CONF-8505408--

SSC-SR-1015

The Superconducting Super Collider

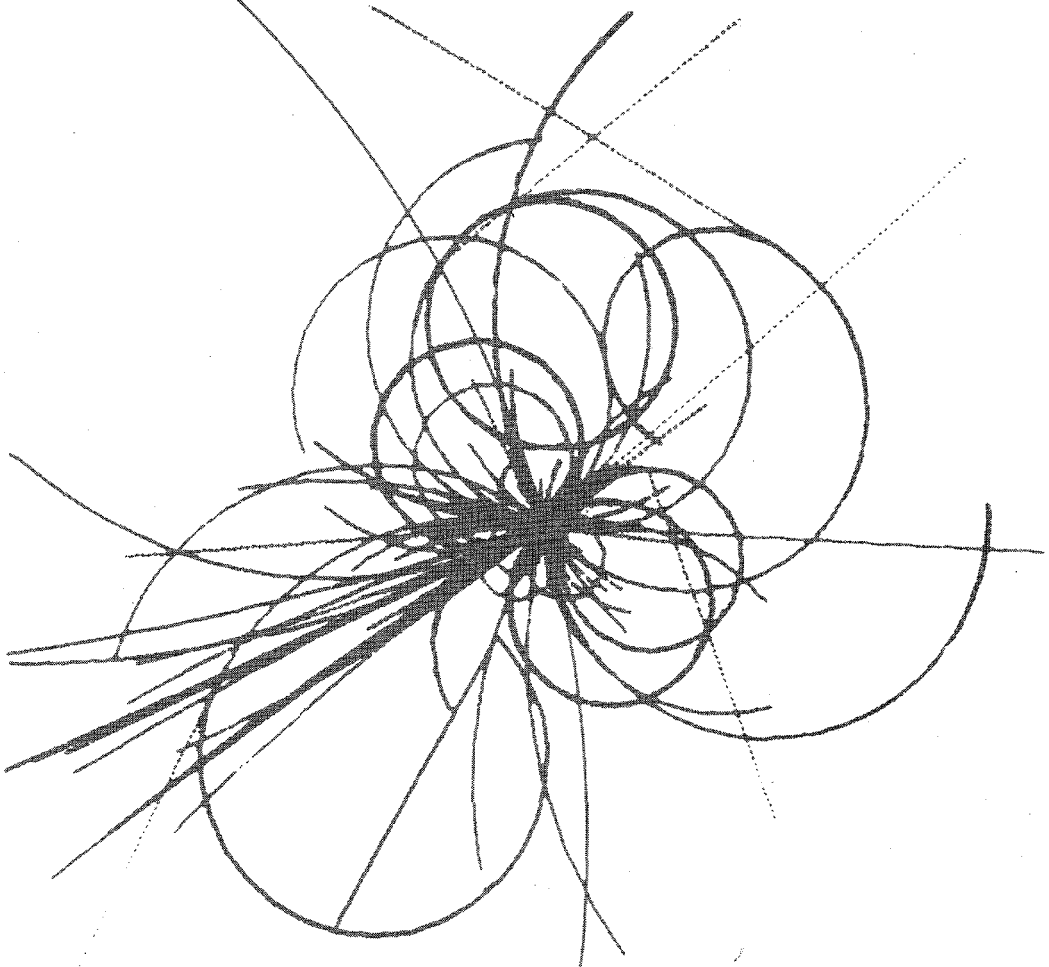

Report of the Workshop on Realistic SSC Lattices

October 1985

LIST OF PARTICIPANTS

Matt Allen, Stanford Linear Accelerator Center
Alex Chao, SSC Central Design Group Berkeley CA
Ernest Courant, Brookhaven National Laboratory
David Douglas, SSC Central Design Group
Al Garren, SSC Central Design Group
Sam Heifets, Texas Accelerator Center
David Johnson, Fermi National Accelerator Laboratory
Beat Leemann, SSC Central Design Group
Christoph Leemann, SSC Central Design Group
Peter Limon, SSC Central Design Group
Zora Parsa, Brookhaven National Laboratory
Steve Peggs, SSC Central Design Group
Jack Peterson, SSC Central Design Group
Lindsay Schachinger, SSC Central Design Group
Klaus Steffen, Deutsches Elektronen Synchrotron
Mike Syphers, Fermi National Accelerator Laboratory

FOREWORD

A workshop was held at the SSC Central Design Group from May 29 to June 4, 1985, on topics relating to the lattice of the SSC. The workshop marked a shift of emphasis from the investigation of simplified test lattices to the development of a realistic lattice suitable for the conceptual design report.

The first day of the workshop was taken up by reviews of accelerator system requirements, of the reference design solutions for these requirements, of lattice work following the reference design, and of plans for the workshop.

The work was divided among four working groups. The first, chaired by David Douglas, concerned the arcs of regular cells. The second group, which studied the utility insertions, was chaired by Beat Leemann. The third group, under David E. Johnson, concerned itself with the experimental insertions, dispersion suppressors, and phase trombones. The fourth group, responsible for global lattice considerations and the design of a new realistic lattice example, was led by Ernest Courant.

The papers resulting from this workshop are roughly divided into three sets: those relating to specific lattice components, to complete lattices, and to other topics.

Among the salient accomplishments of the workshop were additions to and optimization of lattice components, especially those relating to lattices using 1-in-1 magnets, eiher horizontally or vertically separated, and the design of complete lattice examples.

A. A. Garren

TABLE OF CONTENTS

UTILITY STRAIGHT SECTIONS

Beat Leemann, Steve Peggs, and Jack Peterson
SSC Central Design Group

I. REASONS FOR UTILITY STRAIGHT SECTIONS

Utility straight sections are insertions in the SSC lattice to provide relatively free space to facilitate various beam manipulations. These uses include beam-abort, injection (and conceivably ejection), space for the rf system, and collimation. A typical utility straight section is 1500 meters in overall length (ranging from 700 to 2200 meters) with a central inter-doublet length of 1,000 meters (ranging from 500 to 1200 meters). It has zero dispersion and high values of the beta functions. The betatron phase shift across the insertion is about 90° in each plane.

II. ABORT SYSTEM

The principles of the beam-abort system are described in the RDS, pages 117, 253-259, and A-199-218 for Reference Design A, which is a two-in-one configuration with a 0.14-m horizontal beam-line separation. The magnet design D system is an over/under, one-in-one configuration with 0.7-meter beam-line separation. A dog-leg insertion in the central 1,000-meter section is required in the abort system to protect the superconducting magnets from the radiation spray produced by beam loss in the septum magnet, but because of the smaller cryostat diameter and larger beam separation (no extra separation required for kicker magnet) in the present configuration, the dog-leg bend angle is only about two-thirds that in the RDS. Because of the shorter insertion length (1500 vs 2000 meters overall) the vertical kicker is 25% stronger.

The dog-leg is horizontal and in each ring is towards the outside of the ring, so that neither external abort line has to cross under the ring. This arrangement provides more flexibility in the design of the external beam line.

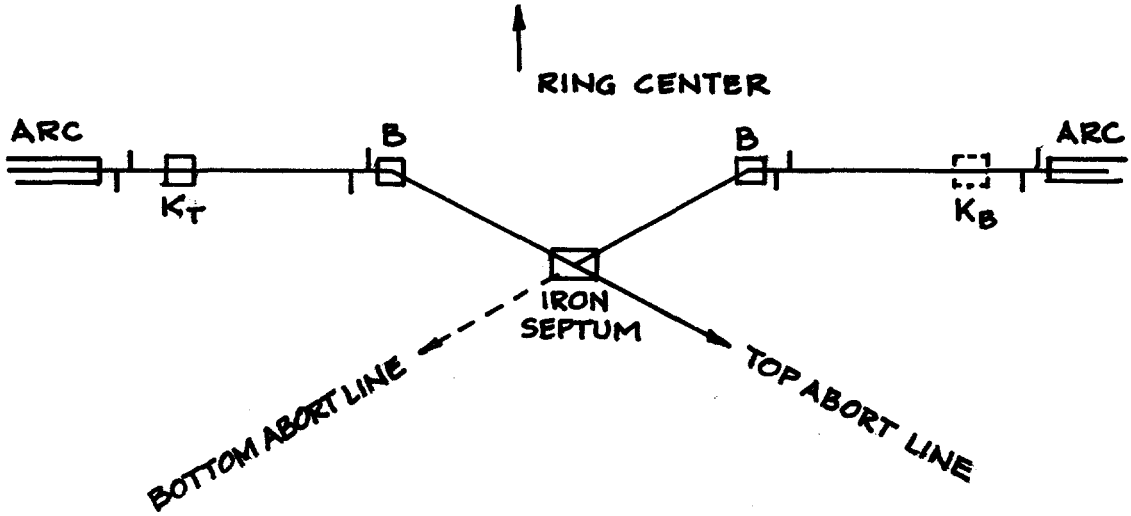

This arrangement of the kicker and septum magnet is basically that considered in the RDS for the two-in-one magnet design A. The use of two one-in-one magnet rings separated by 0.7 meter allows more flexibility in kicker position. The possible advantage of putting the kicker in the 250-meter straight section upstream of the doublet, as shown in the following figure, has not been explored.

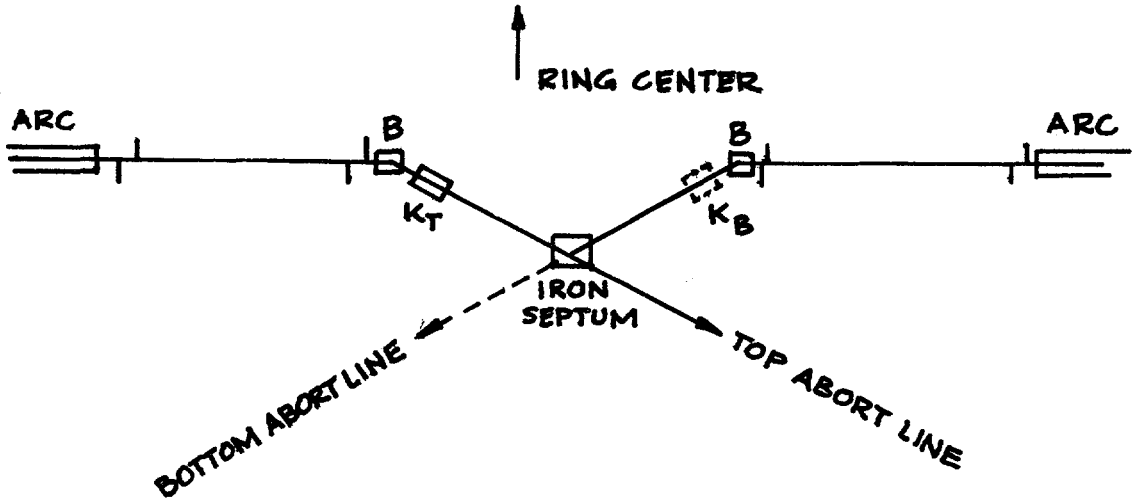

III. INJECTION SYSTEM

The injection system, like the abort system, consists of a septum magnet plus a kicker magnet in each ring. However, in the present one-in-one configuration no dog-leg is required to provide additional clearance for these magnets nor to protect the superconducting magnets from the spray resulting from beam loss in the septum magnet (provided the limiting aperture is at the entrance to the septum magnet).

The injection system could be put in the same utility straight section as the abort system, as has been proposed by Mike Harrison. However, if two or more utility straight sections are required for reasons of lattice symmetry, putting the injection and abort systems in separate insertions is advantageous in that it allows a cleaner design of the injector system, reduces somewhat the kicker requirements, and avoids possible interference between the systems.

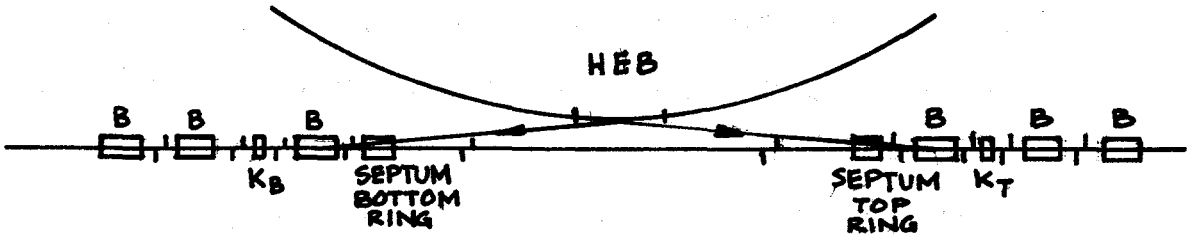

OR

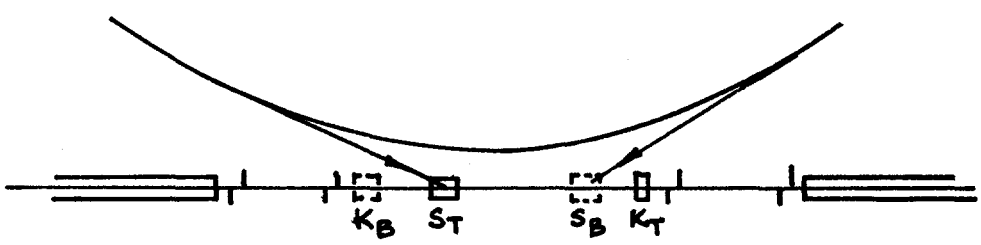

IV. RF SYSTEM

The rf accelerating system is best placed in a zero-dispersion, low-beta lattice position to minimize deleterious beam-cavity interactions. The space needed is 25 meters in each ring. The position best meeting these requirements is in the 250-meter straight section at either end of the utility insertion, at the end toward the adjacent arc. The dispersion there is zero, and the beta functions values approach those of the arc.

The stay-clear radius of the 360 MHz cavity considered in the RDS (p. 244) is 40 cm, so that a dog-leg in the beam line is not necessary. However, the 0.7 meter beam-line separation does require that the top and bottom cavity positions be staggered to avoid mechanical interference.

V. COLLIMATION

Although there will be collimators before and after each of the low-beta triplets to protect the superconducting magnets from beam-beam reaction products, another set of general-purpose collimators should be installed in the abort utility straight section. This position is favorable in that the values of the beta functions are relatively high, the downstream spacing to the nearest superconducting magnet can be made quite large (allowing shielding as well as reduction by $1/r^2$), and any loss signal can be transmitted to the abort system with minimum delay and minimum complexity.

PHASE TROMBONES WITH BENDING

E.D. Courant
Brookhaven National Laboratory

A. Garren
SSC Central Design Group

The phase shifting trombones considered up to now for SSC application [1,2] consisted of sets of evenly spaced quadrupoles separated by drift spaces. One such trombone was placed between a dispersion suppressor and a crossing insertion, so that the trombone had zero dispersion. With such trombones, it is possible to change β^* at constant tune, or to change the tunes by several units without altering the cell phase advances in the arcs.

An objection to the above type of phase trombone is that it adds to the circumference, since no bending is included. This objection may or may not be valid depending on the potential usefulness of the drift spaces in them. In this note we show an alternative trombone design in which dipoles are included between the quadrupoles as in the normal arc cells. Since these trombones have dispersion, they are placed at the ends of the arcs, to be followed in turn by the dispersion suppressors and crossing insertions.

These bending trombones, while economical, do have two probably minor defects. First, they do not contain chromaticity sextupoles, so that the number of normal cells with sextupole will be decreased and their strength increased. For 100 m half-cells these changes are about 10%. Second, when the trombones are adjusted to produce two units of tune change, the maximum beta values occurring within them are 50% above the normal cell maxima. This will increase the sensitivity of the ring to multipole errors in the dipole near the β_{max} points. However, since the fraction of affected dipoles is small, and since others will find their beta values decreased, this effect is likely to be slight.

The bending phase trombones suggested in this note are shown in Fig. 1. The top part of the figure shows the relationship between the trombones for the two rings, and between those on opposite sides of the crossing insertion (which includes dispersion suppressors). The reader will note the opposite polarity between adjacent quadrupoles of the two beam lines, as well as between corresponding quadrupoles for the same beam line on opposite sides of the insertion. Thus the antisymmetric property of all SSC designs to date is maintained.

Each of the four trombones is virtually identical to four regular cells, except that seven of the quadrupoles are powered to have four adjustable gradients. Consider the trombone on the upper left of Fig. 1. It begins with a regular cell QD quadrupole at its left and followed by an array of four adjustable quadrupoles, QFA, QDB, QFC, and 1/2 QDD. This array is then reflected. The four variables are constrained to produce a beam waist ($\alpha_x = \alpha_y = \eta' = 0$) at the center of the trombone and to produce a specified phase advance. The reason for the beam waist is to reproduce the normal cell orbit functions from the entrance to the exit of the trombone.

The four trombones have two sets of gradients. The two top trombones are identical to each other as are the two bottom ones, but each beam encounters one top and one bottom trombone on the opposite sides of the crossings.

The gradients of two adjacent top and bottom quadrupoles, for example of QFA and AQD, are opposite in sign and nearly equal in magnitude. If the rings are adjusted to make the horizontal and vertical tunes equal, then the gradients will be strictly equal in magnitude. To the extent that ν_x and ν_y are to be separated, so will be the magnitudes of the corresponding

Bending Phase Trombones

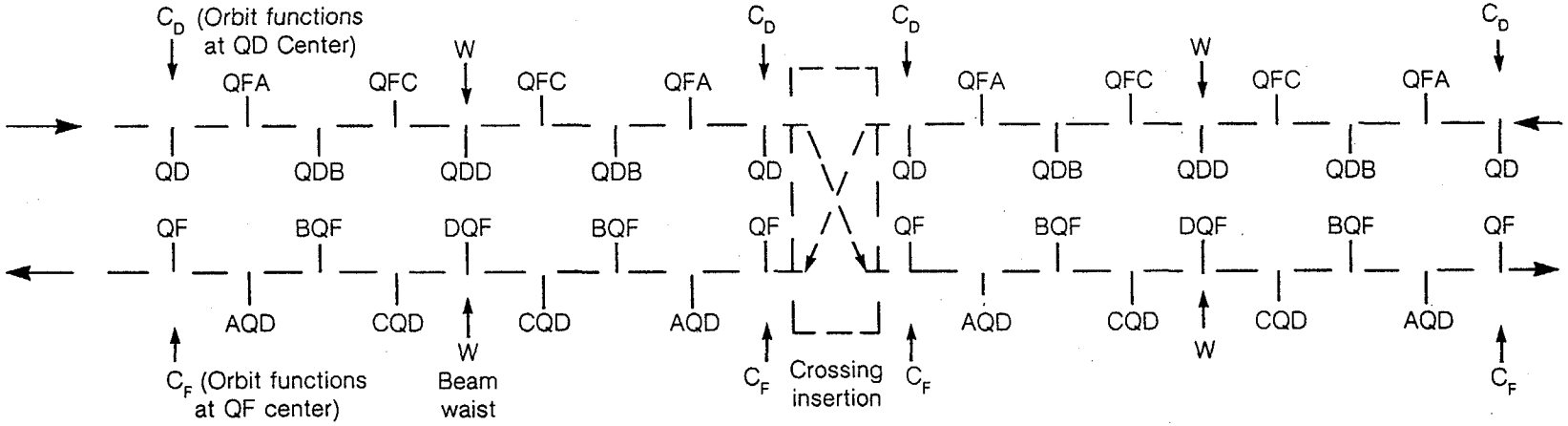

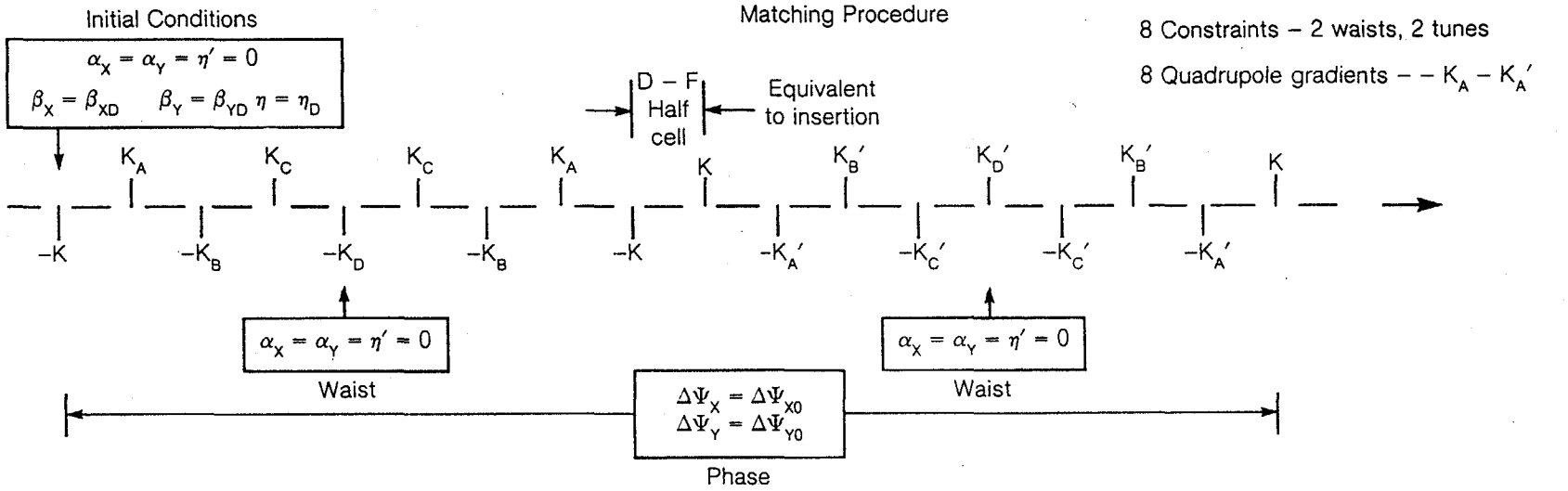

XBL 859-12150

Fig. 1

gradients. It is likely that the trombones will be used to produce or compensate for a couple of units tune change along the diagonal of the tune diagram, but less than 0.1 unit of tune splitting, so the departure from antisymmetry will be slight.

The method of matching the phase trombones encountered by the left-to-right beam to be placed one after the other, separated by a normal QD to QF half-cell.

One tracks the orbit functions (β_x, α_x, β_y, α_y, η, η') from the center of the QD at the left to the center of the QF at the right, beginning with the matched normal cell functions occurring at a QD center. The eight independent gradients K_A, $-K_B$, K_C, $-K_D$ and $-K'_A$, K'_B, $-K'_C$, K'_D are adjusted to meet the following eight conditions:

$\alpha_x = \alpha_y = \eta' = 0$ at center of QDD and DQF

$\Delta\Psi_x = \Delta\Psi_{xo}$ (desired phase advance, horizontal)

$\Delta\Psi_y = \Delta\Psi_{yo}$ (desired phase advance, vertical)

The first waist condition causes the second QD to have the same normal cell functions as the first; the D-F half-cell maps then to normal center QF values; the second waist maps these to the normal QF at the right end; the phase conditions produce the desired horizontal and vertical tune contributions from the trombones.

Since the right-to-left beam encounters the same beam line sequence as does the left-to-right beam, one matching run takes care of both beams.

The difference between the matching procedure for trombones with and without bending magnets is that the latter have zero dispersion. Therefore the two $\eta' = 0$ conditions at the centers of the trombones are unnecessary. As a result, six independent gradients rather than eight suffice, and each

trombone can be shortened by one cell, e.g., the upper left trombone at the top of Fig. 1 becomes

1/2 QD QFA QDB QFC QDB QFA 1/2 QD

with drift spaces and no bends between the quadrupoles.

Returning to the trombones with bending, for an SSC ring with twelve such trombones adjusted to change the tune by two units, some of the quadrupoles must be 50% stronger than those in the cells. Therefore the quadrupoles will need to be made longer and/or with higher gradients than normal ones.

References

1. D.E. Johnson, A Trombone Design Using 1/2 Length Cells - No Bends (Private Communication).
2. A. Garren, Test Lattice Trombones - Three Full Length Cells - No Bends.

DISPERSION SUPPRESSORS WITH BENDING

A. Garren
SSC Central Design Group

Dispersion suppressors of two main types are usually used. In one the cell quadrupole focussing structure is the same as in normal cells but some of the dipoles are replaced by drifts. In the other, the quadrupole strengths and/or spacings are different from those of the normal cells, but the bending is about the same as it is in the cells.

In SSC designs to date, dispersion suppressors of the former type have been used, consisting of two cells with bending equivalent to one. In this note a suppressor design with normal bending and altered focussing is presented. The advantage of this scheme is that circumference is reduced. The disadvantages are that additional special quadrupoles must be provided (however, they need not be adjustable), and the maximum beta values within them are about 30% higher than the cell maxima.

The bending suppressors to be considered are shown in Fig. 1. The upper part of the figure shows the four suppressors, two for each ring, on the opposite sides of a crossing insertion. The quadrupole spacing and the bending are identical to that found in regular cells. Each of the four suppressors has six half-cells and five special quadrupole strengths. The focussing pattern is strictly antisymmetric. The adjacent quadrupoles for the two beams above and below each other are exactly equal and opposite as are corresponding quadrupoles of the same beam line on opposite sides of the crossing insertion. Thus, for example, QFG and GQD have equal and opposite gradients and equal length.

The trombones border the areas so that the orbit functions at their ends farthest from the crossing point are those of normal cells at the center of QF

Bending Dispersion Suppressor

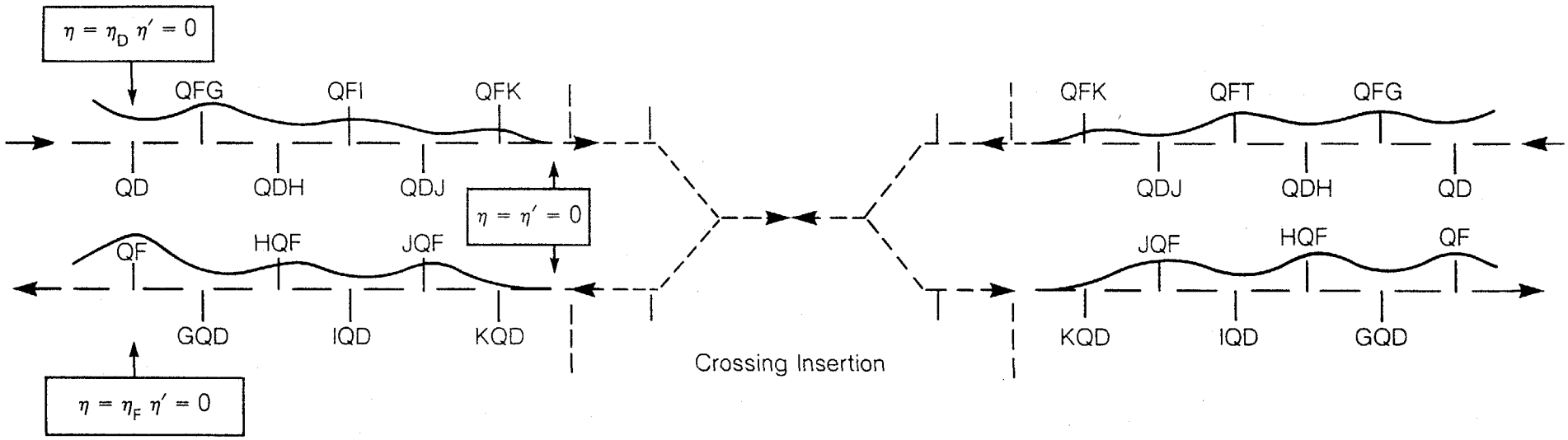

Matching Procedure

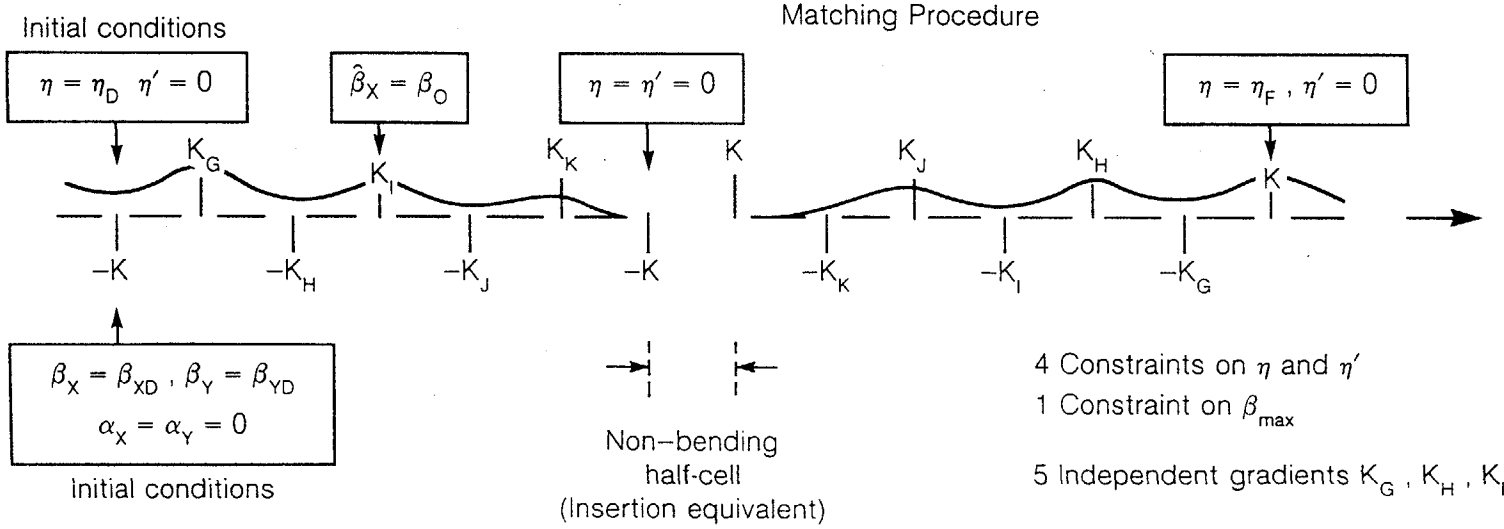

4 Constraints on η and η'

1 Constraint on β_{max}

5 Independent gradients K_G , K_H , K_I , K_J, K_K

XBL 859-12151

Fig. 1

or QD quadrupoles. The matching procedure is shown in the lower part of Fig. 2. The two suppressors of the left-to-right beam line are placed in sequence with the crossing insertion replaced by a normal half-cell without dipoles.

One trades the orbit functions from the center of the QD at the left to the center of the QF at the right, beginning with the normal cell functions at the center of a QD. The five independent gradients K_G, $-K_H$, K_I, $-K_J$, K_K are adjusted to meet the following five conditions:

$\eta = \eta' = 0$ in the non-bending half-cell

$\eta = \eta_F$, $\eta' = 0$ at the QF center on the right

$\beta_x = \beta_o$ in QFI (the point where β_x is maximum)

The maximum beta value β_o, is lowered as far as possible consistent with meeting the dispersion constraints and not producing a larger β at some other point in the suppressor.

During fitting run the β, α values are correct for the left suppressor but not for the right one, since the fictitious half-cell does not have the same effect on β, α as does the crossing insertion. However it (or any non-bending structure) has no effect on η, η' once they are reduced to zero.

The result of the above fitting procedure is that two quadrupole strengths are above 45% above the normal cell values, and the maximum beta is about 30% above normal. In a ring with twelve suppressors and 100 m half-cell length, 2.4 km of circumference is saved. If the ring also has two utility insertions, the savings are 2.8 km.

It should be noted that the β, α values at the interfaces between the suppressors and the crossing insertion are <u>not</u> those of normal cells. Therefore to match the insertions, one must include the suppressors and begin

at the left end of the suppressor with the cell orbit function values. This has been done and no ill effects on the crossing insertion result. Another design of bending dispersion suppressor consists of a half-betatron wavelength block of shortened cells, with length and bending strength adjusted to make the material dispersion of the shortened cells equal to half that of the normal cells. Thus with 60° or 90° regular cells, the suppressors would contain 3 or 2 shortened cells respectively, about $1/\sqrt{2}$ in length compared to normal cells. In contrast to the suppressor of Fig. 1, the shortened cell suppressor would map the cell β, α values from entrance to exit.

HORIZONTALLY SEPARATED 1-IN-1 CROSSING INSERTIONS

M.J. Syphers
Fermi National Accelerator Laboratory

Previous to this workshop, realistic lattices have been developed for vertically separated 1-in-1 (e.g., D.E. Johnson, A.A. Garren) and 2-in-1 (e.g., S. Heifets) magnets as well as for horizontally separated 2-in-1 magnets (e.g., SSC RDS). Bringing together the widely separated (~60-70 cm) beams in a reasonable length of tunnel and keeping the dispersion zero at the interaction point has been difficult in the vertical 1-in-1 case. Most designs have required spacial 2-in-1 quadrupoles near the interaction point where the beams are separated by 15 cm or less. It is not clear that such magnets, as dictated by some of these lattice designs, can easily be built.

The purpose of this exercise is to provide a crossing insertion for a realistic lattice which involves horizontally separated 1-in-1 magnets. The following horizontal crossing insertions, which incorporate the dispersion suppressors and phase trombones into the major arcs, need no special 2-in-1 magnets near the interaction point. The dispersion at the IP created by the horizontal crossing can be cancelled by the dispersion suppressor and one set of triplets.

Insertion Description

The basic lattice of this machine is that generated by A.A. Garren for the vertical 1-in-1 scheme. The phase trombones are taken to lie in the major arcs and hence the insertions are fit to standard cell betatron functions at each end.

There are two different crossings in the horizontal 1-in-1 design as shown in Fig. 1. Since the dispersion generated by crossing from inside to outside

Horizontally Separated 1 – in – 1

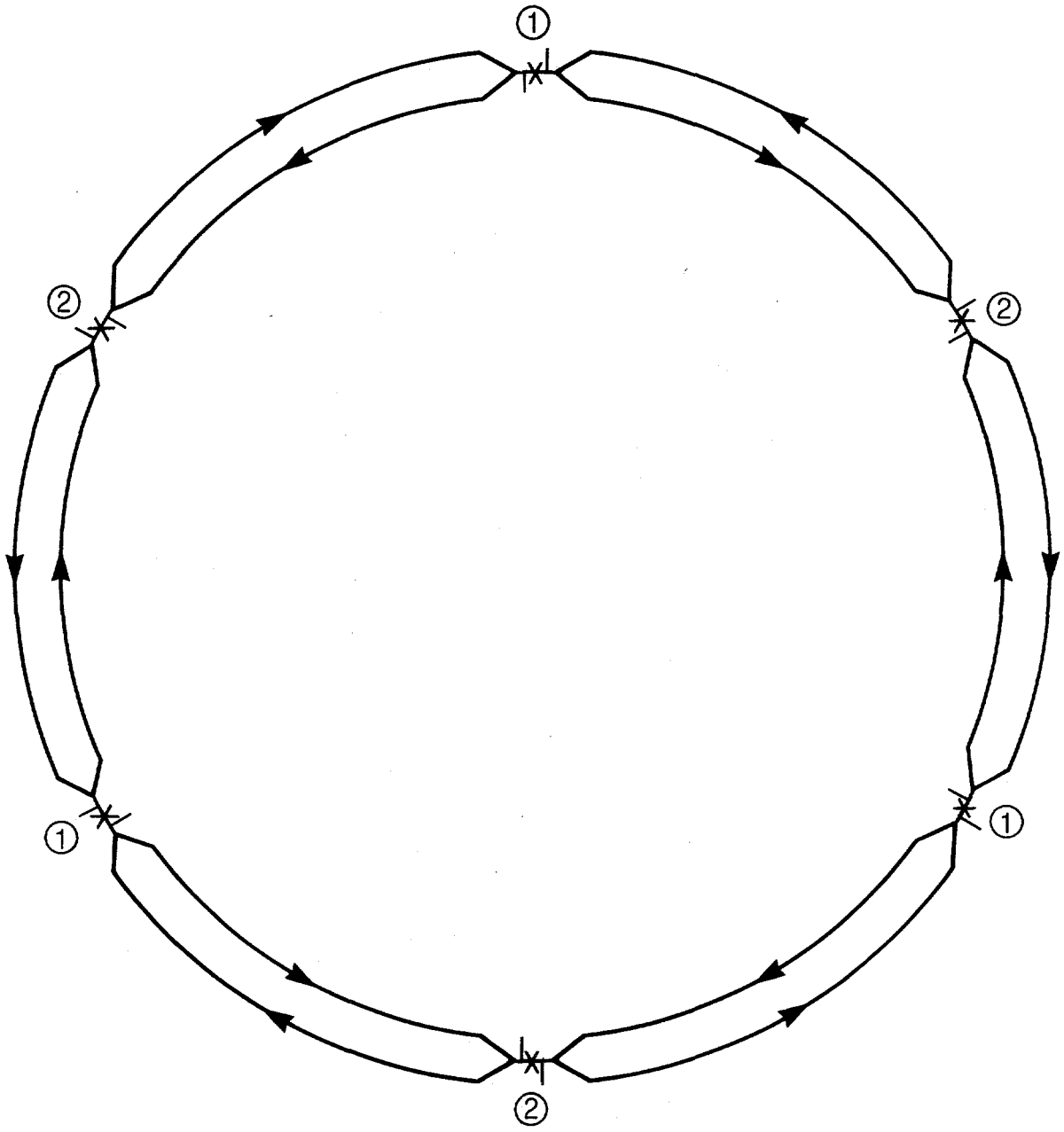

XBL 859-12141

Fig. 1

is different from the dispersion generated by crossing from outside to inside, two different solutions to the dispersion suppressors and crossing insertions must be obtained. In each of these solutions, the dispersion at the end of the suppressor is finally canceled by the crossing magnets.

Figures 2-4 shown the TYPE 1 crossing insertion in more detail as well as the beta functions and momentum dispersion throughout the insertion. Figures 5-7 shown the TYPE 2 crossing insertion. Differences between the quadrupole strengths in the two insertions are displayed in Table I. In each

Table I

	Strength (1/meters)	
Quad	Crossing 1	Crossing 2
G	0.0090570	-0.0088520
H	-0.0114876	0.0112580
I	0.0138696	-0.0138660
J	-0.0139890	0.0143180
K	0.0109856	-0.0100646
6	-0.0007656	0.0007656
5	0.0173496	-0.0173496
4	-0.0103756	0.0103756
3	-0.0411534	0.0414824
2	0.0382972	-0.0381020
1	-0.0243638	0.0231812

example the crossing is created by four bending magnets, two at each end of the long drift region, each with a field strength of 3.75 tesla and a length equivalent to that of a standard cell dipole. At first it was hoped that the dispersion created by the horizontal crossing could be handled solely by the dispersion suppressor quadrupoles. However, by changing these quadrupoles the beta and alpha functions at the IP are altered. In order to fit the betatron functions at the interaction point as well as fitting the dispersion at the

Horizontally Separated 1 – in – 1

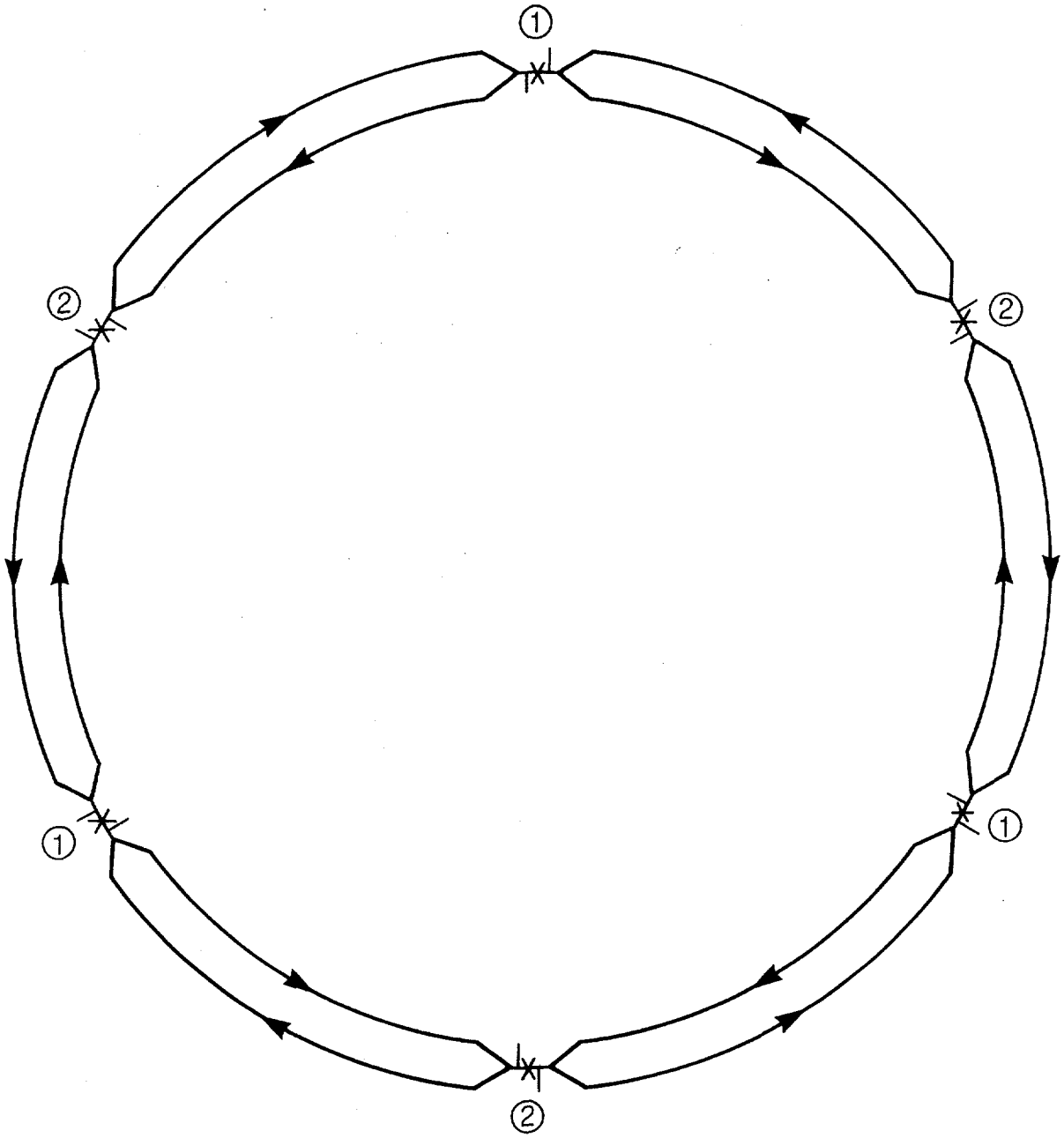

XBL 859-12141

Fig. 1

Crossing 1

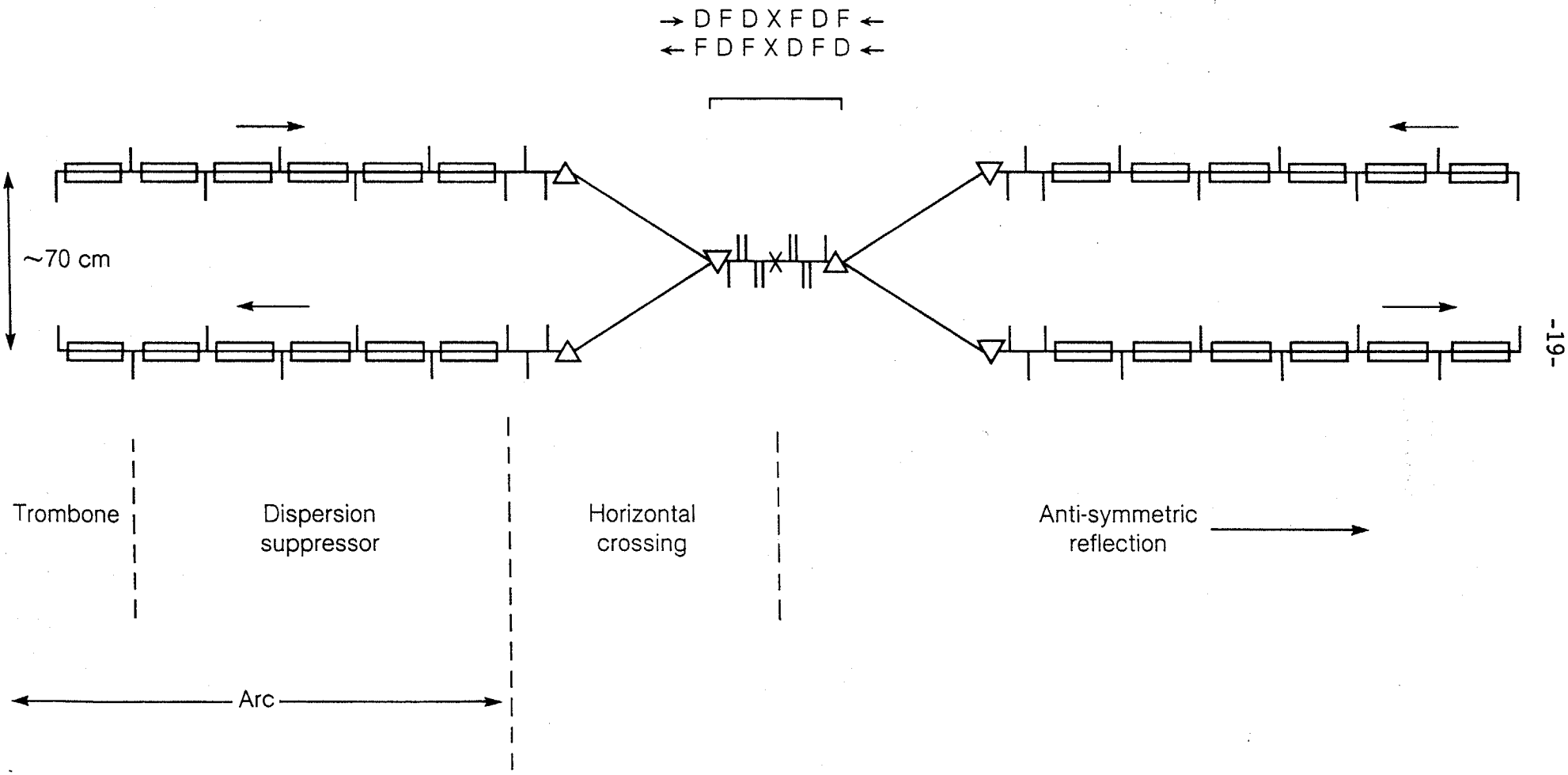

XBL 859-12142

Fig. 2

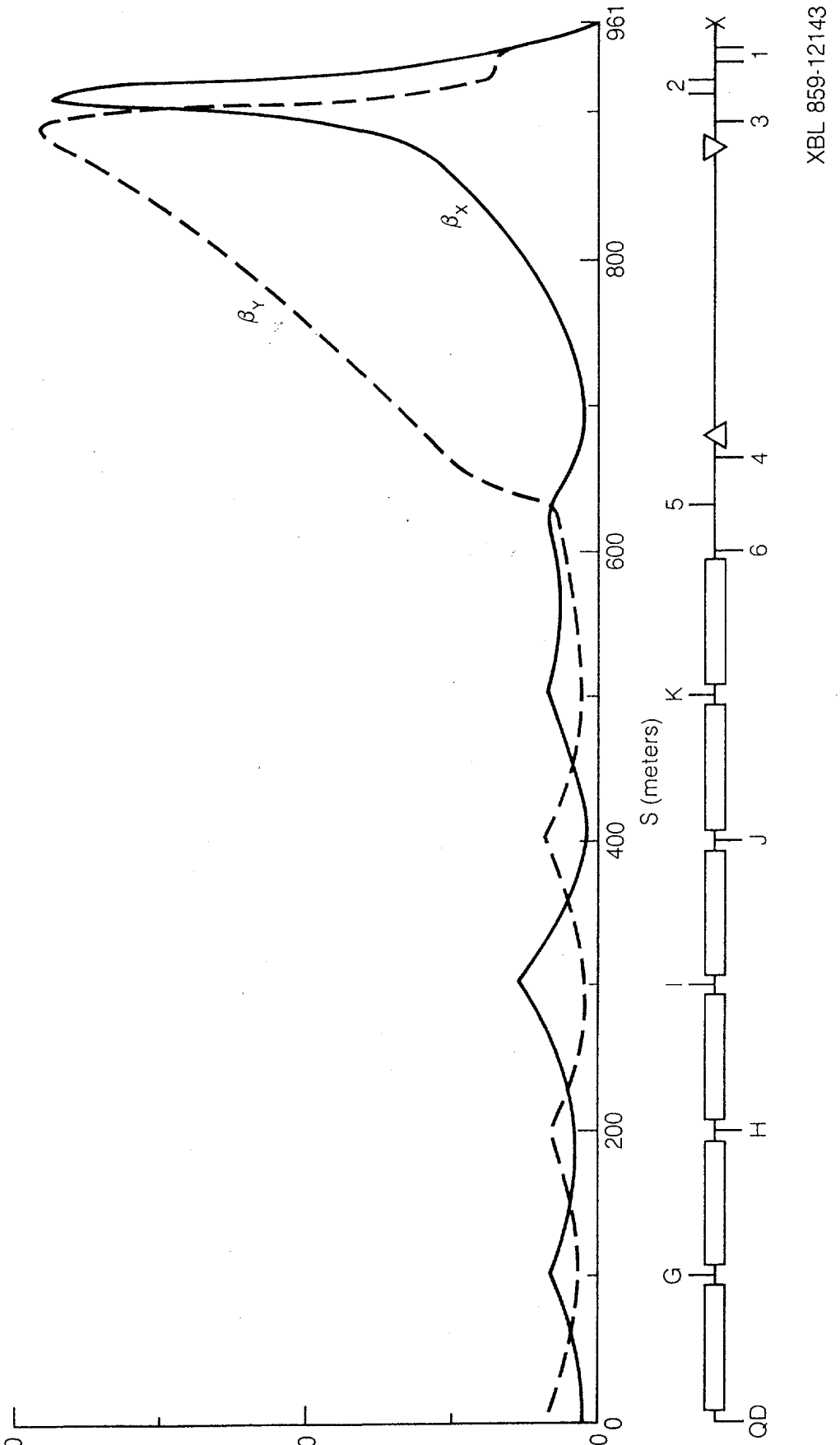
Beta Functions Through Crossing Insertion #1
4000
2000
0
β(m)
0
200
400
600
800
961
β_Y
β_X
S (meters)
QD
G
H
I
J
K
1
2
3
4
5
6
X
XBL 859-12143

Fig. 3

Dispersion Function Through Crossing Insertion #1

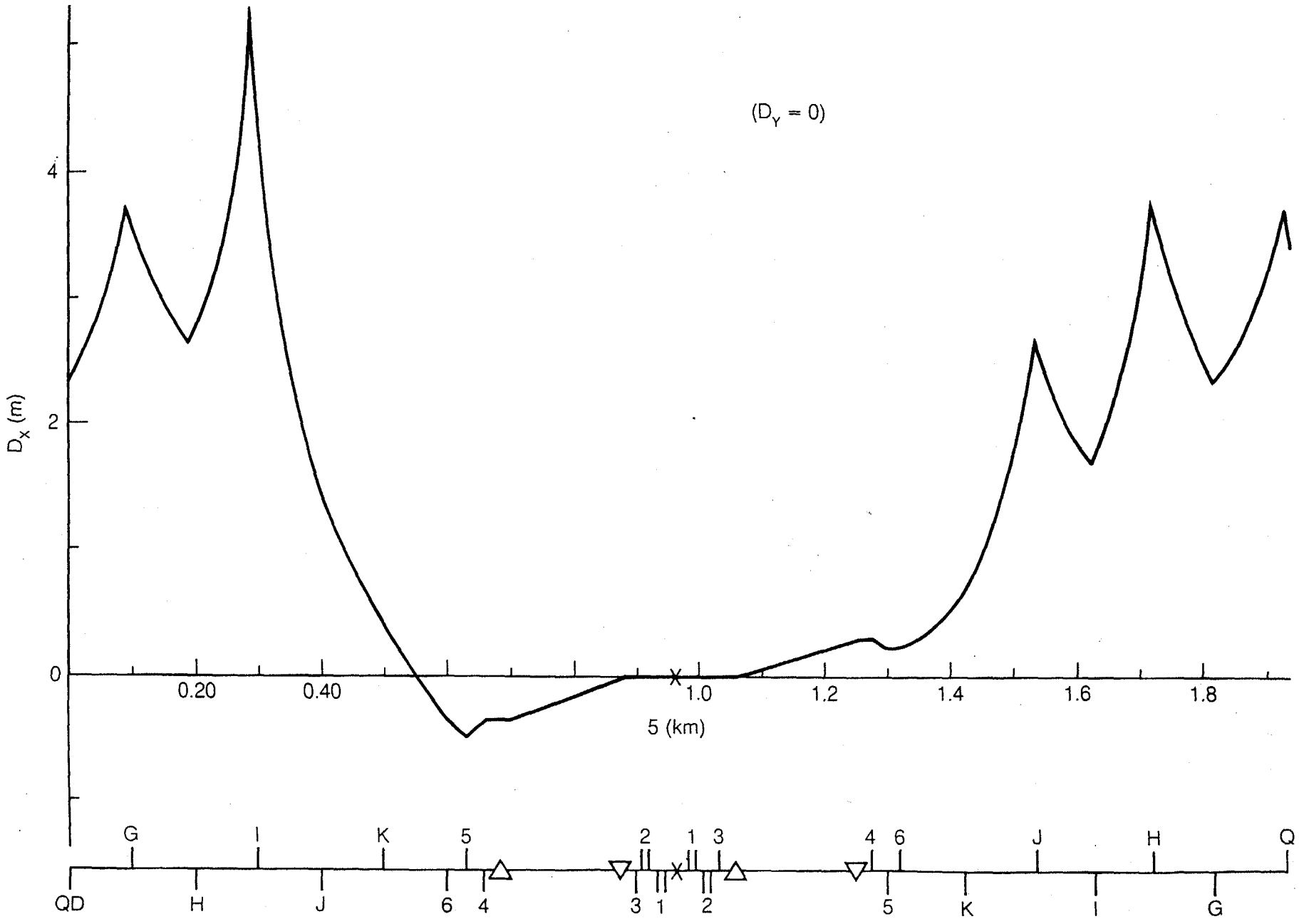

Fig. 4

XBL 859-12144

Crossing 2

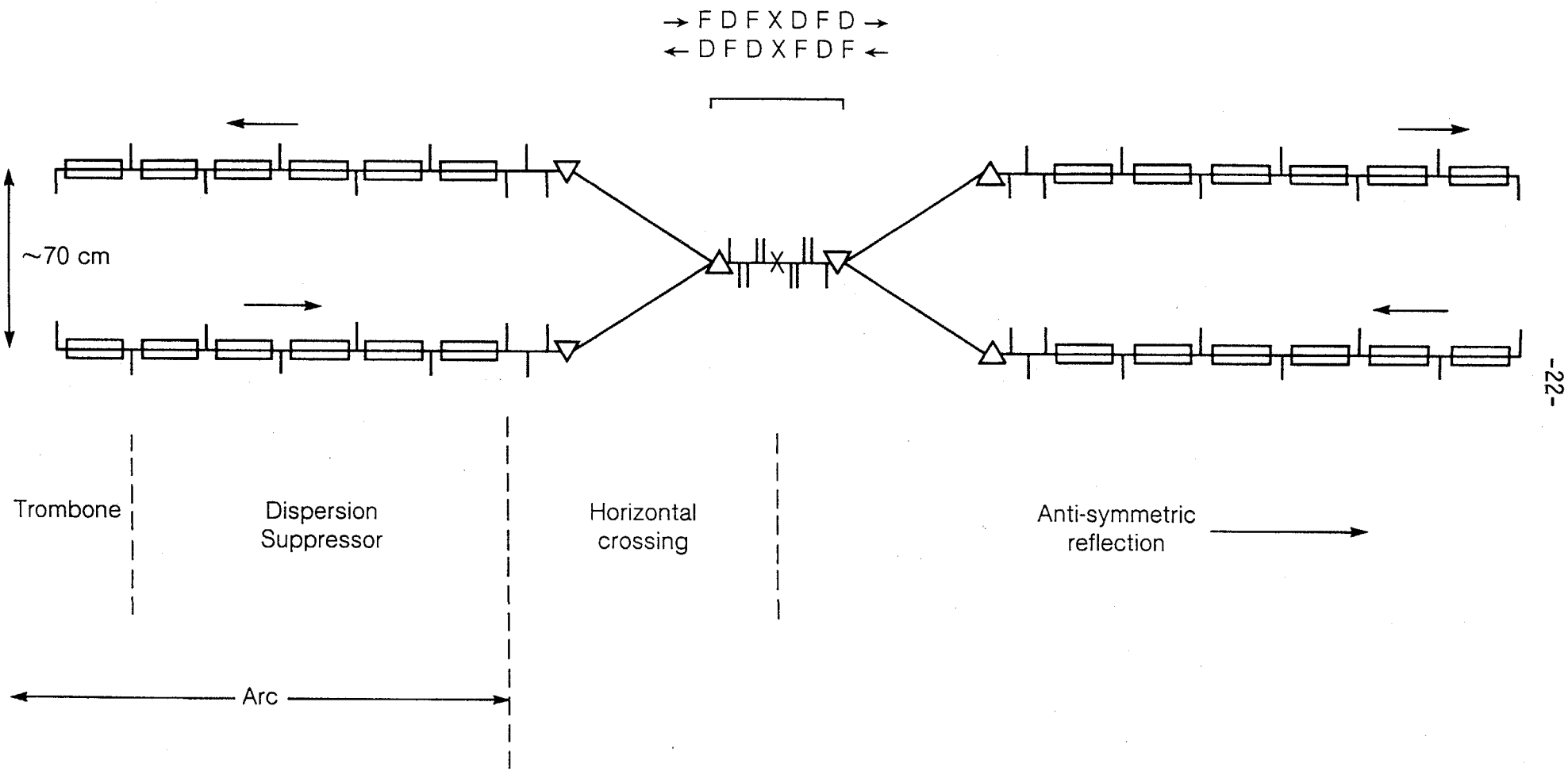

XBL 859-12145

Fig. 5

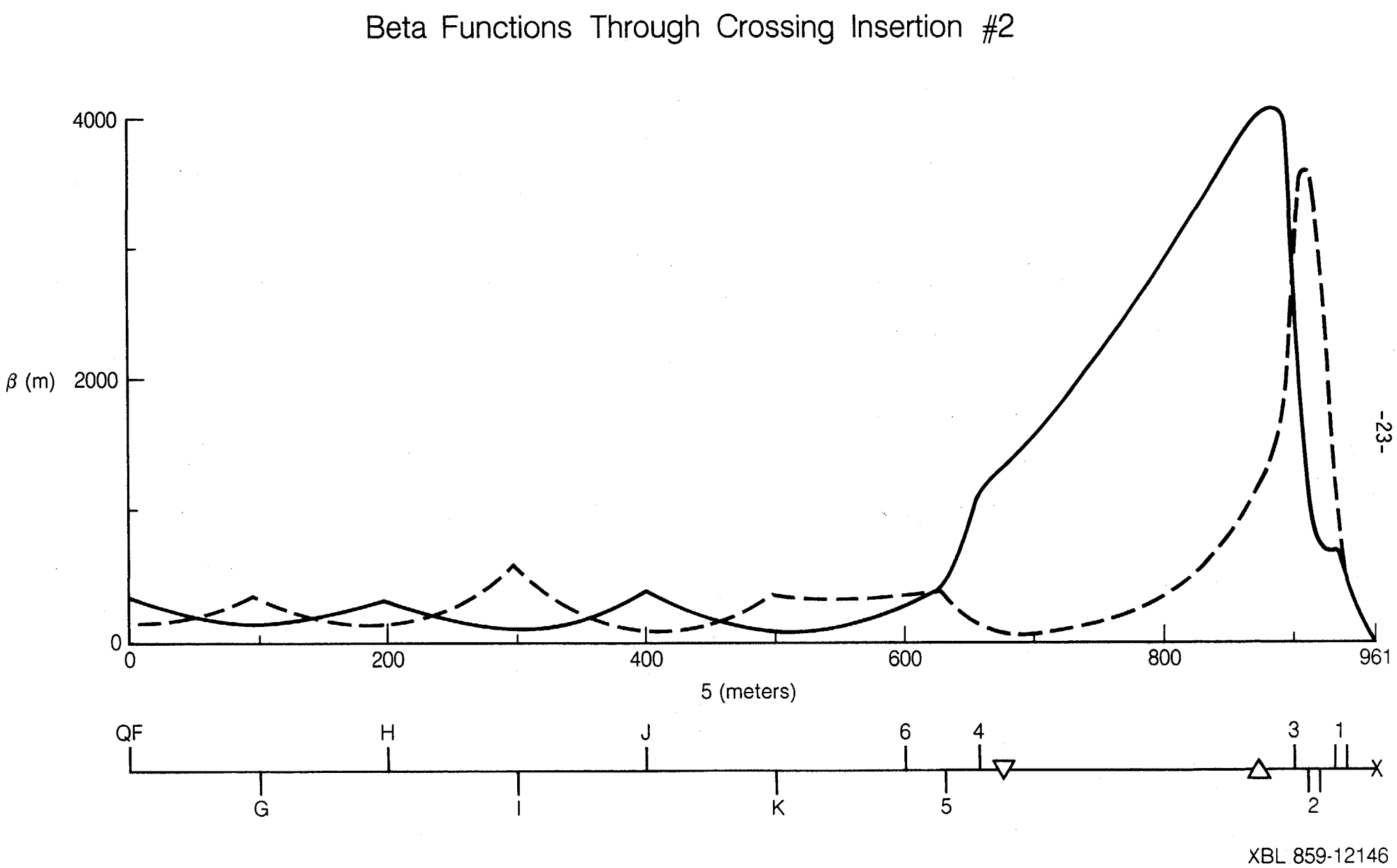

XBL 859-12146

Fig. 6

Dispersion Function Through Crossing Insertion #2

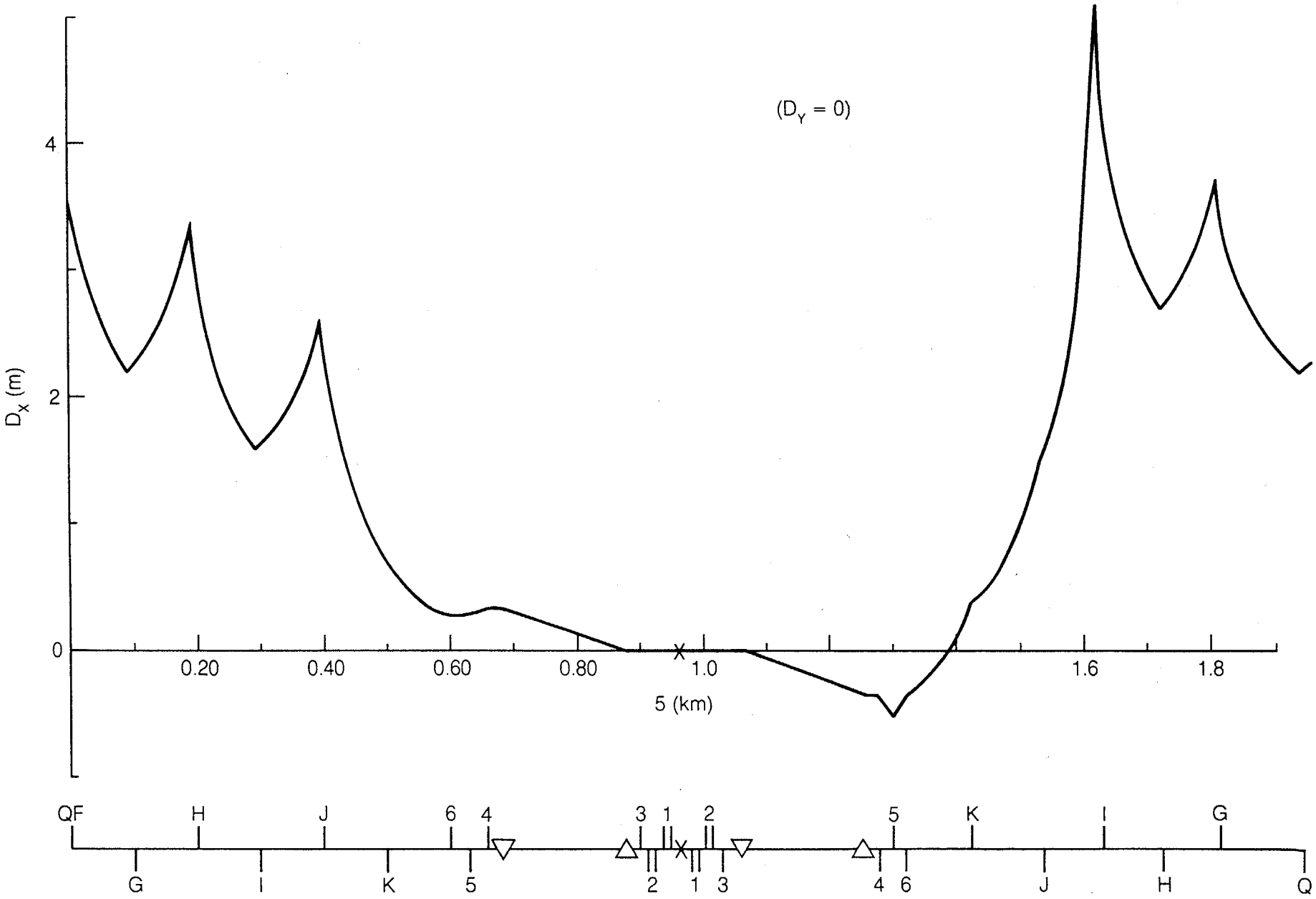

Fig. 7

XBL 859-12147

interaction point and the dispersion at the end of the insertion, 8 different knobs are necessary. Thus, one must tune three of the triplet quadrupoles in addition to the dispersion killer quadrupoles. In this example, quads 1, 2, and 3 were chosen.

Conculsion

With these insertions, examples now exist for each of the four cases being studied: horizontal vs. vertical crossings with 2-in-1 magnets or 1-in-1 magnets. The advantages of the insertions shown in this study include the fact that there is no vertical dispersion to worry about and no special 2-in-1 magnets near the interaction point. On the other hand, the superperiodicity of the machine is reduced to 3 since every other crossing needs a different dispersion suppressor. (Of course this would naturally be the case in a horizontally separated machine since the inner and outer rings are of different radii.)

Another important point to consider is the tuning of β^*. As noted above, in order to tune the dispersion and betatron functions one must use 8 quadrupoles. Thus, one must also re-tune the dispersion suppressor whenever the insertion is altered from one value of β^* to another. This requires that the dispersion suppressor magnets be on separate power supplies as opposed to having a single dispersion suppressor design which uses different length quadrupoles all in series with the dipole magnets. An alternative may be to make the dispersion suppressor contain more quadrupoles. Since it is already incorporated into the arcs, it would not take up any more tunnel. As of yet, this alternative has not been attempted.

The lack of a crossing angle through the interaction point may be yet another concern. The distance between the separator magnets is approximately

140 m which may lead to unacceptable bunch spacing. Of course none of these issues is new. It is clear that many other variations of this scheme are possible and that the horizontal 1-in-1 lattice raises many questions which must be addressed. Now, at least, an example exists which may be used in such discussions.

VERTICAL SEPARATION OF THE TWO BEAMS

S. Heifets
Texas Accelerator Center

Let us consider the possibility of separating two beams in the vertical plane without a vertical dispersion suppressor (D.S.).

It is very desirable to reduce the length of the insertions. For example, one suggested by D. Johnson has the length ≃ 600 m, demanding about 3 km additional space is the clustered insertion with 3 IP's.

The example of a race-track lattice shows that it is possible to have beams separation of 12.5 cm with $\eta_y^* < 5.05$ cm and η_{max} (cell) ≃ 35 cm.

The first question: what η_y should be allowed?

At IP

At E = 20 TeV with $E = 10^{-6}$ m, $\beta^* = 1$ m, $\delta = 10^{-3}$, $\sigma^* = (2E\beta^*)^{1/2}$ $\simeq 10^{-3}$ cm is comparable with $x^* = \eta^* \delta$, if $\eta^* \simeq 10$ cm.

From this point of view η^* of several centimeters does not cause problems.

In the Arc

As A. Chao pointed out, η_y in the regular cells is equivalent to skew multipoles. Indeed, with $\eta_y \neq 0$

$$B_z = \sum_n bn\,(x + i\,\eta_y + y_\beta)^n = \sum_n b(x + iy_\beta)^n + \sum_n inb_n\eta_y\,\delta\,(x+iy_\beta)^{n-1}\ ,$$

which means that there is a induced skew multipole $a_{n-1} = nb_n \eta_y \delta$

If η_y = 35 cm; $\delta = 10^{-3}$, then $a_{n-1}/b_n = n.\ 3.5.10^{-2}$. This should be compared with magnet skew multipoles, which was estimated (J. Peterson) for design A as

$$a_1/b_2 = 0.35$$
$$a_2/b_3 = 1.74$$
$$a_3/b_4 = 1.17$$
$$a_4/b_5 = 2.37$$
$$a_5/b_6 = 2.13$$
$$a_9/b_{10} = 4.66$$

Thus the induced skew multipole is negligibly small when compared with intrinsic skew multipoles in the magnets. Even so, we might ask how the system may be optimized to reduce η_y without use of a vertical dispersion suppressor? Consider the IP with a magnet separator in its vicinity.

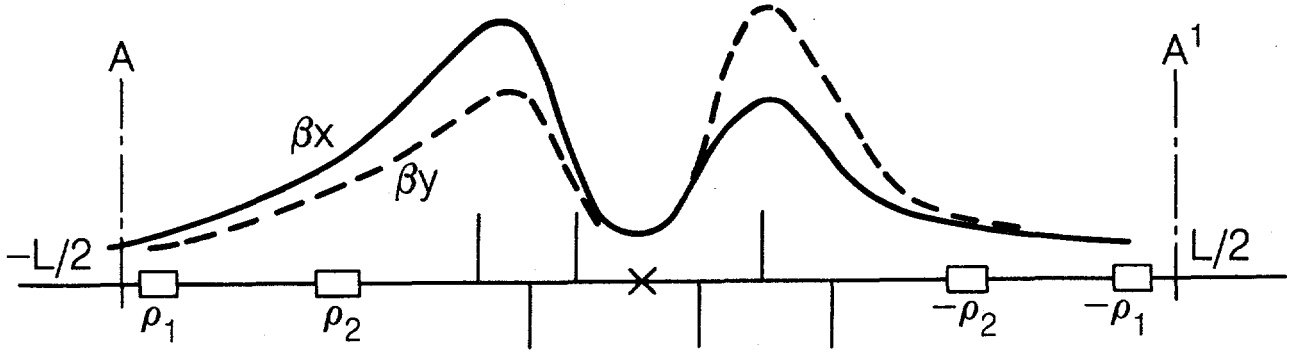

Two short bend magnets and drift in between work as a separator in y-plane. Given beam displacement, there are three independent parameters in a separator ρ_1, ρ_2, Θ

The symmetry of the system for the beams implies that two separators are antisymmetric, as shown.

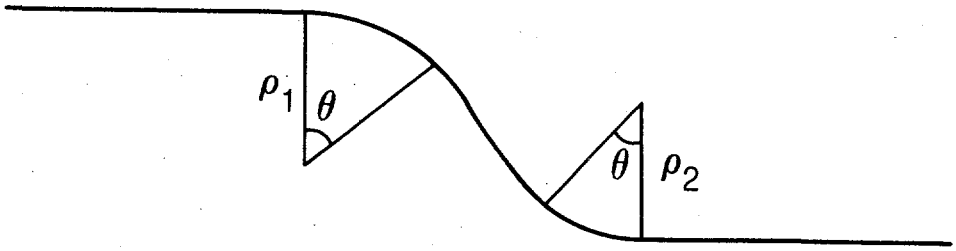

The conditions of matching η_y from the point A ($s = -L/2$; $\eta_y = 0$; $\eta'_y = 0$) to the point A' ($s = +L/2$, $\eta_y = 0$, $\eta'_y = 0$) demand

$$(\eta_y) = \int_{-L/2}^{L/2} ds' \frac{wz(s')}{\rho(s')} \sin \mu_z(s') = 0$$

$$(\eta'_y) = \int_{-L/2}^{L/2} ds' \frac{wz(s')}{\rho(s')} \cos \mu_z(s') = 0$$

The condition $\eta^* = 0$ gives

$$\int_{-L/2}^{\circ} ds' \frac{wz(s')}{\rho(s')} \sin (\mu_z^* - \mu (s')) = 0$$

There are 3 parameters ρ_1, ρ_2 and the position of the separator relative to the IP.

It seems, that it is possible to satisfy two first conditions and, probably, have rather small η_y^* [probably, not zero because β_x (left) $\neq \beta_x$ (right)].

A DESIGN FOR VERTICAL CROSSING INSERTIONS

A. Garren
SSC Central Design Group

A crossing insertion designed for an SSC with vertically separated 1-in-1 beam lines is presented in this note. We suppose that the beam lines consist of separate magnets in separate cryostats separated by about 70 cm.

The insertion proposed is shown schematically in Fig. 1. The vertical separation is done with four vertical dipoles producing a steplike beam line. Consider the right-hand branch of the left-to-right beam line. The beam proceeds from the IP through the common triplet F1, D2, F3 along the horizontal axis with zero vertical (and horizontal) dispersion. It then passes through the first vertically bending dipole B+, which splits to two beams. It then descends through a drift space L to a second dipole B- with opposite bending to the first, so the orbit and the dispersion leave B- with zero slope. The beam proceeds from B- horizontally to another B+ dipole. Between B- and B+ there are 5 quadrupoles adjusted to make two 90° cells, with transfer matrix $M = -1$.

The $M = -1$ array of 5 quadrupoles changes the sign of the dispersion and leaves the slope zero, so that the remaining B+ L B- part of the separator restores the vertical dispersion and its slope to zero.

Since the $M = -1$ array along the step has no net effect on the β, α values, the triplets Q1 Q2 Q3 and Q4 Q5 Q6 can be adjusted to produce the low beta waist at the IP as if it were not there, so the vertical dispersion match is completely decoupled from the beta matching problem, and β^* can be altered at will without worrying about it.

Another advantage of the proposed scheme is that the step containing the center two dipoles and the five quadrupoles is separated from that of the

Vertical Crossing Insertion

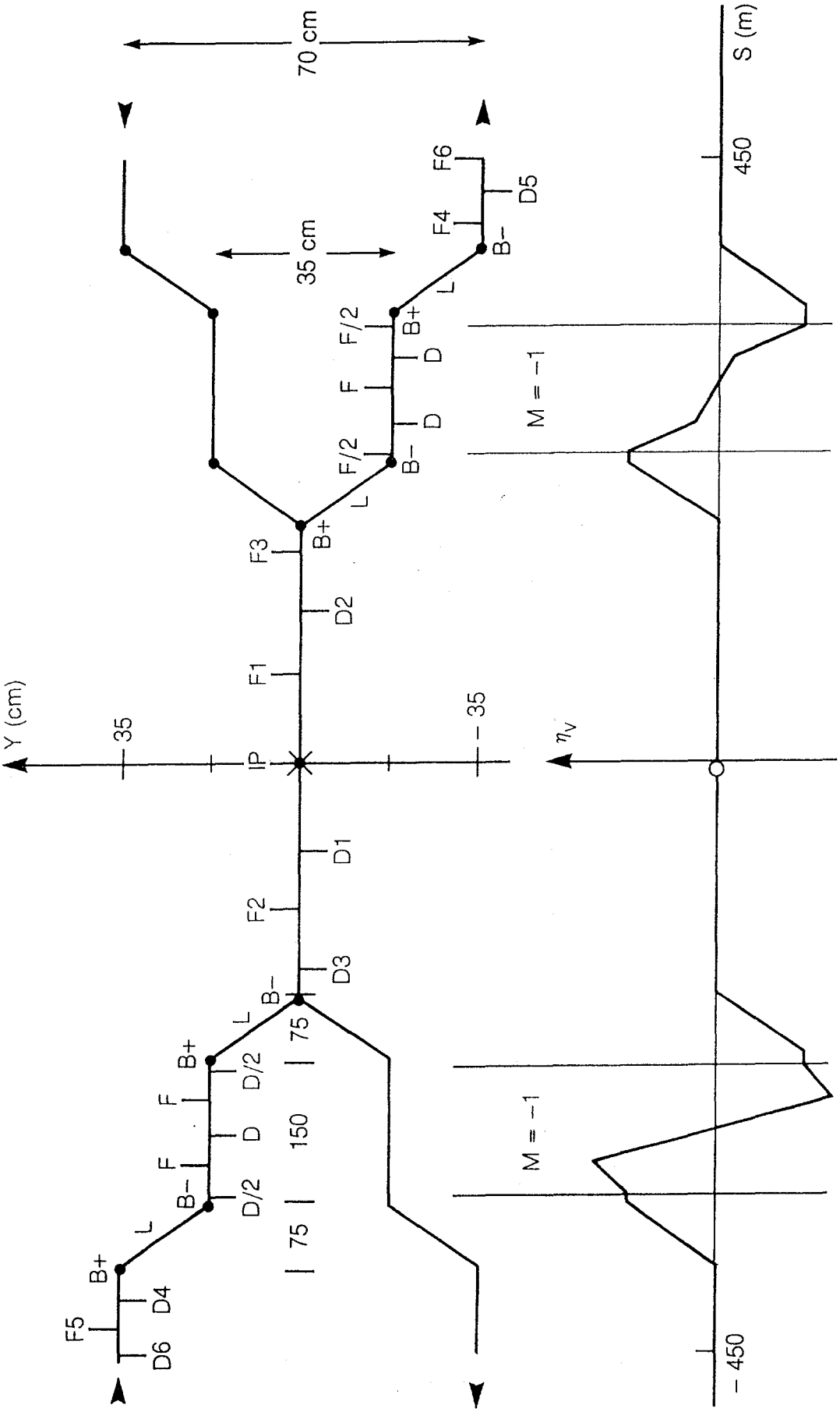

Fig. 1

other beam line by half of the final separation. This separation should be sufficient to permit use of separate magnets in common cryostats along the step, so that the loss of independence and design problems of 2-in-1 magnets can be avoided.

A REALISTIC LATTICE EXAMPLE

E.D. Courant and A.A.Garren

1 INTRODUCTION

A realistic, distributed interaction region (IR) lattice has been designed that includes new components discussed in the June 1985 lattice workshop. Unlike the test lattices, the lattice presented here includes utility straights and the mechanism for crossing the beams in the experimental straights. Moreover, both the phase trombones and the dispersion suppressors contain the same bending as the normal cells.

Vertically separated beams and 6 Tesla, 1-in-1 magnets are assumed. Since the cells are 200 meters long, and have 60 degree phase advance, this lattice has been named RLD1, in analogy with the corresponding test lattice, TLD1 [1]. The quadrupole gradient is 136 tesla/meter in the cells , and has similar values in other quadrupoles except in those in the IR's, where the maximum gradient is 245 tesla/meter.

RLD1 has distributed IR's; however, clustered realistic lattices can easily be assembled from the same components, as was recently done in a version that utilizes the same type of experimental and utility straights as those of RLD1.

2 GLOBAL STRUCTURE

The RLD1 lattice, Fig. 1, contains six equally spaced experimental straights X, and three utility straights U, which are placed in the centers of every other arc joining the X's. Thus the ring has three superperiods, resembling the SSC Reference Design [2] in this respect. The X's are identical except that in one, called Xd, the clockwise beam crosses downwards from top to bottom, and in the next, called Xu, it crosses upwards from botton to top.

The X and U straights are connected by arcs A1, A2, and A2~. Each superperiod may be written, for one of the rings:

$$SP = A1\ Xd\ A2\ U\ A2\sim\ Xu$$

For the other ring, the Xd and Xu are interchanged, every F-quadrupole is changed into a D-quadrupole, and conversely. The reason for this relationship is that in the IR's both beams pass through common quadrupoles, which have opposite foccussing on the two beams. This F-D reversal exists between adjacent quadrupoles of the two rings above and below each other, and, within each ring, between quadrupoles that have mirror-symmetric positions relative to the IP's.

The arcs A1, A2, and A2~ contain three substructures: sets C1, C2 of regular cells C, phase trombones T, T~ and dispersion suppressors D, D~. A T~ trombone is the antisymmetric reflection

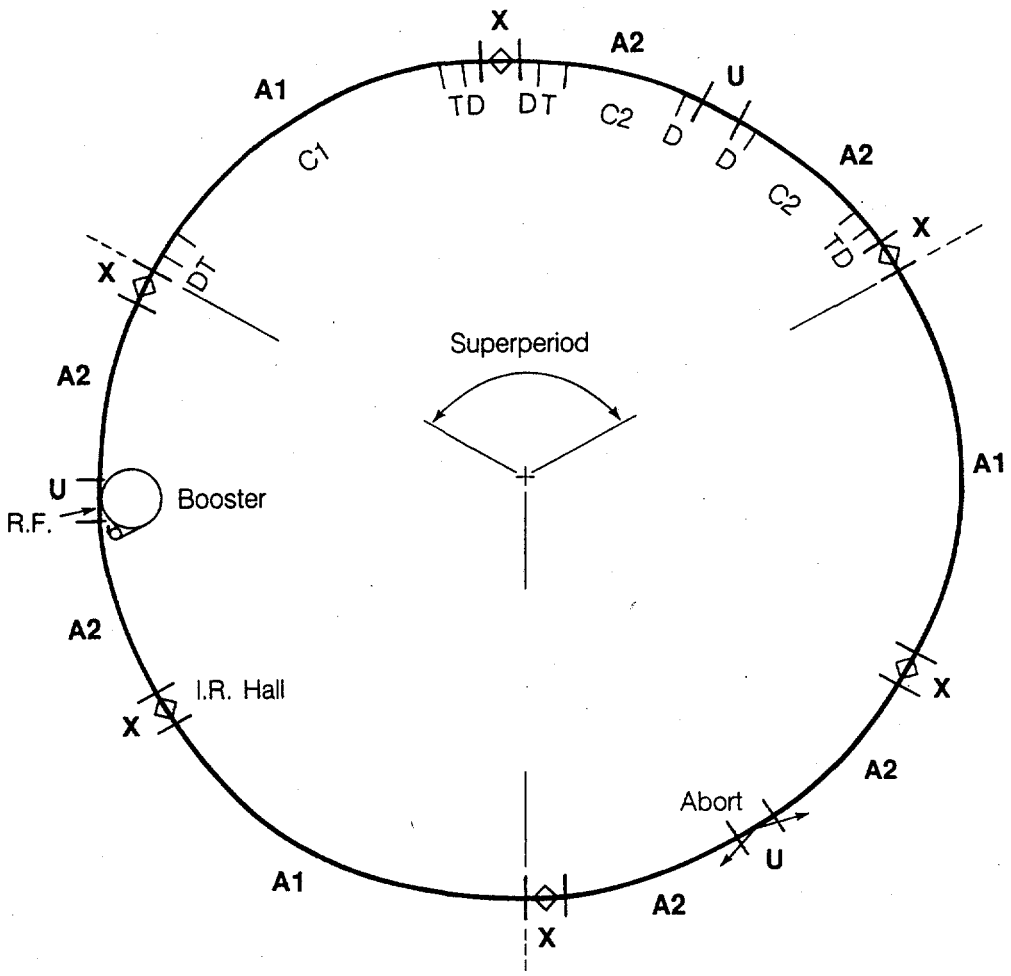

DISTRIBUTED LATTICE RLD1
6 TESLA, 60° CELLS

Circumference 97.2 km Arc Radius 13.5 km Distance between I.P.'s 16.2 km

Component	Type	Length (km)	Angle (deg)	Number Cells (equiv)
X	Exp't straight	1.3	0	6 1/2
U	Utility straight	1.5	0	7 1/2
A1	Arc	14.9	63.2	74 1/2
A2	Arc	6.7	28.4	33 1/2
C1	Reg. Cells	11.7	49.6	58 1/2
C2	Reg. Cells	4.5	19.1	22 1/2
T	Trombone	1.0	4.2	5
D	Suppressor	0.6	2.5	3

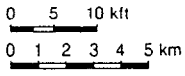

SSC CENTRAL DESIGN GROUP
DWG. NO. B1A025
10-15-85

Fig. 1

of a T , i.e., the structure is mirror-reflected and corresponding quadrupoles have equal and opposite gradients, and likewise with D ,D~. The three arcs may be written:

$$A1 = D\sim\ T\sim\ C1\ T\ D, \qquad A2 = D\sim\ T\sim\ C2\ D, \qquad A2\sim = D\sim\ C2\ T\ D$$

Note that in RLD1, the phase trombones are located toward the centers of the arcs, due to their bending, while in the test lattices, where the trombones have no bending or dispersion, they are located at the ends of the arcs.

2.1 Phase Relationships

In order to reduce the mismatch of the insertions for off-momentum particles two phase constraints were imposed . First, the phase advance between the two IP's separated by the long arc A1 was made to be an odd number of multiples of 90 degrees. This causes the contribution of the strong IR triplets to the half-integer structure resonance to vanish. Second, the same constraint was imposed on the superperiod phase advance, which places the tune as far as possible from these resonances.

3 COMPONENTS OF THE LATTICE

We now turn to a more detailed discussion of the five basic componenets of the lattice: C, T, D, X, and U.

3.1 Arc Cells C

The regular cells C in the arcs take up roughly 85% of the circumference. A diagram of a cell is shown schematically in Fig. 2. The 100 m long half-cells contain five 16.6 m dipoles, separated from each other by 0.9 m drifts, and centered between 5 m quadrupoles. The centering, a temporary artifact used to simplify the design, could be removed later at the cost of a small dispersion mismatch. In addition there are two 4.2 meter drift spaces in each half-cell for sextupoles, correction elements, pumps, etc.

Periodic strings of cells are assembled into the arc structures C1 and C2. Each has an odd number of half-cells -- C1 has 58 1/2 cells and C2 has 22 1/2 cells -- and each begins with a QF and ends with a QD quadrupole.

There are two types of regular cells: those that contain two chromaticity correcting sextupoles and those that have none. Those with sextupoles occurr in multiples of six, i.e., in integral numbers of betatron wavelengths. This strategy, which was also adopted for the test lattices, helps to reduce adverse chromatic and geometric effects.

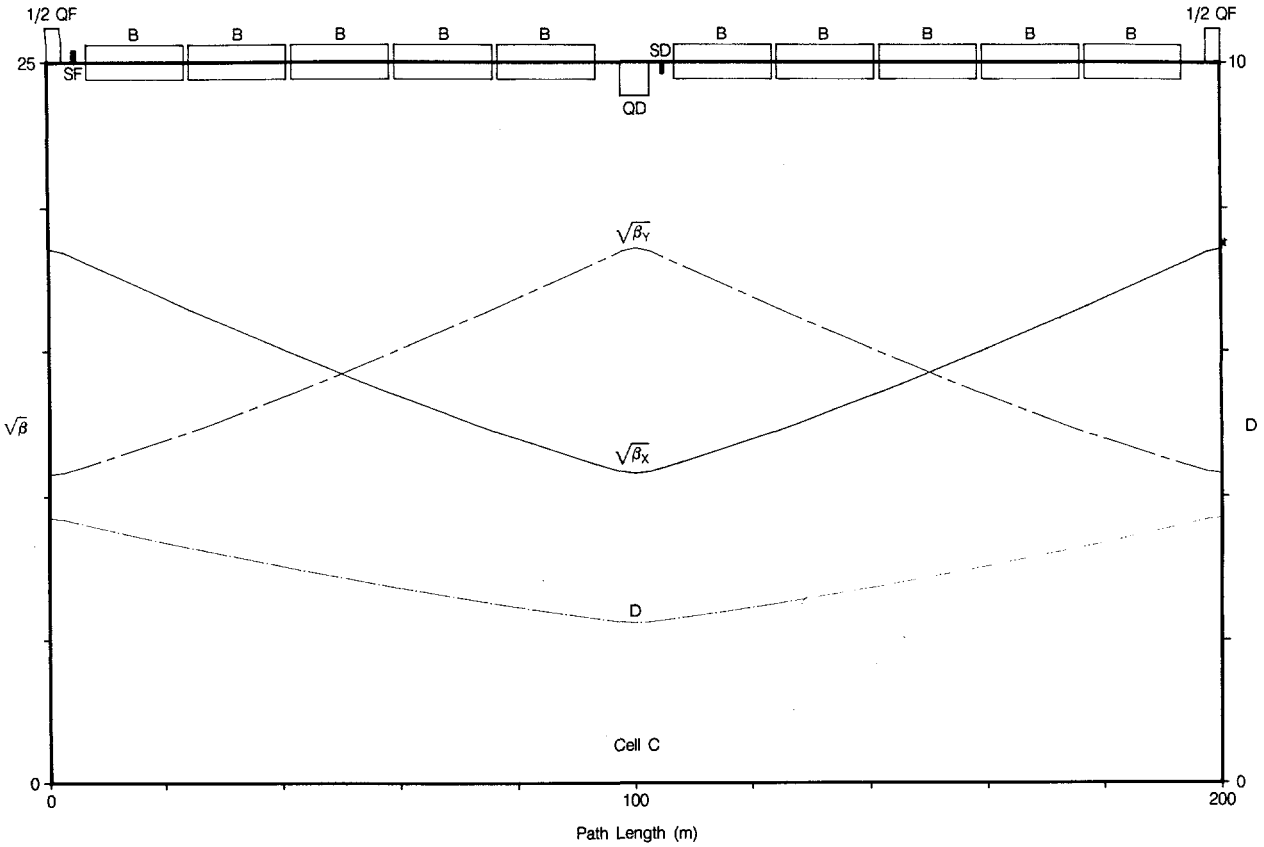

Fig. 2

XBL 859-12140

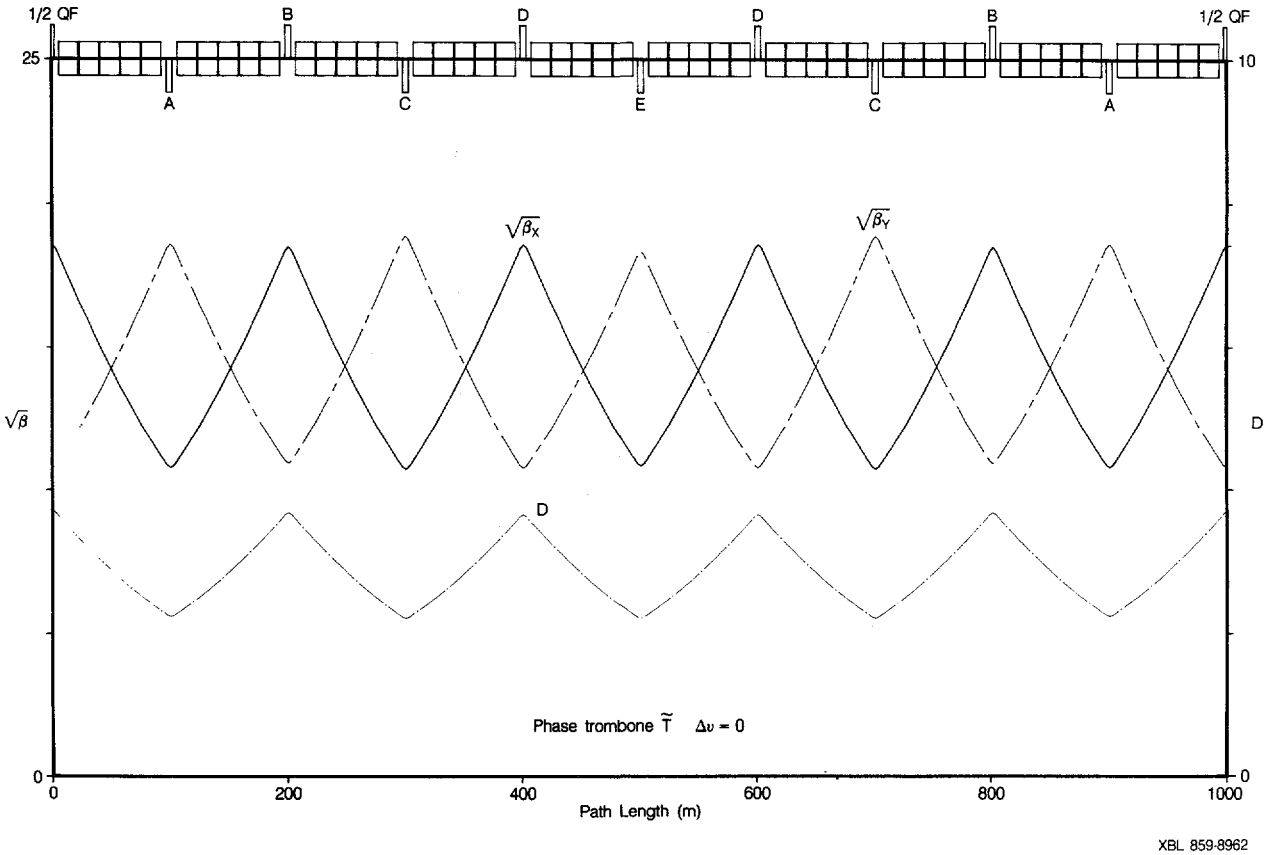

XBL 859-8962

Fig. 3

3.2 Phase Trombones T, T~

The colloquially named phase trombones are used to adjust the tunes of the ring, and to compensate for tune changes when the beta function at the IP is tuned to different values for injection and for experiments. The trombone used in RLD1, shown in Fig. 3, consists of five cells identical to regular ones, except that its nine quadrupoles are powered by five independent circuits, A-E, so as to match the cell beta functions and dispersion at both ends and to produce the desired phase advances. The quadrupole pattern, symmetric about the center of the trombone, produces a corresponding symmetry in the orbit functions. In Fig. 3, the quadrupoles have the normal cell gradients, so the tune contribution is that of five cells, or 5/6. In Figs. 4-5 they are adjusted to raise and lower the tunes respectively.

Each superperiod contains two T and two T~ trombones (Figs. 3-4 show a T~ and Fig. 5 shows a T). Since betax, betay and the gradients are interchanged between T and T~, a pair moves the tunes along the diagonal. In order to split the tunes, the circuits in T must be powered differently from those in T~; however it seems likely that the tune splitting needed will be small compared to diagonal tune changes, so that the corresponding currents in T and T~ will be nearly equal and opposite. Further details on this type of trombone is given in another paper in this report.

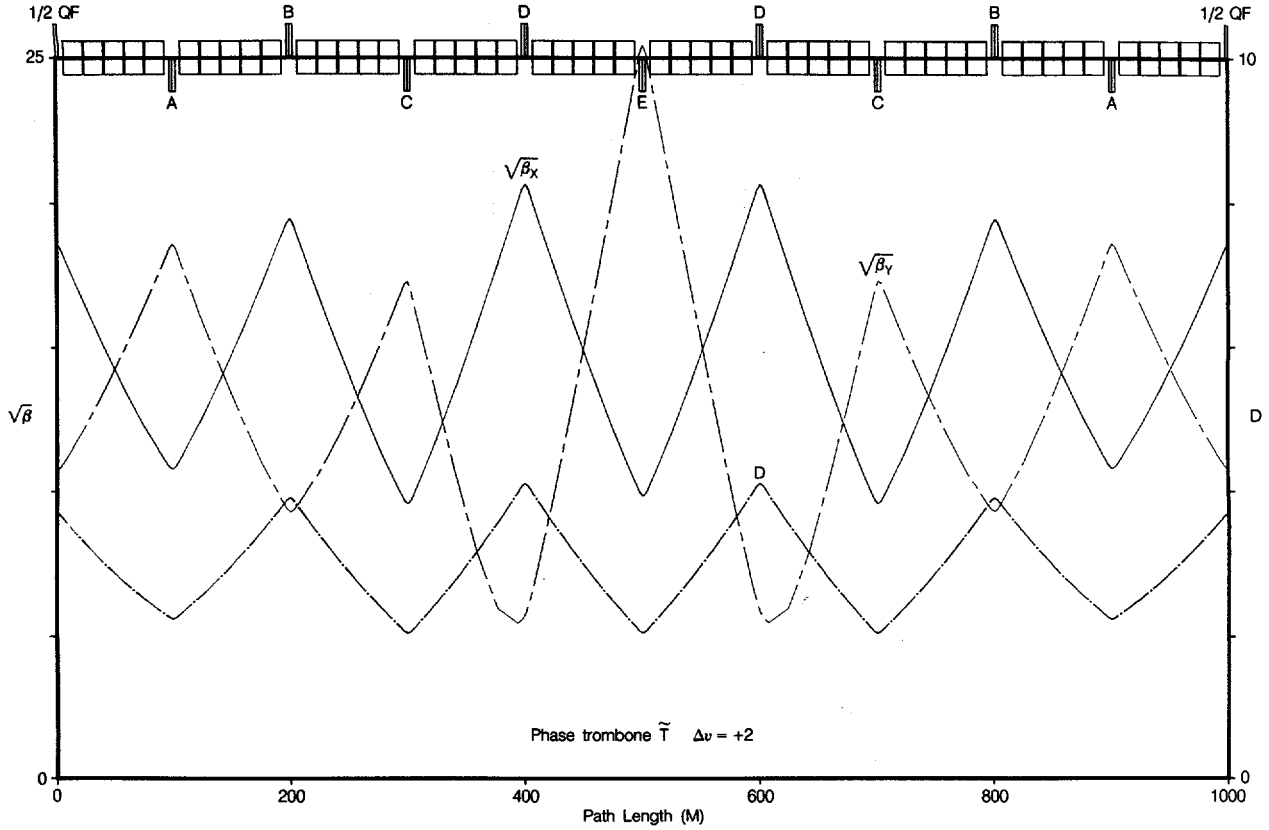
1/2 QF
B
D
D
B
1/2 QF
25
10
A
C
E
C
A
$\sqrt{\beta_x}$
$\sqrt{\beta_y}$
$\sqrt{\beta}$
D
D
Phase trombone $\tilde{T}$ $\Delta\nu = +2$
0
0
0
200
400
600
800
1000
Path Length (M)
XBL 8510-12155

Fig. 4

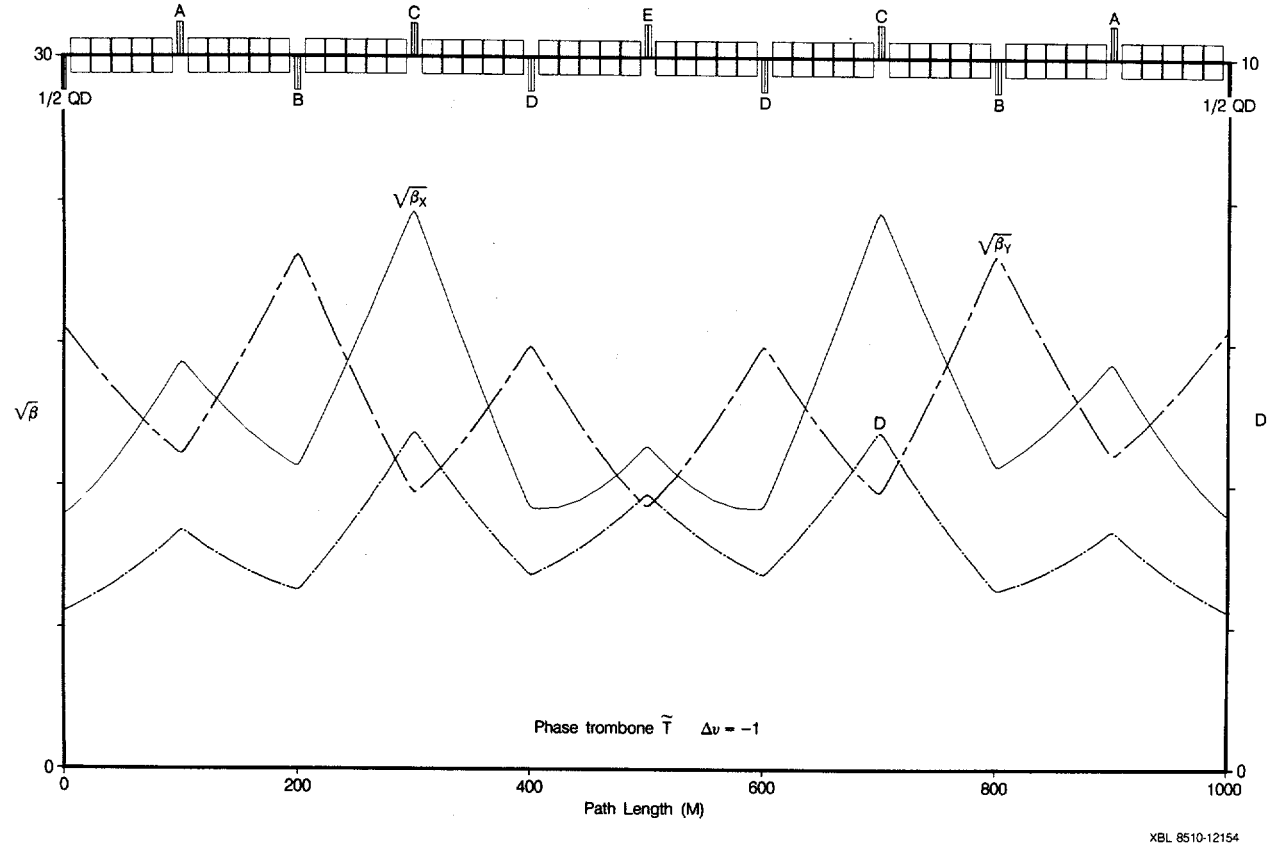
A
C
E
C
A
30
10
1/2 QD
B
D
D
B
1/2 QD
$\sqrt{\beta_x}$
$\sqrt{\beta_y}$
$\sqrt{\beta}$
D
D
Phase trombone $\tilde{T}$ $\Delta\nu = -1$
0
0
0
200
400
600
800
1000
Path Length (M)
XBL 8510-12154

Fig. 5

3.3 Dispersion Suppressors D, D~

The dispersion suppressors D and D~ are interfaces between the arc cells and the straight sections, whose function is to change the dispersion and its slope from the characteristic values at the match points in the cells to zero values in the straight sections X or U. Each straight section is bordered by a D suppressor upstream and a D~ suppressor downstream.

The suppressor design used in RLD1 consists of three cells identical to regular ones, except that five of the quadrupoles are powered by circuits G-K so as to match the cell dispersion and slope values at one end to zero values at the other. The matching is done in such a way that the two suppressors D and D~, which have equal and opposite gradients in the corresponding quadrupoles, respectively match the dispersion to the centers of QD and QF quadrupoles in the cells. A D-type suppressor is shown on the left side of Fig. 6, and a D~-type suppressor is shown on the right side of Fig. 7. Further details are given in a separate note in this report.

This type of suppressor, having the same dipole and quadrupole structure as the regular cells but irregular gradients, contrasts with the two cell, regular gradient, missing dipole suppressor used in previous designs. The advantage of the full bending suppressor is economy of tunnel length needed; those of the missing dipole type are that no new power supplies are needed and that the beta functions are the same as those in the regular cells.

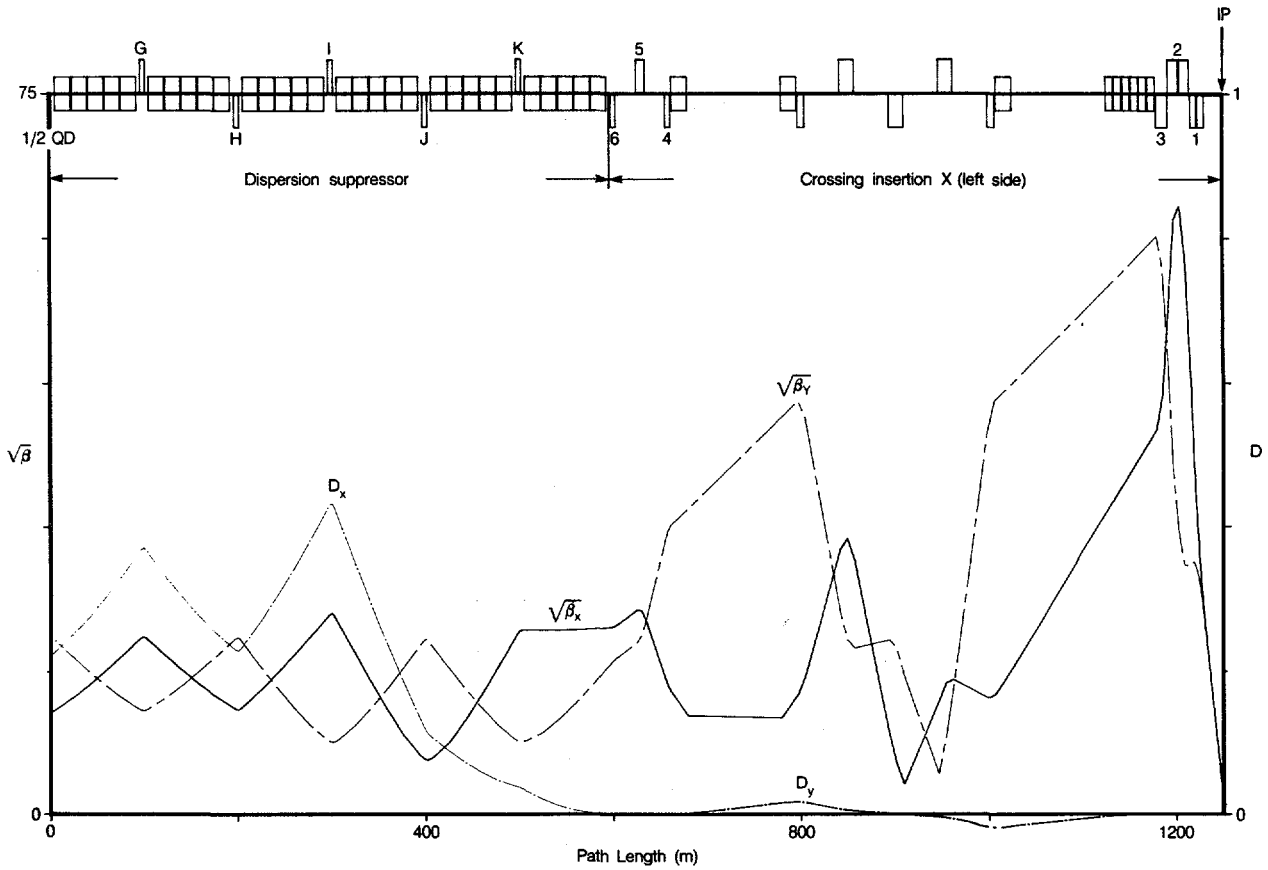
IP
G
I
K
5
2
75
1
1/2 QD
H
J
6
4
3
1
Dispersion suppressor
Crossing insertion X (left side)
$\sqrt{\beta}$
D
$\sqrt{\beta_Y}$
D_x
$\sqrt{\beta_x}$
D_y
0
0
400
800
1200
Path Length (m)
XBL 859-8963

Fig. 6

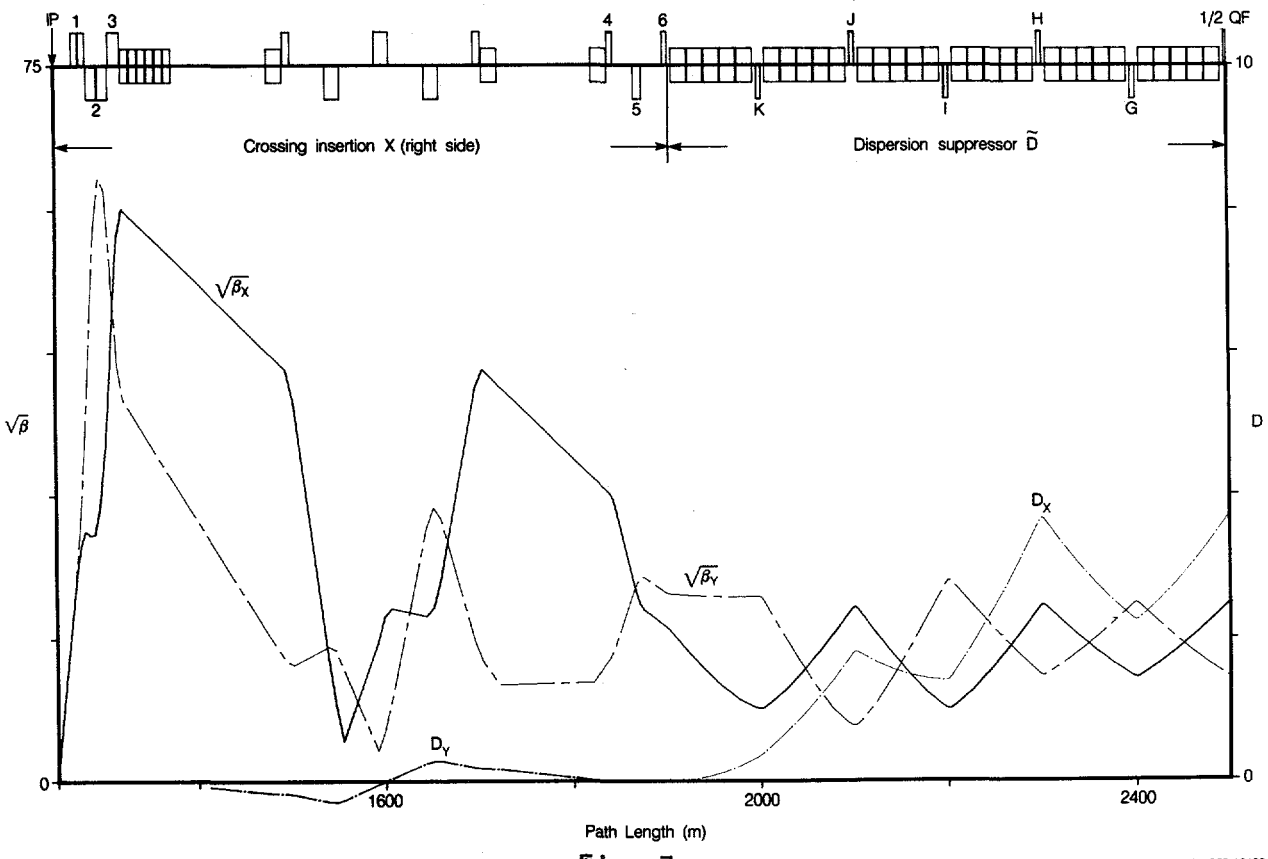
IP
1
3
4
6
J
H
1/2 QF
75
10
2
5
K
I
G
Crossing insertion X (right side)
Dispersion suppressor $\tilde{D}$
$\sqrt{\beta}$
D
$\sqrt{\beta_X}$
D_X
$\sqrt{\beta_Y}$
D_Y
0
0
1600
2000
2400
Path Length (m)
XBL 859-12139

Fig. 7

3.4 Crossing Insertions X

The two proton beams collide at the IP at the center of each crossing insertion. There are 20 meters of magnet-free space on either side of the IP for the detectors. The crossing insertion has two functions: to reduce the beta function values at the IP, beta*, to a low value (1 meter for experiments) in order to produce high luminosity, and to bend the orbits of the two beams from their separated, parallel state at the ends to a nearly colinear state in the interaction region, with a collision angle of only about 0.1 mrad.

The low beta values at the IP imply large values in the quadrupole triplets located along the colinear IR on either side. Just beyond these triplets the beams are separated by dipole splitter magnets and led into separated, parallel beamlines.

3.4.1 Beta Function Matching -

Fig. 6 shows the left half of X, called XL, preceded by the dispersion suppressor D; Fig. 7 shows the right half of X, called XR, followed by the dispersion suppressor D~. XR is the antisymmetric reflection of XL, i.e. XR = XL~. D suppresses the horizontal dispersion Dx and its slope, so that the gradients of its quadrupoles QFG,QDH,QFI,QDJ,QFK are determined by this function alone. The beamline (D XL) changes the beta functions from matched cell values at the center of a QD to a waist with values beta* at the IP, and this function is accomplished by the six quadrupoles

6QD,--,2QF,1QD (the vertically bending dipoles and the quadrupoles included among them are equivalent to a drift space, as will be explained below). The redundancy in this system is used to minimize the beta function peaks in the triplets, and to control the phase advances through the straight section.

Once the beta matching from a QD to the IP through the left side beamline (D XL) has been accomplished, the backwards matching of the interchanged betax and betay from a QF to the IP through the right side beamline (XL~ D~) is automatic, since the gradients of QF6,--,QD2,QF1 are equal and opposite to those of 6QD--1QD.

3.4.2 Vertical Beam Combining, Splitting And Dispersion Matching -

Fig. 8 shows the complete crossing straight section X, with a side view of the vertical beamlines of the two rings superimposed. At the extreme left and right ends of the figure the beamlines are separated vertically by 70 cm, a distance suitable for separate magnets in separate cryostats for the two beamlines. Moving towards the IP, the beams are brought to horizontally parallel sections, separated by 35 cm from each other, by pairs of vertical dipoles that bend through equal and opposite angles. A set of five quadrupoles is located along each of these sections between two dipoles. The seven magnets in each of the two beamlines along these sections are separate magnets in common cryostats. Following these sections the beams are brought to the collinear beamline containing the IR by additional pairs of equal and opposite vertical bends. Along the collinear region, the quadrupoles and

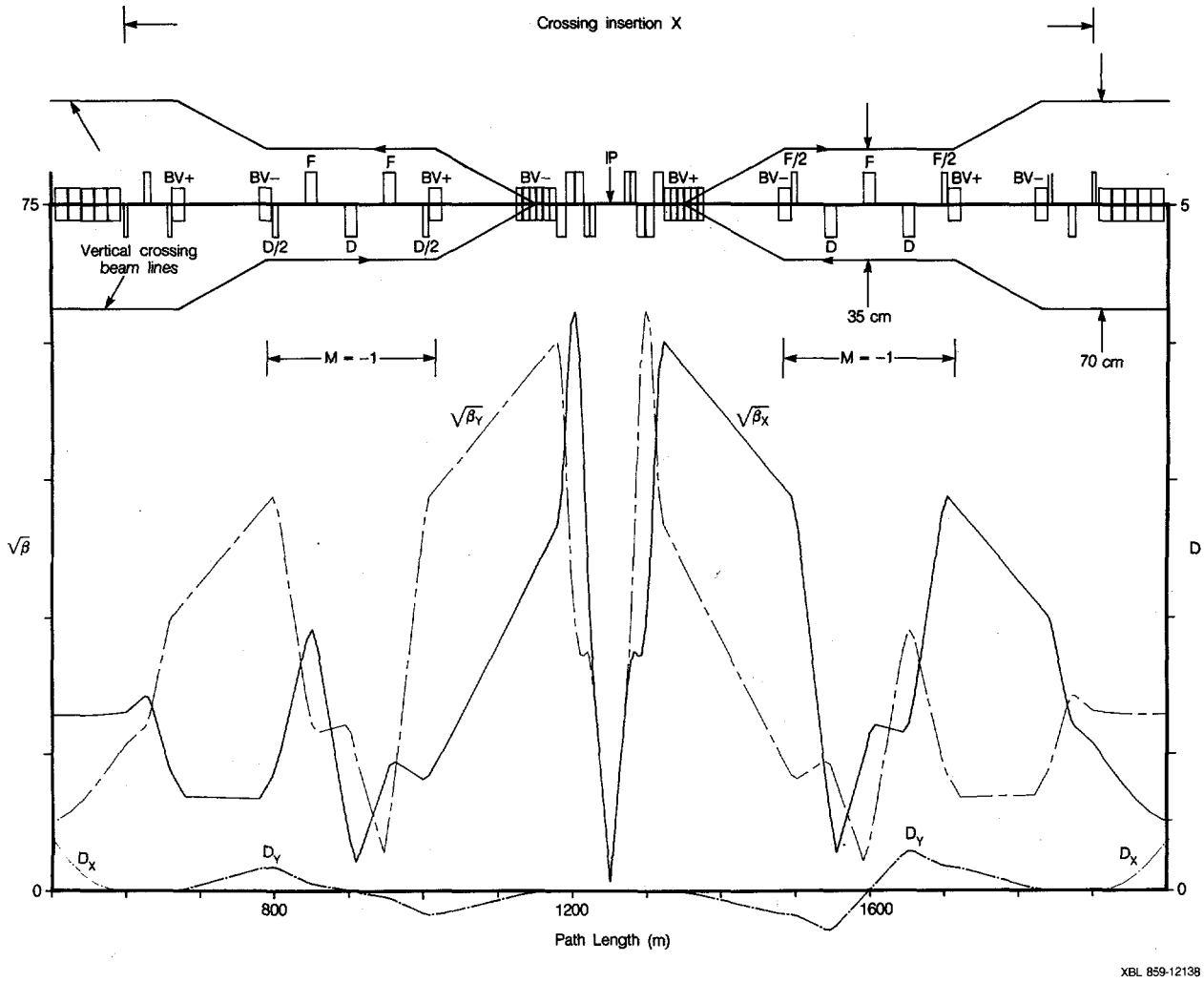
Crossing insertion X
BV+
BV−
F
F
BV+
BV−
IP
BV+
BV−
F/2
F
F/2
BV+
BV−
75
5
Vertical crossing beam lines
D/2
D
D/2
D
D
35 cm
70 cm
M = −1
M = −1
$\sqrt{\beta_Y}$
$\sqrt{\beta_X}$
$\sqrt{\beta}$
D
D_X
D_Y
D_Y
D_X
0
0
800
1200
1600
Path Length (m)
XBL 859-12138

Fig. 8

splitting dipoles are common to both beams.

The intermediate step between the cells and the collinear region matches the vertical dispersion caused by the vertical bending, by means of the set of five quadrupoles along the 35 cm separated section which comprise two 90 degree FODO cells. The transfer matrix for the two cells is M = -1, which reverses the vertical dispersion and exactly cancels the effects of the vertical bends. Moreover the section is invisible for the beta function matching between the cells and the IP.

3.5 Utility Insertion U

A utility insertion U and its dispersion suppressors D and D~ are shown in Fig. 9. These insertions are used for the injection, beam abort and radiofrequency acceleration systems. The vertical dipoles in the center produce doglegs needed for the beam abort and injection systems; they produce a vertical bump in the orbits, which is mirrored by the vertical dispersion plotted beneath them. Since there is no quadrupole focussing included in these doglegs, they do not effect the optics. The RF system is to be located in one of the end regions, between a QP and a QM. The 980 meter quadrupole free space between QFN and QDN allows long drifts between kicker and septum magnets for injection and extraction, and good clearance between the extracted beam and the superconducting magnets downstream.

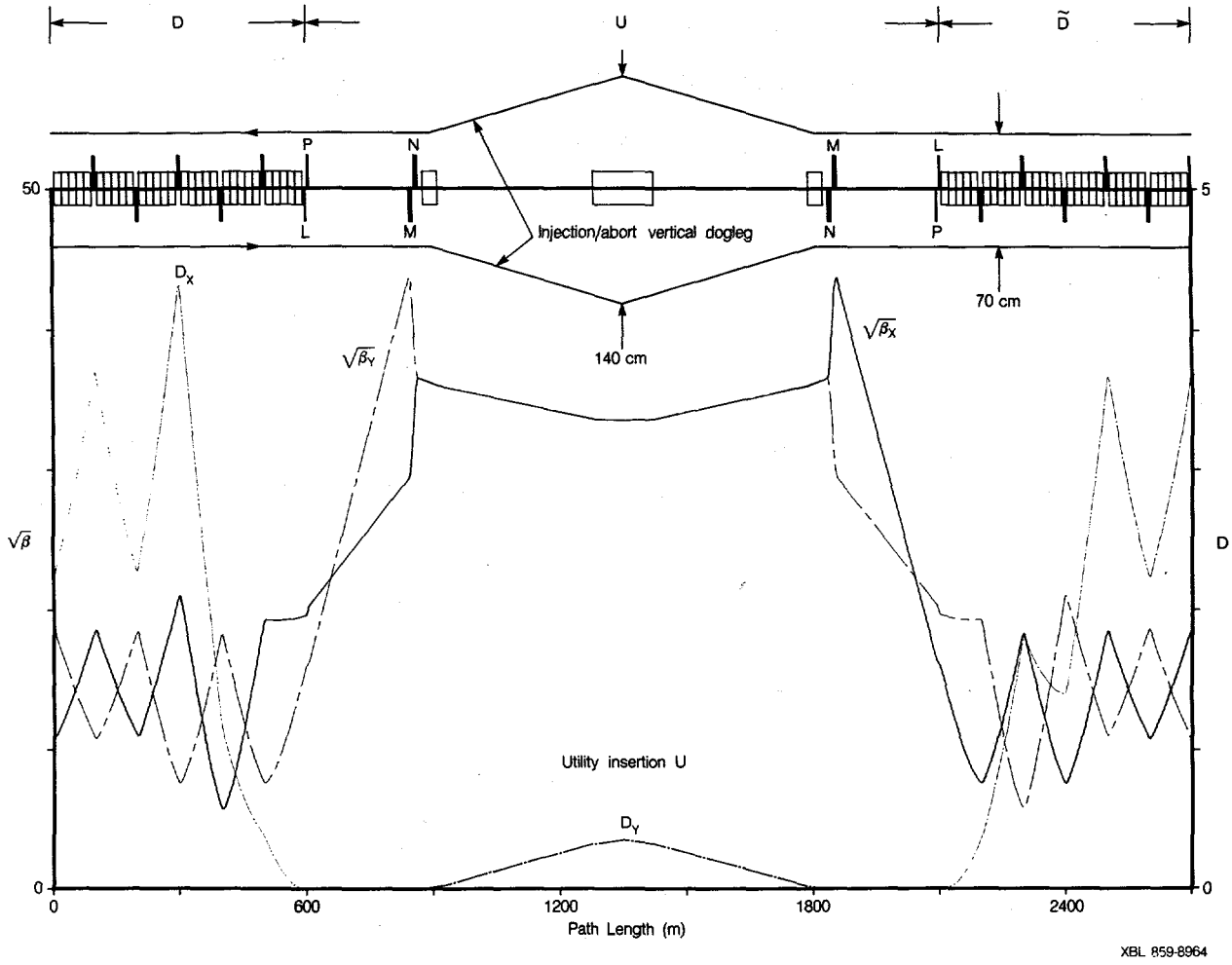
D
U
D̃
P
N
M
L
50
5
L
M
N
P
Injection/abort vertical dogleg
70 cm
140 cm
D_x
$\sqrt{\beta_y}$
$\sqrt{\beta_x}$
$\sqrt{\beta}$
D
Utility insertion U
D_y
0
0
600
1200
1800
2400
Path Length (m)
XBL 859-8964

Fig. 9

The design of the utility is antisymmetric about its center. The four quadrupole circuits that power QDL, QFP, QDM and QFN on one side, and their opposite partners QFL, QDP, QFM, and QDN on the other, match the beta functions from the center of a QD in a cell on the left, through the beamline (D U D~), to the center of a QF in a cell on the right. Of the four variables, two are needed to match the betas and alphas, one to produce a waist at the center of U, and one to achieve a desirable value of the phase advance. The waist at the center serves to reduce the maximum beta function values.

4 ACKNOWLEGEMENTS

We wish to thank the other participants in the Realistic Lattice Workshop held at the CDG in LBL on May 29-June 4 1985 for many stimulating discussions and useful ideas that contributed to the design discussed in this paper.

5 REFERENCES

[1] E.D. Courant, D.R.Douglas, A.A. Garren, and D.E. Johnson, "SSC Test Lattice Designs", Proceedings of the 1985 Particle Accelerator Conference, Vancouver, May 1985, page 1669.

[2] Superconducting Super Collider, Reference Designs Study for U.S. Depar of Energy, May 8, 1984.

6 APPENDICES

Table I --- Dimensions and Orbit Parameters of the RLD1 Lattice

Phase deg	Field tesla	Gradient tesla/m	Lcell m	Lslot m	Ldip m	Lquad m	Lcorr m	Rho km
60	5.948	135.7	200	86.6	16.6	5.0	4.2	11.215

L(C) km	L(X) km	L(U) km	L(D) km	L(T) km	L(A1) km	L(A2) km	L(IR) m	Theta(cell) mrad
0.2	1.3	1.5	0.6	1.0	14.2	6.7	40	14.8014

Circum. km	Tune	Beta(cell) m	D(cell) m	Beta(max) m	D(max) m	Chromat-icity
97.2	86.28	345	3.69	4009	4.31	-227

Table II Chromatic Properties

dp/p o/oo	Nux-86	Nuy-86	Betax* m	Betay* m	Betxmax m	Betymax m	Betxarc m	Betyarc m
-2	.2486	.2444	1.268	1.268	3365	3363	533	569
-1	.2741	.2716	1.099	1.100	3725	3722	410	434
0	.2805	.2786	1.000	1.000	4009	4008	345	345
1	.2770	.2747	.9541	.9550	4231	4232	452	454
2	.2734	.2692	.9559	.9611	4387	4386	596	597

Table III
SYNCH RUN RLD1 Realistic Lattice D1 --- 6 T, 133 T/m, 60 degree cells

E.D. Courant and A.A. Garren

100 meter half-cells, 86.6 m dipole slot centered with five 16.6 m dipoles, 5.0 m quadrupole, 4.2 m spoolpiece drifts, 0.9 m dipole separation drifts.

Full bending three cell dispersion suppressor, full bending five cell phase trombone.

Six 1300 meter crossing straights with a vertical beam separating section containing a step with two 90 degree cells for vertical dispersion matching beam splitter consists of six conventional dipoles.

Three 1500 meter utility straights with superconducting quadrupoles three superperiods, crossings equally spaced and all with df sequence

Tune 86.3

```
    Parameters:
***  BRHO   =     0   0 //  66712.8
***  B0     =     0   0 //  5.94844232
***  RHO    =     0   0 //  11215.1714
***  RHI    =     0   0 //  1.        /        RHO
***  B*     =     0   0 //  1.0
***  MUX    =     0   0 //  .166666667
***  MUY    =     0   0 //  .166666667
***  BR     =     0   0 //  1.0
***  KF     =     0   0 //   .00203404
***  KD     =     0   0 //  -.00203416
***  KSF    =     0   0 //   .01459838
***  KSD    =     0   0 //  -.02340243
***  LB     =     0   0 //  16.6
***  LQ     =     0   0 //  2.5
***  LH     =     0   0 //  100.0

    Drift Spaces:
***  O      DRF   0   0 //  0.9
***  OO     DRF   0   0 //  2.1
***  OOC    DRF   0   0 //  4.2
***  OOO    DRF   0   0 //  95.0

    Markers
***  #QF    DRF   0   0 //
***  #QD    DRF   0   0 //

    Dipole:
***  B      MAG   0   0 //  LB        0.        BR        RHI

    Sextupoles
***  SF     SXTP  0   0 //  0.        KSF       1.
***  SD     SXTP  0   0 //  0.        KSD       1.
```

```
      --                  CELLS
***   .BB     BML    0    0 //  B     O     B     O     B     O     B     O     B
***   .FD     BML    0    0 //  #QF   QF    OO    SF    OO    .BB   OOC   QD
***   .DF     BML    0    0 //  #QD   QD    OO    SD    OO    .BB   OOC   QF
***   .C      BML    0    0 //  .FD   .DF
***   QF      MAG    0    0 //  LQ          KF          BR
***   QD      MAG    0    0 //  LQ          KD          BR
***   CELL    BEST   0    1 //  .C
```

POS		S (M)	NUX	NUY	BETAX (M)	BETAY (M)	XEQ (M)	YEQ (M)	ZEQ (M)	ALPHAX	ALPHAY	DXEQ	DYEQ
0		0.0000	0.00000	0.00000	344.94437	115.95226	3.69552	0.00000	0.00000	0.00000	0.00000	0.00000	0.00000
1	#QF	0.0000	0.00000	0.00000	344.94437	115.95226	3.69552	0.00000	0.00000	0.00000	0.00000	0.00000	0.00000
2	QF	2.5000	0.00116	0.00342	340.59577	117.48671	3.67205	0.00000	0.00000	1.73206	-0.61638	-0.01875	0.00000
3	OO	4.6000	0.00215	0.00623	333.37290	120.12732	3.63267	0.00000	0.00000	1.70740	-0.64105	-0.01875	0.00000
4	SF	4.6000	0.00215	0.00623	333.37290	120.12732	3.63267	0.00000	0.00000	1.70740	-0.64105	-0.01875	0.00000
5	OO	6.7000	0.00316	0.00898	326.25362	122.87152	3.59329	0.00000	0.00000	1.68274	-0.66571	-0.01875	0.00000
6	B	23.3000	0.01201	0.02861	273.62238	148.20975	3.29429	0.00000	0.00509	1.48782	-0.86069	-0.01727	0.00000
7	O	24.2000	0.01254	0.02957	270.95383	149.76850	3.27874	0.00000	0.00509	1.47725	-0.87126	-0.01727	0.00000
8	B	40.8000	0.02324	0.04560	225.14504	181.93081	3.00430	0.00000	0.00974	1.28232	-1.06623	-0.01579	0.00000
9	O	41.7000	0.02388	0.04639	222.84639	183.85954	2.99008	0.00000	0.00974	1.27175	-1.07680	-0.01579	0.00000
10	B	58.3000	0.03695	0.05945	183.86047	222.84593	2.74020	0.00000	0.01398	1.07680	-1.27178	-0.01431	0.00000
11	O	59.2000	0.03773	0.06009	181.93174	225.14463	2.72732	0.00000	0.01398	1.06623	-1.28235	-0.01431	0.00000
12	B	75.8000	0.05376	0.07080	149.76906	270.95509	2.50201	0.00000	0.01785	0.87128	-1.47732	-0.01283	0.00000
13	O	76.7000	0.05472	0.07132	148.21027	273.62378	2.49046	0.00000	0.01785	0.86071	-1.48789	-0.01283	0.00000
14	B	93.3000	0.07435	0.08017	122.87112	326.25830	2.28971	0.00000	0.02138	0.66575	-1.68286	-0.01135	0.00000
15	OOC	97.5000	0.07992	0.08218	117.48605	340.60155	2.24202	0.00000	0.02138	0.61641	-1.73219	-0.01135	0.00000
16	QD	100.0000	0.08333	0.08333	115.95151	344.95048	2.22784	0.00000	0.02138	0.00000	0.00000	0.00000	0.00000
17	#QD	100.0000	0.08333	0.08333	115.95151	344.95048	2.22784	0.00000	0.02138	0.00000	0.00000	0.00000	0.00000
18	QD	102.5000	0.08675	0.08449	117.48605	340.60155	2.24202	0.00000	0.02138	-0.61641	1.73219	0.01135	0.00000
19	OO	104.6000	0.08956	0.08548	120.12679	333.37813	2.26586	0.00000	0.02138	-0.64108	1.70753	0.01135	0.00000
20	SD	104.6000	0.08956	0.08548	120.12679	333.37813	2.26586	0.00000	0.02138	-0.64108	1.70753	0.01135	0.00000
21	OO	106.7000	0.09231	0.08650	122.87112	326.25830	2.28971	0.00000	0.02138	-0.66575	1.68286	0.01135	0.00000
22	B	123.3000	0.11194	0.09534	148.21027	273.62378	2.49046	0.00000	0.02492	-0.86071	1.48789	0.01283	0.00000
23	O	124.2000	0.11290	0.09587	149.76906	270.95509	2.50201	0.00000	0.02492	-0.87128	1.47732	0.01283	0.00000
24	B	140.8000	0.12894	0.10657	181.93174	225.14463	2.72732	0.00000	0.02878	-1.06623	1.28235	0.01431	0.00000
25	O	141.7000	0.12972	0.10721	183.86047	222.84593	2.74020	0.00000	0.02878	-1.07680	1.27178	0.01431	0.00000
26	B	158.3000	0.14279	0.12028	222.84639	183.85954	2.99008	0.00000	0.03302	-1.27175	1.07680	0.01579	0.00000
27	O	159.2000	0.14343	0.12106	225.14504	181.93081	3.00430	0.00000	0.03302	-1.28232	1.06623	0.01579	0.00000
28	B	175.8000	0.15413	0.13710	270.95383	149.76850	3.27874	0.00000	0.03767	-1.47725	0.87126	0.01727	0.00000
29	O	176.7000	0.15466	0.13806	273.62238	148.20975	3.29429	0.00000	0.03767	-1.48782	0.86069	0.01727	0.00000
30	B	193.3000	0.16350	0.15769	326.25362	122.87152	3.59329	0.00000	0.04276	-1.68274	0.66571	0.01875	0.00000
31	OOC	197.5000	0.16551	0.16325	340.59577	117.48671	3.67205	0.00000	0.04276	-1.73206	0.61638	0.01875	0.00000
32	QF	200.0000	0.16667	0.16667	344.94437	115.95226	3.69552	0.00000	0.04276	0.00000	0.00000	0.00000	0.00000

```
CIRCUMFERENCE =   200.0000 M          THETX =   0.01480138 RAD      NUX =    0.16667      DNUX/(DP/P) =    0.71629
      RADIUS =    31.8310 M          THETY =   0.00000000 RAD      NUY =    0.16667      DNUY/(DP/P) =    0.71612
(DS/S)/(DP/P)=  0.0002138             TGAM=(  68.38971,   0.00000)

MAXIMA    --- BETX(   32) =   344.94437    BETY(   17) =   344.95048     XEQ(    1) =     3.69552     YEQ(   32) =     0.00000
MINIMA    --- BETX(   17) =   115.95151    BETY(    1) =   115.95226     XEQ(   17) =     2.22784     YEQ(   32) =     0.00000
```

```
***   CD      MMM    0    0 //  .DF   .FD
```

```
      --              DISPERSION SUPPRESSORS

***   .OBO    BML    0    0 //  OOC  .BB  OOC
***   OBO     MMM    0    0 //  .OBO

***   $DSF    BML    0    0 //  QD   OBO  QFG  OBO  QDH  OBO  QFI  OBO  QDJ  OBO  QFK  OBO
***   $DSD    BML    0    0 //  QF   OBO  GQD  OBO  HQF  OBO  IQD  OBO  JQF  OBO  KQD  OBO

***   DSD$    BML   -1    0 //  $DSD
***   $SUP    BML    0    0 //  $DSF DSD$

***   KGG     =      0    0 //   .00201022
***   KHH     =      0    0 //  -.00247162
***   KII     =      0    0 //   .00280844
***   KJJ     =      0    0 //  -.00290762
***   KKK     =      0    0 //   .00181001
***   LQQ     =      0    0 //  5.0


***   SRDS    SUB    0    0 //
.....................................................................................................................
***   QFG     MAG    0    0 //  LQQ        KGG        BR
***   QDH     MAG    0    0 //  LQQ        KHH        BR
***   QFI     MAG    0    0 //  LQQ        KII        BR
***   QDJ     MAG    0    0 //  LQQ        KJJ        BR
***   QFK     MAG    0    0 //  LQQ        KKK        BR
***   GQD     MAG    0    0 //  LQQ        -KGG       BR
***   HQF     MAG    0    0 //  LQQ        -KHH       BR
***   IQD     MAG    0    0 //  LQQ        -KII       BR
***   JQF     MAG    0    0 //  LQQ        -KJJ       BR
***   KQD     MAG    0    0 //  LQQ        -KKK       BR
***           END    0    0 //
.....................................................................................................................


***           CALL   0    0 //  SRDS

      ---             Lumped suppressors:

***   *DSF    MMM    0    0 //  $DSF
***   DSD*    MMM    0    0 //  DSD$
```

```
      ---               Track through both suppressors.  Note: only the dispersion
                        is valid for the second suppressor DSD (positions 13-24)

 ***   TDS    TRKB        //  $SUP CD
  *                       //
  *                       //
```

POS		S	QX	BX	AX	GX	X	DX	QY	BY	AY	GY	Y	DY
0		0.00000	0.00000	115.95151	0.0000	0.00862	2.22784	0.00000	0.00000	344.95048	0.0000	0.00290	0.00000	0.00000
1	QD	2.50000	0.00342	117.48605	-0.6164	0.01175	2.24202	0.01135	0.00116	340.60155	1.7322	0.01175	0.00000	0.00000
2	OBO	97.50000	0.08218	340.59577	-1.7321	0.01174	3.67205	0.01875	0.07992	117.48671	0.6164	0.01175	0.00000	0.00000
3	QFG	102.50000	0.08449	340.79862	1.6922	0.01134	3.67315	-0.01832	0.08675	117.41681	-0.6022	0.01160	0.00000	0.00000
4	OBO	197.50000	0.16177	121.58730	0.6153	0.01134	2.28449	-0.01092	0.16605	336.56253	-1.7046	0.01160	0.00000	0.00000
5	QDH	202.50000	0.16834	123.13632	-0.9314	0.01517	2.30028	0.01727	0.16840	332.82791	2.4361	0.02084	0.00000	0.00000
6	OBO	297.50000	0.23550	436.96722	-2.3720	0.01516	4.29204	0.02467	0.28822	58.00751	0.4567	0.02084	0.00000	0.00000
7	QFI	302.50000	0.23731	429.99409	3.7338	0.03475	4.26414	-0.03576	0.30213	57.92547	-0.4399	0.02061	0.00000	0.00000
8	OBO	397.50000	0.38067	34.16464	0.4327	0.03475	1.21812	-0.02836	0.42327	327.47630	-2.3974	0.02061	0.00000	0.00000
9	QDJ	402.50000	0.40473	33.05890	-0.2062	0.03154	1.11912	-0.01148	0.42567	327.57512	2.3781	0.02032	0.00000	0.00000
10	OBO	497.50000	0.57418	356.84386	-3.2020	0.03153	0.38037	-0.00408	0.54529	59.09484	0.4480	0.02032	0.00000	0.00000
11	QFK	502.50000	0.57635	372.77751	0.0634	0.00269	0.35157	-0.00740	0.55904	57.70912	-0.1667	0.01781	0.00000	0.00000
12	OBO	597.50000	0.61669	385.00881	-0.1922	0.00269	0.00003	0.00000	0.70419	250.10432	-1.8586	0.01781	0.00000	0.00000
13	OBO	692.50000	0.65351	445.80437	-0.4478	0.00269	0.35155	0.00740	0.73906	763.96180	-3.5505	0.01781	0.00000	0.00000
14	KQD	697.50000	0.65526	470.96545	-4.6601	0.04823	0.39681	0.01077	0.74009	764.79244	3.3869	0.01631	0.00000	0.00000
15	OBO	792.50000	0.67175	1791.63191	-9.2413	0.04823	1.77186	0.01817	0.77371	268.45302	1.8378	0.01631	0.00000	0.00000
16	JQF	797.50000	0.67219	1753.69883	16.6432	0.15852	1.79763	-0.00793	0.77670	269.58069	-2.0687	0.01958	0.00000	0.00000
17	OBO	892.50000	0.75229	22.12461	1.5835	0.15853	1.39567	-0.00053	0.80870	839.39646	-3.9293	0.01958	0.00000	0.00000
18	IQD	897.50000	0.80440	11.18498	0.6554	0.12781	1.44226	0.01928	0.80965	819.78589	7.7592	0.07466	0.00000	0.00000
19	OBO	992.50000	1.13291	1040.11646	-11.4860	0.12780	3.62517	0.02668	0.94569	19.34402	0.6665	0.07466	0.00000	0.00000
20	HQF	997.50000	1.13365	1090.47678	1.6223	0.00333	3.64576	-0.01848	0.99276	15.52639	0.1127	0.06522	0.00000	0.00000
21	OBO	1092.50000	1.14974	812.24442	1.3064	0.00333	2.24133	-0.01108	1.23469	582.76550	-6.0836	0.06522	0.00000	0.00000
22	GQD	1097.50000	1.15071	840.33098	-7.0175	0.05979	2.24200	0.01135	1.23601	614.38752	-0.1345	0.00166	0.00000	0.00000
23	OBO	1192.50000	1.16073	2713.16576	-12.6961	0.05978	3.67201	0.01875	1.25994	654.89369	-0.2919	0.00166	0.00000	0.00000
24	QF	1195.00000	1.16088	2742.13595	1.1572	0.00085	3.69547	0.00000	1.26054	664.73684	-3.6620	0.02168	0.00000	0.00000

```
      ---               Quadrupoles split and flags added at their centers
                        in order to get betas of complete ring at those locations:

 ***   LQQ    =       0    0 //  2.5
 ***          CALL    0    0 //  SRDS

 ***   .DSF   BML     0    0 //  #QD  QD   .OBO QFG  #QFG QFG  .OBO QDH  #QDH QDH  .OBO
  *                             //  QFI  #QFI QFI  .OBO QDJ  #QDJ QDJ  .OBO QFK  #QFK QFK  .OBO

 ***   .DSD   BML     0    0 //  QF   .OBO GQD  #GQD GQD  .OBO HQF  #HQF HQF  .OBO
  *                             //  IQD  #IQD IQD  .OBO JQF  #JQF JQF  .OBO KQD  #KQD KQD  .OBO
 ***   DSD.   BML    -1    0 //  .DSD
 ***   DSF.   BML    -1    0 //  .DSF

 ***   #QFG   DRF     0    0 //
 ***   #QDH   DRF     0    0 //
 ***   #QFI   DRF     0    0 //
 ***   #QDJ   DRF     0    0 //
 ***   #QFK   DRF     0    0 //
 ***   #GQD   DRF     0    0 //
 ***   #HQF   DRF     0    0 //
 ***   #IQD   DRF     0    0 //
 ***   #JQF   DRF     0    0 //
 ***   #KQD   DRF     0    0 //
```

```
      --              UTILITIY INSERTION

***   .UDF    BML    0   0 //  QDL  LUD  QFP  LUE  QDM  LUD  QFN  LUC
***   .UFD    BML    0   0 //  QFL  LUD  QDP  LUE  QFM  LUD  QDN  LUC

***   UDF.    BML   -1   0 //  .UDF
***   UFD.    BML   -1   0 //  .UFD

***   .UTD    BML    0   0 //  .UDF #CEN UFD.

***   $UTL    BML    0   0 //  *DSF .UTD DSD*

***   LQL     =      0   0 //  2.5
***   LQP     =      0   0 //  2.5
***   LQM     =      0   0 //  8.0
***   LQN     =      0   0 //  8.0
***   KL      =      0   0 //   .00179234
***   KP      =      0   0 //   .00139626
***   KM      =      0   0 //   .00203964
***   KN      =      0   0 //   .00192118
***   LUD     DRF    0   0 //  5.0
***   LUC     DRF    0   0 //  486.0
***   LUE     DRF    0   0 //  235.5
***   #CEN    DRF    0   0 //


***   SUTL    SUB    0   0 //
.....................................................................................................................
***   QFL     MAG    0   0 //  LQL       KL        1.
***   QFP     MAG    0   0 //  LQP       KP        1.
***   QFM     MAG    0   0 //  LQM       KM        1.
***   QFN     MAG    0   0 //  LQN       KN        1.
***   QDL     MAG    0   0 //  LQL       -KL       1.
***   QDP     MAG    0   0 //  LQP       -KP       1.
***   QDM     MAG    0   0 //  LQM       -KM       1.
***   QDN     MAG    0   0 //  LQN       -KN       1.
***           END    0   0 //
.....................................................................................................................


***           CALL   0   0 //  SUTL
```

```
      ---               Track through utility insertion, with lumped suppressors:

 ***   TUTL   TRKB        //  $UTL CD
  *                       //
  *                       //
```

POS		S	QX	BX	AX	GX	X	DX	QY	BY	AY	GY	Y	DY
0		0.00000	0.00000	115.95151	0.0000	0.00862	2.22784	0.00000	0.00000	344.95048	0.0000	0.00290	0.00000	0.00000
1	*DSF	597.50000	0.61669	385.00881	-0.1922	0.00269	0.00003	0.00000	0.70419	250.10432	-1.8586	0.01781	0.00000	0.00000
2	QDL	600.00000	0.61772	390.32287	-1.9414	0.01222	0.00003	0.00000	0.70576	256.64751	-0.7489	0.00608	0.00000	0.00000
3	LUD	605.00000	0.61971	410.04200	-2.0025	0.01222	0.00003	0.00000	0.70881	264.28894	-0.7793	0.00608	0.00000	0.00000
4	QFP	607.50000	0.62067	416.50440	-0.5750	0.00319	0.00003	0.00000	0.71030	270.55958	-1.7362	0.01484	0.00000	0.00000
5	LUE	843.00000	0.68486	864.49636	-1.3273	0.00319	0.00001	0.00000	0.763411911.19295		-5.2304	0.01484	0.00000	0.00000
6	QDM	851.00000	0.686251005.68938		-17.0832	0.29118	0.00000	0.00000	0.764091749.88029		24.5094	0.34386	0.00000	0.00000
7	LUD	856.00000	0.686981183.80038		-18.5390	0.29118	0.00000	0.00000	0.764581513.38312		22.7901	0.34386	0.00000	0.00000
8	QFN	864.00000	0.687971334.89948		0.4322	0.00089	0.00000	0.00000	0.765491334.86360		0.4320	0.00089	0.00000	0.00000
9	LUC	1350.00000	0.752881124.80799		0.0001	0.00089	-0.00004	0.00000	0.830401124.89617		0.0000	0.00089	0.00000	0.00000
10	#CEN	1350.00000	0.752881124.80799		0.0001	0.00089	-0.00004	0.00000	0.830401124.89617		0.0000	0.00089	0.00000	0.00000
11	LUC	1836.00000	0.817791334.69219		-0.4320	0.00089	-0.00008	0.00000	0.895301334.87149		-0.4320	0.00089	0.00000	0.00000
12	QDN	1844.00000	0.818711513.18856		-22.7871	0.34381	-0.00008	0.00000	0.896301183.77368		18.5388	0.29118	0.00000	0.00000
13	LUD	1849.00000	0.819201749.65521		-24.5062	0.34381	-0.00009	0.00000	0.897031005.66553		17.0829	0.29118	0.00000	0.00000
14	QFM	1857.00000	0.819881910.94694		5.2297	0.01484	-0.00009	0.00000	0.89842	864.47394	1.3274	0.00320	0.00000	0.00000
15	LUE	2092.50000	0.87299	270.53058	1.7359	0.01484	-0.00005	0.00000	0.96261	416.45890	0.5750	0.00320	0.00000	0.00000
16	QDP	2095.00000	0.87448	264.26097	0.7792	0.00608	-0.00004	0.00000	0.96358	409.99687	2.0023	0.01222	0.00000	0.00000
17	LUD	2100.00000	0.87753	256.62110	0.7488	0.00608	-0.00004	0.00000	0.96557	390.27926	1.9412	0.01222	0.00000	0.00000
18	QFL	2102.50000	0.87910	250.07897	1.8583	0.01781	-0.00004	0.00000	0.96659	384.96548	0.1922	0.00269	0.00000	0.00000
19	DSD*	2700.00000	1.58333	344.94218	0.0000	0.00290	3.69554	0.00000	1.58323	116.00767	-0.0001	0.00862	0.00000	0.00000

```
      ---               Split quads and add markers:

 ***   LQL    =      0    0 //  1.25
 ***   LQP    =      0    0 //  1.25
 ***   LQM    =      0    0 //  4.0
 ***   LQN    =      0    0 //  4.0

 ***          CALL   0    0 //  SUTL

 ***   .UDF   BML    0    0 //  QDL  #QDL QDL  LUD  QFP  #QFP QFP  LUE
  *                          //  QDM  #QDM QDM  LUD  QFN  #QFN QFN  LUC

 ***   .UFD   BML    0    0 //  QFL  #QFL QFL  LUD  QDP  #QDP QDP  LUE
  *                          //  QFM  #QFM QFM  LUD  QDN  #QDN QDN  LUC

 ***   .UTL   BML    0    0 //  .DSF .UTD DSD.

 ***   #QFL   DRF    0    0 //
 ***   #QFP   DRF    0    0 //
 ***   #QFM   DRF    0    0 //
 ***   #QFN   DRF    0    0 //
 ***   #QDL   DRF    0    0 //
 ***   #QDP   DRF    0    0 //
 ***   #QDM   DRF    0    0 //
 ***   #QDN   DRF    0    0 //
```

```
      --                PHASE TROMBONES

***   .TRF    BML    0    0 //  QD    OBO  QFA   OBO  QDB   OBO  QFC   OBO  QDD   OBO
  *                          //  QFE   OBO  QDD   OBO  QFC   OBO  QDB   OBO  QFA   OBO  QD

***   .TRD    BML    0    0 //  QF    OBO  AQD   OBO  BQF   OBO  CQD   OBO  DQF   OBO
  *                          //  EQD   OBO  DQF   OBO  CQD   OBO  BQF   OBO  AQD   OBO  QF

***   TRD.    BML   -1    0 //  .TRD

***   $TRM    BML    0    0 //  .TRF QD   OBO  QF    TRD.


***   KFA     =      0    0 //   .00201429
***   KDB     =      0    0 //  -.00203447
***   KFC     =      0    0 //   .00203497
***   KDD     =      0    0 //  -.00203419
***   KFE     =      0    0 //   .00201389
***   LQT     =      0    0 //  5.0


***   TRMB    SUB    0    0 //
.....................................................................................................................
***   QFA     MAG    0    0 //  LQT        KFA        BR
***   QDB     MAG    0    0 //  LQT        KDB        BR
***   QFC     MAG    0    0 //  LQT        KFC        BR
***   QDD     MAG    0    0 //  LQT        KDD        BR
***   QFE     MAG    0    0 //  LQT        KFE        BR
***   AQD     MAG    0    0 //  LQT        -KFA       BR
***   BQF     MAG    0    0 //  LQT        -KDB       BR
***   CQD     MAG    0    0 //  LQT        -KFC       BR
***   DQF     MAG    0    0 //  LQT        -KDD       BR
***   EQD     MAG    0    0 //  LQT        -KFE       BR
***           END    0    0 //
.....................................................................................................................


***           CALL   0    0 //  TRMB
```

--- Track through both phase trombones on either side of insertion, which is replaced by a half-cell.

```
***   TTR    TRKB        //  $TRM CD
 *            //
 *           //
```

POS		S	QX	BX	AX	GX	X	DX	QY	BY	AY	GY	Y	DY
0		0.00000	0.00000	115.95151	0.0000	0.00862	2.22784	0.00000	0.00000	344.95048	0.0000	0.00290	0.00000	0.00000
1	QD	2.50000	0.00342	117.48605	-0.6164	0.01175	2.24202	0.01135	0.00116	340.60155	1.7322	0.01175	0.00000	0.00000
2	OBO	97.50000	0.08218	340.59577	-1.7321	0.01174	3.67205	0.01875	0.07992	117.48671	0.6164	0.01175	0.00000	0.00000
3	QFA	102.50000	0.08449	340.76396	1.6990	0.01141	3.67296	-0.01839	0.08675	117.42875	-0.6046	0.01163	0.00000	0.00000
4	OBO	197.50000	0.16202	120.88003	0.6155	0.01141	2.27723	-0.01099	0.16596	337.25034	-1.7093	0.01163	0.00000	0.00000
5	QDB	202.50000	0.16865	121.05704	-0.6515	0.01177	2.27996	0.01209	0.16830	337.19130	1.7209	0.01175	0.00000	0.00000
6	OBO	297.50000	0.24488	351.03073	-1.7692	0.01177	3.77982	0.01949	0.24795	116.24838	0.6048	0.01175	0.00000	0.00000
7	QFC	302.50000	0.24713	350.86028	1.8027	0.01211	3.78069	-0.01914	0.25485	116.30700	-0.6167	0.01187	0.00000	0.00000
8	OBO	397.50000	0.32456	117.65045	0.6521	0.01211	2.31381	-0.01174	0.33405	340.59165	-1.7442	0.01187	0.00000	0.00000
9	QDD	402.50000	0.33140	117.29947	-0.5807	0.01140	2.31369	0.01169	0.33636	340.71071	1.7208	0.01163	0.00000	0.00000
10	OBO	497.50000	0.41153	330.50416	-1.6635	0.01140	3.77591	0.01909	0.41467	118.68759	0.6163	0.01163	0.00000	0.00000
11	QFE	502.50000	0.41392	330.50414	1.6635	0.01140	3.77591	-0.01909	0.42144	118.68759	-0.6163	0.01163	0.00000	0.00000
12	OBO	597.50000	0.49405	117.29898	0.5807	0.01140	2.31374	-0.01169	0.49975	340.71095	-1.7208	0.01163	0.00000	0.00000
13	QDD	602.50000	0.50089	117.64993	-0.6521	0.01211	2.31386	0.01174	0.50206	340.59189	1.7442	0.01187	0.00000	0.00000
14	OBO	697.50000	0.57832	350.85879	-1.8027	0.01211	3.78085	0.01914	0.58126	116.30709	0.6167	0.01187	0.00000	0.00000
15	QFC	702.50000	0.58057	351.02925	1.7692	0.01177	3.77998	-0.01949	0.58816	116.24847	-0.6048	0.01175	0.00000	0.00000
16	OBO	797.50000	0.65680	121.05700	0.6515	0.01177	2.28007	-0.01209	0.66781	337.19130	-1.7209	0.01175	0.00000	0.00000
17	QDB	802.50000	0.66343	120.88004	-0.6155	0.01141	2.27734	0.01099	0.67015	337.25033	1.7093	0.01163	0.00000	0.00000
18	OBO	897.50000	0.74096	340.76534	-1.6990	0.01141	3.67312	0.01839	0.74936	117.42867	0.6046	0.01163	0.00000	0.00000
19	QFA	902.50000	0.74328	340.59718	1.7321	0.01174	3.67221	-0.01875	0.75619	117.48663	-0.6164	0.01175	0.00000	0.00000
20	OBO	997.50000	0.82203	117.48657	0.6164	0.01175	2.24208	-0.01135	0.83495	340.60131	-1.7322	0.01175	0.00000	0.00000
21	QD	1000.00000	0.82545	115.95201	0.0000	0.00862	2.22790	0.00000	0.83611	344.95024	0.0000	0.00290	0.00000	0.00000
22	QD	1002.50000	0.82887	117.48655	-0.6164	0.01175	2.24207	0.01135	0.83727	340.60131	1.7322	0.01175	0.00000	0.00000
23	OBO	1097.50000	0.90763	340.59588	-1.7321	0.01174	3.67206	0.01875	0.91603	117.48671	0.6164	0.01175	0.00000	0.00000
24	QF	1100.00000	0.90878	344.94445	0.0000	0.00290	3.69552	0.00000	0.91944	115.95226	0.0000	0.00862	0.00000	0.00000
25	QF	1102.50000	0.90994	340.59583	1.7321	0.01174	3.67205	-0.01875	0.92286	117.48672	-0.6164	0.01175	0.00000	0.00000
26	OBO	1197.50000	0.98870	117.48558	0.6164	0.01175	2.24197	-0.01135	1.00162	340.60179	-1.7322	0.01175	0.00000	0.00000
27	AQD	1202.50000	0.99553	117.42724	-0.6046	0.01163	2.24141	0.01113	1.00394	340.77101	1.6989	0.01140	0.00000	0.00000
28	OBO	1297.50000	1.07474	337.22287	-1.7090	0.01163	3.65009	0.01853	1.08145	120.90168	0.6155	0.01140	0.00000	0.00000
29	BQF	1302.50000	1.07708	337.16250	1.7209	0.01175	3.64952	-0.01876	1.08809	121.08015	-0.6518	0.01177	0.00000	0.00000
30	OBO	1397.50000	1.15675	116.22040	0.6048	0.01175	2.21897	-0.01136	1.16430	351.12301	-1.7697	0.01177	0.00000	0.00000
31	CQD	1402.50000	1.16365	116.27806	-0.6165	0.01187	2.21838	0.01112	1.16654	350.95301	1.8031	0.01211	0.00000	0.00000
32	OBO	1497.50000	1.24287	340.50716	-1.7438	0.01187	3.62628	0.01852	1.24396	117.68227	0.6523	0.01211	0.00000	0.00000
33	DQF	1502.50000	1.24519	340.62659	1.7203	0.01162	3.62628	-0.01852	1.25079	117.33024	-0.5808	0.01140	0.00000	0.00000
34	OBO	1597.50000	1.32351	118.66593	0.6161	0.01163	2.21827	-0.01112	1.33091	330.53517	-1.6635	0.01140	0.00000	0.00000
35	EQD	1602.50000	1.33028	118.66725	-0.6163	0.01163	2.21827	0.01112	1.33330	330.53360	1.6638	0.01140	0.00000	0.00000
36	OBO	1697.50000	1.40860	340.70301	-1.7208	0.01163	3.62631	0.01852	1.41343	117.29855	0.5808	0.01140	0.00000	0.00000
37	DQF	1702.50000	1.41091	340.58487	1.7441	0.01187	3.62631	-0.01852	1.42026	117.64894	-0.6520	0.01211	0.00000	0.00000
38	OBO	1797.50000	1.49011	116.30510	0.6167	0.01187	2.21840	-0.01112	1.49770	350.85604	-1.8028	0.01211	0.00000	0.00000
39	CQD	1802.50000	1.49701	116.24611	-0.6047	0.01175	2.21900	0.01136	1.49995	351.02756	1.7691	0.01176	0.00000	0.00000
40	OBO	1897.50000	1.57667	337.16274	-1.7206	0.01175	3.64957	0.01876	1.57617	121.07729	0.6515	0.01176	0.00000	0.00000
41	BQF	1902.50000	1.57901	337.22050	1.7093	0.01163	3.65015	-0.01853	1.58280	120.90201	-0.6158	0.01141	0.00000	0.00000
42	OBO	1997.50000	1.65823	117.40097	0.6046	0.01163	2.24144	-0.01113	1.66031	340.86079	-1.6995	0.01141	0.00000	0.00000
43	AQD	2002.50000	1.66506	117.45802	-0.6162	0.01175	2.24200	0.01135	1.66263	340.69323	1.7325	0.01175	0.00000	0.00000
44	OBO	2097.50000	1.74384	340.51866	-1.7318	0.01174	3.67208	0.01875	1.74136	117.52053	0.6167	0.01175	0.00000	0.00000
45	QF	2100.00000	1.74500	344.86697	-0.0001	0.00290	3.69555	0.00000	1.74478	115.98494	0.0001	0.00862	0.00000	0.00000

```
---                Split quads and add markers:

***   LQT     =      0    0 //  2.5

***           CALL   0    0 //  TRMB


***   ^TRF    BML    0    0 //  QD    .OBO QFA  #QFA QFA  .OBO QDB  #QDB QDB  .OBO
  *                             //  QFC  #QFC QFC  .OBO QDD  #QDD QDD  .OBO QFE

***   TRF^    BML   -1    0 //  ^TRF

***   .TRF    BML    0    0 //  #QD  ^TRF #QFE TRF^


***   ^TRD    BML    0    0 //  QF    .OBO AQD  #AQD AQD  .OBO BQF  #BQF BQF  .OBO
  *                             //  CQD  #CQD CQD  .OBO DQF  #DQF DQF  .OBO EQD

***   TRD^    BML   -1    0 //  ^TRD

***   .TRD    BML    0    0 //  ^TRD #EQD TRD^ #QF

***   TRD.    BML   -1    0 //  .TRD


***   #QFA    DRF    0    0 //
***   #AQD    DRF    0    0 //
***   #QDB    DRF    0    0 //
***   #BQF    DRF    0    0 //
***   #QFC    DRF    0    0 //
***   #CQD    DRF    0    0 //
***   #QDD    DRF    0    0 //
***   #DQF    DRF    0    0 //
***   #QFE    DRF    0    0 //
***   #EQD    DRF    0    0 //
```

```
--              BEAM SEPARATION/DISPERSION CORRECTION
                SYSTEM FOR CROSSING INSERTION (VERTICAL)

                i) M=-1 horizontal step made of two 90 deg FODO cells:
***   .FDV   BML    0   0 //  QFV  OOV  QDV
***   .DFV   BML    0   0 //  QDV  OOV  QFV
***   .CFV   BML    0   0 //  .FDV .DFV
***   .CDV   BML    0   0 //  .DFV .FDV
***   LQV    =      0   0 //  7.75
***   KFV    =      0   0 //   .00194100
***   KDV    =      0   0 //  -.00194100
***   OOV    DRF    0   0 //  37.0
***   QFV    MAG    0   0 //  LQV       KFV       BR
***   QDV    MAG    0   0 //  LQV       KDV       BR

                ii) Vertical steps
***   .BC+   BML    0   0 //    6( D    BCV+    )
***   .BC-   BML    0   0 //    6( D    BCV-    )
***   .C+-   BML    0   0 //  BC+  DV1  BSV- D
***   .C-+   BML    0   0 //  BC-  DV1  BSV+ D
***   .V+-   BML    0   0 //  D    BV+  DV   BV-  D
***   .V-+   BML   -1   0 //  .V+-
***   .VD+   BML    0   0 //  .C+- .CDV .CDV .V+-
***   .VF-   BML    0   0 //  .C-+ .CFV .CFV .V-+
***   .VD-   BML    0   0 //  .C-+ .CDV .CDV .V-+
***   .VF+   BML    0   0 //  .C+- .CFV .CFV .V+-
***   VD+.   BML   -1   0 //  .VD+
***   VF-.   BML   -1   0 //  .VF-
***   VD-.   BML   -1   0 //  .VD-
***   VF+.   BML   -1   0 //  .VF+

***   LBVC   =      0   0 //  8.0
***   BV1    =      0   0 //  1.79633493
***   BV2    =      0   0 //  5.19422149
***   BV3    =      0   0 //  6.04207552
***   RI1    =      0   0 //  BV1       /         BRHO
***   RI2    =      0   0 //  BV2       /         BRHO
***   RI3    =      0   0 //  BV3       /         BRHO
***   R1     =      0   0 //  1.        /         RI1
***   R2     =      0   0 //  1.        /         RI2
***   R3     =      0   0 //  1.        /         RI3
***   D      DRF    0   0 //  1.0
***   DV     DRF    0   0 //  99.8
***   DV1    DRF    0   0 //  100.6
***   BCV+   MAGV   0   0 //  LBVC      0.        BR        RI1
***   BCV-   MAGV   0   0 //  LBVC      0.        BR        -RI1
***   BSV+   MAGV   0   0 //  LB        0.        BR        RI2
***   BSV-   MAGV   0   0 //  LB        0.        BR        -RI2
***   BV+    MAGV   0   0 //  LB        0.        BR        RI3
***   BV-    MAGV   0   0 //  LB        0.        BR        -RI3
***   BC+    MMM    0   0 //  .BC+
***   BC-    MMM    0   0 //  .BC-
```

```
--                LOW BETA INSERTION
***   TPI.   BML    0   0 //       D0     2( 1QD  D       )   2( 2QF  D       ) 3QD
***   SSI.   BML    0   0 //  4QD  D45  5QF  D56  6QD
***   .TPI   BML   -1   0 //  TPI.
***   .SSI   BML   -1   0 //  SSI.
***   .DUD   BML    0   0 //  .SSI VD-. .TPI
***   .DDU   BML    0   0 //  .SSI VD+. .TPI

***   TPO.   BML    0   0 //  #IP--D0     2( QF1  D       )   2( QD2  D       ) QF3
***   SSO.   BML    0   0 //  QF4  D45  QD5  D56  QF6
***   .TPO   BML   -1   0 //  TPO.
***   .SSO   BML   -1   0 //  SSO.
***   .FUD   BML    0   0 //  .SSO VF-. .TPO
***   .FDU   BML    0   0 //  .SSO VF+. .TPO
***   FDU.   BML   -1   0 //  .FDU
***   FUD.   BML   -1   0 //  .FUD
***   $UD    BML    0   0 //  *DSF .DUD FUD. DSD*

***   LQ1    =      0   0 //  3.40
***   LQ2    =      0   0 //  5.45
***   LQ3    =      0   0 //  6.05
***   LQ4    =      0   0 //  2.9
***   LQ5    =      0   0 //  4.5
***   LQ6    =      0   0 //  2.5
***   LQ1    =      0   0 //  6.80
***   LQ2    =      0   0 //  10.9
***   LQ3    =      0   0 //  12.1
***   LQ4    =      0   0 //  5.8
***   LQ5    =      0   0 //  9.0
***   LQ6    =      0   0 //  5.0
***   K1     =      0   0 //   .00367913
***   K2     =      0   0 //  -.00348474
***   K3     =      0   0 //   .00332400
***   K4     =      0   0 //   .00179708
***   K5     =      0   0 //  -.00191929
***   K6     =      0   0 //   .00059091
***   D      DRF    0   0 //  1.0
***   D0     DRF    0   0 //  20.
***   D56    DRF    0   0 //  22.5
***   D45    DRF    0   0 //  21.5
***   D34    DRF    0   0 //  307.2
***   #IP-   DRF    0   0 //  0.0

***   SRS    SUB    0   0 //
.....................................................................................................
***   QF1    MAG    0   0 //  LQ1       K1        BR
***   QD2    MAG    0   0 //  LQ2       K2        BR
***   QF3    MAG    0   0 //  LQ3       K3        BR
***   QF4    MAG    0   0 //  LQ4       K4        BR
***   QD5    MAG    0   0 //  LQ5       K5        BR
***   QF6    MAG    0   0 //  LQ6       K6        BR
***   1QD    MAG    0   0 //  LQ1       -K1       BR
***   2QF    MAG    0   0 //  LQ2       -K2       BR
***   3QD    MAG    0   0 //  LQ3       -K3       BR
***   4QD    MAG    0   0 //  LQ4       -K4       BR
***   5QF    MAG    0   0 //  LQ5       -K5       BR
***   6QD    MAG    0   0 //  LQ6       -K6       BR
***          END    0   0 //
.....................................................................................................
```

```
***          CALL   0   0 //  SRS

     ---             Track through crossing insertion, including
                     lumped suppressors *DSF and DSD*.  Strings
                     of six conventional dipoles, BC+, BC-,
                     used as splitters, are also lumped.

***   TINS   TRKB        //  $UD  CD
 *                       //
 *                       //
```

POS		S	QX	BX	AX	GX	X	DX	QY	BY	AY	GY	Y	DY
0		0.00000	0.00000	115.95151	0.0000	0.00862	2.22784	0.00000	0.00000	344.95048	0.0000	0.00290	0.00000	0.00000
1	*DSF	597.50000	0.61669	385.00881	-0.1922	0.00269	0.00003	0.00000	0.70419	250.10432	-1.8586	0.01781	0.00000	0.00000
2	6QD	602.50000	0.61874	392.73300	-1.3603	0.00726	0.00003	0.00000	0.70727	265.27390	-1.1604	0.00885	0.00000	0.00000
3	D56	625.00000	0.62719	457.61856	-1.5235	0.00726	0.00003	0.00000	0.71954	321.97008	-1.3594	0.00885	0.00000	0.00000
4	5QF	634.00000	0.63039	415.31386	5.9779	0.08845	0.00002	0.00000	0.72362	402.51281	-8.0488	0.16343	0.00000	0.00000
5	D45	655.50000	0.64230	199.15031	4.0762	0.08845	0.00001	0.00000	0.72956	824.15623	-11.5625	0.16343	0.00000	0.00000
6	4QD	661.30000	0.64744	165.25758	1.8847	0.02754	0.00001	0.00000	0.73062	909.50157	-2.8545	0.01006	0.00000	0.00000
7	D	662.30000	0.64842	161.51579	1.8571	0.02754	0.00001	0.00000	0.73079	915.22054	-2.8645	0.01006	0.00000	0.00000
8	BV+	678.90000	0.66852	107.44963	1.3999	0.02754	0.00000	0.00000	0.733541013.09173		-3.0313	0.01006	0.01248	0.00150
9	DV	778.70000	0.96828	102.37945	-1.3491	0.02754	-0.00003	0.00000	0.745591718.31855		-4.0351	0.01006	0.16252	0.00150
10	BV-	795.30000	0.98933	154.75894	-1.8063	0.02754	-0.00004	0.00000	0.747071855.04993		-4.2018	0.01006	0.17500	0.00000
11	D	796.30000	0.99035	158.39912	-1.8339	0.02754	-0.00004	0.00000	0.747151863.46351		-4.2118	0.01006	0.17500	0.00000
12	QDV	804.05000	0.99724	210.00018	-5.0811	0.12770	-0.00004	0.00000	0.747831715.43779		22.5638	0.29737	0.16490	-0.00258
13	OOV	841.05000	1.01200	760.82545	-9.8061	0.12770	-0.00008	0.00000	0.75451	452.81887	11.5610	0.29737	0.06938	-0.00258
14	QFV	848.80000	1.01353	823.35125	2.0542	0.00634	-0.00008	0.00000	0.75775	332.80767	4.5215	0.06443	0.05306	-0.00167
15	QFV	856.55000	1.01512	701.97995	12.9932	0.24192	-0.00007	0.00000	0.76172	301.50299	-0.3264	0.00367	0.04299	-0.00095
16	OOV	893.55000	1.04149	71.67148	4.0421	0.24192	-0.00002	0.00000	0.78042	330.67967	-0.4622	0.00367	0.00769	-0.00095
17	QDV	901.30000	1.06980	27.82337	1.8339	0.15681	-0.00001	0.00000	0.78425	300.43539	4.2118	0.06237	0.00000	-0.00101
18	QDV	909.05000	1.14709	10.29923	0.5145	0.12280	0.00000	0.00000	0.78907	210.02705	6.9969	0.23786	-0.00770	-0.00095
19	OOV	946.05000	1.43400	140.33553	-4.0290	0.12280	0.00004	0.00000	1.18591	17.88371	-1.8038	0.23786	-0.04300	-0.00095
20	QFV	953.80000	1.44142	189.40225	-2.0542	0.02756	0.00004	0.00000	1.22311	65.08447	-4.5215	0.32947	-0.05306	-0.00167
21	QFV	961.55000	1.44765	199.18103	0.8419	0.00858	0.00004	0.00000	1.23511	169.19959	-9.4308	0.53156	-0.06938	-0.00258
22	OOV	998.55000	1.48215	148.62794	0.5244	0.00858	0.00004	0.00000	1.246451594.78526		-29.0985	0.53156	-0.16490	-0.00258
23	QDV	1006.30000	1.49035	158.39912	-1.8339	0.02754	0.00004	0.00000	1.247151863.46361		-4.2118	0.01006	-0.17500	0.00000
24	D	1007.30000	1.49134	162.09439	-1.8614	0.02754	0.00004	0.00000	1.247241871.89730		-4.2219	0.01006	-0.17500	0.00000
25	BSV+	1023.90000	1.50500	231.48322	-2.3186	0.02754	0.00004	0.00000	1.248602014.83131		-4.3886	0.01006	-0.16427	0.00129
26	DV1	1124.50000	1.53892	976.75614	-5.0896	0.02754	0.00008	0.00000	1.255112999.58230		-5.4002	0.01006	-0.03425	0.00129
27	BC-	1178.50000	1.545791606.75671		-6.5770	0.02754	0.00010	0.00000	1.257733612.11613		-5.9430	0.01005	0.00130	0.00000
28	3QD	1190.60000	1.546782744.88723		-102.2688	3.81069	0.00013	0.00000	1.258352224.25879		101.4022	4.62329	0.00100	-0.00005
29	D	1191.60000	1.546842953.23560		-106.0795	3.81069	0.00013	0.00000	1.258432026.07775		96.7789	4.62329	0.00095	-0.00005
30	2QF	1202.50000	1.547314008.90066		22.9796	0.13197	0.00015	0.00000	1.25982	874.40375	23.0737	0.61001	0.00059	-0.00002
31	D	1203.50000	1.547353963.07337		22.8477	0.13197	0.00015	0.00000	1.26001	828.86645	22.4636	0.61001	0.00057	-0.00002
32	2QF	1214.40000	1.547902178.66378		117.6176	6.35018	0.00011	-0.00001	1.26250	668.61635	-5.7867	0.05158	0.00046	0.00000
33	D	1215.40000	1.547971949.77877		111.2674	6.35018	0.00011	-0.00001	1.26274	680.24137	-5.8383	0.05158	0.00046	0.00000
34	1QD	1222.20000	1.54880	920.59247	48.5705	2.56367	0.00007	0.00000	1.26433	643.88197	10.8786	0.18535	0.00042	-0.00001
35	D	1223.20000	1.54899	826.01519	46.0068	2.56367	0.00007	0.00000	1.26458	622.31020	10.6932	0.18535	0.00040	-0.00001
36	1QD	1230.00000	1.55092	401.00196	19.9999	0.99999	0.00005	0.00000	1.26669	400.91928	19.9967	0.99988	0.00029	-0.00002
37	D0	1250.00000	1.79294	1.00001	0.0002	0.99999	0.00000	0.00000	1.50886	1.00013	-0.0008	0.99988	-0.00013	-0.00002

38	#IP-	1250.00000	1.79294	1.00001	0.0002	0.99999	0.00000	0.00000	1.50886	1.00013	-0.0008	0.99988	-0.00013	-0.00002
39	D0	1270.00000	2.03502	400.98734	-19.9995	0.99999	-0.00005	0.00000	1.75078	400.98123	-19.9983	0.99988	-0.00054	-0.00002
40	QF1	1276.80000	2.03712	622.40630	-10.6943	0.18536	-0.00006	0.00000	1.75272	825.96045	-46.0032	2.56343	-0.00074	-0.00004
41	D	1277.80000	2.03738	643.98022	-10.8796	0.18536	-0.00006	0.00000	1.75290	920.53020	-48.5666	2.56343	-0.00077	-0.00004
42	QF1	1284.60000	2.03897	680.33723	5.8397	0.05160	-0.00007	0.00000	1.753731949.63472		-111.2586	6.34964	-0.00109	-0.00006
43	D	1285.60000	2.03920	668.70941	5.7881	0.05160	-0.00006	0.00000	1.753812178.50155		-117.6082	6.34964	-0.00115	-0.00006
44	QD2	1296.50000	2.04170	828.96654	-22.4658	0.61005	-0.00007	0.00000	1.754363962.76190		-22.8453	0.13195	-0.00153	-0.00001
45	D	1297.50000	2.04188	874.50813	-23.0758	0.61005	-0.00007	0.00000	1.754404008.58438		-22.9772	0.13195	-0.00154	-0.00001
46	QD2	1308.40000	2.043282026.29861		-96.7888	4.62374	-0.00011	-0.00001	1.754872952.99220		106.0714	3.81042	-0.00130	0.00005
47	D	1309.40000	2.043352224.50001		-101.4126	4.62374	-0.00012	-0.00001	1.754922744.65985		102.2610	3.81042	-0.00125	0.00005
48	QF3	1321.50000	2.043983612.49104		5.9442	0.01006	-0.00015	0.00000	1.755921606.61167		6.5770	0.02755	-0.00092	0.00001
49	BC-	1375.50000	2.046592999.84122		5.4011	0.01006	-0.00013	0.00000	1.76278	976.61608	5.0895	0.02755	-0.03480	-0.00129
50	DV1	1476.10000	2.053102014.92538		4.3893	0.01006	-0.00011	0.00000	1.79672	231.39275	2.3183	0.02755	-0.16413	-0.00129
51	BSV+	1492.70000	2.054461871.97232		4.2223	0.01006	-0.00010	0.00000	1.81038	162.01744	1.8610	0.02755	-0.17474	0.00001
52	D	1493.70000	2.054551863.53771		4.2123	0.01006	-0.00010	0.00000	1.81137	158.32303	1.8334	0.02755	-0.17473	0.00001
53	QFV	1501.45000	2.055251594.84458		29.0999	0.53159	-0.00009	0.00000	1.81958	148.54999	-0.5238	0.00858	-0.18496	-0.00267
54	OOV	1538.45000	2.06660	169.19880	9.4310	0.53159	-0.00003	0.00000	1.85409	199.05268	-0.8412	0.00858	-0.28384	-0.00267
55	QDV	1546.20000	2.07859	65.08130	4.5215	0.32950	-0.00002	0.00000	1.86032	189.27845	2.0530	0.02755	-0.28777	0.00167
56	QDV	1553.95000	2.11579	17.88059	1.8037	0.23788	-0.00001	0.00000	1.86775	140.24298	4.0264	0.12273	-0.25847	0.00582
57	OOV	1590.95000	2.51264	210.06508	-6.9979	0.23788	0.00004	0.00000	2.15464	10.30546	-0.5146	0.12273	-0.04321	0.00582
58	QFV	1598.70000	2.51745	300.48547	-4.2123	0.06238	0.00005	0.00000	2.23190	27.82673	-1.8334	0.15674	0.00022	0.00550
59	QFV	1606.45000	2.52129	330.73085	0.4625	0.00367	0.00005	0.00000	2.26021	71.66338	-4.0410	0.24182	0.04367	0.00582
60	OOV	1643.45000	2.53998	301.53080	0.3267	0.00367	0.00004	0.00000	2.28659	701.75633	-12.9885	0.24182	0.25919	0.00582
61	QDV	1651.20000	2.54395	332.83368	-4.5215	0.06443	0.00004	0.00000	2.28818	823.07950	-2.0530	0.00634	0.28850	0.00166
62	QDV	1658.95000	2.54719	452.84900	-11.5615	0.29738	0.00005	0.00000	2.28971	760.56603	9.8033	0.12767	0.28450	-0.00269
63	OOV	1695.95000	2.553871715.51026		-22.5645	0.29738	0.00010	0.00000	2.30447	209.90791	5.0794	0.12767	0.18507	-0.00269
64	QFV	1703.70000	2.554551863.53762		4.2123	0.01006	0.00010	0.00000	2.31137	158.32302	1.8334	0.02755	0.17473	-0.00001
65	D	1704.70000	2.554631855.12312		4.2022	0.01006	0.00010	0.00000	2.31239	154.68371	1.8059	0.02755	0.17473	-0.00001
66	BV-	1721.30000	2.556111718.38100		4.0353	0.01006	0.00010	0.00000	2.33345	102.31919	1.3486	0.02755	0.16213	-0.00151
67	DV	1821.10000	2.568161013.12059		3.0315	0.01006	0.00007	0.00000	2.63323	107.52115	-1.4007	0.02755	0.01139	-0.00151
68	BV+	1837.70000	2.57091	915.24702	2.8645	0.01006	0.00006	0.00000	2.65332	161.61617	-1.8580	0.02755	-0.00120	-0.00001
69	D	1838.70000	2.57108	909.52805	2.8545	0.01006	0.00006	0.00000	2.65429	165.35974	-1.8856	0.02755	-0.00121	-0.00001
70	QF4	1844.50000	2.57214	824.18105	11.5628	0.16343	0.00006	0.00000	2.65943	199.26965	-4.0783	0.08849	-0.00129	-0.00002
71	D45	1866.00000	2.57808	402.52717	8.0490	0.16343	0.00004	0.00000	2.67133	415.54057	-5.9808	0.08849	-0.00171	-0.00002
72	QD5	1875.00000	2.58216	321.98275	1.3594	0.00885	0.00004	0.00000	2.67453	457.86083	1.5248	0.00726	-0.00176	0.00001
73	D56	1897.50000	2.59443	265.28712	1.1604	0.00885	0.00003	0.00000	2.68298	392.92225	1.3614	0.00726	-0.00152	0.00001
74	QF6	1902.50000	2.59751	250.11740	1.8586	0.01781	0.00003	0.00000	2.68503	385.18958	0.1928	0.00269	-0.00148	0.00001
75	DSD*	2500.00000	3.30174	344.89440	0.0001	0.00290	3.69554	0.00000	3.30165	115.96599	0.0005	0.00862	-0.00015	-0.00001

```
    ---                 Split quads and add markers:
***   LQ1     =      0   0 //  3.40
***   LQ2     =      0   0 //  5.45
***   LQ3     =      0   0 //  6.05
***   LQ4     =      0   0 //  2.9
***   LQ5     =      0   0 //  4.5
***   LQ6     =      0   0 //  2.5

***           CALL   0   0 //  SRS

***   .FDV    BML    0   0 //  #QFV QFV  OOV  QDV
***   .DFV    BML    0   0 //  #QDV QDV  OOV  QFV
***   .C+-    BML    0   0 //  .BC+ DV1  BSV- D
***   .C-+    BML    0   0 //  .BC- DV1  BSV+ D
***   .C+-    BML    0   0 //  #BC+ .BC+ DV1  BSV- D    #BS-
***   .C-+    BML    0   0 //  #BC- .BC- DV1  BSV+ D    #BS+
***   .V+-    BML    0   0 //  #BV+ D    BV+  DV   BV-  D    #BV-
***   .VD+    BML    0   0 //  .C+- .CDV .CDV #QDV .V+-
***   .VF-    BML    0   0 //  .C-+ .CFV .CFV #QFV .V-+
***   .VD-    BML    0   0 //  .C-+ .CDV .CDV #QDV .V-+
***   .VF+    BML    0   0 //  .C+- .CFV .CFV #QFV .V+-

***   TPO.    BML    0   0 //  #IP--D0     2( QF1  #QF1 QF1  D       )
  *                          //    2( QD2  #QD2 QD2  D       ) QF3  #QF3 QF3

***   TPI.    BML    0   0 //  #IP--D0     2( 1QD  #1QD 1QD  D       )
  *                          //    2( 2QF  #2QF 2QF  D       ) 3QD  #3QD 3QD

***   SSO.    BML    0   0 //  QF4  #QF4 QF4  D45  QD5  #QD5 QD5
  *                          //  D56  QF6  #QF6 QF6

***   SSI.    BML    0   0 //  4QD  #4QD 4QD  D45  5QF  #5QF 5QF
  *                          //  D56  6QD  #6QD 6QD

***   .UD     BML    0   0 //  .DSF .DUD FUD. DSD.
***   .DU     BML    0   0 //  .DSF .DDU FDU. DSD.

***   #QF1    DRF    0   0 //
***   #QD2    DRF    0   0 //
***   #QF3    DRF    0   0 //
***   #QF4    DRF    0   0 //
***   #QD5    DRF    0   0 //
***   #QF6    DRF    0   0 //
***   #1QD    DRF    0   0 //
***   #2QF    DRF    0   0 //
***   #3QD    DRF    0   0 //
***   #4QD    DRF    0   0 //
***   #5QF    DRF    0   0 //
***   #6QD    DRF    0   0 //
***   #BV+    DRF    0   0 //
***   #BV-    DRF    0   0 //
***   #BC+    DRF    0   0 //
***   #BC-    DRF    0   0 //
***   #BS+    DRF    0   0 //
***   #BS-    DRF    0   0 //
***   #QFV    DRF    0   0 //
***   #QDV    DRF    0   0 //
```

```
      --              ARCS ( . lines contain sextupoles, * lines do not)

***   *FD     BML    0   0 //  #QF  QF   .OBO QD
***   *DF     BML    0   0 //  #QD  QD   .OBO QF


***   .RG1    BML    0   0 //   24( .FD  .DF     )  10( *FD  *DF     )
  *                       //  *FD   24( .DF  .FD    )

***   .RG2    BML    0   0 //   18( .FD  .DF     )   4( *FD  *DF     ) *FD

***   .RG3    BML    0   0 //  *FD    4( *DF  *FD     )  18( .DF  .FD     )


***   .AR1    BML    0   0 //  TRD. .RG1 .TRF

***   .AR2    BML    0   0 //  TRD. .RG2 .UTL .RG3 .TRF



      --              SUPERPERIOD

***   .SP     BML    0   0 //  .AR1 .UD  .AR2 .DU  #QF
```

--- BETA FUNCTIONS THROUGH SUPERPERIOD (from beginning of long arc)---

*** RLD1 CYC -1 3 // .SP SF SD 0. 0.

BETATRON FUNCTIONS OF RLD1

POS		S(M)	NUX	NUY	BETAX(M)	BETAY(M)	XEQ(M)	YEQ(M)	ZEQ (M)	ALPHAX	ALPHAY	DXEQ	DYEQ
1	#QF	0.0000	0.00000	0.00000	344.89768	115.94737	3.69524	0.00000	0.00000	0.00009	0.00020	0.00000	0.00000
15	#AQD	100.0000	0.08335	0.08334	115.91985	344.92492	2.22756	0.00000	0.00000	0.00571	-0.01700	-0.00011	0.00000
29	#BQF	200.0000	0.16715	0.16536	341.49576	119.39455	3.67315	0.00000	0.02138	0.00593	-0.01783	-0.00011	0.00000
43	#CQD	300.0000	0.25143	0.24601	114.74488	355.53440	2.20475	0.00000	0.04268	-0.00580	0.01694	-0.00012	0.00000
57	#DQF	400.0000	0.33525	0.32795	344.96457	115.99384	3.64975	0.00000	0.06389	-0.01197	0.03483	0.00000	0.00000
71	#EQD	500.0000	0.41811	0.41267	117.13316	334.76571	2.20458	0.00000	0.08501	0.00003	0.00029	0.00000	0.00000
85	#DQF	600.0000	0.50097	0.49740	344.94633	115.93516	3.64977	0.00000	0.10614	0.01200	-0.03454	0.00000	0.00000
99	#CQD	700.0000	0.58479	0.57939	114.73879	355.35636	2.20476	-0.00001	0.12726	0.00577	-0.01722	0.00012	0.00000
113	#BQF	800.0000	0.66907	0.66007	341.49601	119.39226	3.67317	0.00000	0.14839	-0.00599	0.01725	0.00011	0.00000
127	#AQD	900.0000	0.75287	0.74206	115.92606	345.09256	2.22757	0.00000	0.16960	-0.00574	0.01669	0.00011	0.00000
141	#QF	1000.0000	0.83622	0.82536	344.91578	116.00708	3.69525	0.00000	0.19090	-0.00006	0.00006	0.00000	0.00000
157	#QD	1100.0000	0.91955	0.90866	115.95289	345.01423	2.22770	0.00000	0.21228	-0.00010	0.00044	0.00000	0.00000
173	#QF	1200.0000	1.00288	0.99200	344.97707	115.91887	3.69537	0.00000	0.23366	-0.00004	0.00038	0.00000	0.00000
189	#QD	1300.0000	1.08621	1.07537	115.96112	344.78746	2.22783	0.00000	0.25504	0.00006	-0.00006	0.00000	0.00000
205	#QF	1400.0000	1.16954	1.15873	344.94026	115.93086	3.69564	0.00000	0.27642	0.00010	-0.00044	0.00000	0.00000
221	#QD	1500.0000	1.25288	1.24206	115.94052	345.04989	2.22797	0.00000	0.29780	0.00004	-0.00038	0.00000	0.00000
237	#QF	1600.0000	1.33622	1.32536	344.91578	116.00708	3.69579	0.00000	0.31918	-0.00006	0.00006	0.00000	0.00000
253	#QD	1700.0000	1.41955	1.40866	115.95289	345.01422	2.22798	0.00000	0.34056	-0.00010	0.00044	0.00000	0.00000
269	#QF	1800.0000	1.50288	1.49200	344.97707	115.91887	3.69567	0.00000	0.36194	-0.00004	0.00038	0.00000	0.00000
285	#QD	1900.0000	1.58621	1.57537	115.96112	344.78746	2.22785	0.00000	0.38332	0.00006	-0.00006	0.00000	0.00000
301	#QF	2000.0000	1.66954	1.65873	344.94026	115.93086	3.69540	0.00000	0.40470	0.00010	-0.00044	0.00000	0.00000
317	#QD	2100.0000	1.75288	1.74206	115.94052	345.04989	2.22771	0.00000	0.42608	0.00004	-0.00038	0.00000	0.00000
333	#QF	2200.0000	1.83622	1.82536	344.91579	116.00708	3.69525	0.00000	0.44746	-0.00006	0.00006	0.00000	0.00000
349	#QD	2300.0000	1.91955	1.90866	115.95289	345.01422	2.22770	0.00000	0.46884	-0.00010	0.00044	0.00000	0.00000
365	#QF	2400.0000	2.00288	1.99200	344.97707	115.91887	3.69537	0.00000	0.49022	-0.00004	0.00038	0.00000	0.00000
381	#QD	2500.0000	2.08621	2.07537	115.96112	344.78746	2.22783	0.00000	0.51160	0.00006	-0.00006	0.00000	0.00000
397	#QF	2600.0000	2.16954	2.15873	344.94026	115.93086	3.69564	0.00000	0.53298	0.00010	-0.00044	0.00000	0.00000
413	#QD	2700.0000	2.25288	2.24206	115.94052	345.04989	2.22797	0.00000	0.55436	0.00004	-0.00038	0.00000	0.00000
429	#QF	2800.0000	2.33622	2.32536	344.91579	116.00708	3.69579	0.00000	0.57574	-0.00006	0.00006	0.00000	0.00000
445	#QD	2900.0000	2.41956	2.40866	115.95289	345.01422	2.22798	0.00000	0.59713	-0.00010	0.00044	0.00000	0.00000
461	#QF	3000.0000	2.50288	2.49200	344.97707	115.91887	3.69567	0.00000	0.61851	-0.00004	0.00038	0.00000	0.00000
477	#QD	3100.0000	2.58621	2.57537	115.96112	344.78746	2.22785	0.00000	0.63989	0.00006	-0.00006	0.00000	0.00000
493	#QF	3200.0000	2.66954	2.65873	344.94026	115.93086	3.69540	0.00000	0.66127	0.00010	-0.00044	0.00000	0.00000
509	#QD	3300.0000	2.75288	2.74206	115.94052	345.04989	2.22771	0.00000	0.68265	0.00004	-0.00038	0.00000	0.00000
525	#QF	3400.0000	2.83622	2.82536	344.91579	116.00708	3.69525	0.00000	0.70403	-0.00006	0.00006	0.00000	0.00000
541	#QD	3500.0000	2.91956	2.90866	115.95289	345.01422	2.22770	0.00000	0.72541	-0.00010	0.00044	0.00000	0.00000
557	#QF	3600.0000	3.00289	2.99200	344.97707	115.91887	3.69537	0.00000	0.74679	-0.00004	0.00038	0.00000	0.00000
573	#QD	3700.0000	3.08621	3.07537	115.96112	344.78746	2.22783	0.00000	0.76817	0.00006	-0.00006	0.00000	0.00000
589	#QF	3800.0000	3.16954	3.15873	344.94026	115.93086	3.69564	0.00000	0.78955	0.00010	-0.00044	0.00000	0.00000
605	#QD	3900.0000	3.25288	3.24206	115.94052	345.04989	2.22797	0.00000	0.81093	0.00004	-0.00038	0.00000	0.00000
621	#QF	4000.0000	3.33622	3.32536	344.91579	116.00708	3.69579	0.00000	0.83231	-0.00006	0.00006	0.00000	0.00000
637	#QD	4100.0000	3.41956	3.40866	115.95289	345.01422	2.22798	0.00000	0.85369	-0.00010	0.00044	0.00000	0.00000
653	#QF	4200.0000	3.50289	3.49200	344.97707	115.91887	3.69567	0.00000	0.87507	-0.00004	0.00038	0.00000	0.00000
669	#QD	4300.0000	3.58621	3.57537	115.96112	344.78746	2.22785	0.00000	0.89646	0.00006	-0.00006	0.00000	0.00000
685	#QF	4400.0000	3.66954	3.65873	344.94026	115.93086	3.69540	0.00000	0.91784	0.00010	-0.00044	0.00000	0.00000

POS		S (M)	NUX	NUY	BETAX (M)	BETAY (M)	XEQ (M)	YEQ (M)	ZEQ (M)	ALPHAX	ALPHAY	DXEQ	DYEQ
701	#QD	4500.0000	3.75288	3.74206	115.94052	345.04989	2.22771	0.00000	0.93922	0.00004	-0.00038	0.00000	0.00000
717	#QF	4600.0000	3.83622	3.82536	344.91579	116.00708	3.69525	0.00000	0.96060	-0.00006	0.00006	0.00000	0.00000
733	#QD	4700.0000	3.91956	3.90866	115.95289	345.01422	2.22770	0.00000	0.98198	-0.00010	0.00044	0.00000	0.00000
749	#QF	4800.0000	4.00289	3.99200	344.97707	115.91887	3.69537	0.00000	1.00336	-0.00004	0.00038	0.00000	0.00000
765	#QD	4900.0000	4.08621	4.07537	115.96112	344.78746	2.22783	0.00000	1.02473	0.00006	-0.00006	0.00000	0.00000
781	#QF	5000.0000	4.16954	4.15873	344.94026	115.93086	3.69564	0.00000	1.04611	0.00010	-0.00044	0.00000	0.00000
797	#QD	5100.0000	4.25288	4.24206	115.94052	345.04989	2.22797	0.00000	1.06750	0.00004	-0.00038	0.00000	0.00000
813	#QF	5200.0000	4.33622	4.32536	344.91579	116.00708	3.69579	0.00000	1.08888	-0.00006	0.00006	0.00000	0.00000
829	#QD	5300.0000	4.41956	4.40867	115.95289	345.01422	2.22798	0.00000	1.11026	-0.00010	0.00044	0.00000	0.00000
845	#QF	5400.0000	4.50289	4.49200	344.97707	115.91887	3.69567	0.00000	1.13164	-0.00004	0.00038	0.00000	0.00000
861	#QD	5500.0000	4.58621	4.57537	115.96112	344.78746	2.22785	0.00000	1.15302	0.00006	-0.00006	0.00000	0.00000
877	#QF	5600.0000	4.66954	4.65874	344.94026	115.93086	3.69540	0.00000	1.17440	0.00010	-0.00044	0.00000	0.00000
893	#QD	5700.0000	4.75288	4.74206	115.94052	345.04989	2.22771	0.00000	1.19578	0.00004	-0.00038	0.00000	0.00000
909	#QF	5800.0000	4.83622	4.82536	344.91579	116.00708	3.69525	0.00000	1.21716	-0.00006	0.00006	0.00000	0.00000
923	#QD	5900.0000	4.91956	4.90867	115.95289	345.01421	2.22770	0.00000	1.23854	-0.00010	0.00044	0.00000	0.00000
937	#QF	6000.0000	5.00289	4.99200	344.97707	115.91887	3.69537	0.00000	1.25992	-0.00004	0.00038	0.00000	0.00000
951	#QD	6100.0000	5.08622	5.07537	115.96112	344.78746	2.22783	0.00000	1.28130	0.00006	-0.00006	0.00000	0.00000
965	#QF	6200.0000	5.16955	5.15874	344.94026	115.93086	3.69564	0.00000	1.30268	0.00010	-0.00044	0.00000	0.00000
979	#QD	6300.0000	5.25288	5.24206	115.94052	345.04990	2.22797	0.00000	1.32406	0.00004	-0.00038	0.00000	0.00000
993	#QF	6400.0000	5.33623	5.32536	344.91579	116.00708	3.69579	0.00000	1.34544	-0.00006	0.00006	0.00000	0.00000
1007	#QD	6500.0000	5.41956	5.40867	115.95289	345.01421	2.22798	0.00000	1.36683	-0.00010	0.00044	0.00000	0.00000
1021	#QF	6600.0000	5.50289	5.49200	344.97707	115.91886	3.69567	0.00000	1.38821	-0.00004	0.00038	0.00000	0.00000
1035	#QD	6700.0000	5.58622	5.57537	115.96112	344.78746	2.22785	0.00000	1.40959	0.00006	-0.00006	0.00000	0.00000
1049	#QF	6800.0000	5.66955	5.65874	344.94026	115.93086	3.69540	0.00000	1.43097	0.00010	-0.00044	0.00000	0.00000
1063	#QD	6900.0000	5.75289	5.74207	115.94052	345.04990	2.22771	0.00000	1.45235	0.00004	-0.00038	0.00000	0.00000
1077	#QF	7000.0000	5.83623	5.82536	344.91579	116.00708	3.69525	0.00000	1.47373	-0.00006	0.00006	0.00000	0.00000
1091	#QD	7100.0000	5.91956	5.90867	115.95289	345.01421	2.22770	0.00000	1.49511	-0.00010	0.00044	0.00000	0.00000
1105	#QF	7200.0000	6.00289	5.99201	344.97707	115.91886	3.69537	0.00000	1.51649	-0.00004	0.00038	0.00000	0.00000
1119	#QD	7300.0000	6.08622	6.07537	115.96112	344.78746	2.22783	0.00000	1.53787	0.00006	-0.00006	0.00000	0.00000
1133	#QF	7400.0000	6.16955	6.15874	344.94026	115.93086	3.69564	0.00000	1.55925	0.00010	-0.00044	0.00000	0.00000
1147	#QD	7500.0000	6.25289	6.24207	115.94052	345.04990	2.22797	0.00000	1.58063	0.00004	-0.00038	0.00000	0.00000
1161	#QF	7600.0000	6.33623	6.32536	344.91579	116.00708	3.69579	0.00000	1.60201	-0.00006	0.00006	0.00000	0.00000
1175	#QD	7700.0000	6.41956	6.40867	115.95289	345.01421	2.22798	0.00000	1.62339	-0.00010	0.00044	0.00000	0.00000
1189	#QF	7800.0000	6.50289	6.49201	344.97707	115.91886	3.69567	0.00000	1.64477	-0.00004	0.00038	0.00000	0.00000
1203	#QD	7900.0000	6.58622	6.57537	115.96112	344.78746	2.22785	0.00000	1.66616	0.00006	-0.00006	0.00000	0.00000
1219	#QF	8000.0000	6.66955	6.65874	344.94026	115.93086	3.69540	0.00000	1.68754	0.00010	-0.00044	0.00000	0.00000
1235	#QD	8100.0000	6.75289	6.74207	115.94052	345.04990	2.22771	0.00000	1.70892	0.00004	-0.00038	0.00000	0.00000
1251	#QF	8200.0000	6.83623	6.82537	344.91579	116.00708	3.69525	0.00000	1.73030	-0.00006	0.00006	0.00000	0.00000
1267	#QD	8300.0000	6.91957	6.90867	115.95289	345.01421	2.22770	0.00000	1.75168	-0.00010	0.00044	0.00000	0.00000
1283	#QF	8400.0000	7.00289	6.99201	344.97707	115.91886	3.69537	0.00000	1.77305	-0.00004	0.00038	0.00000	0.00000
1299	#QD	8500.0000	7.08622	7.07538	115.96112	344.78746	2.22783	0.00000	1.79443	0.00006	-0.00006	0.00000	0.00000
1315	#QF	8600.0000	7.16955	7.15874	344.94025	115.93086	3.69564	0.00000	1.81581	0.00010	-0.00044	0.00000	0.00000
1331	#QD	8700.0000	7.25289	7.24207	115.94052	345.04990	2.22797	0.00000	1.83719	0.00004	-0.00038	0.00000	0.00000
1347	#QF	8800.0000	7.33623	7.32537	344.91579	116.00708	3.69579	0.00000	1.85858	-0.00006	0.00006	0.00000	0.00000
1363	#QD	8900.0000	7.41957	7.40867	115.95289	345.01421	2.22798	0.00000	1.87996	-0.00010	0.00044	0.00000	0.00000

POS		S (M)	NUX	NUY	BETAX (M)	BETAY (M)	XEQ (M)	YEQ (M)	ZEQ (M)	ALPHAX	ALPHAY	DXEQ	DYEQ
1379	#QF	9000.0000	7.50290	7.49201	344.97707	115.91886	3.69567	0.00000	1.90134	-0.00004	0.00038	0.00000	0.00000
1395	#QD	9100.0000	7.58622	7.57538	115.96112	344.78746	2.22785	0.00000	1.92272	0.00006	-0.00006	0.00000	0.00000
1411	#QF	9200.0000	7.66955	7.65874	344.94025	115.93086	3.69540	0.00000	1.94410	0.00010	-0.00044	0.00000	0.00000
1427	#QD	9300.0000	7.75289	7.74207	115.94052	345.04990	2.22771	0.00000	1.96548	0.00004	-0.00038	0.00000	0.00000
1443	#QF	9400.0000	7.83623	7.82537	344.91579	116.00708	3.69525	0.00000	1.98686	-0.00006	0.00006	0.00000	0.00000
1459	#QD	9500.0000	7.91957	7.90867	115.95289	345.01420	2.22770	0.00000	2.00824	-0.00010	0.00044	0.00000	0.00000
1475	#QF	9600.0000	8.00290	7.99201	344.97707	115.91886	3.69537	0.00000	2.02962	-0.00004	0.00038	0.00000	0.00000
1491	#QD	9700.0000	8.08622	8.07538	115.96112	344.78746	2.22783	0.00000	2.05100	0.00006	-0.00006	0.00000	0.00000
1507	#QF	9800.0000	8.16955	8.15874	344.94025	115.93086	3.69564	0.00000	2.07238	0.00010	-0.00044	0.00000	0.00000
1523	#QD	9900.0000	8.25289	8.24207	115.94052	345.04990	2.22797	0.00000	2.09376	0.00004	-0.00038	0.00000	0.00000
1539	#QF	10000.0000	8.33623	8.32537	344.91579	116.00708	3.69579	0.00000	2.11514	-0.00006	0.00006	0.00000	0.00000
1555	#QD	10100.0000	8.41957	8.40867	115.95289	345.01420	2.22798	0.00000	2.13652	-0.00010	0.00044	0.00000	0.00000
1571	#QF	10200.0000	8.50290	8.49201	344.97707	115.91886	3.69567	0.00000	2.15791	-0.00004	0.00038	0.00000	0.00000
1587	#QD	10300.0000	8.58622	8.57538	115.96112	344.78746	2.22785	0.00000	2.17929	0.00006	-0.00006	0.00000	0.00000
1603	#QF	10400.0000	8.66955	8.65874	344.94025	115.93086	3.69540	0.00000	2.20067	0.00010	-0.00044	0.00000	0.00000
1619	#QD	10500.0000	8.75289	8.74207	115.94052	345.04991	2.22771	0.00000	2.22205	0.00004	-0.00038	0.00000	0.00000
1635	#QF	10600.0000	8.83623	8.82537	344.91579	116.00708	3.69525	0.00000	2.24343	-0.00006	0.00006	0.00000	0.00000
1651	#QD	10700.0000	8.91957	8.90867	115.95289	345.01420	2.22770	0.00000	2.26481	-0.00010	0.00044	0.00000	0.00000
1667	#QF	10800.0000	9.00290	8.99201	344.97707	115.91886	3.69537	0.00000	2.28619	-0.00004	0.00038	0.00000	0.00000
1683	#QD	10900.0000	9.08622	9.07538	115.96112	344.78746	2.22783	0.00000	2.30757	0.00006	-0.00006	0.00000	0.00000
1699	#QF	11000.0000	9.16955	9.15874	344.94025	115.93086	3.69564	0.00000	2.32895	0.00010	-0.00044	0.00000	0.00000
1715	#QD	11100.0000	9.25289	9.24207	115.94052	345.04991	2.22797	0.00000	2.35033	0.00004	-0.00038	0.00000	0.00000
1731	#QF	11200.0000	9.33623	9.32537	344.91579	116.00708	3.69579	0.00000	2.37171	-0.00006	0.00006	0.00000	0.00000
1747	#QD	11300.0000	9.41957	9.40867	115.95289	345.01420	2.22798	0.00000	2.39309	-0.00010	0.00044	0.00000	0.00000
1763	#QF	11400.0000	9.50290	9.49201	344.97707	115.91886	3.69567	0.00000	2.41447	-0.00004	0.00038	0.00000	0.00000
1779	#QD	11500.0000	9.58622	9.57538	115.96112	344.78746	2.22785	0.00000	2.43585	0.00006	-0.00006	0.00000	0.00000
1795	#QF	11600.0000	9.66956	9.65874	344.94025	115.93086	3.69540	0.00000	2.45724	0.00010	-0.00044	0.00000	0.00000
1811	#QD	11700.0000	9.75289	9.74207	115.94052	345.04991	2.22771	0.00000	2.47862	0.00004	-0.00038	0.00000	0.00000
1827	#QF	11800.0000	9.83624	9.82537	344.91579	116.00708	3.69525	0.00000	2.50000	-0.00006	0.00006	0.00000	0.00000
1843	#QD	11900.0000	9.91957	9.90867	115.95289	345.01420	2.22770	0.00000	2.52137	-0.00010	0.00044	0.00000	0.00000
1859	#QF	12000.000010.00290		9.99201	344.97707	115.91886	3.69537	0.00000	2.54275	-0.00004	0.00038	0.00000	0.00000
1875	#QD	12100.000010.0862310.07538			115.96112	344.78746	2.22783	0.00000	2.56413	0.00006	-0.00006	0.00000	0.00000
1891	#QF	12200.000010.1695610.15874			344.94025	115.93086	3.69564	0.00000	2.58551	0.00010	-0.00044	0.00000	0.00000
1907	#QD	12300.000010.2528910.24207			115.94052	345.04991	2.22797	0.00000	2.60689	0.00004	-0.00038	0.00000	0.00000
1923	#QF	12400.000010.3362410.32537			344.91579	116.00708	3.69579	0.00000	2.62828	-0.00006	0.00006	0.00000	0.00000
1939	#QD	12500.000010.4195710.40867			115.95289	345.01420	2.22798	0.00000	2.64966	-0.00010	0.00044	0.00000	0.00000
1955	#QF	12600.000010.5029010.49201			344.97707	115.91886	3.69567	0.00000	2.67104	-0.00004	0.00038	0.00000	0.00000
1971	#QD	12700.000010.5862310.57538			115.96112	344.78746	2.22785	0.00000	2.69242	0.00006	-0.00006	0.00000	0.00000
1985	#QFA	12800.000010.6695610.65875			344.98265	115.91649	3.69562	0.00000	2.71380	-0.01686	0.00531	0.00018	0.00000
1999	#QDB	12900.000010.7515710.74253			119.38016	341.62607	2.26405	0.00000	2.73518	-0.01751	0.00558	0.00054	0.00000
2013	#QFC	13000.000010.8322410.82677			355.39890	114.81138	3.80415	0.00000	2.75670	0.01713	-0.00575	0.00017	0.00000
2027	#QDD	13100.000010.9142210.91055			115.94105	345.06095	2.29897	0.00000	2.77861	0.03470	-0.01157	-0.00002	0.00000
2041	#QFE	13200.000010.9989610.99340			334.71148	117.11872	3.79964	0.00000	2.80066	-0.00004	0.00037	0.00000	0.00000
2055	#QDD	13300.000011.0837011.07629			115.94980	344.83826	2.29916	0.00000	2.82269	-0.03474	0.01194	0.00003	0.00000
2069	#QFC	13400.000011.1656711.16012			355.42545	114.73704	3.80470	0.00000	2.84472	-0.01709	0.00537	-0.00017	0.00000

POS	S (M)	NUX	NUY	BETAX (M)	BETAY (M)	XEQ (M)	YEQ (M)	ZEQ (M)	ALPHAX	ALPHAY	DXEQ	DYEQ
2083	#QDB13500.000011.246341	1.24439	119.38049	341.62905	2.26442	0.00000	2.86677	0.01759	-0.00633	-0.00054	0.00000	
2097	#QFA13600.000011.328351	1.32815	344.95764	115.99234	3.69617	0.00000	2.88869	0.01690	-0.00567	-0.00018	0.00000	
2111	#QD 13700.000011.411691	1.41145	115.95222	345.00863	2.22804	0.00000	2.91021	-0.00010	0.00045	0.00000	0.00000	
2125	#QFG13800.000011.495021	1.49479	345.02674	115.90002	3.69596	0.00000	2.93159	-0.02050	0.00730	0.00022	0.00000	
2139	#QDH13900.000011.576741	1.57872	120.44864	339.73856	2.27476	0.00000	2.95297	-0.15328	0.37708	0.00315	0.00000	
2153	#QFI14000.000011.648071	1.70670	441.16282	56.85767	4.31565	0.00000	2.97451	0.70565	0.00764	-0.00560	0.00000	
2167	#QDJ14100.000011.804281	1.83595	32.81468	333.68501	1.15795	0.00000	2.99840	0.10921	-0.00988	-0.01974	0.00000	
2181	#QFK14200.000011.986961	1.96357	368.93942	57.62868	0.36786	0.00000	3.01818	-1.60564	0.13797	-0.00577	0.00000	
2195	#6QD14300.000012.029401	2.11726	387.45180	258.46519	-0.00005	0.00000	3.02323	-0.77060	-1.52041	0.00000	0.00000	
2199	#5QF14329.500012.040431	2.13321	453.61228	347.27376	-0.00003	0.00000	3.02402	2.41253	-4.35972	0.00000	0.00000	
2203	#4QD14358.400012.056431	2.14162	179.05940	879.27934	0.00001	0.00001	3.02402	2.89286	-7.43037	0.00000	0.00000	
2205	#BV+14361.300012.059121	2.14214	165.27333	909.25540	0.00001	0.00001	3.02402	1.88488	-2.85407	0.00000	0.00000	
2211	#BV-14496.300012.402041	2.15868	158.39814	1863.12038	0.00021	0.17501	3.02402	-1.83395	-4.21148	0.00000	0.00000	
2212	#QDV14496.300012.402041	2.15868	158.39814	1863.12038	0.00021	0.17501	3.02377	-1.83395	-4.21148	0.00000	0.00000	
2216	#QFV14548.800012.425221	2.16928	823.37027	332.76632	0.00041	0.05306	3.02377	2.05416	4.52044	0.00000	-0.00167	
2220	#QDV14601.300012.481491	2.19578	27.82564	300.44523	0.00005	0.00000	3.02377	1.83395	4.21148	-0.00001	-0.00101	
2224	#QFV14653.800012.853111	2.63463	189.39026	65.06454	-0.00026	-0.05307	3.02377	-2.05416	-4.52044	0.00000	-0.00167	
2228	#QDV14706.300012.902041	2.65868	158.39815	1863.12048	-0.00021	-0.17501	3.02377	-1.83395	-4.21148	0.00000	0.00000	
2229	#BS+14706.300012.902041	2.65868	158.39815	1863.12048	-0.00021	-0.17501	3.02377	-1.83395	-4.21148	0.00000	0.00000	
2245	#BC-14878.500012.957481	2.66925	1606.85325	3611.66653	-0.00045	0.00000	3.02377	-6.57752	-5.94276	0.00000	0.00000	
2247	#3QD14884.550012.958041	2.66952	1897.66440	3256.34979	-0.00049	0.00000	3.02357	-43.42423	62.27142	-0.00001	0.00000	
2251	#2QF14897.050012.958781	2.67050	3845.64863	1255.90102	-0.00069	0.00000	3.02357	-51.93854	49.34614	-0.00001	0.00000	
2255	#2QF14908.950012.959271	2.67271	3338.61835	674.23926	-0.00064	0.00000	3.02357	87.79247	6.86598	0.00002	0.00000	
2259	#1QD14918.800012.960001	2.67505	1330.16991	690.82755	-0.00040	0.00000	3.02357	73.57614	2.75010	0.00002	0.00000	
2263	#1QD14926.600012.961471	2.67704	569.94968	527.61717	-0.00026	0.00000	3.02357	30.38403	16.74785	0.00001	0.00000	
2266	#IP-14950.000013.204621	2.92031	0.99996	1.00024	0.00002	0.00000	3.02357	0.00027	-0.00031	0.00001	0.00000	
2267	#IP-14950.000013.204621	2.92031	0.99996	1.00024	0.00002	0.00000	3.02357	0.00027	-0.00031	0.00001	0.00000	
2270	#QF114973.400013.447881	3.16344	527.77023	569.78896	0.00028	0.00000	3.02357	-16.75268	-30.37539	0.00001	0.00000	
2274	#QF114981.200013.449871	3.16491	691.02750	1329.79313	0.00032	0.00000	3.02357	-2.75087	-73.55523	0.00000	0.00000	
2278	#QD214991.050013.452201	3.16564	674.43374	3337.67067	0.00031	0.00001	3.02357	-6.86792	-87.76748	0.00000	0.00000	
2282	#QD215002.950013.454411	3.16614	1256.26181	3844.55554	0.00041	0.00001	3.02357	-49.36027	51.92383	0.00002	0.00000	
2286	#QF315015.450013.455391	3.16688	3257.28335	1897.12394	0.00065	0.00000	3.02357	-62.28922	43.41192	0.00001	0.00000	
2288	#BC-15021.500013.455671	3.16744	3612.70134	1606.39496	0.00069	0.00000	3.02357	5.94451	6.57570	0.00000	0.00000	
2304	#BS+15193.700013.466241	3.22289	1863.66567	158.35307	0.00044	-0.17501	3.02357	4.21249	1.83334	0.00000	0.00000	
2305	#QFV15193.700013.466241	3.22289	1863.66567	158.35307	0.00044	-0.17501	3.02336	4.21249	1.83334	0.00000	0.00000	
2309	#QDV15246.200013.490281	3.27183	65.08700	189.35550	0.00006	-0.28859	3.02336	4.52188	2.05355	-0.00001	0.00167	
2313	#QFV15298.700013.929141	3.64342	300.49386	27.81937	-0.00024	0.00000	3.02336	-4.21249	-1.83334	0.00000	0.00551	
2317	#QDV15351.200013.955641	3.69971	332.85305	823.12576	-0.00021	0.28859	3.02336	-4.52188	-2.05355	0.00000	0.00167	
2321	#QFV15403.700013.966241	3.72289	1863.66558	158.35306	-0.00044	0.17501	3.02336	4.21249	1.83334	0.00000	0.00000	
2322	#BV-15403.700013.966241	3.72289	1863.66558	158.35306	-0.00044	0.17501	3.02336	4.21249	1.83334	0.00000	0.00000	
2328	#BV+15538.700013.982771	4.06578	909.60310	165.28101	-0.00025	0.00001	3.02336	2.85464	-1.88466	0.00000	0.00000	
2330	#QF415541.600013.983281	4.06847	879.61857	179.06587	-0.00025	0.00001	3.02311	7.43272	-2.89266	0.00000	0.00000	
2334	#QD515570.500013.991691	4.08447	347.42617	453.60065	-0.00014	0.00001	3.02311	4.36115	-2.41217	0.00000	0.00000	
2338	#QF615600.000014.007631	4.09550	258.60104	387.42554	-0.00009	0.00001	3.02311	1.52083	0.77085	0.00000	0.00000	
2352	#KQD15700.000014.161251	4.13795	57.63434	368.88563	0.37216	0.00000	3.02311	-0.13735	1.60539	0.00904	0.00000	

POS	S (M)	NUX	NUY	BETAX (M)	BETAY (M)	XEQ (M)	YEQ (M)	ZEQ (M)	ALPHAX	ALPHAY	DXEQ	DYEQ
2366	#JQF15800.000014.	2889214.	32062	333.45955	32.82085	1.80144	-0.00001	3.02391	0.01005	-0.10929	0.00517	0.00000
2380	#IQD15900.000014.	4182414.	47681	56.84466	441.17236	1.40672	-0.00003	3.03143	-0.00830	-0.70557	0.00929	0.00000
2394	#HQF16000.000014.	5461914.	54814	339.95094	120.45323	3.66378	-0.00001	3.04274	-0.37742	0.15322	0.00413	0.00000
2408	#GQD16100.000014.	6300714.	62986	115.93680	345.06665	2.22757	0.00000	3.06099	-0.00671	0.02038	0.00013	0.00000
2422	#QF 16200.000014.	7134114.	71317	344.87164	115.98165	3.69518	0.00001	3.08227	0.00015	0.00007	0.00000	0.00000
2436	#AQD16300.000014.	7967714.	79649	115.90990	345.01584	2.22747	0.00002	3.10365	0.00567	-0.01681	-0.00011	0.00000
2450	#BQF16400.000014.	8805714.	87849	341.49241	119.39138	3.67293	0.00002	3.12503	0.00583	-0.01751	-0.00012	0.00000
2464	#CQD16500.000014.	9648514.	95916	114.75365	355.43185	2.20462	0.00003	3.14633	-0.00586	0.01708	-0.00012	0.00000
2478	#DQF16600.000015.	0486615.	04112	344.99387	115.96186	3.64959	0.00001	3.16754	-0.01193	0.03465	0.00000	0.00000
2492	#EQD16700.000015.	1315215.	12585	117.13418	334.77099	2.20454	0.00001	3.18866	0.00012	-0.00003	0.00000	0.00000
2506	#DQF16800.000015.	2143815.	21057	344.92006	115.96891	3.64982	-0.00001	3.20979	0.01205	-0.03469	0.00000	0.00000
2520	#CQD16900.000015.	2982115.	29254	114.72902	355.45325	2.20485	-0.00002	3.23091	0.00573	-0.01705	0.00012	0.00000
2534	#BQF17000.000015.	3825015.	37320	341.49344	119.39165	3.67339	-0.00002	3.25204	-0.00608	0.01758	0.00012	0.00000
2548	#AQD17100.000015.	4662915.	45520	115.93504	344.99568	2.22770	-0.00003	3.27325	-0.00579	0.01685	0.00011	0.00000
2562	#QF 17200.000015.	5496315.	53853	344.94491	115.97447	3.69541	-0.00001	3.29455	-0.00002	-0.00010	0.00000	0.00000
2578	#QD 17300.000015.	6329615.	62184	115.95370	345.01404	2.22774	-0.00001	3.31593	-0.00001	0.00011	0.00000	0.00000
2594	#QF 17400.000015.	7162915.	70517	344.95035	115.95141	3.69531	0.00000	3.33731	0.00001	0.00022	0.00000	0.00000
2610	#QD 17500.000015.	7996315.	78851	115.95133	344.88441	2.22774	0.00002	3.35869	0.00002	0.00010	0.00000	0.00000
2626	#QF 17600.000015.	8829615.	87186	344.93785	115.93090	3.69542	0.00002	3.38007	0.00001	-0.00011	0.00000	0.00000
2642	#QD 17700.000015.	9663015.	95520	115.94950	344.95302	2.22785	0.00003	3.40145	-0.00001	-0.00022	0.00000	0.00000
2658	#QF 17800.000016.	0496316.	03853	344.94491	115.97447	3.69562	0.00001	3.42283	-0.00002	-0.00010	0.00000	0.00000
2674	#QD 17900.000016.	1329616.	12185	115.95370	345.01404	2.22795	0.00001	3.44421	-0.00001	0.00011	0.00000	0.00000
2690	#QF 18000.000016.	2162916.	20517	344.95035	115.95141	3.69572	0.00000	3.46559	0.00001	0.00022	0.00000	0.00000
2706	#QD 18100.000016.	2996316.	28851	115.95133	344.88441	2.22795	-0.00002	3.48697	0.00002	0.00010	0.00000	0.00000
2722	#QF 18200.000016.	3829616.	37186	344.93785	115.93090	3.69562	-0.00002	3.50835	0.00001	-0.00011	0.00000	0.00000
2738	#QD 18300.000016.	4663016.	45521	115.94950	344.95303	2.22784	-0.00003	3.52973	-0.00001	-0.00022	0.00000	0.00000
2754	#QF 18400.000016.	5496316.	53853	344.94491	115.97447	3.69541	-0.00001	3.55111	-0.00002	-0.00010	0.00000	0.00000
2770	#QD 18500.000016.	6329616.	62185	115.95370	345.01404	2.22774	-0.00001	3.57249	-0.00001	0.00011	0.00000	0.00000
2786	#QF 18600.000016.	7163016.	70517	344.95035	115.95141	3.69531	0.00000	3.59387	0.00001	0.00022	0.00000	0.00000
2802	#QD 18700.000016.	7996316.	78851	115.95133	344.88441	2.22774	0.00002	3.61525	0.00002	0.00010	0.00000	0.00000
2818	#QF 18800.000016.	8829616.	87186	344.93785	115.93090	3.69542	0.00002	3.63663	0.00001	-0.00011	0.00000	0.00000
2834	#QD 18900.000016.	9663016.	95521	115.94950	344.95303	2.22785	0.00003	3.65801	-0.00001	-0.00022	0.00000	0.00000
2850	#QF 19000.000017.	0496317.	03853	344.94491	115.97447	3.69562	0.00001	3.67939	-0.00002	-0.00010	0.00000	0.00000
2866	#QD 19100.000017.	1329617.	12185	115.95370	345.01404	2.22795	0.00001	3.70077	-0.00001	0.00011	0.00000	0.00000
2882	#QF 19200.000017.	2163017.	20517	344.95035	115.95141	3.69572	0.00000	3.72216	0.00001	0.00022	0.00000	0.00000
2898	#QD 19300.000017.	2996317.	28851	115.95133	344.88441	2.22795	-0.00002	3.74354	0.00002	0.00010	0.00000	0.00000
2914	#QF 19400.000017.	3829617.	37187	344.93785	115.93090	3.69562	-0.00002	3.76492	0.00001	-0.00011	0.00000	0.00000
2930	#QD 19500.000017.	4663017.	45521	115.94950	344.95303	2.22784	-0.00003	3.78630	-0.00001	-0.00022	0.00000	0.00000
2946	#QF 19600.000017.	5496317.	53853	344.94491	115.97447	3.69541	-0.00001	3.80768	-0.00002	-0.00010	0.00000	0.00000
2962	#QD 19700.000017.	6329717.	62185	115.95370	345.01403	2.22774	-0.00001	3.82906	-0.00001	0.00011	0.00000	0.00000
2978	#QF 19800.000017.	7163017.	70517	344.95035	115.95141	3.69531	0.00000	3.85044	0.00001	0.00022	0.00000	0.00000
2994	#QD 19900.000017.	7996317.	78852	115.95133	344.88441	2.22774	0.00002	3.87182	0.00002	0.00010	0.00000	0.00000
3010	#QF 20000.000017.	8829717.	87187	344.93785	115.93090	3.69542	0.00002	3.89320	0.00001	-0.00011	0.00000	0.00000
3026	#QD 20100.000017.	9663017.	95521	115.94950	344.95303	2.22785	0.00003	3.91458	-0.00001	-0.00022	0.00000	0.00000
3042	#QF 20200.000018.	0496318.	03853	344.94491	115.97447	3.69562	0.00001	3.93596	-0.00002	-0.00010	0.00000	0.00000

POS		S (M)	NUX	NUY	BETAX (M)	BETAY (M)	XEQ (M)	YEQ (M)	ZEQ (M)	ALPHAX	ALPHAY	DXEQ	DYEQ
3058	#QD	20300.000018	.132971	8.12185	115.95370	345.01403	2.22795	0.00001	3.95734	-0.00001	0.00011	0.00000	0.00000
3074	#QF	20400.000018	.216301	8.20517	344.95035	115.95141	3.69572	0.00000	3.97872	0.00001	0.00022	0.00000	0.00000
3090	#QD	20500.000018	.299631	8.28852	115.95133	344.88441	2.22795	-0.00002	4.00010	0.00002	0.00010	0.00000	0.00000
3106	#QF	20600.000018	.382971	8.37187	344.93785	115.93090	3.69562	-0.00002	4.02149	0.00001	-0.00011	0.00000	0.00000
3122	#QD	20700.000018	.466301	8.45521	115.94950	344.95303	2.22784	-0.00003	4.04287	-0.00001	-0.00022	0.00000	0.00000
3138	#QF	20800.000018	.549641	8.53853	344.94491	115.97447	3.69541	-0.00001	4.06425	-0.00002	-0.00010	0.00000	0.00000
3152	#QD	20900.000018	.632971	8.62185	115.95370	345.01403	2.22774	-0.00001	4.08563	-0.00001	0.00011	0.00000	0.00000
3166	#QF	21000.000018	.716301	8.70517	344.95035	115.95141	3.69531	0.00000	4.10701	0.00001	0.00022	0.00000	0.00000
3180	#QD	21100.000018	.799631	8.78852	115.95133	344.88441	2.22774	0.00002	4.12839	0.00002	0.00010	0.00000	0.00000
3194	#QF	21200.000018	.882971	8.87187	344.93785	115.93090	3.69542	0.00002	4.14977	0.00001	-0.00011	0.00000	0.00000
3208	#QD	21300.000018	.966301	8.95521	115.94950	344.95303	2.22785	0.00003	4.17115	-0.00001	-0.00022	0.00000	0.00000
3222	#QF	21400.000019	.049641	9.03853	344.94491	115.97447	3.69562	0.00001	4.19253	-0.00002	-0.00010	0.00000	0.00000
3236	#QD	21500.000019	.132971	9.12185	115.95370	345.01403	2.22795	0.00001	4.21391	-0.00001	0.00011	0.00000	0.00000
3250	#QF	21600.000019	.216301	9.20518	344.95035	115.95141	3.69572	0.00000	4.23529	0.00001	0.00022	0.00000	0.00000
3264	#QD	21700.000019	.299631	9.28852	115.95133	344.88441	2.22795	-0.00002	4.25667	0.00002	0.00010	0.00000	0.00000
3278	#QFG	21800.000019	.382971	9.37187	344.98899	115.91357	3.69589	-0.00002	4.27805	-0.02045	0.00682	0.00022	0.00000
3292	#QDH	21900.000019	.464701	9.45577	120.43622	339.90098	2.27479	-0.00003	4.29943	-0.15333	0.37712	0.00315	0.00000
3306	#QFI	22000.000019	.536041	9.58370	441.15700	56.86444	4.31581	-0.00001	4.32097	0.70552	0.00813	-0.00560	0.00000
3320	#QDJ	22100.000019	.692231	9.71298	32.81853	333.52208	1.15802	0.00001	4.34486	0.10925	-0.00979	-0.01974	0.00000
3334	#QFK	22200.000019	.874911	9.84065	368.90129	57.62425	0.36794	0.00001	4.36465	-1.60541	0.13747	-0.00577	0.00000
3348	#QDL	22298.750019	.916841	9.99352	386.56551	254.09727	-0.00004	0.00002	4.36969	-1.06081	-1.31141	0.00000	0.00000
3352	#QFP	22306.250019	.919821	9.99810	414.15734	266.85807	-0.00004	0.00002	4.37049	-1.29433	-1.25264	0.00000	0.00000
3356	#QDM	22547.000019	.985222	0.05227	903.90686	1891.06172	0.00005	0.00004	4.37049	-8.63535	10.30683	0.00000	0.00000
3360	#QFN	22560.000019	.987132	0.05355	1297.66823	1380.14599	0.00006	0.00003	4.37049	-9.63992	10.93426	0.00000	0.00000
3363	#CEN	23050.000020	.052522	0.11892	1124.81060	1125.10803	0.00016	0.00001	4.37049	0.00009	0.00010	0.00000	0.00000
3366	#QDN	23540.000020	.117902	0.18430	1379.70584	1297.72162	0.00026	-0.00001	4.37049	-10.93084	9.64064	0.00000	0.00000
3370	#QFM	23553.000020	.119182	0.18621	1890.46066	903.93703	0.00030	-0.00001	4.37049	-10.30363	8.63597	0.00000	0.00000
3374	#QDP	23793.750020	.173362	0.25161	266.80383	414.06858	0.00013	-0.00002	4.37049	1.25213	1.29430	0.00000	0.00000
3378	#QFL	23801.250020	.177952	0.25459	254.04942	386.47918	0.00013	-0.00002	4.37049	1.31090	1.06081	0.00000	0.00000
3392	#KQD	23900.000020	.330812	0.29653	57.63803	368.81024	0.37210	-0.00002	4.37049	-0.13758	1.60487	0.00904	0.00000
3406	#JQF	24000.000020	.458462	0.47919	333.53259	32.83014	1.80106	-0.00001	4.37129	0.01012	-0.10935	0.00517	0.00000
3420	#IQD	24100.000020	.587772	0.63536	56.83994	441.13386	1.40656	0.00000	4.37881	-0.00808	-0.70524	0.00929	0.00000
3434	#HQF	24200.000020	.715742	0.70670	339.87902	120.42126	3.66362	0.00001	4.39012	-0.37744	0.15328	0.00413	0.00000
3448	#GQD	24300.000020	.799632	0.78844	115.93386	344.98959	2.22761	0.00002	4.40837	-0.00694	0.02020	0.00013	0.00000
3462	#QF	24400.000020	.882972	0.87176	344.93566	115.98629	3.69544	0.00002	4.42965	0.00001	-0.00021	0.00000	0.00000
3476	#QD	24500.000020	.966302	0.95507	115.94881	345.06404	2.22784	0.00003	4.45103	-0.00002	0.00015	0.00000	0.00000
3490	#QF	24600.000021	.049642	1.03838	344.94505	115.95640	3.69557	0.00001	4.47241	-0.00003	0.00036	0.00000	0.00000
3504	#QD	24700.000021	.132972	1.12173	115.95444	344.84928	2.22791	0.00001	4.49379	-0.00001	0.00021	0.00000	0.00000
3518	#QF	24800.000021	.216302	1.20509	344.95240	115.91410	3.69565	0.00000	4.51517	0.00002	-0.00015	0.00000	0.00000
3532	#QD	24900.000021	.299632	1.28844	115.95128	344.93820	2.22791	-0.00002	4.53655	0.00003	-0.00036	0.00000	0.00000
3546	#QF	25000.000021	.382972	1.37176	344.93566	115.98629	3.69559	-0.00002	4.55793	0.00001	-0.00021	0.00000	0.00000
3560	#QD	25100.000021	.466302	1.45507	115.94881	345.06404	2.22785	-0.00003	4.57931	-0.00002	0.00015	0.00000	0.00000
3574	#QF	25200.000021	.549642	1.53838	344.94505	115.95640	3.69546	-0.00001	4.60069	-0.00003	0.00036	0.00000	0.00000
3588	#QD	25300.000021	.632972	1.62173	115.95444	344.84928	2.22778	-0.00001	4.62207	-0.00001	0.00021	0.00000	0.00000
3604	#QF	25400.000021	.716302	1.70509	344.95240	115.91410	3.69539	0.00000	4.64345	0.00002	-0.00015	0.00000	0.00000

POS		S (M)	NUX	NUY	BETAX (M)	BETAY (M)	XEQ (M)	YEQ (M)	ZEQ (M)	ALPHAX	ALPHAY	DXEQ	DYEQ
3620	#QD	25500.000021.7996321.78844			115.95128	344.93820	2.22777	0.00002	4.66483	0.00003	-0.00036	0.00000	0.00000
3636	#QF	25600.000021.8829721.87176			344.93566	115.98629	3.69544	0.00002	4.68621	0.00001	-0.00021	0.00000	0.00000
3652	#QD	25700.000021.9663021.95507			115.94881	345.06403	2.22784	0.00003	4.70759	-0.00002	0.00015	0.00000	0.00000
3668	#QF	25800.000022.0496422.03838			344.94505	115.95640	3.69557	0.00001	4.72897	-0.00003	0.00036	0.00000	0.00000
3684	#QD	25900.000022.1329722.12173			115.95444	344.84928	2.22791	0.00001	4.75035	-0.00001	0.00021	0.00000	0.00000
3700	#QF	26000.000022.2163022.20509			344.95240	115.91410	3.69565	0.00000	4.77173	0.00002	-0.00015	0.00000	0.00000
3716	#QD	26100.000022.2996422.28844			115.95128	344.93820	2.22791	-0.00002	4.79312	0.00003	-0.00036	0.00000	0.00000
3732	#QF	26200.000022.3829722.37176			344.93566	115.98629	3.69559	-0.00002	4.81450	0.00001	-0.00021	0.00000	0.00000
3748	#QD	26300.000022.4663122.45507			115.94881	345.06403	2.22785	-0.00003	4.83588	-0.00002	0.00015	0.00000	0.00000
3764	#QF	26400.000022.5496422.53838			344.94505	115.95640	3.69546	-0.00001	4.85726	-0.00003	0.00036	0.00000	0.00000
3780	#QD	26500.000022.6329722.62173			115.95444	344.84928	2.22778	-0.00001	4.87864	-0.00001	0.00021	0.00000	0.00000
3796	#QF	26600.000022.7163022.70509			344.95240	115.91410	3.69539	0.00000	4.90002	0.00002	-0.00015	0.00000	0.00000
3812	#QD	26700.000022.7996422.78844			115.95128	344.93820	2.22777	0.00002	4.92140	0.00003	-0.00036	0.00000	0.00000
3828	#QF	26800.000022.8829722.87176			344.93566	115.98629	3.69544	0.00002	4.94278	0.00001	-0.00021	0.00000	0.00000
3844	#QD	26900.000022.9663122.95507			115.94881	345.06403	2.22784	0.00003	4.96416	-0.00002	0.00015	0.00000	0.00000
3860	#QF	27000.000023.0496423.03839			344.94505	115.95640	3.69557	0.00001	4.98554	-0.00003	0.00036	0.00000	0.00000
3876	#QD	27100.000023.1329723.12173			115.95444	344.84928	2.22791	0.00001	5.00692	-0.00001	0.00021	0.00000	0.00000
3892	#QF	27200.000023.2163123.20509			344.95240	115.91410	3.69565	0.00000	5.02830	0.00002	-0.00015	0.00000	0.00000
3908	#QD	27300.000023.2996423.28844			115.95128	344.93820	2.22791	-0.00002	5.04968	0.00003	-0.00036	0.00000	0.00000
3924	#QF	27400.000023.3829723.37176			344.93566	115.98629	3.69559	-0.00002	5.07106	0.00001	-0.00021	0.00000	0.00000
3940	#QD	27500.000023.4663123.45507			115.94881	345.06403	2.22785	-0.00003	5.09244	-0.00002	0.00015	0.00000	0.00000
3956	#QF	27600.000023.5496423.53839			344.94505	115.95640	3.69546	-0.00001	5.11383	-0.00003	0.00036	0.00000	0.00000
3972	#QD	27700.000023.6329723.62173			115.95444	344.84928	2.22778	-0.00001	5.13521	-0.00001	0.00021	0.00000	0.00000
3988	#QF	27800.000023.7163123.70509			344.95240	115.91410	3.69539	0.00000	5.15659	0.00002	-0.00015	0.00000	0.00000
4004	#QD	27900.000023.7996423.78844			115.95128	344.93820	2.22777	0.00002	5.17797	0.00003	-0.00036	0.00000	0.00000
4020	#QF	28000.000023.8829723.87177			344.93566	115.98629	3.69544	0.00002	5.19935	0.00001	-0.00021	0.00000	0.00000
4036	#QD	28100.000023.9663123.95507			115.94881	345.06403	2.22784	0.00003	5.22073	-0.00002	0.00015	0.00000	0.00000
4052	#QF	28200.000024.0496424.03839			344.94505	115.95640	3.69557	0.00001	5.24211	-0.00003	0.00036	0.00000	0.00000
4068	#QD	28300.000024.1329824.12173			115.95444	344.84928	2.22791	0.00001	5.26349	-0.00001	0.00021	0.00000	0.00000
4084	#QF	28400.000024.2163124.20509			344.95240	115.91410	3.69565	0.00000	5.28487	0.00002	-0.00015	0.00000	0.00000
4100	#QD	28500.000024.2996424.28844			115.95128	344.93821	2.22791	-0.00002	5.30625	0.00003	-0.00036	0.00000	0.00000
4116	#QF	28600.000024.3829724.37177			344.93566	115.98629	3.69559	-0.00002	5.32763	0.00001	-0.00021	0.00000	0.00000
4132	#QD	28700.000024.4663124.45507			115.94881	345.06403	2.22785	-0.00003	5.34901	-0.00002	0.00015	0.00000	0.00000
4148	#QF	28800.000024.5496424.53839			344.94505	115.95640	3.69546	-0.00001	5.37039	-0.00003	0.00036	0.00000	0.00000
4164	#QD	28900.000024.6329824.62173			115.95444	344.84928	2.22778	-0.00001	5.39177	-0.00001	0.00021	0.00000	0.00000
4178	#QFA	29000.000024.7163124.70510			344.99481	115.89973	3.69561	0.00000	5.41315	-0.01695	0.00560	0.00018	0.00000
4192	#QDB	29100.000024.7983124.78891			119.39121	341.51544	2.26412	0.00002	5.43453	-0.01752	0.00559	0.00054	0.00000
4206	#QFC	29200.000024.8789824.87317			355.42066	114.79136	3.80434	0.00002	5.45605	0.01720	-0.00602	0.00017	0.00000
4220	#QDD	29300.000024.9609624.95694			115.93765	345.11314	2.29911	0.00003	5.47796	0.03479	-0.01185	-0.00002	0.00000
4234	#QFE	29400.000025.0457025.03978			334.68066	117.15668	3.79985	0.00001	5.50001	-0.00003	0.00036	0.00000	0.00000
4248	#QDD	29500.000025.1304525.12264			115.94286	344.89902	2.29923	0.00001	5.52204	-0.03481	0.01221	0.00003	0.00000
4262	#QFC	29600.000025.2124225.20647			355.43645	114.71988	3.80471	-0.00001	5.54407	-0.01718	0.00566	-0.00017	0.00000
4276	#QDB	29700.000025.2930925.29076			119.39141	341.51831	2.26436	-0.00002	5.56612	0.01758	-0.00631	-0.00054	0.00000
4290	#QFA	29800.000025.3750925.37454			344.97994	115.97266	3.69598	-0.00002	5.58804	0.01697	-0.00595	-0.00018	0.00000
4304	#QD	29900.000025.4584325.45785			115.94915	345.06193	2.22791	-0.00003	5.60956	-0.00001	0.00016	0.00000	0.00000

POS	S (M)	NUX	NUY	BETAX (M)	BETAY (M)	XEQ (M)	YEQ (M)	ZEQ (M)	ALPHAX	ALPHAY	DXEQ	DYEQ
4318	#QFG30000.000025.	5417625.	54116	344.99531	115.93761	3.69575	-0.00001	5.63094	-0.02048	0.00729	0.00022	0.00000
4332	#QDH30100.000025.	6234925.	62507	120.44069	339.79557	2.27468	-0.00001	5.65232	-0.15333	0.37742	0.00315	0.00000
4346	#QFI30200.000025.	6948325.	75306	441.16758	56.84154	4.31560	0.00001	5.67386	0.70556	0.00780	-0.00560	0.00000
4360	#QDJ30300.000025.	8510225.	88234	32.81737	333.63769	1.15800	0.00003	5.69775	0.10926	-0.01018	-0.01974	0.00000
4374	#QFK30400.000026.	0337026.	00996	368.90681	57.64575	0.36808	0.00001	5.71753	-1.60546	0.13788	-0.00577	0.00000
4388	#6QD30500.000026.	0761526.	16361	387.41618	258.47015	0.00014	0.00000	5.72258	-0.77055	-1.52012	0.00000	0.00000
4392	#5QF30529.500026.	0871826.	17956	453.57211	347.25791	0.00017	0.00000	5.72338	2.41229	-4.35920	0.00000	0.00000
4396	#4QD30558.400026.	1031826.	18797	179.04496	879.20965	0.00012	-0.00001	5.72338	2.89258	-7.42947	0.00000	0.00000
4398	#BV-30561.300026.	1058726.	18849	165.26028	909.18148	0.00012	-0.00001	5.72338	1.88468	-2.85353	0.00000	0.00000
4404	#BV+30696.300026.	4487726.	20503	158.39570	1862.85146	0.00005	-0.17502	5.72338	-1.83383	-4.21058	0.00000	0.00000
4405	#QDV30696.300026.	4487726.	20503	158.39570	1862.85146	0.00005	-0.17502	5.72313	-1.83383	-4.21058	0.00000	0.00000
4409	#QFV30748.800026.	4719526.	21563	823.33626	332.70588	0.00006	-0.05307	5.72313	2.05416	4.51989	0.00000	0.00167
4413	#QDV30801.300026.	5282326.	24214	27.82324	300.36726	-0.00002	-0.00001	5.72313	1.83383	4.21058	0.00000	0.00101
4417	#QFV30853.800026.	8998526.	68097	189.39798	65.06120	-0.00011	0.05307	5.72313	-2.05416	-4.51989	0.00000	0.00167
4421	#QDV30906.300026.	9487726.	70503	158.39571	1862.85155	-0.00005	0.17502	5.72313	-1.83383	-4.21058	0.00000	0.00000
4422	#BS-30906.300026.	9487726.	70503	158.39571	1862.85155	-0.00005	0.17502	5.72313	-1.83383	-4.21058	0.00000	0.00000
4438	#BC+31078.500027.	0042226.	71560	1606.73895	3611.01084	0.00004	0.00003	5.72313	-6.57699	-5.94141	0.00000	0.00000
4440	#3QD31084.550027.	0047826.	71588	1897.52860	3255.75557	0.00004	0.00002	5.72292	-43.42106	62.26033	0.00000	0.00000
4444	#2QF31097.050027.	0055226.	71685	3845.37127	1255.66772	0.00007	0.00002	5.72292	-51.93473	49.33724	0.00000	0.00000
4448	#2QF31108.950027.	0060126.	71906	3338.37633	674.10908	0.00006	0.00001	5.72292	87.78616	6.86491	0.00000	0.00000
4452	#1QD31118.800027.	0067426.	72140	1330.07276	690.68895	0.00004	0.00001	5.72292	73.57082	2.74981	0.00000	0.00000
4456	#1QD31126.600027.	0082126.	72339	569.90745	527.50798	0.00003	0.00001	5.72292	30.38184	16.74463	0.00000	0.00000
4459	#IP-31150.000027.	2513726.	96670	1.00003	1.00043	0.00001	0.00000	5.72292	0.00020	-0.00058	0.00000	0.00000

POS	S (M)	NUX	NUY	BETAX (M)	BETAY (M)	XEQ (M)	YEQ (M)	ZEQ (M)	ALPHAX	ALPHAY	DXEQ	DYEQ
4460	#IP-31150.000027.2513726.96670			1.00003	1.00043	0.00001	0.00000	5.72292	0.00020	-0.00058	0.00000	0.00000
4463	#QF131173.400027.4946227.20979			527.73683	569.69695	0.00000	-0.00001	5.72292	-16.75155	-30.37021	0.00000	0.00000
4467	#QF131181.200027.4966127.21126			690.98259	1329.57153	-0.00001	-0.00002	5.72292	-2.75062	-73.54270	0.00000	0.00000
4471	#QD231191.050027.4989427.21200			674.38859	3337.10595	-0.00001	-0.00003	5.72292	-6.86739	-87.75236	0.00000	0.00000
4475	#QD231202.950027.5011527.21249			1256.17546	3843.89850	-0.00002	-0.00003	5.72292	-49.35682	51.91524	0.00000	0.00000
4479	#QF331215.450027.5021327.21323			3257.05693	1896.79488	-0.00004	-0.00002	5.72292	-62.28483	43.40467	0.00000	0.00000
4481	#BC+31221.500027.5024127.21379			3612.44943	1606.11321	-0.00005	-0.00002	5.72292	5.94416	6.57482	0.00000	0.00000
4497	#BS-31393.700027.5129827.26926			1863.52141	158.30404	-0.00008	0.17500	5.72292	4.21222	1.83287	0.00000	0.00000
4498	#QFV31393.700027.5129827.26926			1863.52141	158.30404	-0.00008	0.17500	5.72271	4.21222	1.83287	0.00000	0.00000
4502	#QDV31446.200027.5370227.31821			65.08117	189.29705	-0.00003	0.28857	5.72271	4.52150	2.05282	0.00000	-0.00167
4506	#QFV31498.700027.9758827.68977			300.48022	27.81696	-0.00003	0.00000	5.72271	-4.21222	-1.83287	0.00000	-0.00551
4510	#QDV31551.200028.0023827.74607			332.82985	822.90451	0.00001	-0.28857	5.72271	-4.52150	-2.05282	0.00000	-0.00167
4514	#QFV31603.700028.0129827.76926			1863.52132	158.30403	0.00008	-0.17500	5.72271	4.21222	1.83287	0.00000	0.00000
4515	#BV+31603.700028.0129827.76926			1863.52132	158.30403	0.00008	-0.17500	5.72271	4.21222	1.83287	0.00000	0.00000
4521	#BV-31738.700028.0295128.11214			909.52429	165.31580	0.00010	0.00000	5.72271	2.85443	-1.88481	0.00000	0.00000
4523	#QF431741.600028.0300228.11482			879.54216	179.10205	0.00010	0.00000	5.72246	7.43211	-2.89299	0.00000	0.00000
4527	#QD531770.500028.0384428.13082			347.39487	453.66747	0.00008	0.00000	5.72246	4.36079	-2.41223	0.00000	0.00000
4531	#QF631800.000028.0543728.14185			258.57688	387.46659	0.00009	0.00000	5.72246	1.52070	0.77124	0.00000	0.00000
4545	#KQD31900.000028.2080028.18429			57.63584	368.86179	0.37217	0.00000	5.72246	-0.13744	1.60561	0.00904	0.00000
4559	#JQF32000.000028.3356628.36702			333.48927	32.81445	1.80129	0.00000	5.72326	0.01008	-0.10953	0.00517	0.00000
4573	#IQD32100.000028.4649828.52319			56.84274	441.31093	1.40663	0.00000	5.73078	-0.00821	-0.70587	0.00929	0.00000
4587	#HQF32200.000028.5929428.59450			339.92167	120.48451	3.66361	0.00000	5.74210	-0.37743	0.15346	0.00413	0.00000
4601	#GQD32300.000028.6768228.67620			115.93560	345.05559	2.22754	0.00000	5.76034	-0.00680	0.02070	0.00013	0.00000
4615	#QF 32400.000028.7601628.75953			344.89768	115.94737	3.69524	0.00000	5.78162	0.00009	0.00020	0.00000	0.00000

CIRCUMFERENCE = 97200.0000 M THETX = 6.28318529 RAD NUX = 86.28048 DNUX/(DP/P) = -0.00220
RADIUS = 15469.8605 M THETY = 0.00000000 RAD NUY = 86.27860 DNUY/(DP/P) = -0.00255
(DS/S)/(DP/P)= 0.0001791 TGAM=(74.72160, 0.00000)

MAXIMA --- BETX(2252) = 4009.14771 BETY(2280) = 4008.00883 XEQ(3306) = 4.31581 YEQ(2309) = -0.28859
MINIMA --- BETX(2267) = 0.99996 BETY(2267) = 1.00024 XEQ(4461) = 0.00000 YEQ(134) = 0.00000

SEXTUPOLE CORRECTIONS ----- DKSF = 0.14773875E-06 DKSD =-0.25354771E-06 KSF = 0.14598528E-01 KSD =-0.23402684E-01

END OF SYNCH RUN RLD1

Modules for 6.0 Tesla, Vertically Separated, Clustered or Distributed Lattices

S Peggs
SSC Central Design Group

1.0 INTRODUCTION

A total of four lattices have been designed for distributed and (3,3) clustered versions of the SSC, and are available in the SSC database, SSCDB. These lattices are constructed of the same four basic modules, which with only minor tuning can be re-organised to form many conceivable realistic geometries. One module is trivial, consisting of regular cells in a long main arc. The description of the other three modules is the central theme of this report. Potential improvements in both the modules and their implementation are also mentioned.

The lattices, with the generic name VSD1bnn.DAT, are in MAD/standard input format in the [SSCDB.LATTICES] directory of the database. Lower case letters in the generic name represent variable characters, where "b" is either C or D, according to whether the lattice is (3,3) Clustered or Distributed, and where "nn" is 01 or 10, according to whether the collision beta is $\beta^* = 1.0$ or 10.0 metres, in luminosity or injection lattices. The general title "VS" stands for the Vertical Separation of the two beam lines, with a (total) separation in the main arcs of 0.70 metres, while the notation "D1" reflects the regular cell dipoles of 6.0 Tesla ("D"), with a phase advance per cell of 60 degrees ("1"). The half cell length is 100 metres.

It would be useful for lattice designers and users in the SSC design community to agree on some such lattice naming convention, even if the agreement is merely informal. Two criticisms of the above convention are first, that since the magnet selection for the SSC has fixed the dipole field to be close to 6.4 Tesla, the "D" definition of dipole strength is redundant, and second, that collision betas of less than 1.0 metre can not be handled unless three digits, "nnn", are included. In the future other information,

such as the half cell length, might also be coded into the lattice name. The trick will be to maximise the information content while retaining a mnemonically useful, i.e. short, name length.

2.0 LATTICE MODULES

Figure 1 shows how the four main modules, LOB, VSEP, PT and ARC, are arranged between consecutive intersection points (IPs) in the clustered and distributed lattices. Starting from an IP of the distributed lattice sextant shown in figure 1a, the first module is LOB, for LOw Beta, which matches the collision betas into regular cell betas. It consists solely of quadrupoles and drifts, so that the horizontal and vertical dispersion functions η_h and η_v are zero throughout, and so that the beam, assumed to have zero vertical crossing angle, is not displaced from the horizontal plane. Except in LOB, and at its boundary with VSEP, the quadrupoles in all the modules are spaced by 100 metres, and have strengths which differ only slightly, if at all, from the regular cell quadrupole strengths. Consequently the beta functions are exactly, or very close to, their regular cell values everywhere, except in LOB.

After LOB comes VSEP, the Vertical SEParator, which displaces the beam vertically by means of vertical dipoles, arranged so that there is no vertical dispersion in the rest of the lattice. VSEP also includes horizontal dipoles to act as a horizontal dispersion suppressor, matching the horizontal dispersion function and its slope from zero at the entrance to regular cell values at the exit. The third module is PT, a Phase Trombone, which is made of regular cells full of horizontal dipoles, with variable strength quadrupoles. It enables the tune of the whole machine, or the phase advance between neighboring IPs, to be varied at will. Such variations will be necessary, for example, when going from injection optics to luminosity optics.

Finally comes ARC, with a self-evident name, consisting of a large number of regular cells - and half a cell at the end, to maintain the correct symmetry between IRs. The uninteresting details of the regular cells in the ARC will be put aside here, and attention will be focussed instead on the three other modules, which combine to make a clustered lattice 'segment', as shown in figure 1b. The behaviour of these modules, and their interfaces, will be described using the segments of the injection and luminosity lattices VSD1C10.DAT and VSD1C01.DAT as concrete examples. In practice the modules have to be tuned slightly differently for the clustered and distributed lattices, but these differences can be ignored for present purposes. There are no utility modules in any of the four lattices.

Figure 2 shows the layout and optical parameters of the segment in the β^*=1.0 metre lattice, with a total of just less than 3 kilometres between adjacent IPs. The drifts, dipoles and quadrupoles which make up the segment are shown in the linear display across the top of the figure, and correspond to the (root) beta functions and dispersion functions shown at the bottom. The layout display shows a quadrupole as a narrow rectangle, with a vertical height proportional to the field gradient or strength. Dipoles are shown as constant height broad rectangles, and drifts are not explicitly drawn. Those dipoles which are broken into two equal length pieces, such as BV4, BV5, BV10 and BV11, are consecutive vertical dipoles of opposite polarities, which displace the closed orbit from the horizontal plane in vertical 'steps'. The very small vertical dispersion inside VSEP which is caused by these steps is just visible, close to the horizontal axis at the bottom of the optical function display.

3.0 THE LOW BETA MATCHING MODULE, LOB

The layout and optical functions of LOB are shown in more detail in figure 3, which is an expansion of the first 10% of figure 2, with a total length of 185 metres between the IP and the first (vertical) dipole of the VSEP module. The first quad in VSEP is slightly more (60 metres) than a quarter cell length from the boundary of LOB, a separation which is vital to the operation of LOB, as is explained below. Since the roles of LOB and VSEP are combined in this region, the clear cut LOB/VSEP boundary, which is shown in the figures for the sake of clarity, does not truly exist.

LOB consists of four quadrupoles, of which the first three are arrranged in the usual triplet, with an experimental free space of L^*= 20 metres. After the triplet there is a drift of 120 metres before the fourth quadrupole. In this region the functions $b_h=\sqrt{\beta_h}$ and $b_v=\sqrt{\beta_v}$ vary almost exactly as straight lines (even after allowing for the graphical resolution), except that b_h 'collides' with, and then 'bounces' off, the horizontal axis. This important behaviour is easily understood by examining the differential equation for beta function propogation,

$$b''(s) + K(s)\, b(s) - b^{-3}(s) = 0 \qquad (1)$$

where K(s) is the quadrupole field gradient (which acquires a different sign according to whether b(s) is horizontal or vertical).

In the quadrupole free region (K=0) between the triplet and the fourth quadrupole, the propogation of b or β is well represented by the piecemeal matching of solutions of equation (1), in the limits of slow and rapid betatron phase advance. If b is large (that is, over small phase advances), then b"= 0, with the straight line behavior of b noted above. However, if β is small the phase variation cannot be ignored, and the solution is

$$\beta(s) = \beta_0 + (s - s_0)^2 / \beta_0 \qquad (2)$$

which is already familiar from the behaviour of β near the IP. The solution (2) shows that the beta bounce of b_h is 'elastic', since

$$b_h'(s<<s_0) = -b_h'(s>>s_0) \qquad (3)$$

as also observed in figure 3.

It is (apparently) quite natural for an IR triplet controling the beta functions coming from an IP to launch them at its exit with equal slopes, $b'_h \approx b'_v$, so that after the beta bounce, according to (3), the slopes are approximately equal and opposite. Now, if the fourth quadrupole of length L_4 is located at a position where $b_h = b_v = b_4$, it can be used to control the magnitude of these equal and opposite slopes, since according to (1)

$$\Delta b'_h \approx (K_4 L_4) . b_h = (K_4 L_4) . b_v \approx -\Delta b'_v \qquad (4)$$

If the fourth quadrupole is followed one quarter of a cell length later by a regular strength quadrupole, the strength K_4 can be adjusted to match into the regular cell beta functions, provided that the value of b_4 is correctly chosen. Loosely speaking, then, the IR triplet is tuned to produce b_h and b_v functions which have equal slopes on exit from the triplet, and which eventually cross with an appropriate value b_4 at the fourth quadrupole.

It is wise to increase the triplet-to-fourth-quad drift length as much as possible, in order to make the triplet focussing as weak as possible, because this decreases the chromaticity contribution of LOB to the natural chromaticity of the whole machine. This in turn will allow lower collision betas to become operationally acceptable in the luminosity lattice. As the collision beta is lowered with constant triplet

quadrupole strengths, almost the only effect, according to (1), is to scale up $\sqrt{\beta}$ by a constant factor. In practice the triplet needs to be only slightly retuned to hold the value b_4 constant, in order to match into the regular cells. Collision betas as low as 0.4 metres have been obtained in this way, with no lower limit from unacceptable magnet strengths in sight.

However, there is an upper limit to the collision beta possible for injection optics, causing the need for 10.0 metre injection optics to place an upper limit on the triplet-to-fourth quad drift length. It is in this sense that the injection optics determine the geometry of the LOB module. This is indirectly illustrated in the LOB module of VSD1C10.DAT shown in figure 4, where the strength K_4 has been reduced almost to zero, and where the fourth quadrupole can only be moved out a few more metres before matching solutions can no longer be found.

4.0 THE VERTICAL SEPARATION MODULE, VSEP

Seven full length half cells follow the 'quarter' cell (60 metre) section BV4 to comprise VSEP, as shown in detail in figure 5, for a total length of 760 metres. All quadrupoles in VSEP always have the regular cell strength, so that the phase advance between half cells is fixed at 30 degrees, a crucial characteristic for a vertical dispersion cancellation scheme which is independent of the collision beta. VSEP is also a conventional horizontal dispersion suppressor, with two half cells full of horizontal dipoles followed by two empty half cells, a function which only needs the module to be be four (and a half) half cells long. The additional three half cells are needed to pair BV4 with BV10, and BV5 with BV11, in a configuration where the ends of the members of each pair of vertical 'steps' are separated by 180 degrees.

The vertical dispersion downstream of VSEP is

$$\eta_v \,/\, \sqrt{\beta_v} \quad = \quad \sum_i -(\Delta z_i \,/\, \sqrt{\beta_{vi}}) \,.\, \cos(\phi - \phi_i) \qquad (5)$$

where β_i and ϕ_i are the vertical betatron function and phase at the end of the i'th vertical step of size Δz_i, the amount by which the closed orbit of the beam is shifted. This shows that for the cancellation of vertical dispersion the BV4 step size should equal that of BV10, and the step size of BV5 should equal that of BV11, since the beta functions at the end of two steps 180 degrees apart are identical. (Expression

(5) assumes that the vertical dispersion entering from LOB is zero, an assumption which is justified post facto, since the downstream dispersion does indeed vanish.)

This scheme of vertical dispersion suppression using vertical steps is quite similar to those reported elsewhere in this workshop summary, in two notes by Garren, and by Garren and Steffen. Those schemes differ principally by not having regular cell betatron functions in the separation module, and by using half quadrupoles at the end of a '-I' transfer line, which separates two steps of a single pair. The phase difference between the end of the first step and the beginning of the second step is slightly larger than 180 degrees.

Figure 5 shows how the closed orbit in VSEP is stepped to 6.5, 17.5, 24.0 and 35.0 centimetres, numbers which must be doubled to get the total separation of the two beams. This unfortunately means that the quadrupole between BV4 and BV5, where the total separation is only 13.0 centimetres, needs to be a 2-in-1 magnet. It is not possible to increase this separation appreciably, with a short 60 metre BV4, because its dipole field is already 5.86 Tesla. (The other fields are 3.27, 1.93 and 3.27 Tesla, respectively). In the next design iteration VSEP will have only one pair of 17.5 centimetre steps, with the first step after the fifth quadrupole, which can then be a 1-in-1 magnet. This will shift the focus of the practical problems to the first vertical step, which will be a mechanically awkward set of dipoles, starting with a 1-in-1 and ending in a double 1-in-1 configuration, possibly with a 2-in-1 low field large bore intermediary. However, it should be possible to make this first step significantly longer than 100 metres.

It is not trivially obvious that the first major separation of the two beams can be postponed beyond the fourth (or even the fifth) quadrupole from the IP. However, the step scheme presented here depends on such a postponement, since the quadrupole strengths between the first and last steps must be constant over a wide range of collision betas. In order to show that this is possible, consider the (vertical) tune shift ΔQ due to the series of long range beam-beam collisions which occur between the IP and the first vertical step.

$$\Delta Q = \sum 2\,(\varepsilon\beta/\gamma)\,.\,\xi\,.\,1/p^2 \qquad (6)$$

$$= \sum 2\xi\,.\,(p/\sigma)^{-2} \qquad (7)$$

Here ε is the normalised emittance, ξ is the head on tune shift parameter, γ is the relativistic factor, and p is the total beam separation, which, according to (7), is naturally measured in units of σ, the size

of the beam under consideration. Equation 7 also implies that postponement is acceptable if the value of p / σ can be maintained at (or increased beyond) its value at the IR triplet, for the interval between the triplet and the first separation step.

If both beams have a crossing angle of $\pm\alpha^*$ at the collision point, and if they both receive a trim separator kick of size $\pm\alpha_1$ just beyond the triplet, at a phase very close to $\pi/2$ for both beams, the separation beyond the triplet is

$$p / \sigma = (\gamma / \varepsilon)^{1/2} . [\, \alpha^* \sqrt{\beta^*} . \sin(\phi_v) + \alpha_1 \sqrt{\beta_{v1}} . \sin(\phi_v - \pi/2) \quad (8)$$

$$+ \alpha^* \sqrt{\beta^*} . (\beta_h / \beta_v)^{1/2} \sin(\phi_h) + \alpha_1 \sqrt{\beta_{h1}} . (\beta_h / \beta_v)^{1/2} \sin(\phi_h - \pi/2) \,]$$

where it should be noted that horizontal betas and phases for one beam translate directly into vertical betas and phases for the other. This equation shows that adequate separation can be maintained through the beta bounce, where the phase advances through 180 degrees, with a very small trim of approximately

$$\alpha_1 \approx (\beta^*/\beta_{v1})^{1/2} . \alpha^* << \alpha^* \approx 50 \ \mu\text{radians} \quad (9)$$

If necessary, additional small trim separators can be added between the triplet and the fourth quadrupole.

While it might be objected that these trim separators are a source of vertical dispersion around the lattice, another more important source which is also being ignored is the dipole field due to the closed orbit offset in each of the triplet quadrupoles, which is related to the non-zero crossing angle. While crossing angle and trim separator effects need to be examined together, in a more thorough analysis of SSC lattices, postponement of the first vertical separation step beyond the fourth or fifth quadrupole from the IP seems reasonable.

5.0 THE PHASE TROMBONE MODULE, PT

When the '2π' phase trombone is relaxed, it consists of five and a half regular 60 degree cells full of dipoles, with a total length of 1100 metres and a phase advance of $(11/12) * 2\pi$ in both planes. Figure 6 shows how the beta and horizontal dispersion functions are distorted in the $\beta^* = 10.0$ injection

lattice, when the segment tune advance is forced from its natural value of 2.951 to a value of 3 + 1/6, in both planes. Two periods of beta perturbation waves can be seen in PT, but only one period of a dispersion perturbation wave, while the optical functions in the VSEP modules on either side remain unaltered.

When the trombone is active, the 6 quadrupoles in each plane of PT (including those at the VSEP/PT boundary) are independently adjusted to match the exterior optics. Taken together with the 2 phase advances which are requested, the 6 matching conditions lead to a total of only 8 constraints, so that some of the 12 quadrupoles can be ganged together to have identical strengths. While the phase trombone could therefore be made shorter, with a minimum of only three and a half cells, a 2π phase trombone has natural advantages which justify the presence of the extra two cells in PT. (A major advantage of a 2π phase trombone built from 90 degree cells, with a natural length of three and a half cells, is that it would have exactly as many quadrupole variables as there are constraints.)

The natural advantages of a 2π phase trombone can be seen by considering the dispersion and beta function perturbation waves leaving the module, under the assumption that no errors enter from upstream. Downstream of PT the beta error, to first order, is

$$\Delta\beta / \beta \quad = \quad \sum_i \; 2\beta_i \; . \; \Delta q_i \; . \; \sin (2 (\phi - \phi_i)) \qquad (10)$$

and the downstream horizontal dispersion error is

$$\Delta\eta_x / \sqrt{\beta} \quad = \quad \sum_i \; \sqrt{\beta_i}\eta_{xi} \; . \; \Delta q_i \; \sin (\phi - \phi_i) \qquad (11)$$

while the change in the phase advance is

$$\Delta \phi \quad = \quad \sum_i \; \beta_i \; . \; \Delta q_i \; / \; 2 \qquad (12)$$

In these expressions q_i is the focal strength KL of the i'th quadrupole, assumed thin, and Δq_i is the deviation away from the regular strength, with a different sign for the different transverse planes.

The scalar sensitivity of a given quadrupole location is $2\beta_i$ in (10) for producing beta errors, and $\sqrt{\beta_i}\eta_{xi}$ in (11) for producing horizontal dispersion errors. Figure 7 shows a phasor representation of these two equations, in which all the sensitivity vectors for the six quadrupoles in a given plane of the

phase trombone are of equal length, with an angular spacing of 60 or 120 degrees. Since the resultant vector is of zero length for both beta and dispersion perturbations, if all the (say) horizontal quadrupoles are perturbed by the same amount Δq_h, there will be no first order optical perturbation downstream of the phase trombone.

While this analysis seems to make it possible to have a 2π phase trombone such as PT work with only two power supplies, one for all of the quadrupoles in each plane, it is practically advisable to keep the quadrupoles independent of one another. This is true even for the idealised case considered so far, with no optical errors and zero crossing angle, because the higher order effects of PT can not be ignored. In practice the phase advances in both planes are usually changed by about the same amount, and the strengths of both horizontal and vertical quadrupoles are quite similar. The moderately strong squeezing of 0.216 tune units shown in figure 6, for example, was acheived using 12 different quadrupole strengths, with a mean and standard deviation of 1.199 ± 0.052 times the regular cell quadrupole strength.

Another major reason for keeping the quadrupole strengths independent is that flexible 'phase trombones' at the ends of the long main arcs, (which can have their regular cells slightly retuned to adjust the phase advance), could also be used to correct the large optical errors which must be expected to accumulate in the arcs. Finally, flexible phase trombones may be very useful in the dynamic control of vertical dispersion for variable crossing angles, acting in concert with vertical dipole correctors.

6.0 CONCLUSIONS

Three non-trivial lattice modules, and a main arc module, are sufficient to construct clustered and distributed lattices, with only minor modifications between lattice variants. Lattices constructed in this way and installed in the SSC database handle a 'first round' of realistic lattice problems, like the transition from injection to luminosity optics, and the need for vertical separation, in addition to the basic need for optical matching. While adjacent modules may overlap their roles in an ill-defined boundary area (for example, LOB/VSEP), or while those roles may be superimposed (for example, VSEP), it is still conceptually very useful to associate roles with modules. Eventually, however, under the pressure of an increasing number of realistic constraints, it may not be possible to maintain a one-to-one relationship between conceptual function and geographical location.

In the next iteration of clustered lattice design, the segment modules will be based on 90 degree cells, while the modules between clusters will still be built from 60 degree cells. Since the lengths of both VSEP and PT are determined by the need for a given phase advance, this will lead to a VSEP module 200 metres shorter, and a PT module 400 metres shorter, for a total length between interaction points of about 2.2 kilometres. Utility sections, which have already been designed, will also be included.

Only slightly further off in the future, attention must be paid to the integrally related problems of non-zero crossing angles, trim separator dipoles, and radiation loads on intersection region magnets. The possibility of injection matching from the injector into the utilities must also be established, and a scheme to compensate the expected optical errors entering from the main arcs must be devised.

ACKNOWLEDGEMENTS

I would like to thank Al Garren for many fruitful and interesting conversations, and Ruth Hinkins for creating the plotting routines used as a basis for most of the figures.

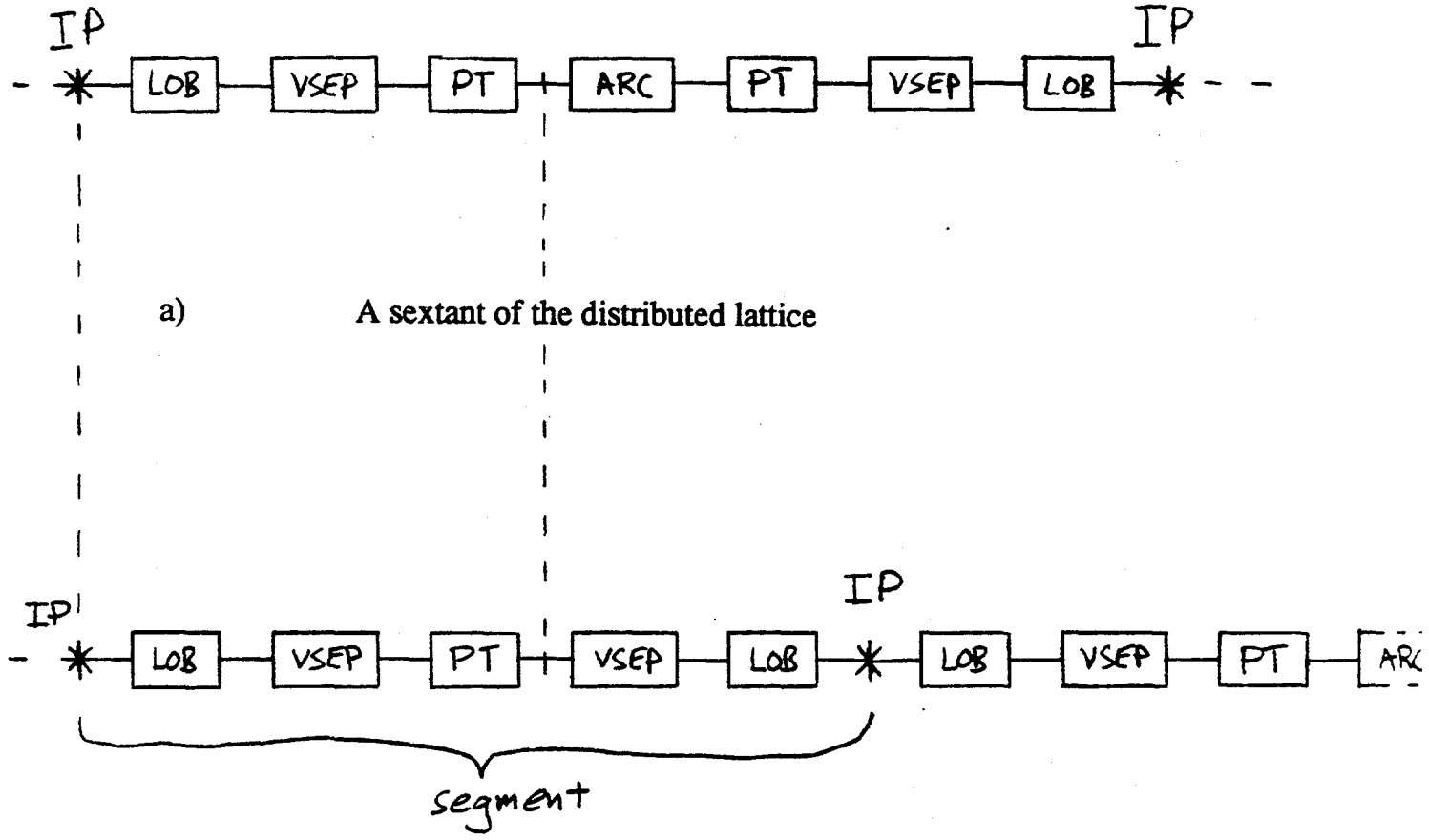

a) A sextant of the distributed lattice

b) A segment and the beginning of a main arc in the (3,3) clustered lattice

Figure 1 Schematic arrangement of the lattice modules in a) the distributed lattices, and b) the clustered lattices

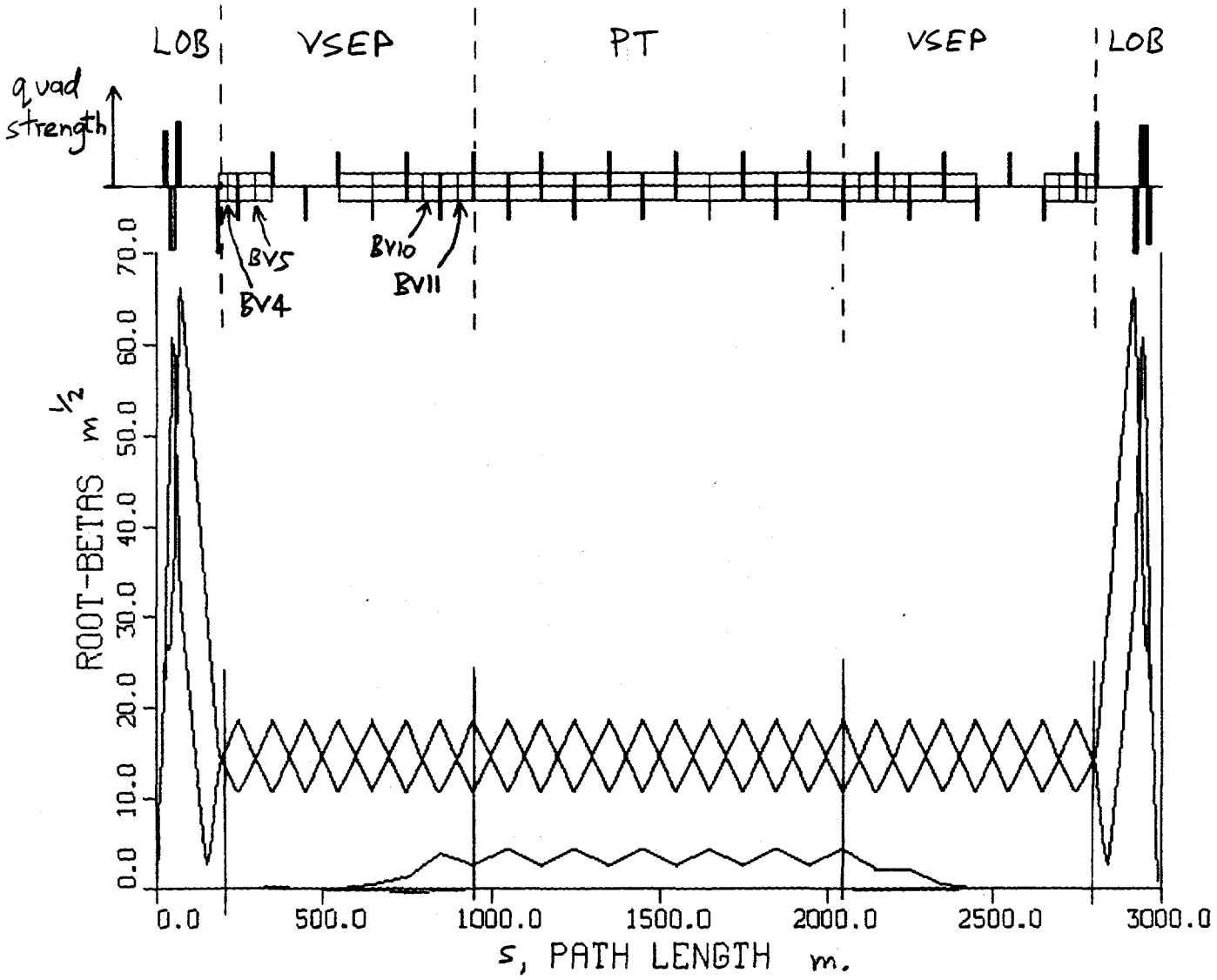

Figure 2 **Layout and optical parameters of the cluster segment in the $\beta^* = 1.0$ metre luminosity lattice, with the phase trombone PT at rest**

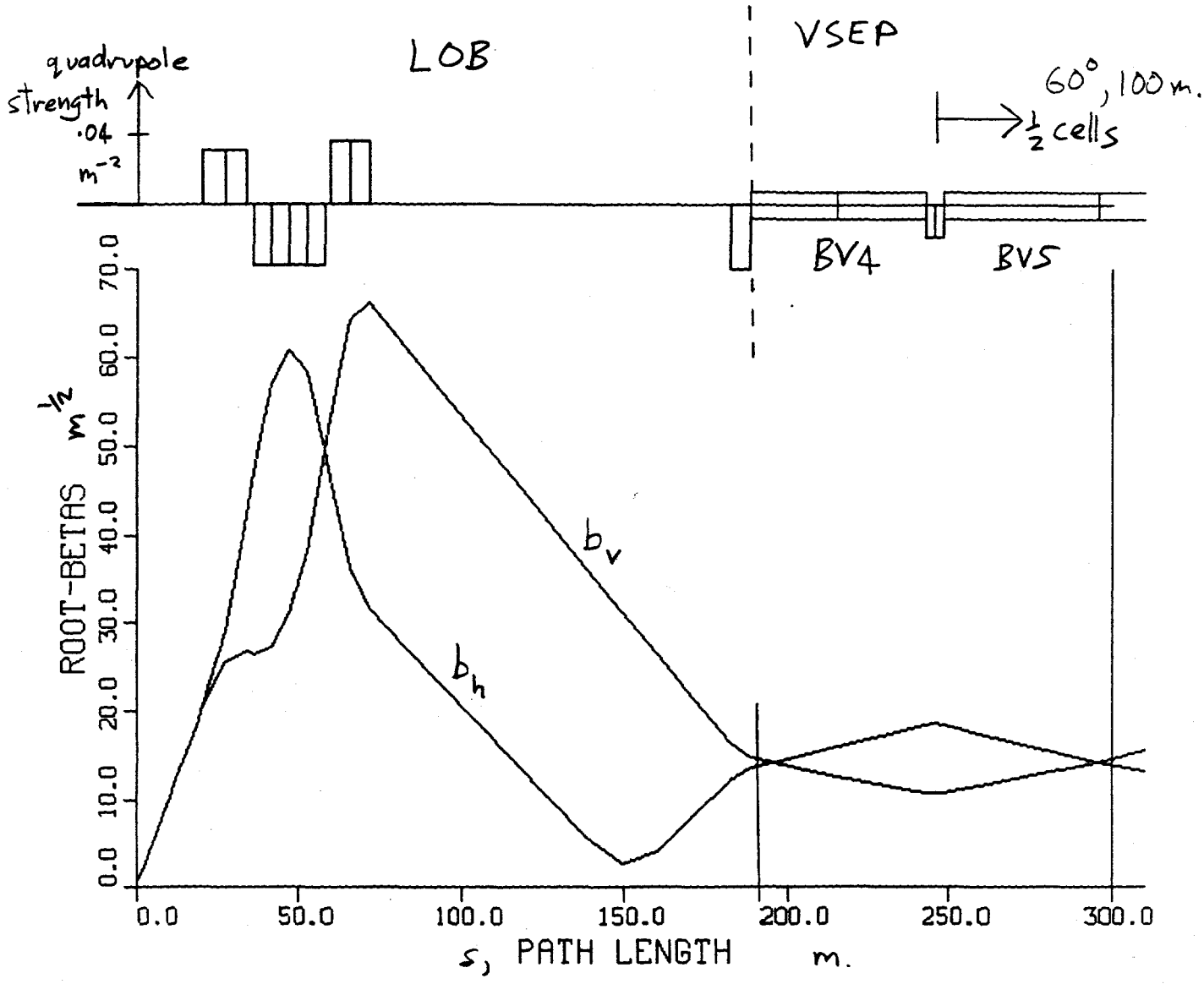

Figure 3 The low beta matching module LOB, in the $\beta^* = 1.0$ metre luminosity lattice

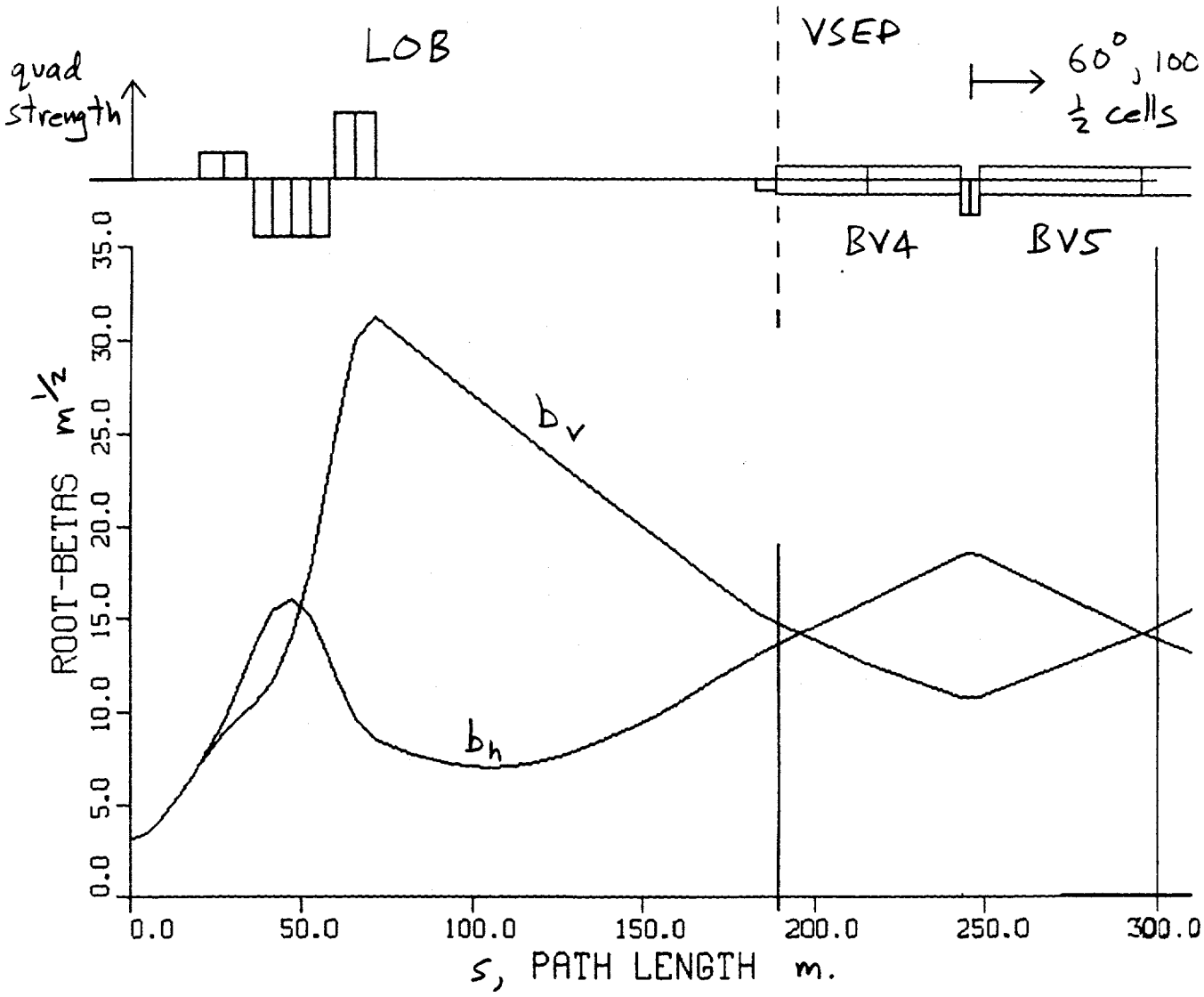

Figure 4 The low beta matching module LOB, in the $\beta^* = 10.0$ metre injection lattice

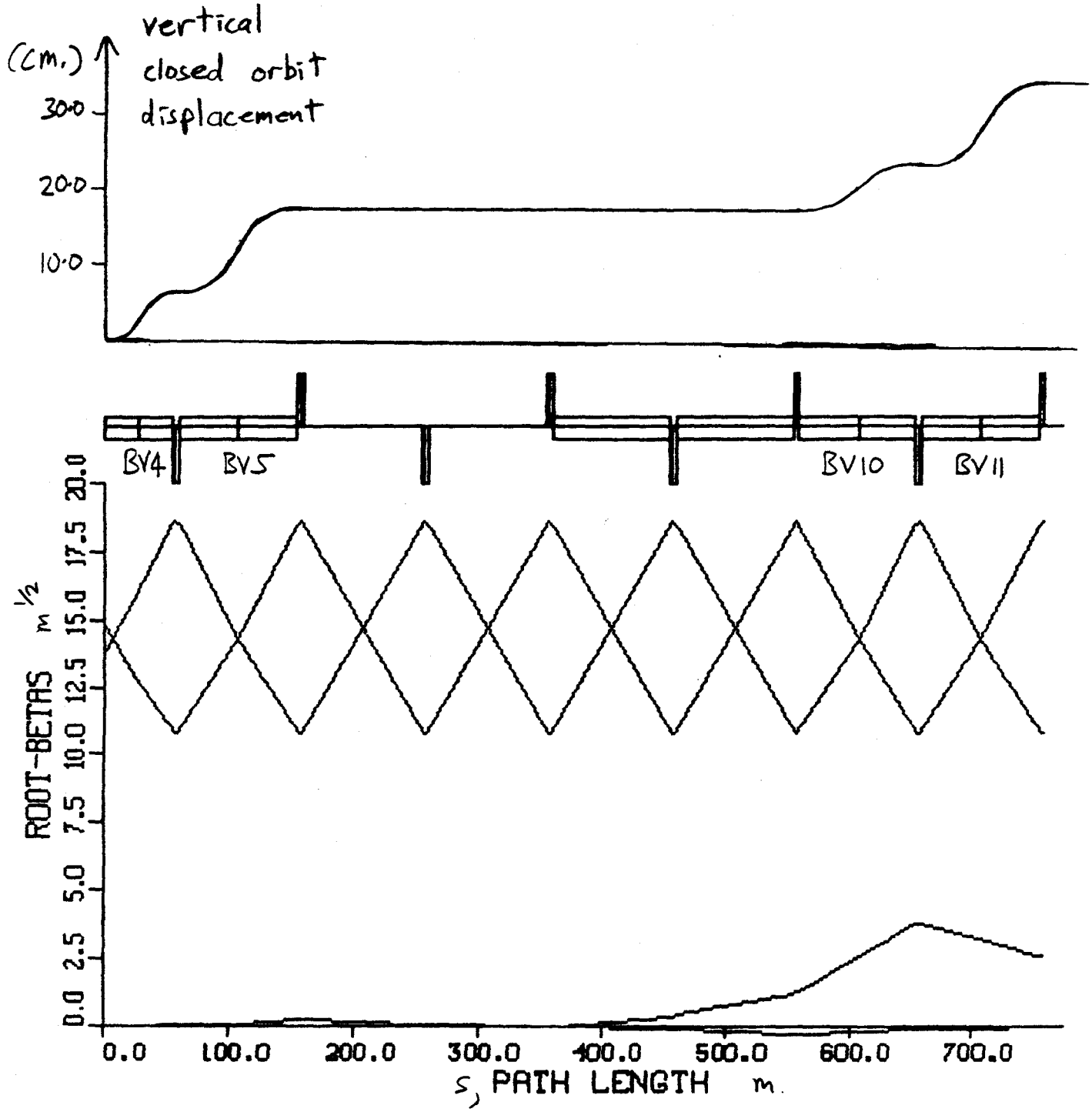

Figure 5 The vertical separation module VSEP, showing the steps in the vertical closed orbit

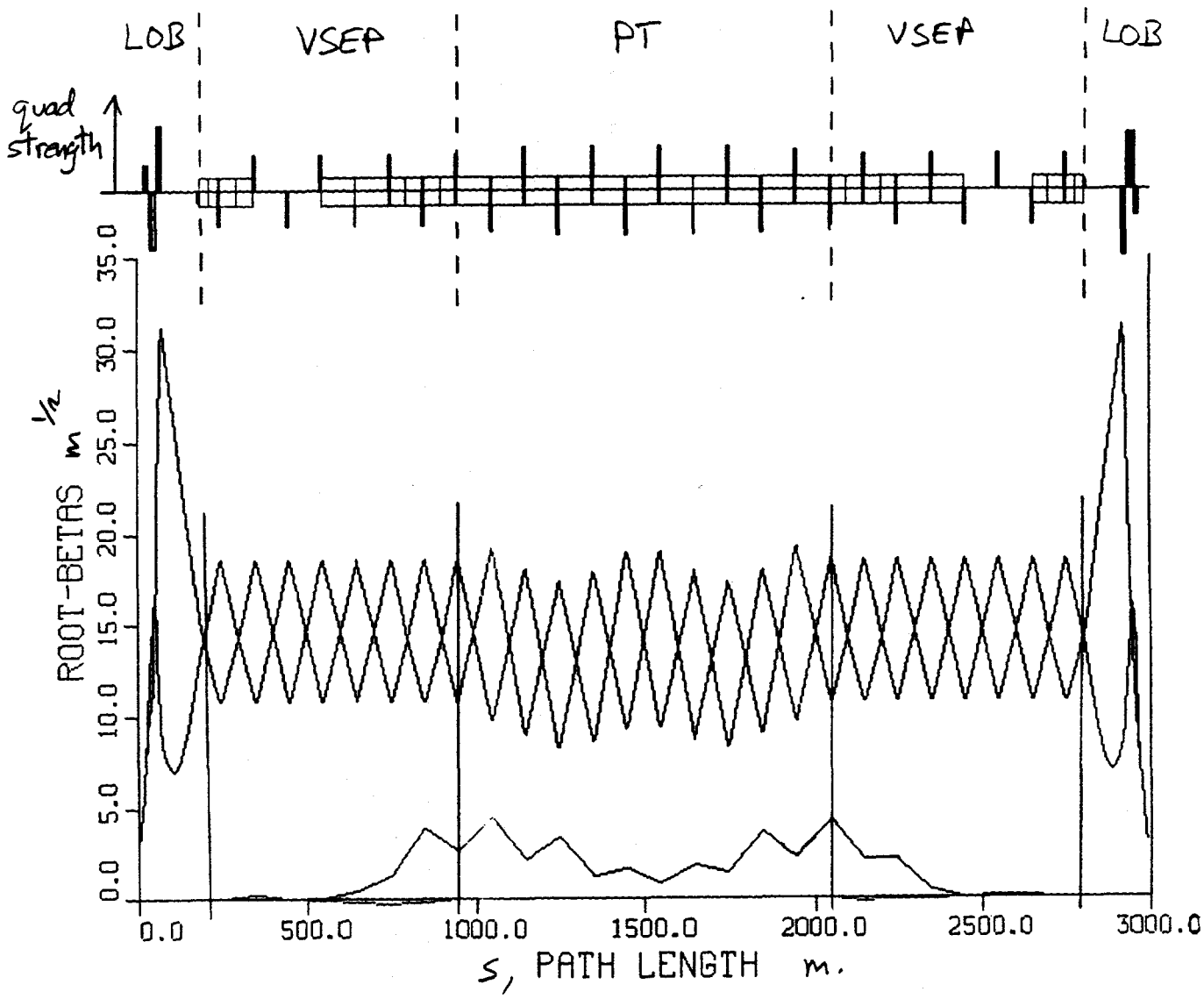

Figure 6 Layout and optical parameters of the cluster segment in the $\beta^* = 10.0$ metre injection lattice, with the phase trombone PT active

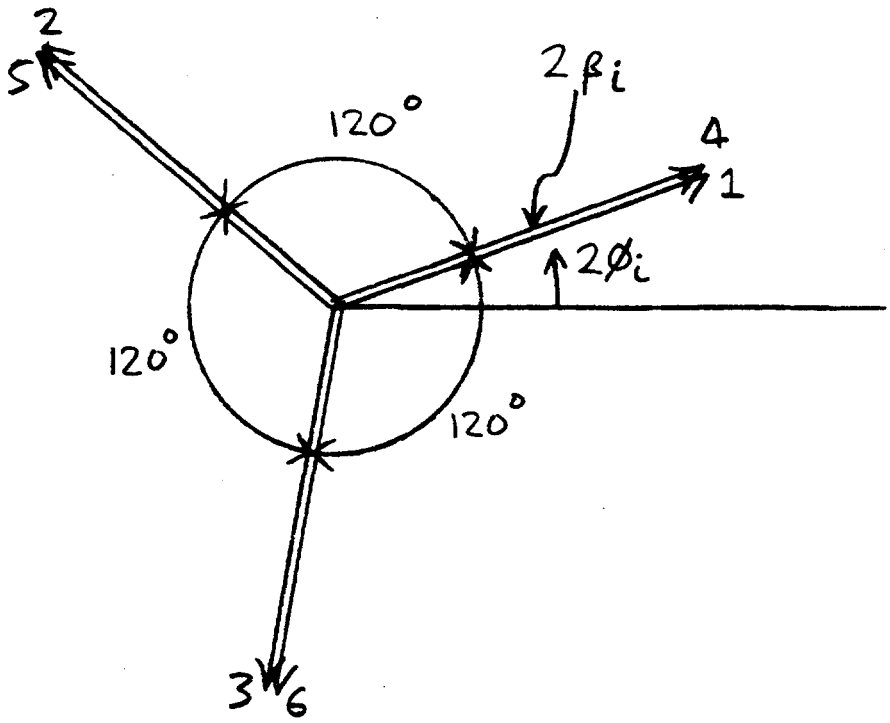

a) Betatron error phasors

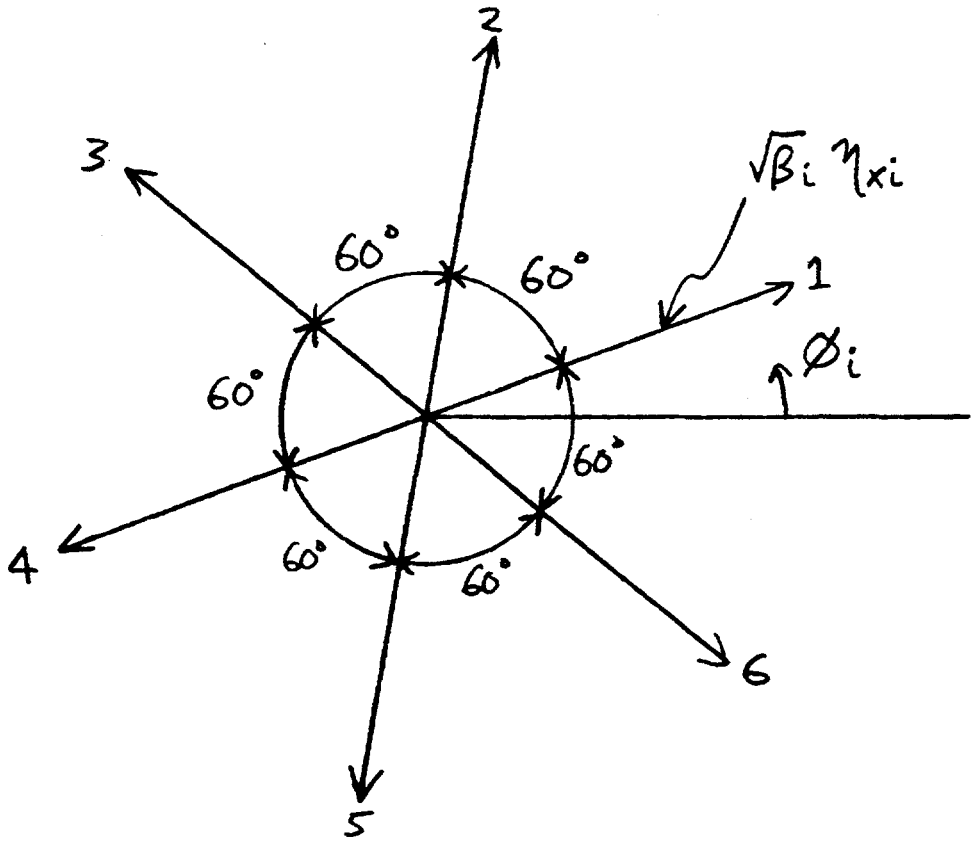

b) Horizontal dispersion error phasors

Figure 7 Phasor representation of the first order a) betatron, and b) horizontal dispersion optics errors caused by the '2π' phase trombone PT, with 60 degree cells

TOWARD AN SSC TEST LATTICE DESIGN WITH TWO CHROMATIC CLUSTERS OF INTERACTION REGIONS

A. Garren
SSC Central Design Group
and
K. Steffen
DESY

Introduction

Various ideas on how to design a cluster of interaction regions (IR) with local chromaticity correction were investigated, all of them employing pairs of sextupoles with betatron phase advances of $(2n+\lambda)\pi$ between them so that their geometric aberrations cancel. Some of these ideas were discarded, for example those which had an interaction region within the pair or those employing interleaved pairs. Even when, at the sextupoles, one amplitude function is made very small as compared to the other, and the two interleaving pairs are thus decoupled regarding their horizontal and vertical chromaticity correction, they can still not be considered "non-interleaved" regarding their compensation of chromatic aberrations.

What remains, then, are schemes that have one or more complete sextupole pairs in a periodic focusing structure between interaction points. This periodic structure may be specially tailored to suit the purpose, or it may even be the normal arc FODO structure. In any case, it must have a strong horizontal dispersion for the sextupoles to act on. Probably the best and most elegant structure we found is the one described at the end of this note; it has a 2200 m long periodic channel of arc cells with four pairs of sextupoles between interaction points. In this scheme, the three interaction points forming a "cluster" are within five miles of each other, and thus the denotation

may still be justified. However, the FODO channels may be increased in this scheme to any length, until an equidistant spacing of IR's is obtained. The elegance of the scheme lies in the way the vertical separation and the horizontal and vertical dispersions are handled at the end of the FODO channel and matched into the interaction region, and it is applicable to clustered as well as distributed IR's.

However at first a simpler scheme will be described which has only one pair of sextupoles between IR's, placed in a specially tailored FODO channel with long cells and very large dispersion.

Scheme With One Pair of Sextupoles in a Special 360° FODO Channel Between IR's

The half cell of the special FODO channel is shown in Fig. 1. It is very long in order to create a large periodic dispersion, containing 12 bending magnets each 16.6 m long. The phase advance in a full cell is 90°. Figure 2 shows the optical arrangement of the 360° FODO channel between interaction points. The insertion quadrupole quintet matches the beta functions across a drift space into the periodic channel. The drift space contains a pair of vertical bends with opposite polarity, which translates the beam vertically and generates a vertical dispersion that enters the FODO channel with zero slope and, after passing the 360° channel, is transformed into itself at the end of the channel. For the horizontal dispersion, the first half of the channel acts like an inverse dispersion suppressor that generates a dispersion which, in the second half of the channel, is subsequently eaten up again. The sextupoles for correcting the, say, horizontal insertion chromaticity are placed ±90° away from the center line of the channel, where the horizontal dispersion has half of its maximum

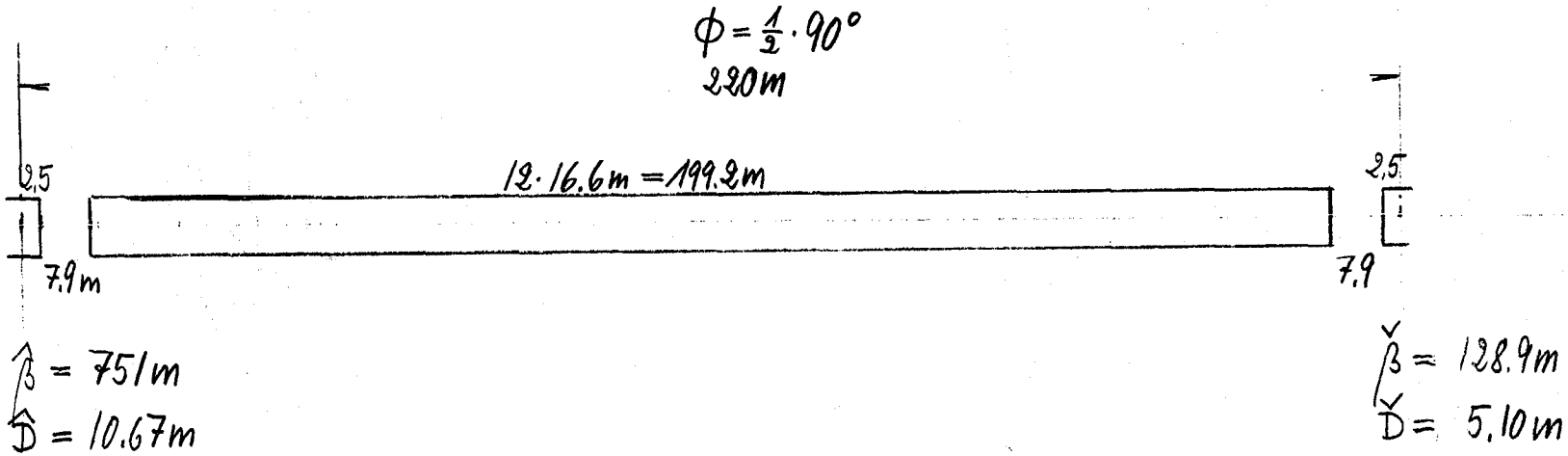

Fig. 1. Half cell for the special 360° FODO channel with one 180° sextupole pair between IR's.

Fig. 2. Cluster with one 180° sextupole pair between IP's.

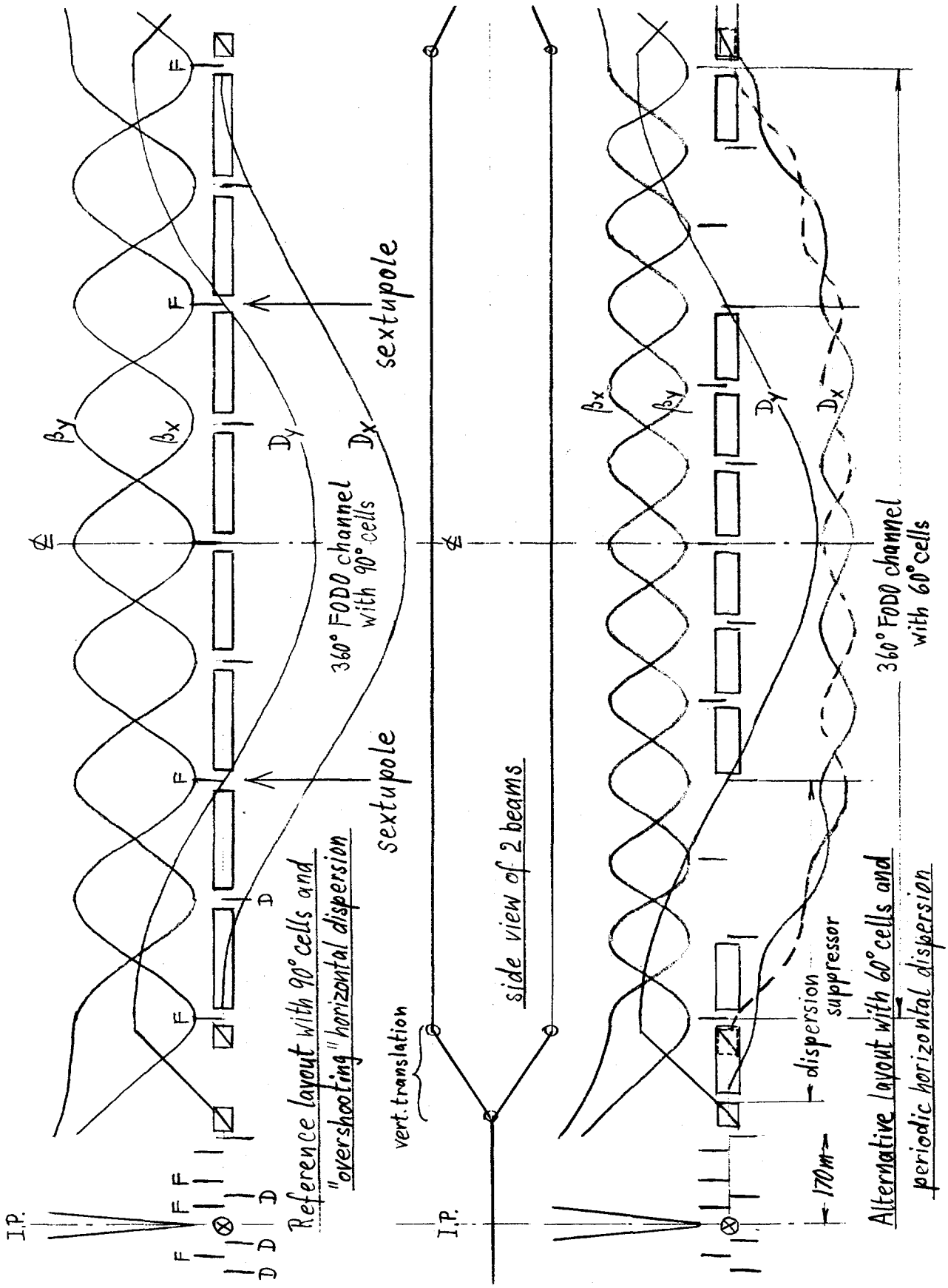

value (i.e., 10.7 m) and the vertical dispersion is zero. On the other side of the interaction point, all quadrupole polarities are inverted, and the FODO channel will, at the same location, carry a sextupole pair for vertical chromaticity correction. Thus, in a cluster of three IR's, with special FODO channels around and between, there will be two pairs of horizontal sextupoles and two pairs of vertical sextupoles.

Applying the word "cluster" to this compound, including the outer two 360° FODO channels in full, we have joined two "clusters" in three slightly different ways to form three simple test rings that do not contain the arcs of the machine and serve only to give a feeling of the chromatic behavior of the "chromatic IR cluster" itself. The three different ways of joining the clusters are explained in Fig. 3. Ring A is created by simply joining the cluster with its mirror image, giving the superperiodicity one. Ring B has the cluster identically repeated, and in order to join the two clusters, a half cell of the same polarity is inserted in each joint. This ring has superperiodicity two. In order to move the betatron tune to a better value, we defined Ring C by merely adding another 90° cell in one of the joints.

Information about the chromatic behavior of these IR test rings obtained from a quick investigation is comprised in Table I and, for the most well-behaved Ring B, shown graphically in Fig. 4.

The lower part of Fig. 2 shows an alternative arrangement with the 360° FODO channel composed of 60° cells. The horizontal dispersion is periodic in this case, with a dispersion suppressor at each end which reduces the required aperture. However, the beta functions are less decoupled in this case (factor 3 instead of 5.8).

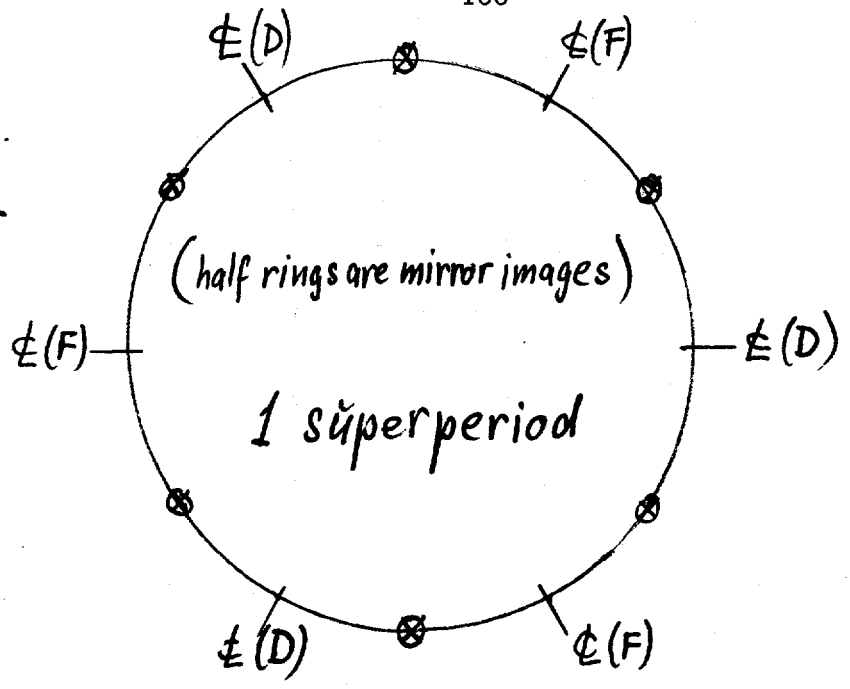

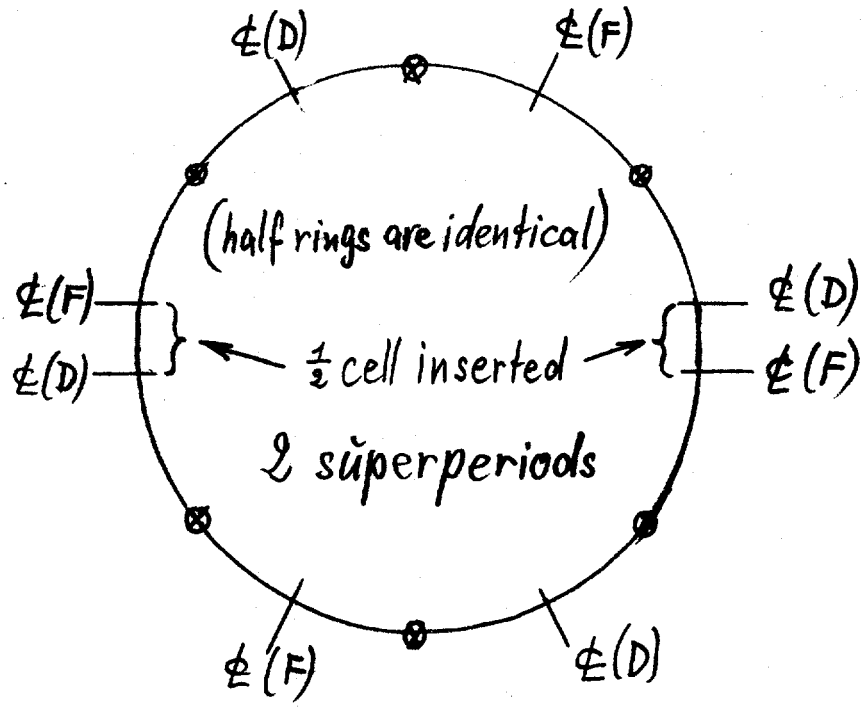

Ring C: Same as ring B, but on one side 3 half cells inserted instead of 1 half cell (↘ different tune)

Fig. 3. Cluster ring configurations for test runs. One sextupole pair between IP's, arcs not included.

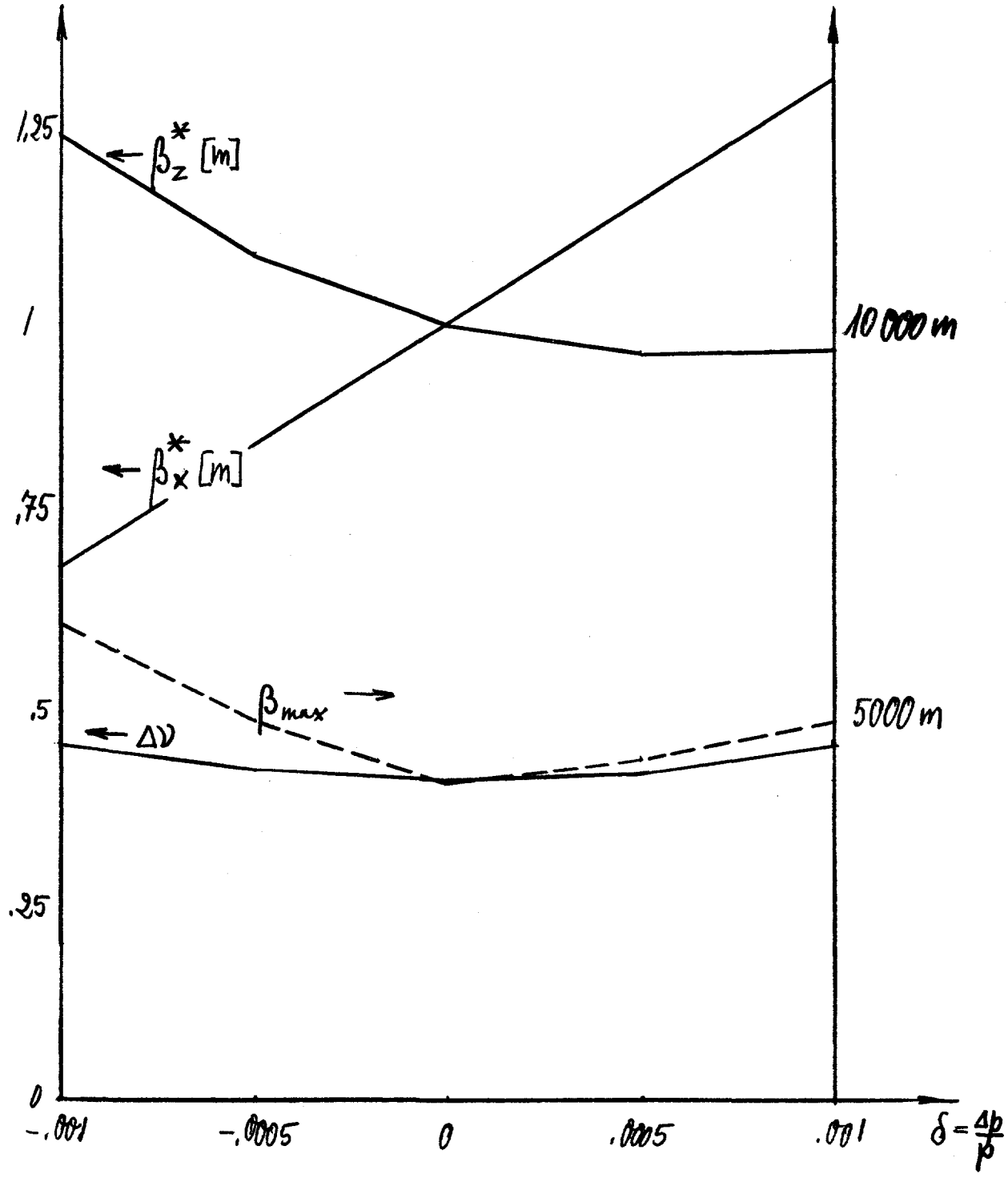

Fig. 4. Variation of $\Delta\nu$, β^* and β_{max} with energy for the clusters with one sextupole pair between IP's; two superperiods, without arcs (Ring B).

Scheme With 4 Pairs of Sextupoles in a Regular Arc-Type FODO Channel Between IR's

The scheme is shown in Figs. 5 and 6. It has a basically different symmetry. While the previous scheme is antisymmetric about the IP and symmetric about the center of the FODO channel, this scheme is antisymmetric also about the center of the FODO channel. From the center of one FODO channel to the center of the next one, therefore, the system repeats identically, and three of these periods S (see lower part of Fig. 5) form what we call the "cluster" in this case. In order to give room for three non-interleaved pairs of sextupoles, two horizontal and two vertical, the FODO channel has 19 half cells, of the type shown in Fig. 6 with a maximum periodic dispersion 2.88 m.

In order to have the dispersion periodic in the channel, a horizontal dispersion suppressor is needed at each end. On the other hand, due to the fact that the 19 half cells give a phase advance of 19 x 45° = 2.375 x 360°, also the vertical dispersion generated by beam separation requires some special adaptation. We found a way of combining these two functions in a single dispersion transformer, as shown in Fig. 6. It consists of a 180° FODO channel of similar cells, but "loaded" with horizontal bending magnets of half the usual strength. It thus acts as an inverse suppressor that generates the proper periodic horizontal dispersion value of the entrance of the periodic channel. In the vertical plane, the translation is divided in two equal steps, one before and one after the 180° "dispersion transformer." The vertical dispersion owing to the first step will then be inverted by the transformer and subsequently be eaten up by the second step.

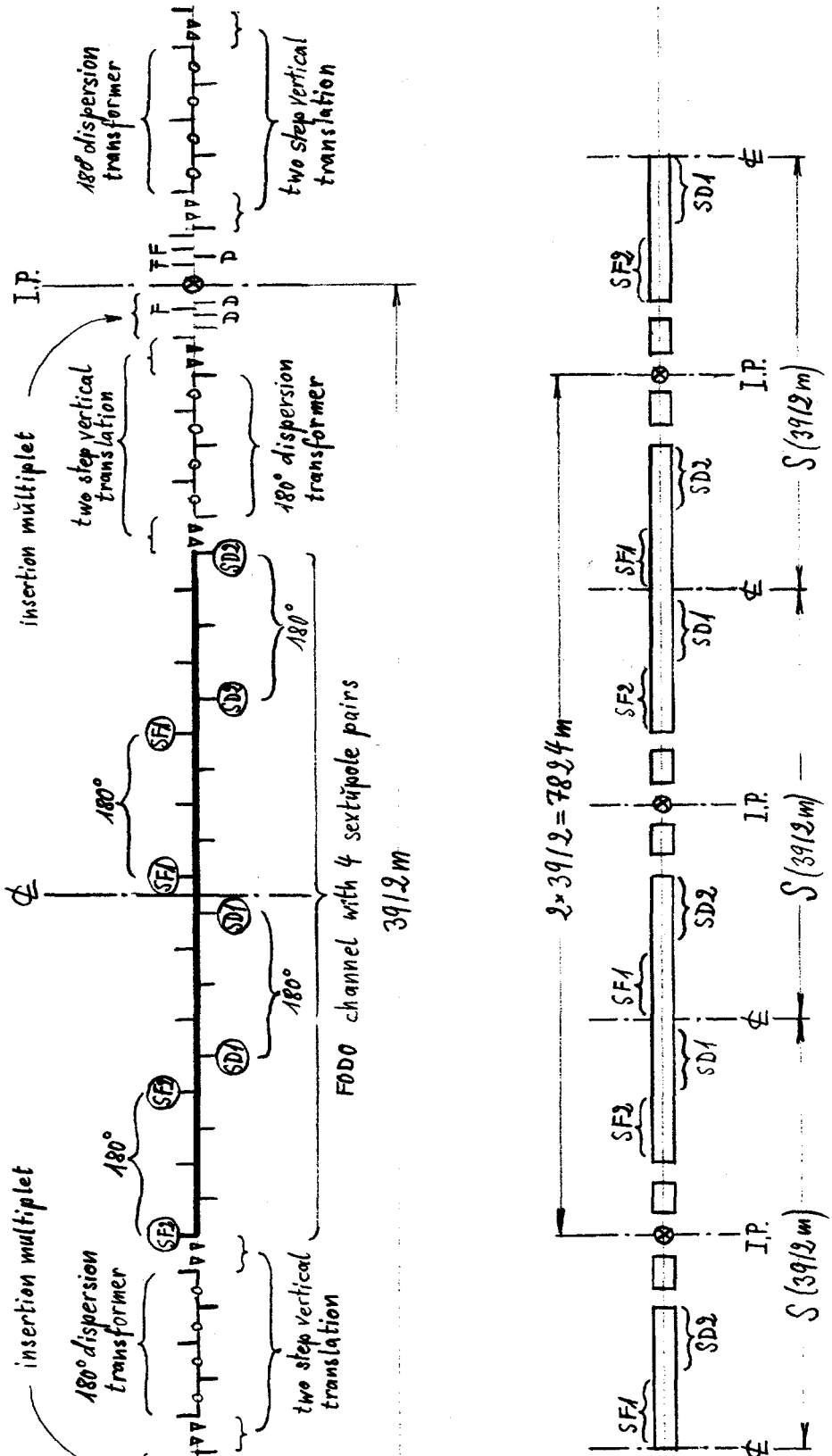

Fig. 5. Partial and full overviews of a cluster with four 180° sextupole pairs between IP's. The cluster consists of three identical periods S.

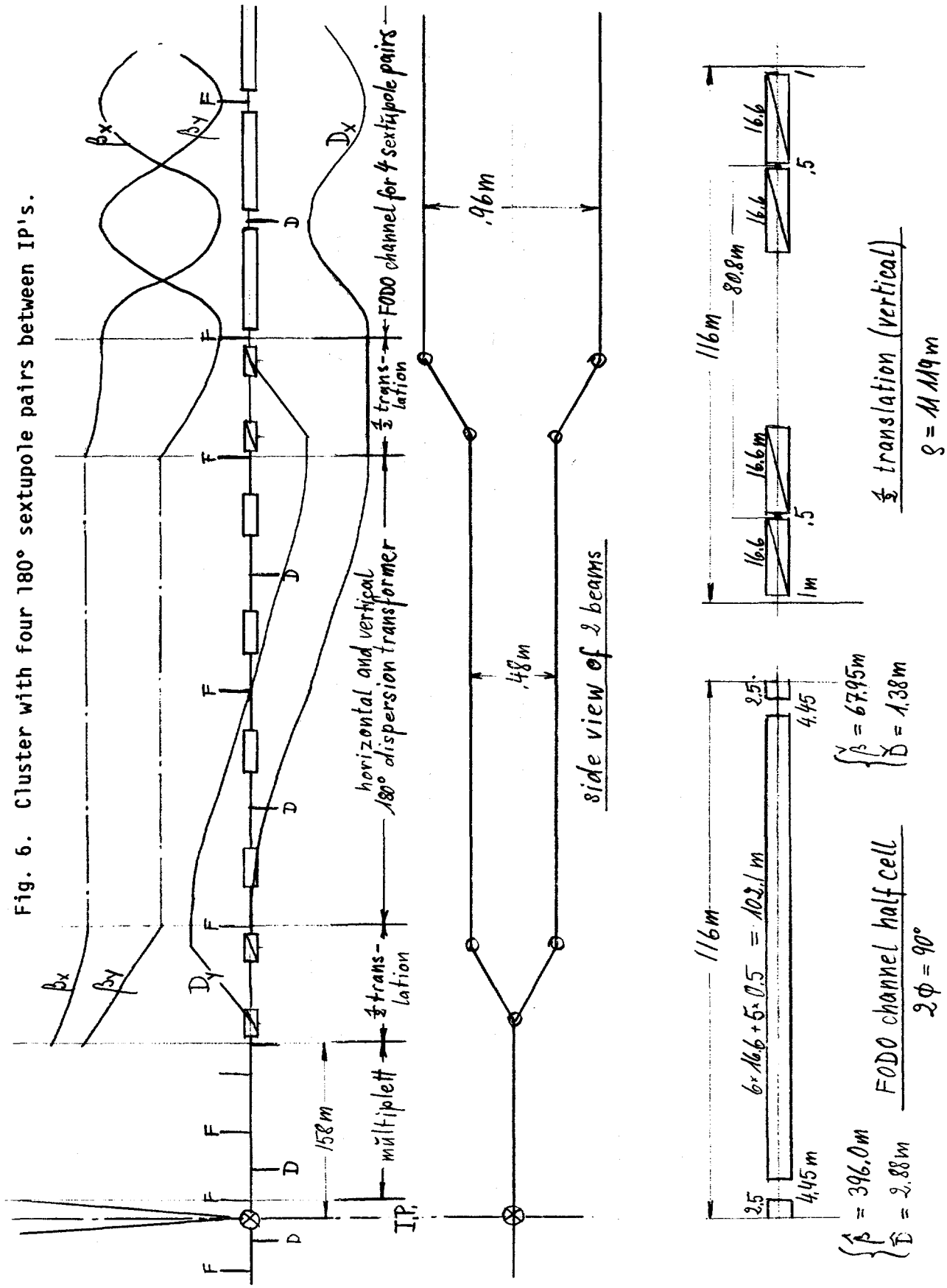
Fig. 6. Cluster with four 180° sextupole pairs between IP's.
βx
βy
Dy
Dx
F
D
158m
multiplett
½ trans-lation
IP
horizontal and vertical 180° dispersion transformer
½ trans-lation
FODO channel for 4 sextupole pairs
side view of 2 beams
,96m
,48m
116m
80.8m
16.6
16.6m
.5
1m
½ translation (vertical)
S = 11.119m
6x16.6+5.0.5 = 102.1m
2.5
4.45
4.45m
2.5
β = 396.0m
D̂ = 2.88m
FODO channel half cell
2Φ = 90°
β̌ = 67.95m
Ď = 1.38m

In order to get a feeling for the chromatic behavior of this scheme, we have again joined two identical "clusters" into an IR test ring D. Ring D thus has the superperiodicity six. The results are shown in Table II and partly displayed in Fig. 7. The υ-variation with energy is very small over the range of $-0.001 \leq \delta \leq 0.001$, and the variations of β^* and β_{max} are moderate.

We then extended the test ring to include the arcs, by inserting between the two clusters two arcs of 135 normal cells each. The chromaticity of the arc is compensated within itself by noninterleaved pairs of sextupoles acting on the horizontal and vertical chromaticity, respectively. The results for this ring E are given in Table II and partly displayed graphically in Fig. 8. The tune variation is again very small, the β_{max}-variation is moderate, but the variation of β^*_x and β^*_y is larger than for ring D with IR clusters only.

Acknowledgments

We gratefully acknowledge fruitful discussions with members of the SSC lattice design group, especially with A. Chao who contributed to various phases of this work.

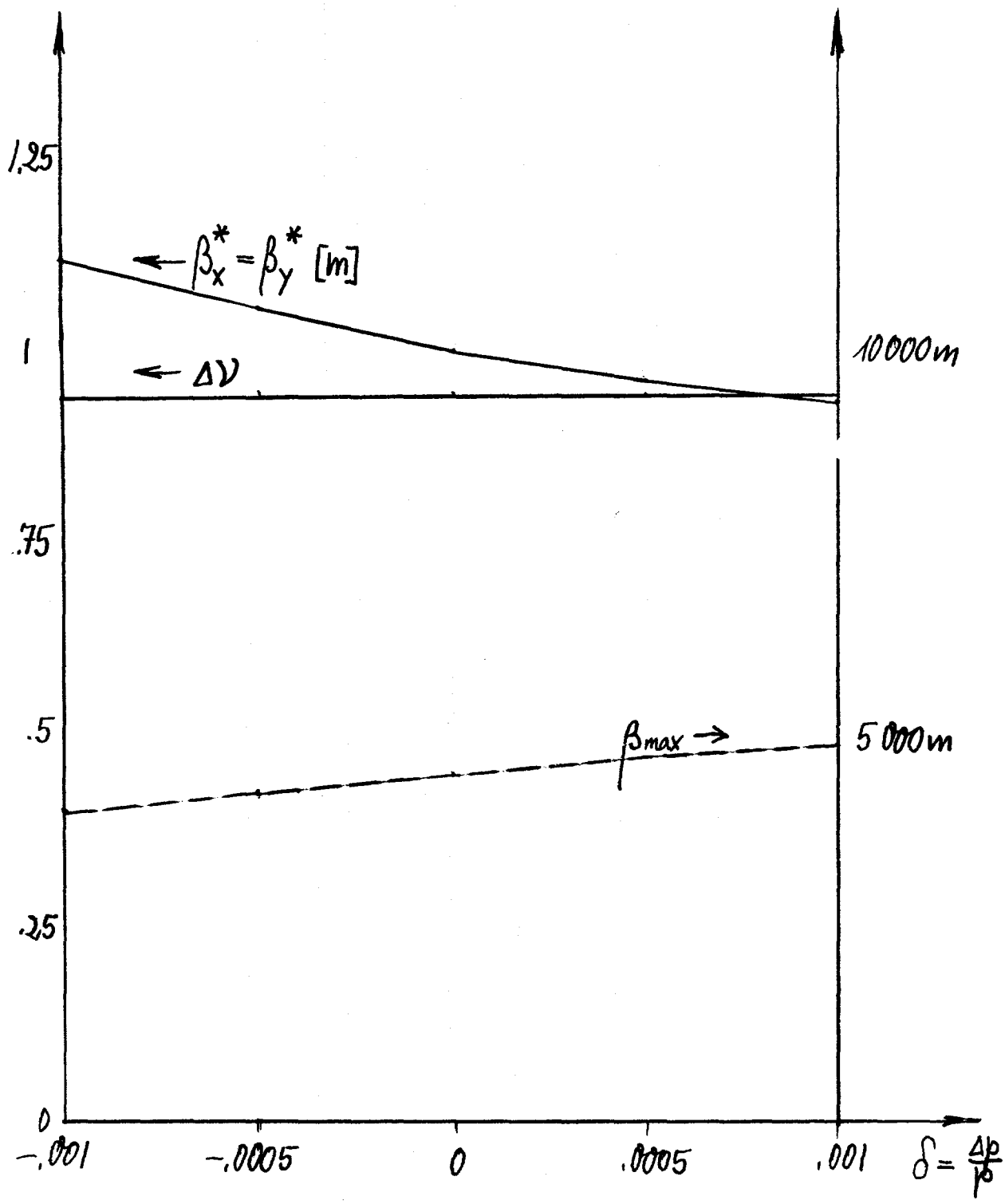

Fig. 7. Variation of $\Delta\nu$, β^* and β_{max} with energy for the clusters with four sextupole pairs between IP's; arcs not yet included (Ring D).

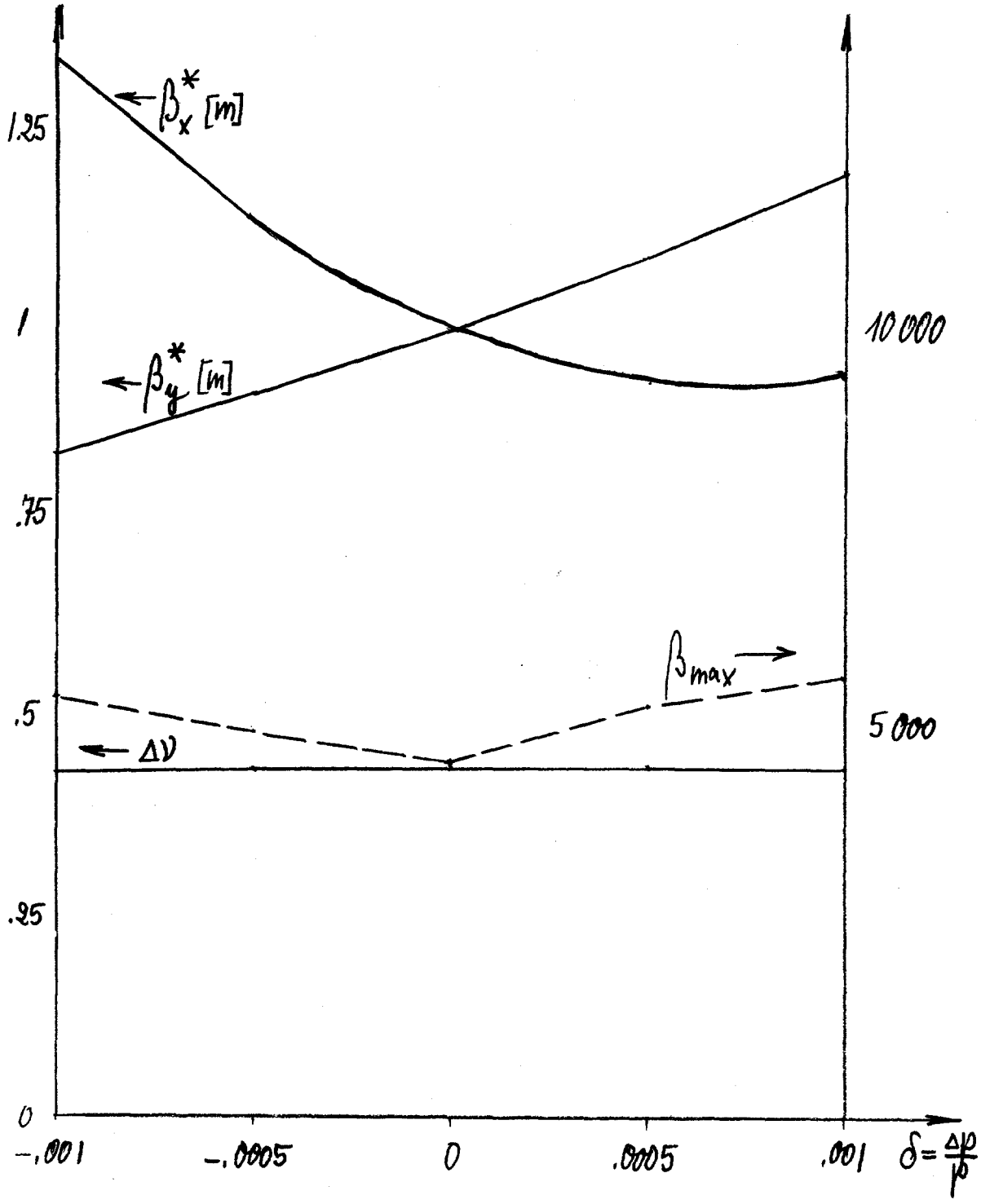

Fig. 8. Variation of $\Delta\nu$, β^* and β_{max} with energy for the clusters with 4 sextupole pairs between IP's; 2 arcs with 135 normal cells each inserted. Arcs are chromaticity corrected by 27 non-interleaved sextupole pairs each (Ring E).

Table I. Effect of Energy Variation in Test Ring Configurations A, B and C

	δ	$(\nu-15)$	β	β^*	β_{end}	
		KSF = 0		KSD = 0		
Ring A without sextupoles	-0.001	0.3244	0.5330	0.8695	221.6	(H)
		0.3248	0.5337	0.8632	552.2	(V)
	-0.0005	0.2391	0.4398	0.9452	158.8	(H)
		0.2394	0.4400	0.9456	687.4	(V)
	0	0.1634	0.4085	1.0	129.2	(H)
		0.1637	0.4086	1.0	749.1	(V)
	0.0005	0.0912	0.3976	1.0284	110.2	(H)
		0.0915	0.3976	1.0281	771.8	(V)
	0.001	0.0200	0.4018	1.0375	97.7	(H)
		0.0203	0.4017	1.0224	759.2	(V)
		KSF = 0.03489		KSD = -0.07282		
Ring A with sextupoles	-0.001	0.3224	12334	0.8371	516.4	(H)
		0.3232	12395	1.0322	116.0	(V)
	-0.0005	0.1913	0.5732	0.8683	224.9	(H)
		0.1917	0.5736	0.9743	541.8	(V)
	0	0.1634	0.4085	1.0000	129.2	(H)
		0.1637	0.4086	1.0000	749.1	(V)
	0.0005	0.1814	0.4738	1.2191	0.72.3	(H)
		0.1818	0.4738	0.9621	860.7	(V)
	0.001	0.2217	0.6492	1.5926	0.40.4	(H)
		0.2226	0.6501	0.9601	957.7	(V)

(continued)

Table I (Continued)

	δ	(υ-15)	β	β*	β end	
		KSF = 0.03497		KSD = -0.07297		
	-0.001	0.4588	0.6137	0.6847	574.6	(H)
		0.4593	0.6141	1.2456	263.7	(V)
	-0.0005	0.4235	0.4935	0.8408	635.6	(H)
		0.4240	0.4937	1.0904	180.2	(V)
Ring B						
	0	0.4134	0.4086	0.9998	749.0	(H)
		0.4137	0.4087	1.0001	129.3	(V)
	0.0005	0.4216	0.4402	1.1580	894.5	(H)
		0.4221	0.4853	0.9632	96.2	(V)
	0.001	0.4424	0.4853	1.3146	1050.8	(H)
		0.4431	0.4852	0.9717	73.0	(V)
		KSF = 0.03505		KSD = -0.07312		
	-0.001	0.6939	13174	0.3268	825.0	(H)
		0.6947	13173	2.5148	607.8	(V)
	-0.0005	0.6673	0.7245	0.5666	620.9	(H)
		0.6678	0.7246	1.4430	272.1	(V)
Ring C						
	0	0.6633	0.4087	1.0000	749.2	(H)
		0.6637	0.4088	1.0000	129.3	(V)
	0.0005	0.6660	0.6170	1.6722	1191.2	(H)
		0.6672	0.6165	0.9815	71.4	(V)
	0.001	0.6799	0.9055	2.5428	1887.1	(H)
		0.6808	0.9047	1.2359	5.2	(V)

TABLE II. Effect of Energy Variation in Test Ring Configurations.

Ring D (6 IR's only):

δ	ν_y-97	ν_y-27	β_x	β_y	β^*_x	β^*_y	β_x end	β_y end
-0.001	0.9394	0.9405	4028	4026	1.118	1.119	0.225	0.225
-0.0005	0.9440	0.9449	4272	4270	1.054	1.054	0.198	0.198
0	0.9451	0.9460	4504	4501	1.000	1.000	174.7	174.9
0.0005	0.9446	0.9446	4717	4714	0.959	0.960	0.155	0.155
0.001	0.9445	0.9456	4902	4898	0.935	0.936	0.139	0.139

Ring E (6 IR's plus 2 arcs):

$\delta(\delta)$	ν_x-95	ν_y-95	β_x	β_y	β^*_x	β^*_y	Arc SF β_x	β_y
-0.02	0.3988	0.4010	6418	6407	2.0293	0.7169	337.2	65.0
-0.15	0.4234	0.4250	5847	5842	1.6259	0.7760	359.9	66.3
-0.1	0.4371	0.4383	5359	5356	1.3384	0.8428	374.6	67.1
-0.05	0.4434	0.4444	4915	4913	1.1341	0.9173	385.1	67.7
0	0.4451	0.4460	4506	4502	0.999	1.0003	394.0	68.3
0.05	0.4441	0.4451	5231	5222	0.9330	1.0925	402.8	68.9
0.1	0.4424	0.4438	6077	6065	0.9385	1.1950	411.8	69.5
0.15	0.4427	0.4446	7020	7004	1.0285	1.3109	419.9	70.0
0.2	0.4482	0.4511	8006	7982	1.2218	1.4475	424.4	70.1

TOWARD A REALISTIC LOW-FIELD SSC LATTICE

S. Heifets
University of Houston
and
Texas Accelerator Center

ABSTRACT

Three six-fold lattices for 3 T superferric SSC have been generated at TAC. The program based on the first order canonical transformation was used to compare lattices. On this basis the realistic race-track lattices were generated.

Foreword

The low-field SSC design can be very attractive because the effect of persistent currents is diminished, and there are more possibilities for shuffling to reduce random error. At the same time, the design probably demands longer dipoles to reduce the cost of the accelerator.

In this paper we compare different lattices to make a reasonable choice of the main parameters of the accelerator and use them in the design of realistic lattices. In the first section we compare different single cells. In the second section we describe the structure of three six-fold model lattices, and we compare their properties in the third section. The fourth section describes the realistic race-track lattices.

The emittances $\varepsilon_{x,y} = \sigma_{x,y}^2/\beta_{x,y}$ are assumed to be $\gamma\varepsilon = 1$ μm, as they are given in the Reference Design.[1]

The rms momentum spread $\delta = \Delta p/p = 5 \times 10^{-4}$ at injection energy 1 TeV. It is based on the estimate[2] of collective instabilities which demand $\delta > 1.5 \times 10^{-4}$. On the other hand, with a dispersion function $\eta \sim 2$ m the momentum spread rms value $\delta = 5 \times 10^{-4}$ is reasonable.

1° Cells

We compared seven different cells with phase advances (60°, 72°, 80°, 90°) and dipole lengths 100 m and 140 m.

The momentum dependence of β,η functions, nonlinear tune shift, and the amplitude dependence of the tune were calculated with the program HARMON, assuming two sextupole families in the lattice made of regular cells only. The sextupoles were set to cancel the linear chromaticity. Some results are presented in the Table I.

Table I. Chromatic Properties of Single Cells.

	Qx/δ^2	$(\partial Qx/\partial\varepsilon)10^{-2}$	$\eta'(IP)$	$(\beta'/\beta)10^{-2}$
140,60°	-16.4	-4.1	-0.47	-3.31
140,80°	-20.8	-9.3	-0.37	-5.48
140,90°	-22.9	-6.4	-0.34	-6.67
100,90°	-23.7	-19.2	-0.18	-8.01
100,80°	-22.5	-31.8	-0.19	-6.51
100,72°	-19.8	-26.1	-0.22	-8.53
100,60°	-18.1	-14.5	-0.25	-6.16

The chromatic properties are slightly better for phase advance 60°, but are rather good in all cases.

The tracking of the same cells with MARYLIE values shows that the length 140 m is favorable (see Fig. 1). Because the effect of higher multipoles is less for shorter cells, in the following we keep looking for two half cell lengths, about 110 m and 140 m.

2° Six-fold Lattices

The comparison of lattices made of cells only is not very satisfactory, because the periodicity of such lattices is very big; therefore, three model six-fold lattices were generated with half cell length and phase advance per cell (140 m, 60°), (140 m, 90°), (110 m, 90°).

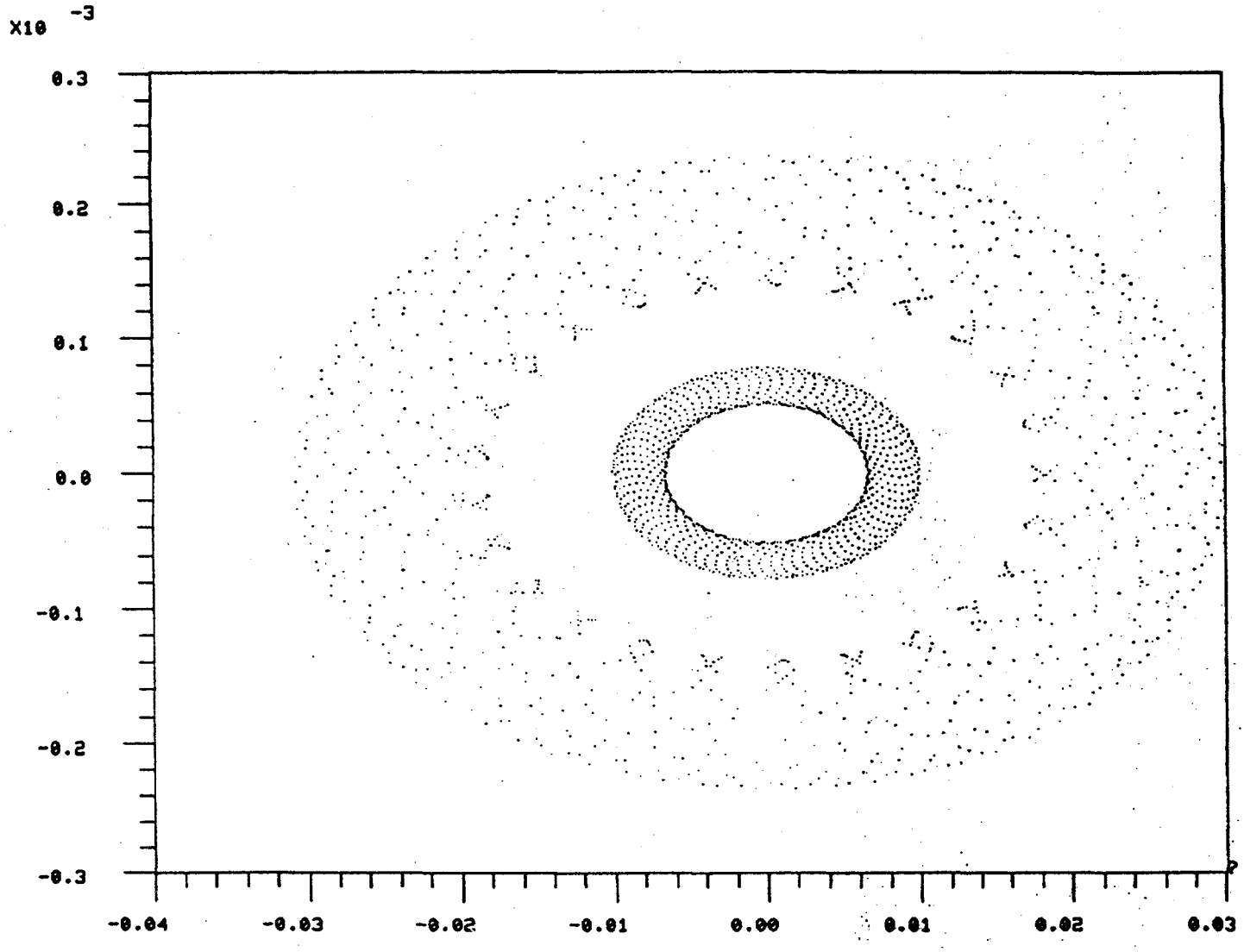

Fig. 1. Cell Tracking with MARYLIE.

The main parameters of the lattices are given in the Table II. The layout of a period of the lattices is shown in Fig. 2 and the typical β,η functions are plotted in Fig. 3.

The lattices are very similar. A period contains an arc and an asymmetric insertion. In all three cases the radius of curvature, fractional part of the tune per ring and per period were the same. The fractional part of the tune per ring, is close to 0.3. The nearest resonances are on the order of 13.[4] The SPS experience also makes this point favorable.

The number of cells N_s with sextupoles in the arc was such that N_s x Q_c = integer, where Q_c is the tune per cell.

The regular cell has a centered dipole and two sextupoles (F,D) in one half of each cell (A. Chao scheme). The dipoles are made of 10 subdipoles with small slots between them. The drift in a cell is rather long, as recommended by CDG. Each half of the insertion contains a dispersion suppressor (DS), a matching section (M), a trombone (T) and a low-beta triplet (LB).

The low-beta triplet was suggested by A. Garren. It gives $\beta_x^* = \beta_y^* = 1$ m at IP, $\alpha_x^* = \alpha_y^* = 0$ and $\beta_{max} = 3956$ m. The total length is 71.5 m, drift to IP is 20 m long. It is possible to modify the low-beta triplet to $\beta_{max} = 3057$ m.

The drift between LB and M has a length 120 m and is reserved for the magnet separator of two beams.

Matching is made with three quadrupoles. The DS basically is two regular cells with dipoles of special length.[3]

The use of a trombone was suggested by D. Johnson. The trombone has at symmetry point $\alpha_x = \alpha_y = 0$. With given phase advances it determines the strength of four independent quadrupoles.

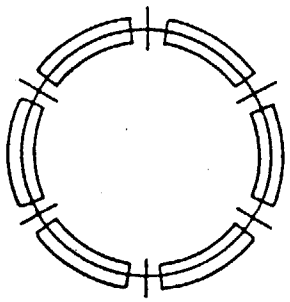

6 - FOLD LATTICES

L = 140 : $\Phi = 60^{o}$: Q = 6 x 16.216 : ρ = 19934.16

L = 140 : $\Phi = 90^{o}$: Q = 6 x 24.216 : ρ = 19934.16

L = 110 : $\Phi = 90^{o}$: Q = 6 x 31.216 : ρ = 19337.329

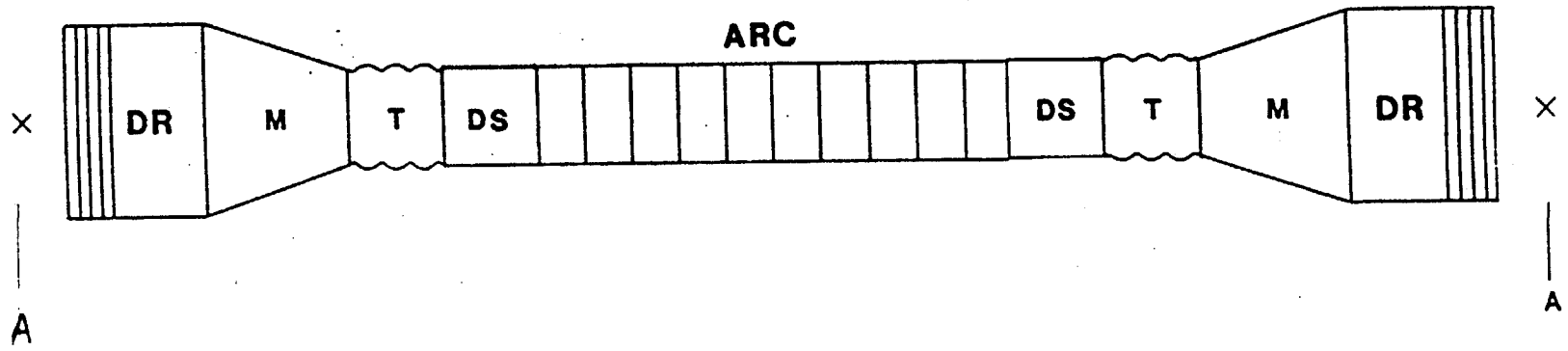

Fig. 2. Layout of six-fold lattices.

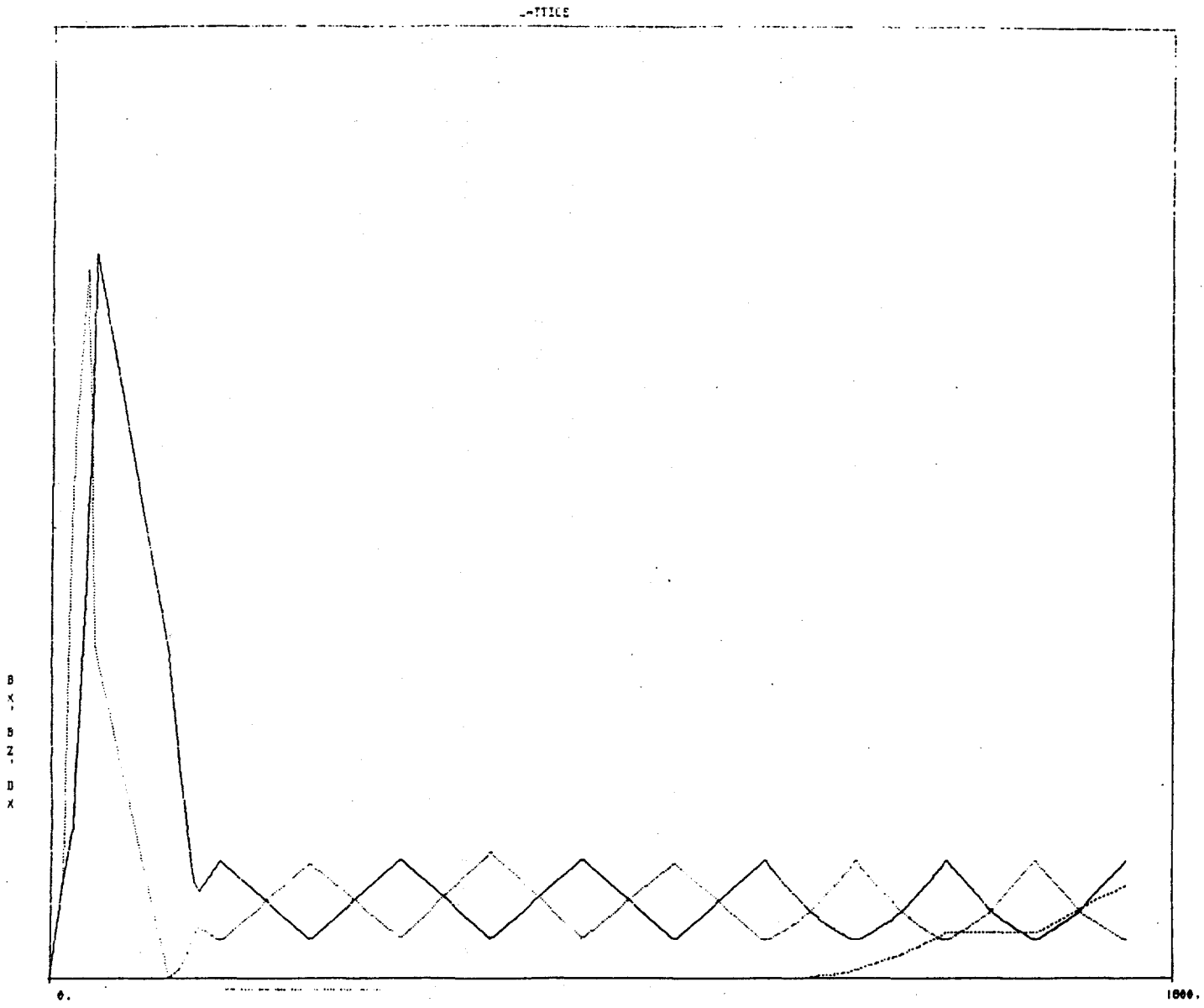

BETX,BETZ,DX FUCTIONS FOR THE
SIXFOLD LATTICE TAC14060

Fig. 3. ß, η, functions for six-fold lattices.

Table II. Main Parameters of 6-Fold Lattices.

	140,60°	140,90°	110,90°
1 Length of a period	27154.450	27189.5654	27159.762
2 Radius of curvature	19934.16	19934.16	19333.329
3 No. of cells/arc	81.5	81.5	110.5
4 Half cell length	145.207	145.00	110.00
5 Dipole length	125	125	100
6 Qx,y/ring	97.3028 97.2969	145.297 145.291	187.300 187.295
7 η_x max	3.978	2.459	1.384
8 β_{max} cell	501.94	493.3	373.48
9 β_{min} cell	169.02	85.3	64.78
10 $Q_{x,y}$/period	-36.27	-49.33	-57.96
11 $(B''/B\rho)_F$	-2.16791 E-03	-4.16433 E-03	-8.80005 E-03
12 $(B''/B\rho)_D$	3.50745 E-03	8.34872 E-03	1.73982 E-03

The trombone is very convenient for local tuning, but increases the total length of an insertion. The increase of β-function with the change of a tune can enhance chromatic effects at injection. The same tuning $\Delta Q \sim 0.5$ could be obtained by small (2%) change of quadrupole strength in regular cells, with η-function is still negligibly small. Nevertheless, we use two trombones per period at this time.

3° Comparison, Program CANON

To compare the lattices, the program CANON was used, based on the formulas obtained with the first order canonical transformation. This approach seems to be reasonable for the first screening of the parameters and can fill a gap between time-consuming tracking programs and crude analytic estimations. It provides also a basis for interpretation of tracking results.

With magnet field of a form $B = (1/2)\, B_o\ b_n\ (x + iy)^n + c.c.$,
the following formulas have been obtained for the tune shift per ring and the distortion $\Delta\varepsilon/\varepsilon$ with accuracy of $O(b_n^{\,2})$

$$\Delta Q_x = - \Sigma\langle(R/\rho)(2m_x/\varepsilon_x)\ C_m b_{n-1} \sigma_x^{\,2m1}\ \sigma_y^{\,2m_2}\ x_c^{\,n-2m1-2m2}\rangle \qquad (1)$$

$$(\Delta\varepsilon_x/\varepsilon_x)_k = \sum \frac{2\pi\ (m_1 - m_2)\ C}{N_s\ \varepsilon_x\ \sin\ (\alpha/2)}\ (m_1,m_2,m_3,m_4)\ . \qquad (2)$$

$$\langle(R/\rho)\ \ b_{n-1}\ \sigma_x^{\,m1\ +\ m2}\ \ \sigma_y^{\,m3\ +\ m4}\ \ X_c^{\,n-\Sigma m}\ \cos\ (\beta+K\alpha)\rangle\ ,$$

where

$$\sigma_x^{\,2} = (\varepsilon_x/2)\beta_x(s);\quad X_c = (\Delta p/p)\ .\ n_x$$

$$\alpha = (2\pi/N_s).\ \ [m_1 - m_2)\ Q_x + (m_3 - m_4)\ Q_y]$$

$$\beta(s) = (m_1 - m_2)\ \ (\mu_x + \phi_x - \pi/2 - \pi Q_x/N_s) +$$

$$(m_3 - m_4)\ \ (\mu_y + \phi_y - \pi Q_y/N_s)\ ;$$

$$C\ (m_1m_2m_3m_4) = \frac{(n-1)!\ [(-)^{m3} + (-)^{m4}]}{4\ (n-\Sigma m)!\ m_1!\ m_2!\ m_3!\ m_4!}$$

$$C_m = C(m_1,m_1,m_2,m_2)\ ;$$

m_1, m_2, m_3, m_4 are integers.

The tune shift $\Delta Q_{x,y}$ is included in $Q_{x,y}$ and $\mu_{x,y}(s)$. The study of the distortion functions was initiated by T. Collins.[5] The emittances ε and initial phases ϕ are related to the coordinates of the particle as

$$x = (\Delta p/p) \quad \eta_x(s) + \sqrt{2\varepsilon_x \beta_x(s)} \sin [\phi_x + \mu_x + O(b_n)].$$

The beta-functions $\beta_{x,y}(s)$, phase advances $\mu_{x,y}(s)$ and $\eta_x(s)$ are determined for a linear lattice and given $\Delta p/p$.

In the linear approximation the emittances ε are constant along the lattice. Equation (2) gives the distortion at the exit of the k-th period; N_s is the number of periods per ring. The brackets $<>$ mean an averaging along a period.

The factor $\sin(\alpha/2)$ in Eq. (2) describes the resonance enhancement of the distortion. For decapole errors there is a coupling resonance $(m_1,m_2,m_3,m_4) = (2,0,0,2)$, $(0,2,2,0)$ which gives a big distortion near the diagonal $Q_x \sim Q_y$. The resonance is narrow and goes down 10 times with $|Q_x - Q_y| \sim 0.05$. The similar enhancement of the distortion exists also for sextupole errors in the second order in b_2.[4]

The crude estimation of the nonlinear tune shift and distortion can be done using Eq. (1) and (2). It gives tune shifts due to systematic multipoles

$$(\Delta Q)_S \sim (R/Q) \quad \Delta x^{n-2} \; b_{n-1},$$

tune shift due to random multipoles

$$(\Delta Q)_R \sim <b_{n-1}> (R/Q) \; (\Delta x)^{n-2}/\sqrt{N_c},$$

distortion due to systematic multipoles

$$(\Delta\varepsilon/\varepsilon)_S \sim (\Delta Q/Q)_S \; \pi/\sin(\alpha/2), \text{ and}$$

distortion due to random multipoles

$$(\Delta\varepsilon/\varepsilon)_R \sim (\Delta\varepsilon/\varepsilon)_S \; Q/\sqrt{N_c}.$$

Here N_c is the number of uncorrelated kicks per ring, Δx is the effective beam size $\Delta x \sim X_c + \sigma_x + \sigma_y$.

The last formula shows, that the distortion due to random multipoles can be comparable or even bigger than the distortion due to systematic multipoles.

The program was developed on the base of the Eqs. (1), (2). The program uses β_x, β_y, η_x functions as they are given by the program MAD for a linear lattice for a given $\Delta p/p$. The program can be used:

1. To calculate strength of two regular sextupole families in the lattice to cancel the linear chromaticity.

2. To calculate the tune shift due to systematic or random multipoles of a given order. For random multipoles rms value of b_n has to be given.

3. To calculate the distortion. The result of this calculation can be plotted on a phase plane or as distortion versus number of turns, or as variation of the distortion along a period to study the local distortion.

The program is rather fast. It takes 20 seconds of CPU time for tracking with sextupole errors instead of 16 minutes for tracking with MARYLIE under MAD for the same lattice on the VAX 780. Of course, time increases with multipole order.

The calculations of the distortion after each period, as it is given by Eq. (2) was done for comparison with the tracking programs (see Figs. 4-6).

Usually, only the amplitude of distortion variation with the number of periods is important. As it could be seen from the Eq. (2) this amplitude is given by Eq. (2) where the factor 2 has to be used instead of Cos $(\beta+K\alpha)$. So, there is no need to go through number of periods, and this makes the calculations much faster. The program was used to compare three six-fold lattices and the results are given in Table III.

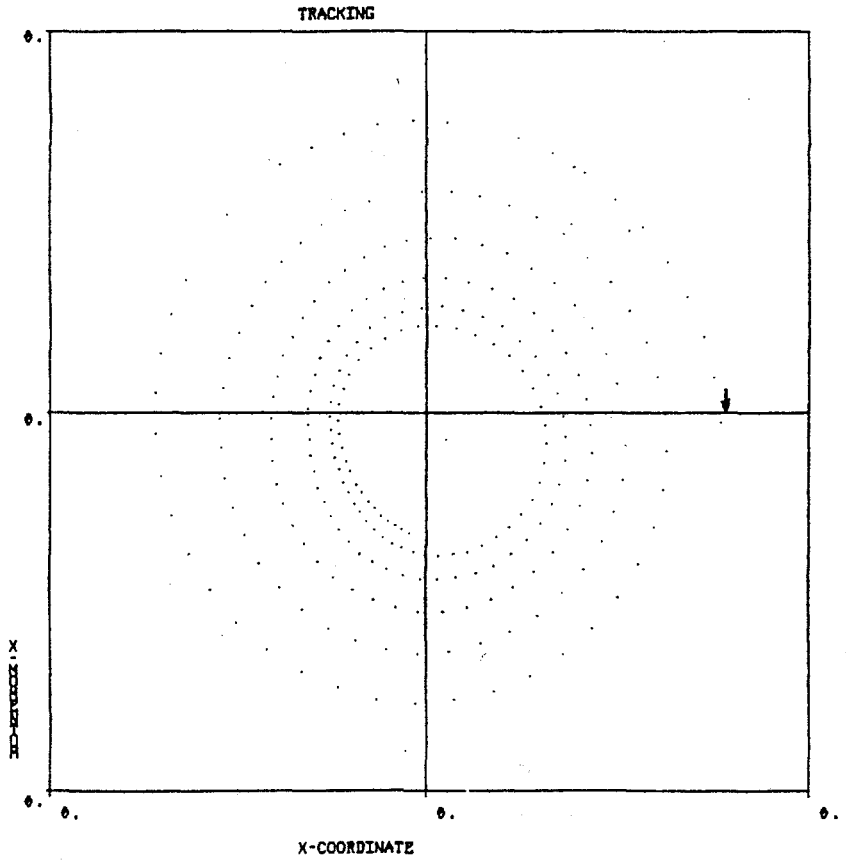

Fig. 4. Tracking results with MARYLIE for the lattice 140, 60°.

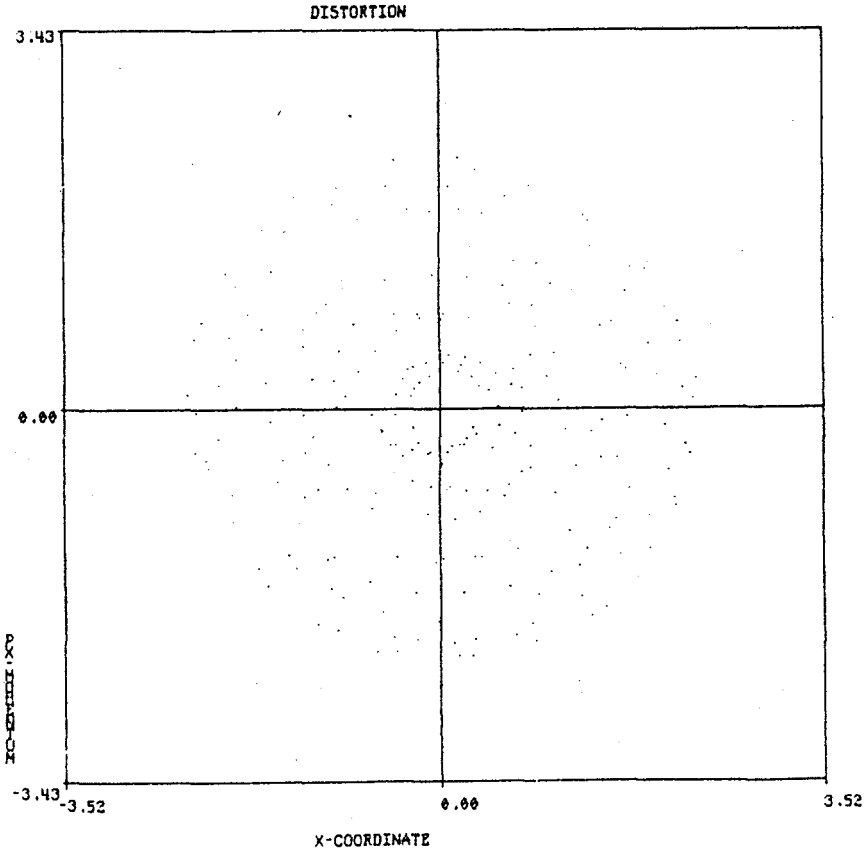

Fig. 5. Tracking with CANON (parameter the same as on Fig. 4)

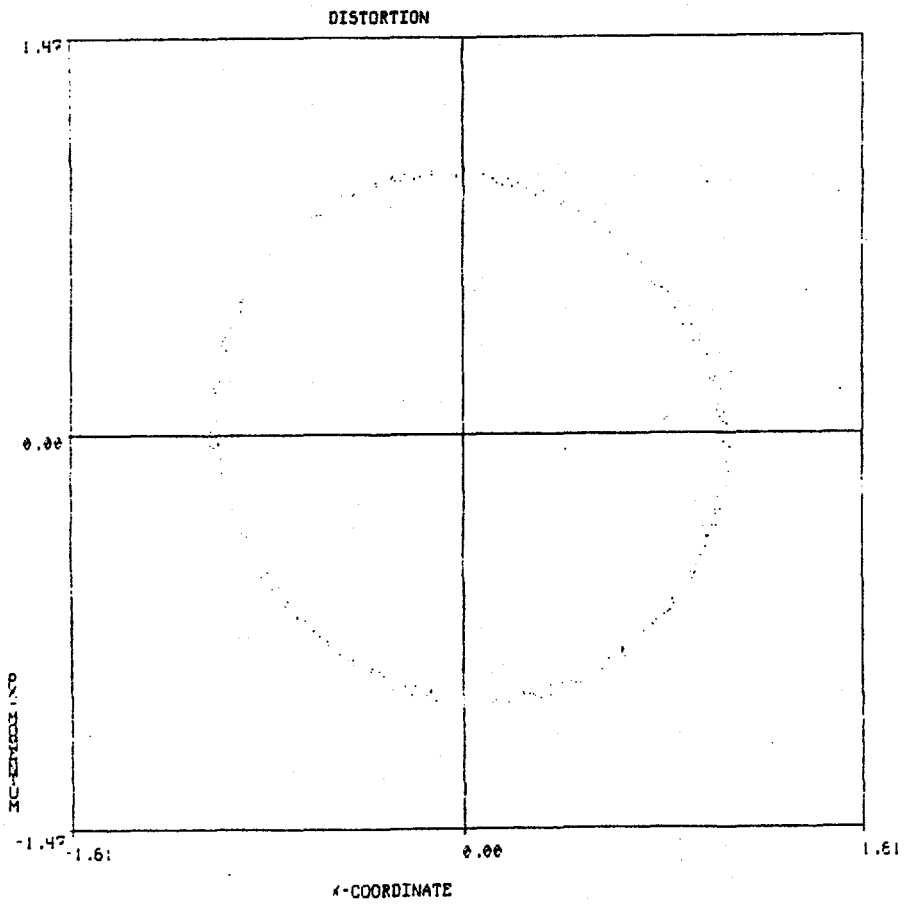

Fig. 6. The same as on Fig. 5, but without coupling resonance (0 2, 2, 0)

In all cases <bn> in dipoles was assumed to be equal 1 unit (in 10^{-4} cm^{-n}).

There were 4 kicks per dipole for the lattices (140 m, 60°,90°) and 3 kicks per dipole for the lattice (110 m, 90°).

The emittances $\varepsilon x = \varepsilon y = 0.5 \times 10^{-7}$ were used that correspond to 10σ at 1 TeV. The momentum spread was $\delta = 5 \times 10^{-4}$. The initial conditions were $p_x(0) = p._y(0) = 0$, $x_0 = y_0 = 0.316$ mm at IP.

For random multipoles <bn> was considered as the rms value. The distribution of the random numbers was chopped off at 2 rms value. The dependence on initial seed was studied and a seed which gives a typical distortion variation was used. The sensitivity of the results to the initial seed indicates that shuffling can be important for the beam dynamics.

In all cases two regular sextupole families were set to cancel linear chromaticity. Table III shows the distortion variation $\delta\varepsilon/\varepsilon$ and the tune shift per period ΔQ due to given multipole errors. For the control the tune per ring is given also.

Analysis of the data shows that the tune shift and distortion significantly depend on the cell length, making shorter cells favorable. For higher multipoles, stronger focusing is better. The nonlinear chromaticity due to sextupoles is better for 60°, than for 90°, at least for on-momentum particles. The best choice for the phase advance needs more consideration.

The results show that the tune shifts due to random multipoles are much less than those due to systematic multipoles, as could be expected. As the same time, the distortions due to random and systematic multipoles are comparable, in agreement with the estimates given below.

Table III.

		Q_x	Q_y	Q_x	Q_y	$\Delta\varepsilon_x/\varepsilon_x$	$\Delta\varepsilon_y/\varepsilon_y$
140,60	Regular b_x	97.30335	97.29750			+0.016	0.016
	Rand b_2	97.3035	97.2975	$0.47\ 10^{-3}$	$-0.245\ 10^{-2}$	0.160	0.186
	Syst.b_4	96.9985	96.9084	0.0508	0.0648	0.1375	0.156
	Rand b_4	97.3256	97.2995	$-0.37\ 10^{-2}$	$-0.33\ 10^{-3}$	0.284	0.280
	Syst.b_6	96.7045	97.1331	0.0998	-0.0726	1.435	0.940
	Rand b_6	97.3028	97.2595	$0.94\ 10^{-4}$	$0.63\ 10^{-2}$	0.397	0.437
140,90	Regular b_x	145.2979	145.2920			0.022	0.022
	Rand b_2	145.2979	145.2920	$-0.26\ 10^{-3}$	$-0.1097\ 10^{-2}$	0.089	0.071
	Syst.b_4	145.2358	145.1932	0.0103	0.0164	0.283	0.426
	Rand b_4	145.3089	145.2918	$-0.18\ 10^{-2}$	$0.28\ 10^{-4}$	0.1851	0.1972
	Syst.b_6	145.1860	145.3611	0.018	-0.011	0.457	0.539
	Rand b_6	145.2963	145.2784	$0.27\ 10^{-3}$	$0.23\ 10^{-2}$	0.129	0.151
110,90	Regular b_x	187.3008	187.2961			0.0278	0.0281
	Rand b_2	187.3008	187.2961	$-0.60\ 10^{-4}$	$-0.53\ 10^{-3}$	0.1093	0.1857
	Syst.b_4	187.2817	187.2651	$0.317\ 10^{-2}$	$0.517\ 10^{-2}$	0.091	0.072
	Rand b_4	187.3036	187.2949	$-0.46\ 10^{-3}$	$0.201\ 10^{-3}$	0.1026	0.082
	Syst.b_6	187.2738	187.3125	$0.45\ 10^{-2}$	$-0.27\ 10^{-2}$	0.134	0.125
	Rand b_6	187.2995	187.2936	$0.212\ 10^{-3}$	$0.425\ 10^{-3}$	0.041	0.045

The effects of decapole (b_4) and dodecapole (b_6) errors are comparable. Even in the best case (110 m, 90°) the systematic errors of 1 unit seem to be marginal.

The random sextupole has to be less than several units to keep motion in the linear aperture. There is a tendency to follow the analytic estimation, given before, although there is a significant difference, especially for dodecapoles. It can be explained by an increase of the number of terms in Eqs. (1) and (2) and interference between them. As a result, the numerical factor is difficult to take into account and it changes with the ratio (σ/X_c). In general, the analytic estimations are not very reliable for the systems like SSC, where there is no safety factor. The use of the simple programs, like CANON, seems therefore reasonable.

4° Realistic Lattice

The three race-track lattices were generated with phase advances 60° and 80° per cell and with the half cell length 115 m. They are basically the same as in the Reference Design.[6]

The race-track lattices with clustering IP are cheaper and easy to exploit. Some loss of periodicity probably is not crucial, if the main systematic errors are eliminated. Random multipoles and difference in IP's make the periodicity for the ring equal unity anyway.

The influence of the clustering on the beam beam interaction needs more analysis and may be crucial. A symbolic layout of the accelerator is shown on Fig. 7. Two sextupole families are placed in two subarcs with 162 cells each according to the scheme

325.5 = 0.5 + 162 + 0.5 + 162 + 0.5 (arc, 80°)

324.5 = 165 + 0.5 + 165 (arc, 60°A)

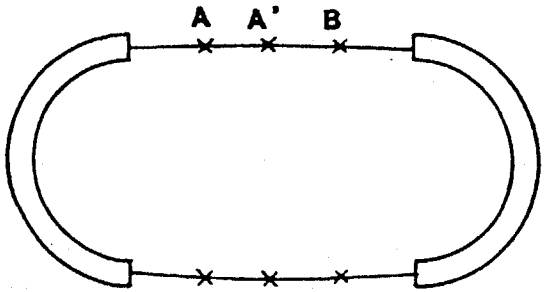

RACE - TRACK LATTICE, TOTAL LENGTH 162080.48 m.

CELL 115 m. : 60° AND 80° : B' = 125 T/m

CLUSTERED IR-S

INSERTION, TOTAL LENGTH 6359.24 m.

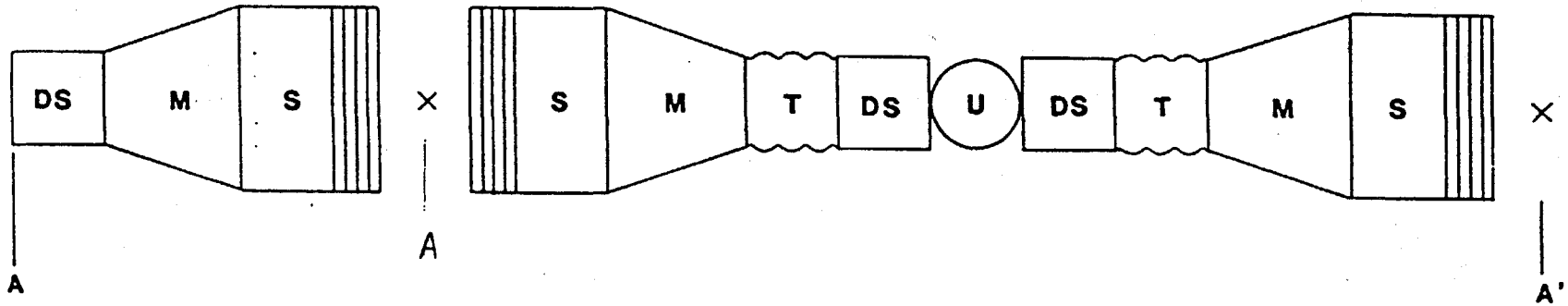

Fig. 7. Layout of race-track lattice.

The structure of the cell is as follows: half cell = (1/2 QF, dipole, drift, sext, 1/2 DQ). The dipole is 105 m long and made as 3 subdipoles 35 m each. The gradient of the field in quads is 125 T/m. With length of sextupole magnets 1 m, the sextupole strength to cancel linear chromaticity is (for 60°)

$$(B''/B)_F = 91.42\ 1/m^2;\ (B''/B)_D = -55.66\ 1/m^2$$

which seems reasonable.

The drift is 4 m long, and is enough to provide room for the thermal expansion (0.1% of 105 m dipole length), for correctors and monitors. The radius of curvature is ρ = 22225.992 m; $B_0\rho$ = 66677.976 T/m.

The length of a quad L_Q, a cell L_c, and the arc L_a are given in Table IV.

Two arcs are connected with two slightly convex insertions with 3 IP in each insertion. The layout of the half of the insertion is shown in Fig. 7. See also Table V for length and phase advance for each element.

The total length of the insertion is about 7800 m or 9.4% of the length of a half ring. We use a model utility section U as a half of a regular cell. Generally it could contain n + 1/2 of regular cells. The additional sextupoles can be placed in the utility sections for local corrections. It was done in the (60°B) lattice with 314.5 cells in the arc and 9 cells in the insertion (see Table V).

The dipoles in the utility sections and in 6 dispersion suppressors per insertion make an insertion convex. It reduces the mutual influence of experimental areas in the insertion.

The four trombones per insertion provide the local tuning. The utility sections and free space in trombones can be used to place rf cavities, abortion, extraction, and injection systems.

Table V. The Main Parameters of the Race Track Lattices.

	80°			60°A			60°B		
	Qx	Qy	L	Qx	Qy	L	Qx	Qy	L
Ring	164.30348	164.29904	166563.81	124.2992	124.2818	164600.18	125.30783	125.30242	163682.44
Period	82.15174	82.14952	83281.907	62.1496	62.1409	82300.090	62.653917	62.651212	81841.22082
Arc	72.334	72.332	75528.297	54.0843	54.082	74451.567	52.418	52.415	72157.219
Insert	9.8173	9.8173	7753.61(9.3%)	8.065	8.065	7848.523(9.5%)	10.236	10.236	9684.002
(IP)to(IP)	3.903	3.903	3087.285	2.979	2.979	3113.283	4.065	4.065	4031.022
LBT	0.248	0.251	71.5	0.247	0.250	71.5	0.248	0.251	71.5
Separ	0.241	0.009	120.0	0.241	0.010	120.0	0.241	0.009	120.0
Match	0.309	0.065	133.944	0.263	0.428	160.609	0.428	0.254	160.609
Tromb	0.854	0.926	696.114	0.369	0.421	688.304	0.579	0.63	688.305
D. Supr.	0.444	0.445	464.076	0.333	0.333	458.869	0.333	0.333	458.869
Util	0.111	0.111	116.019	0.084	0.083	114.718	0.75	0.75	1032.456

Table IV. Some Parameters of Race-Track Lattices.

	80°		60°A		60°B	
ρ	22227.588		22162.623		22028.93	
L_a	6.01889		4.71736		4.71736	
L_c	232.03777		229.43472		229.43472	
$B'/B\rho$	0.18737×10^{-2}		0.18737×10^{-2}		0.18737×10^{-2}	
# cells/arc	325.5		324.5		314.5	
# cells/ins	1		1		9	
	x	y	x	y	x	y
β cell	384.86	84.64	395.87	132.87	396.01	132.91
η max cell	1.87	0.38	2.80	0.76	2.75	0.32
η min cell	0.81	-0.44	1.58	-0.76	1.62	-0.32
β^*	1.0	1.0	1.0	1.0	1.0	1.0
α^*	0.0	0.0	0.0	0.0	0.0	0.0
η^* max	0.010	0.006	0.001	0.006	0.003	0.002
Q'/Q	-1.883	-1.883	-2.033	-2.033	-2.055	-2.055
(Q'/Q) cell	-1.207	-1.202	-1.102	-1.102	-1.102	-1.102

The magnet separator S of two beams in vertical plane is made as two magnet dipoles with drift in between. The separation of the two beams is explained in Fig. 8. The crossing angle at IP is taken equal zero, although it can be any. The real lattice has to have vertical dispersion suppressor in any case, because the accelerator of the SSC size cannot be planar.

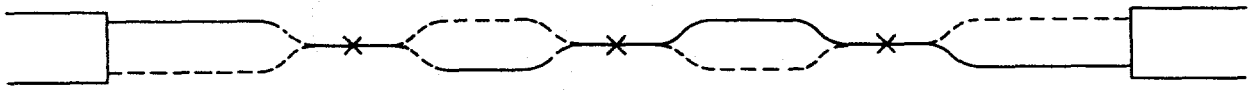

Fig. 8. Separation of the 2 beams

In this step we do not use a vertical dispersion suppressor that causes the vertical η-function. It is less than 1 cm at IP and about 35 cm in regular cells and seems appropriate. The magnitude of the η_y- function in cells depends on the phase advance between IP and has minimum if the phase advance proportional to 2π. The uncorrected linear chromicity is comparable with the chromicity in 6-fold lattices where $\eta = 0$: $Q'/Q = 2.236$ (140, 60°); 2.037 (140, 90°); 1.856 (110, 90°).

The tracking of the lattice will be done in the near future.

I am thankful to M. Donald, who provided me with the programs HARMON and MAD and to E. Courant, A. Garren, and D. Neuffer for useful discussions.

REFERENCES

1. SSC Reference Design report, May 1984

2. S. Heifets, Collective Effects for the Superferric SSC Design. U of H and TAC report, 1985.

3. R. H. Helm, Ann Arbor workshop, December, 1983, p. 67.

4. E. J. N. Wilson, private communication (1985).

5. T. L. Collins, Distortion Functions, Fermilab -84/114.

6. D. Neuffer, Superferric Supercollider Reference Design, TAC 384-21, 1984.

1101S

```
TITLE'
THE RACETRACK LATTICE 110M,60/DEGREE,REF.DES.LBTR

  DATE AND TIME: 00/00/00     00:00:00

ORC0:     DRIFT,L=4.00000000000
ORC1:     DRIFT,L=LU
ORC2:     DRIFT,L=LSEXT
ORM1:     DRIFT,L=65.0646000000
ORM2:     DRIFT,L=68.0689000000
ORLB0:    DRIFT,L=20.0000000000
ORLB:     DRIFT,L=1.00000000000
ORTR0:    DRIFT,L=1.00000000000
ORTR:     DRIFT,L=LQ
ORS1:     DRIFT,L=0.500000000000*(LBEND*(1.00000000000-LS1)*SM+ORC0[L]&
          +LSEXT)
ORS2:     DRIFT,L=0.500000000000*(LBEND*(1.00000000000-LS2)*SM+ORC0[L]&
          +LSEXT)
ORB1:     DRIFT,L=LNG2
ORB2:     DRIFT,L=LH
QFH:      QUADRUPO,L=LM/2.00000000000,K1=NEG(FOC)
QDH:      QUADRUPO,L=LM/2.00000000000,K1=FOC
QF:       QUADRUPO,L=LM,K1=NEG(FOC)
QD:       QUADRUPO,L=LM,K1=FOC
QM1:      QUADRUPO,L=7.47577000000,K1=0.200000000000E-02
QM2:      QUADRUPO,L=10.0000000000,K1=-0.200000000000E-02
QM3:      QUADRUPO,L=10.0000000000,K1=0.287507000000E-03
QTR1:     QUADRUPO,L=LM/2.00000000000,K1=0.135424000000E-02
QTR2:     QUADRUPO,L=LM,K1=-0.118475000000E-02
QTR3:     QUADRUPO,L=LM,K1=0.157055000000E-02
QTR4:     QUADRUPO,L=LM/2.00000000000,K1=-0.177766000000E-02
QDLB1:    QUADRUPO,L=LBD1,K1=-0.367300000000E-02
QFLB:     QUADRUPO,L=LBF,K1=0.365800000000E-02
QDLB2:    QUADRUPO,L=LBD2,K1=-0.361700000000E-02
SF:       SEXTUPOL,L=LSEXT,K2=0.000000000000E+00
SD:       SEXTUPOL,L=LSEXT,K2=0.000000000000E+00
QM1R:     QUADRUPO,L=7.47577000000,K1=-0.200000000000E-02
QM2R:     QUADRUPO,L=10.0000000000,K1=0.200000000000E-02
QM3R:     QUADRUPO,L=10.0000000000,K1=-0.287507000000E-03
QTR1R:    QUADRUPO,L=LM/2.00000000000,K1=-0.135424000000E-02
QTR2R:    QUADRUPO,L=LM,K1=0.118475000000E-02
QTR3R:    QUADRUPO,L=LM,K1=-0.157055000000E-02
QTR4R:    QUADRUPO,L=LM/2.00000000000,K1=0.177766000000E-02
QDLB1R:   QUADRUPO,L=LBD1,K1=0.367300000000E-02
QFLBR:    QUADRUPO,L=LBF,K1=-0.365800000000E-02
QDLB2R:   QUADRUPO,L=LBD2,K1=0.361700000000E-02
BDF:      SBEND,L=LBEND,ANGLE=LBEND/RADIUS,HGAP=0.125000000000E-01
BDS1:     SBEND,L=LBEND*LS1,ANGLE=LS1*LBEND/RADIUS,HGAP=&
          0.125000000000E-01
BDS2:     SBEND,L=LBEND*LS2,ANGLE=LS2*LBEND/RADIUS,HGAP=&
          0.125000000000E-01
BDD:      SBEND,L=LNG,ANGLE=LNG/RADIUS,TILT=1.57079632679,HGAP=&
          0.125000000000E-01
BDU:      SBEND,L=LNG,ANGLE=NEG(LNG)/RADIUS,TILT=1.57079632679,HGAP=&
          0.125000000000E-01
  :       MARKER
BEND:     LINE=(BDF,BDF,BDF)
BEND1:    LINE=(BDS1,BDS1,BDS1)
BEND2:    LINE=(BDS2,BDS2,BDS2)
CELLF:    LINE=(QFH,BEND,ORC0,ORC2,QDH)
```

```
CELLD:    LINE=(QDH,BEND,DRC0,DRC2,QFH)
CELLSF:   LINE=(QFH,BEND,DRC0,SF,QDH)
CELLSD:   LINE=(QDH,BEND,DRC0,SD,QFH)
DSUP:     LINE=(QFH,DRS1,BEND1,DRS1,QD,DRS1,BEND1,DRS1,QF,DRS2,BEND2,&
          DRS2,QD,DRS2,BEND2,DRS2,QFH)
MATCH:    LINE=(QM1,DRM1,QM2,DRM2,QM3)
LBT:      LINE=(QDLB1,DRLB,QFLB,DRLB,QFLB,DRLB,QDLB2,DRLB,QDLB2,DRLB0)
TROMBH:   LINE=(QTR1,DRTR,QTR2,DRTR,QTR3,DRTR,QTR4)
TROMB:    LINE=(TROMBH,-(TROMBH))
DSUPR:    LINE=(QDH,DRS1,BEND1,DRS1,QF,DRS1,BEND1,DRS1,QD,DRS2,BEND2,&
          DRS2,QF,DRS2,BEND2,DRS2,QDH)
MATCHR:   LINE=(QM1R,DRM1,QM2R,DRM2,QM3R)
LBTR:     LINE=(QDLB1R,DRLB,QFLBR,DRLB,QFLBR,DRLB,QDLB2R,DRLB,QDLB2R,&
          DRLB0)
TROMBHR:  LINE=(QTR1R,DRTR,QTR2R,DRTR,QTR3R,DRTR,QTR4R)
TROMBR:   LINE=(TROMBHR,-(TROMBHR))
ARC:      LINE=(162*(CELLSD,CELLSF),CELLD,162*(CELLSF,CELLSD))
SEPAR:    LINE=(DRB1,BDD,DRB2,BDU,DRB1)
INSR:     LINE=(DSUP,MATCHR,SEPAR,LBT)
INS:      LINE=(-(LBTR),SEPAR,-(MATCH),-(DSUPR))
INST:     LINE=(-(MATCH),TROMB,-(DSUPR))
INSTR:    LINE=(DSUP,TROMBR,MATCHR)
LINE1:    LINE=(-(LBTR),SEPAR,INST,CELLD,INSTR,-(SEPAR),LBT)
LINE2:    LINE=(-(LBTR),-(SEPAR),INST,CELLD,INSTR,SEPAR,LBT)
STRAIGHT: LINE=(INSR,LINE1,LINE2,INS)
PERIOD:   LINE=(ARC,STRAIGHT)
PARA,LU=0.500000000000*(LSEXT+DRC0[L])
PARA,LSEXT=1.00000000000
PARA,LQ=LBEND*SM+LSEXT+DRC0[L]
PARA,LBEND=35.0000000000
PARA,LS1=0.174371000000E-01
PARA,SM=3.00000000000
PARA,LS2=0.991232000000
PARA,LNG2=0.500000000000*(120.000000000-LH-2.00000000000*LNG)
PARA,LH=0.619125000000E-01*RADIUS/LNG-LNG
PARA,LM=4.71736000000
PARA,FOC=0.187370200000E-02
PARA,LBD1=12.1000000000
PARA,LBF=10.9000000000
PARA,LBD2=6.80000000000
PARA,RADIUS=SM*(N+12.0000000000*(LS1+LS2))*LBEND/PI
PARA,LNG=13.5000000000
PARA,N=651.000000000
PARA,PI=3.14159265359
RETURN
```

```
TITLE'
THE RACETRACK LATTICE 110M,60βDEGREE,REF.DES.LETR

   DATE AND TIME: 00/00/00      00:00:00

DRC0:      DRIFT,L=4.00000000000
DRC1:      DRIFT,L=LU
DRC2:      DRIFT,L=LSEXT
DRM1:      DRIFT,L=65.0646000000
DRM2:      DRIFT,L=68.0689000000
DRLB0:     DRIFT,L=20.0000000000
DRLB:      DRIFT,L=1.00000000000
DRTR0:     DRIFT,L=1.00000000000
DRTR:      DRIFT,L=LQ
DRS1:      DRIFT,L=0.500000000000*(LBEND*(1.00000000000-LS1)*SM+DRC0[L]&
           +LSEXT)
DRS2:      DRIFT,L=0.500000000000*(LBEND*(1.00000000000-LS2)*SM+DRC0[L]&
           +LSEXT)
DRB1:      DRIFT,L=LNG2
DRB2:      DRIFT,L=LH
QEH:       QUADRUPO,L=LM/2.00000000000,K1=NEG(FOC)
QDH:       QUADRUPO,L=LM/2.00000000000,K1=FOC
QF:        QUADRUPO,L=LM,K1=NEG(FOC)
QD:        QUADRUPO,L=LM,K1=FOC
QM1:       QUADRUPO,L=7.47577000000,K1=0.200000000000E-02
QM2:       QUADRUPO,L=10.0000000000,K1=-0.200000000000E-02
QM3:       QUADRUPO,L=10.0000000000,K1=0.287507000000E-03
QTR1:      QUADRUPO,L=LM/2.00000000000,K1=0.100648000000E-02
QTR2:      QUADRUPO,L=LM,K1=-0.194440000000E-02
QTR3:      QUADRUPO,L=LM,K1=0.274447000000E-02
QTR4:      QUADRUPO,L=LM/2.00000000000,K1=-0.239527000000E-02
QDLB1:     QUADRUPO,L=LBD1,K1=-0.367300000000E-02
QELB:      QUADRUPO,L=LBE,K1=0.365800000000E-02
QDLB2:     QUADRUPO,L=LBD2,K1=-0.361700000000E-02
SF:        SEXTUPOL,L=LSEXT,K2=0.000000000000E+00
SD:        SEXTUPOL,L=LSEXT,K2=0.000000000000E+00
QM1R:      QUADRUPO,L=7.47577000000,K1=-0.200000000000E-02
QM2R:      QUADRUPO,L=10.0000000000,K1=0.200000000000E-02
QM3R:      QUADRUPO,L=10.0000000000,K1=-0.287507000000E-03
QTR1R:     QUADRUPO,L=LM/2.00000000000,K1=-0.100648000000E-02
QTR2R:     QUADRUPO,L=LM,K1=0.194440000000E-02
QTR3R:     QUADRUPO,L=LM,K1=-0.274447000000E-02
QTR4R:     QUADRUPO,L=LM/2.00000000000,K1=0.239527000000E-02
QDLB1R:    QUADRUPO,L=LBD1,K1=0.367300000000E-02
QELBR:     QUADRUPO,L=LBE,K1=-0.365800000000E-02
QDLB2R:    QUADRUPO,L=LBD2,K1=0.361700000000E-02
BDF:       SBEND,L=LBEND,ANGLE=LBEND/RADIUS,HGAP=0.125000000000E-01
BDS1:      SBEND,L=LBEND*LS1,ANGLE=LS1*LBEND/RADIUS,HGAP=&
           0.125000000000E-01
BDS2:      SBEND,L=LBEND*LS2,ANGLE=LS2*LBEND/RADIUS,HGAP=&
           0.125000000000E-01
BDD:       SBEND,L=LNG,ANGLE=LNG/RADIUS,TILT=1.57079632679,HGAP=&
           0.125000000000E-01
BDU:       SBEND,L=LNG,ANGLE=NEG(LNG)/RADIUS,TILT=1.57079632679,HGAP=&
           0.125000000000E-01
 :         MARKER
BEND:      LINE=(BDF,BDF,BDF)
BEND1:     LINE=(BDS1,BDS1,BDS1)
BEND2:     LINE=(BDS2,BDS2,BDS2)
CELLF:     LINE=(QFH,BEND,DRC0,DRC2,QDH)
```

```
CELLD:     LINE=(QDH,BEND,DRCO,DRC2,QEH)
CELLSF:    LINE=(QEH,BEND,DRCO,SF,QDH)
CELLSD:    LINE=(QDH,BEND,DRCO,SD,QEH)
DSUP:      LINE=(QEH,DRS1,BEND1,DRS1,QD,DRS1,BEND1,DRS1,QF,DRS2,BEND2,&
           DRS2,QD,DRS2,BEND2,DRS2,QEH)
MATCH:     LINE=(QM1,DRM1,QM2,DRM2,QM3)
LBT:       LINE=(QDLB1,DRLB,QFLB,DRLB,QFLB,DRLB,QDLB2,DRLB,QDLB2,DRLBO)
TROMBH:    LINE=(QTR1,DRTR,QTR2,DRTR,QTR3,DRTR,QTR4)
TROMB:     LINE=(TROMBH,-(TROMBH))
DSUPR:     LINE=(QDH,DRS1,BEND1,DRS1,QF,DRS1,BEND1,DRS1,QD,DRS2,BEND2,&
           DRS2,QF,DRS2,BEND2,DRS2,QDH)
MATCHR:    LINE=(QM1R,DRM1,QM2R,DRM2,QM3R)
LBTR:      LINE=(QDLB1R,DRLB,QFLBR,DRLB,QFLBR,DRLB,QDLB2R,DRLB,QDLB2R,&
           DRLBO)
TROMBHR:   LINE=(QTR1R,DRTR,QTR2R,DRTR,QTR3R,DRTR,QTR4R)
TROMBR:    LINE=(TROMBHR,-(TROMBHR))
SUBARC:    LINE=(156*(CELLSD,CELLSF))
ARC:       LINE=(CELLD,CELLF,SUBARC,CELLD,156*(CELLSF,CELLSD),CELLF,&
           CELLD)
SEPAR:     LINE=(DRB1,BDD,DRB2,BDU,DRB1)
INSR:      LINE=(DSUP,MATCHR,SEPAR,LBT)
INS:       LINE=(-(LBTR),SEPAR,-(MATCH),-(DSUPR))
INST:      LINE=(-(MATCH),TROMB,-(DSUPR))
INSTR:     LINE=(DSUP,TROMBR,MATCHR)
UTIL:      LINE=(CELLD,4*(CELLSF,CELLSD))
LINE1:     LINE=(-(LBTR),SEPAR,INST,UTIL,INSTR,-(SEPAR),LBT)
LINE2:     LINE=(-(LBTR),-(SEPAR),INST,UTIL,INSTR,SEPAR,LBT)
STRAIGHT:  LINE=(INSR,LINE1,LINE2,INS)
PERIOD:    LINE=(ARC,STRAIGHT)
PARA,LU=0.500000000000*(LSEXT+DRCO[L])
PARA,LSEXT=1.00000000000
PARA,LQ=LBEND*SM+LSEXT+DRCO[L]
PARA,LBEND=35.0000000000
PARA,LS1=0.174371000000E-01
PARA,SM=3.00000000000
PARA,LS2=0.991232000000
PARA,LNG2=0.500000000000*(120.000000000-LH-2.00000000000*LNG)
PARA,LH=0.619125000000E-01*RADIUS/LNG-LNG
PARA,LM=4.71736000000
PARA,EOC=0.187370200000E-02
PARA,LBD1=12.1000000000
PARA,LBF=10.9000000000
PARA,LBD2=6.80000000000
PARA,RADIUS=SM*(N+12.0000000000*(LS1+LS2))*LBEND/PI
PARA,LNG=13.5000000000
PARA,N=647.000000000
PARA,PI=3.14159265359
RETURN
```

```
SF:    LINE=(QFH,BEND,DRCØ,SF,QDH)
SD:    LINE=(QDH,BEND,DRCØ,SD,QFH)
:      LINE=(QFH,DRS1,BEND1,DRS1,QD,DRS1,BEND1,DRS1,QF,DRS2,BEND2,&
       DRS2,QD,DRS2,BEND2,DRS2,QFH)
M:     LINE=(QM1,DRM1,QM2,DRM2,QM3)
       LINE=(QDLB1,DRLB,QFLB,DRLB,QFLB,DRLB,QDLB2,DRLB,QDLB2,DRLBØ)
TH:    LINE=(QTR1,DRTR,QTR2,DRTR,QTR3,DRTR,QTR4)
:      LINE=(TROMBH,-(TROMBH))
R:     LINE=(QDH,DRS1,BEND1,DRS1,QF,DRS1,BEND1,DRS1,QD,DRS2,BEND2,&
       DRS2,QF,DRS2,BEND2,DRS2,QDH)
MR:    LINE=(QM1R,DRM1,QM2R,DRM2,QM3R)
:      LINE=(QDLB1R,DRLB,QFLBR,DRLB,QFLBR,DRLB,QDLB2R,DRLB,QDLB2R,&
       DRLBØ)
THR:   LINE=(QTR1R,DRTR,QTR2R,DRTR,QTR3R,DRTR,QTR4R)
BR:    LINE=(TROMBHR,-(TROMBHR))
       LINE=(CELLD,162*(CELLSF,CELLSD),CELLF,162*(CELLSD,CELLSF),&
       CELLD)
R:     LINE=(DRB1,BDD,DRB2,BDU,DRB1)
:      LINE=(DSUP,MATCHR,SEPAR,LBT)
       LINE=(-(LBTR),SEPAR,-(MATCH),-(DSUPR))
:      LINE=(-(MATCH),TROMB,-(DSUPR))
P:     LINE=(DSUP,TROMBR,MATCHR)
I:     LINE=(-(LBTR),SEPAR,INST,CELLD,INSTR,-(SEPAR),LBT)
C:     LINE=(-(LBTR),-(SEPAR),INST,CELLD,INSTR,SEPAR,LBT)
IGHT:  LINE=(INSR,LINE1,LINE2,INS)
OD:    LINE=(ARC,STRAIGHT)
.LU=Ø.5ØØØØØØØØØØØ*(LSEXT+DRCØ[L])
.LSEXT=1.ØØØØØØØØØØØ
.LQ=LBEND*SM+LSEXT+DRCØ[L]
.LBEND=35.ØØØØØØØØØØ
.LS1=Ø.41Ø476ØØØØØØ
.SM=3.ØØØØØØØØØØØ
.LS2=Ø.5935Ø5ØØØØØØ
.LNG2=Ø.5ØØØØØØØØØØØ*(12Ø.ØØØØØØØØØ-LH-2.ØØØØØØØØØØØ*LNG)
.LH=Ø.619125ØØØØØE-Ø1*RADIUS/LNG-LNG
.LM=6.Ø1889ØØØØØ
.FOC=Ø.18737Ø2ØØØØE-Ø2
.LBD1=12.1ØØØØØØØØ
.LBF=1Ø.9ØØØØØØØØ
.LBD2=5.8ØØØØØØØØØ
.RADIUS=SM*(1+12.ØØØØØØØØØ*(LS1+LS2))*LBEND/PI
.LNG=13.5ØØØØØØØØ
.N=653.ØØØØØØØØ
.PI=3.14159265359
DFN
```

```
ITLE!
HE FACETRACK LATTICE 110M,80 DEGREE,REF.DES.LBTR

 DATE AND TIME: 00/00/00      00:00:00

RC0:      DRIFT,L=4.000000000000
RC1:      DRIFT,L=LU
RC2:      DRIFT,L=LSEXT
RM1:      DRIFT,L=79.088800000C
RM2:      DRIFT,L=33.553300000C
RLB0:     DRIFT,L=20.000000000C
RLB:      DRIFT,L=1.000000000000
RTP0:     DRIFT,L=1.000000000000
RTP:      DRIFT,L=LQ
RS1:      DRIFT,L=0.500000000000C*LBEND*(1.000000000000-LS1)*SM+DRC0[L]&
          +LSEXT)
RS2:      DRIFT,L=0.500000000000C*LBEND*(1.000000000000-LS2)*SM+DRC0[L]&
          +LSEXT)
RB1:      DRIFT,L=LNG2
RB2:      DRIFT,L=LH
FH:       QUADRUPO,L=LM/2.000000000000,K1=NEG(FOC)
DH:       QUADRUPO,L=LM/2.000000000000,K1=FOC
F:        QUADRUPO,L=LM,K1=NEG(FOC)
D:        QUADRUPO,L=LM,K1=FOC
M1:       QUADRUPO,L=1.378820000000,K1=0.250429000000E-02
M2:       QUADRUPO,L=10.82060000000,K1=-0.247939000000E-02
M3:       QUADRUPO,L=9.102210000000,K1=0.379127000000E-03
TR1:      QUADRUPO,L=LM/2.000000000000,K1=0.237729000000E-02
TR2:      QUADRUPO,L=LM,K1=-0.220049000000E-02
TR3:      QUADRUPO,L=LM,K1=0.239704000000E-02
TR4:      QUADRUPO,L=LM/2.000000000000,K1=-0.244562000000E-02
DLB1:     QUADRUPO,L=LBD1,K1=-0.367300000000E-02
FLB:      QUADRUPO,L=LBF,K1=0.365800000000E-02
DLB2:     QUADRUPO,L=LBD2,K1=-0.361700000000E-02
F:        SEXTUPOL,L=LSEXT,K2=0.000000000000E+00
D:        SEXTUPOL,L=LSEXT,K2=0.000000000000E+00
M1R:      QUADRUPO,L=1.378820000000,K1=-0.250429000000E-02
M2R:      QUADRUPO,L=10.82060000000,K1=0.247939000000E-02
M3R:      QUADRUPO,L=9.102210000000,K1=-0.379127000000E-03
TR1R:     QUADRUPO,L=LM/2.000000000000,K1=-0.237729000000E-02
TR2R:     QUADRUPO,L=LM,K1=0.220049000000E-02
TR3R:     QUADRUPO,L=LM,K1=-0.239704000000E-02
TR4R:     QUADRUPO,L=LM/2.000000000000,K1=0.244562000000E-02
DLB1R:    QUADRUPO,L=LBD1,K1=0.367300000000E-02
FLBR:     QUADRUPO,L=LBF,K1=-0.365800000000E-02
DLB2R:    QUADRUPO,L=LBD2,K1=0.361700000000E-02
DF:       SBEND,L=LBEND,ANGLE=LBEND/RADIUS,HGAP=0.125000000000E-01
DS1:      SBEND,L=LBEND*LS1,ANGLE=LS1*LBEND/RADIUS,HGAP=&
          0.125000000000E-01
DS2:      SBEND,L=LBEND*LS2,ANGLE=LS2*LBEND/RADIUS,HGAP=&
          0.125000000000E-01
DD:       SBEND,L=LNG,ANGLE=LNG/RADIUS,TILT=1.570796326?9,HGAP=&
          0.125000000000E-01
DU:       SBEND,L=LNG,ANGLE=NEG(LNG)/RADIUS,TILT=1.570796326?9,HGAP=&
          0.125000000000E-01
:         MARKER
END:      LINE=(DDF,DDF,BDF)
END1:     LINE=(DB1,BDS1,BDS1)
END2:     LINE=(BDS2,BDS2,BDS2)
ELLF:     LINE=(QFH,BEND,DRC0,DRC2,QDH)
ELLD:     LINE=(QDH,BEND,DRC0,DRC2,QFH)
```

Don Groom

04 June 1985

PRELIMINARY COMMENTS ABOUT BEAM LOSS

A variety of beam loss questions are being investigated. They affect several design issues, ranging from machine-associated background in the detectors to the radiation lifetime of the main-ring magnets:

1. *Muons.* Oppositly directed muon beams from prompt muon production, primary meson decay, and a variety of other processes radiate from each IR. If they were not fanned by the insertion diopoles, the beams would be sufficiently intense and energetic that they would present a radiation hazard even after penetrating 2 km of soil or rock.

Details depend upon the origin of the muons:

(*a*) *Prompt muons.* Muons from heavy flavor decay form an irreducible background. Since their spectrum is quite hard, this source dominates above some energy which is geometry dependent, but for the SSC is about 1 TeV.

(*b*) *Meson decay.* About half of inelastically produced mesons are inside 30 mr, and so they travel in the beam pipe at least as far as the first insertion dipole, 72 m from the IR. A meson with lifetime τ and energy γmc^2 decays with probability $(\gamma c\tau)^{-1}$ per unit length. For a 1 TeV pion, this probability is 2×10^{-5} per meter; 1.5×10^{-3} of them decay before reaching the first dipole. (Their production rate at the SSC is several GigaHertz, so that the decay contribution to the muon flux is substantial.) Using the RDS figures for this dipole (3T excitation, 16.6 m long), we find that particles with < 7 GeV/c are swept into the beam tube walls. Hadronic interaction then effectively terminates primary meson decay as a muon souce.

(*c*) *Bethe-Heitler muon production.* This process is quite important, contributing muon pairs from both direct and shower-produced photons.

(*d*) *Decay of shower-produced mesons.* This process contributes a few soft muons, but is unimportant at energies of interest.

Given the contribution of meson-decay muons, it is not surprising that the flux is exceedingly sensitive to the initial geometry. Moreover, the "beam spot" shape will be sensitive to the magnetic history of the particles. Detailed modeling is planned for the coming months, but results to date are based on a very simple geometry. A. Van Ginniken has made several Monte Carlo runs at our request, using a version of CASIM in which muons are included. In the most relevant, particles leaving the IR travel 80 m in vacuum, then enter "Fermilab rock." The attached figures are based upon this geometry. Fig. 1 shows the depedence of the radially integrated flux upon depth (z). Fig. 2 shows the relative importance of different contributions as a function of z, and Fig. 3 the muon flux and radiation dose as a function of radial distance from the center of the beam spot, at selected depths typical of proposed clustered IR separations. The important results are that (i) prompt muon production dominates the flux after about 1 km ($\sim$1 TeV), (ii) even after 2 km, the intensity in an 8 m diameter circle exceeds the surface cosmic ray intensity, and (iii) at distances of up to 2 km, the muons present a substantial radiation hazard.

Several observations are in order:

(*a*) The muon/parent meson beam has been "fanned" by the dipole. An integrated field of 20 Tesla-meters near the IR is sufficient to deflect a 1 TeV particle by 1 m at 1 km, so the effect is important. This effect substantially reduces the radiation dosage in an adjacent IR, should the beam be permitted to emerge there.

(*b*) With an over/under bore arrangement, the deflection is vertical, so that a vertically fanned muon beam emerges from the surface. Since the upward-going muons are all of the same sign, inclusion of a magnetized "iron reflector" might essentially contain then in the earth.

(*c*) If the beam orientation is side-by-side, part of the the beam would sweep

across the detectors in adjacent IR's.

(*d*) In the over/under case, it is important that this fan not intercept the detector at the next IR. In practice this means sufficient bend that the muon beam spot is about 30 m or more "outboard" of the ring *and the staging area* at the next IR. A minimal separation and bend from a lattice point of view (4 dispersion supressors at half the nominal ring stregth, or 800 m at 3 T) would result in a 14 m displacement.

(*e*) We can see little motivation for contriving to use these muons as a "test beam" in the staging area near the next IR. It is not dependable (particularly when both detector and machine are being commissioned), its direction is wrong (axial, with all but the endcaps designed for radial particles), it could be a radiation hazard, and it illuminates only a small region. We would propose that the IR staging area be inboard of the ring.

2. *Machine-associated background in the IR's.* About 30 mb of the total cross section is elastic or quasi-elastic, and most of the protons are in a Gaussian spot with sigma = 9 mr. These particles are well within the machine acceptance, but there is a grey area in the tail of the distributions in which the scattered particles "almost" remain in orbit—they continue for some distance but eventually hit a wall. In the worst case, they will strike the wall in a low-beta quadrupole as they enter the IR, creating a hadronic splash in the detector. Although such a flux is probably not large enough to be otherwise harmful, it is imperative that it strike collimators elsewhere.

3. *Cryogenic load.* We have previously mentioned the effectiveness of the first dipole in sweeping the products of inelastic scattering. This problem has been addressed to some degree in the RDS, but considerably more detail is needed. It appears that a very large fraction of the inelastic particle energy will be deposited here. The drift space between the insertion dipoles must contain tight collimators on the outgoing legs, perhaps including magnetized iron.

4. *Radiation damage in the ring.* The lifetime of both magnets and electonics

in the tunnel might be limited by radiation due to particle loss. Early results are not reassuring: Tevatron measurements, reported to us by John Elias, indicate that most of the tunnel background comes from particle loss due to beam-gas collisions. He calculates lifetimes of about 10 years for both electronics and magnets, with a sufficient margin of error for worry. In addition to ionizing radiation, an isotropic flux of boil-off neutrons is present. Further measurements and detailed calculations are planned.

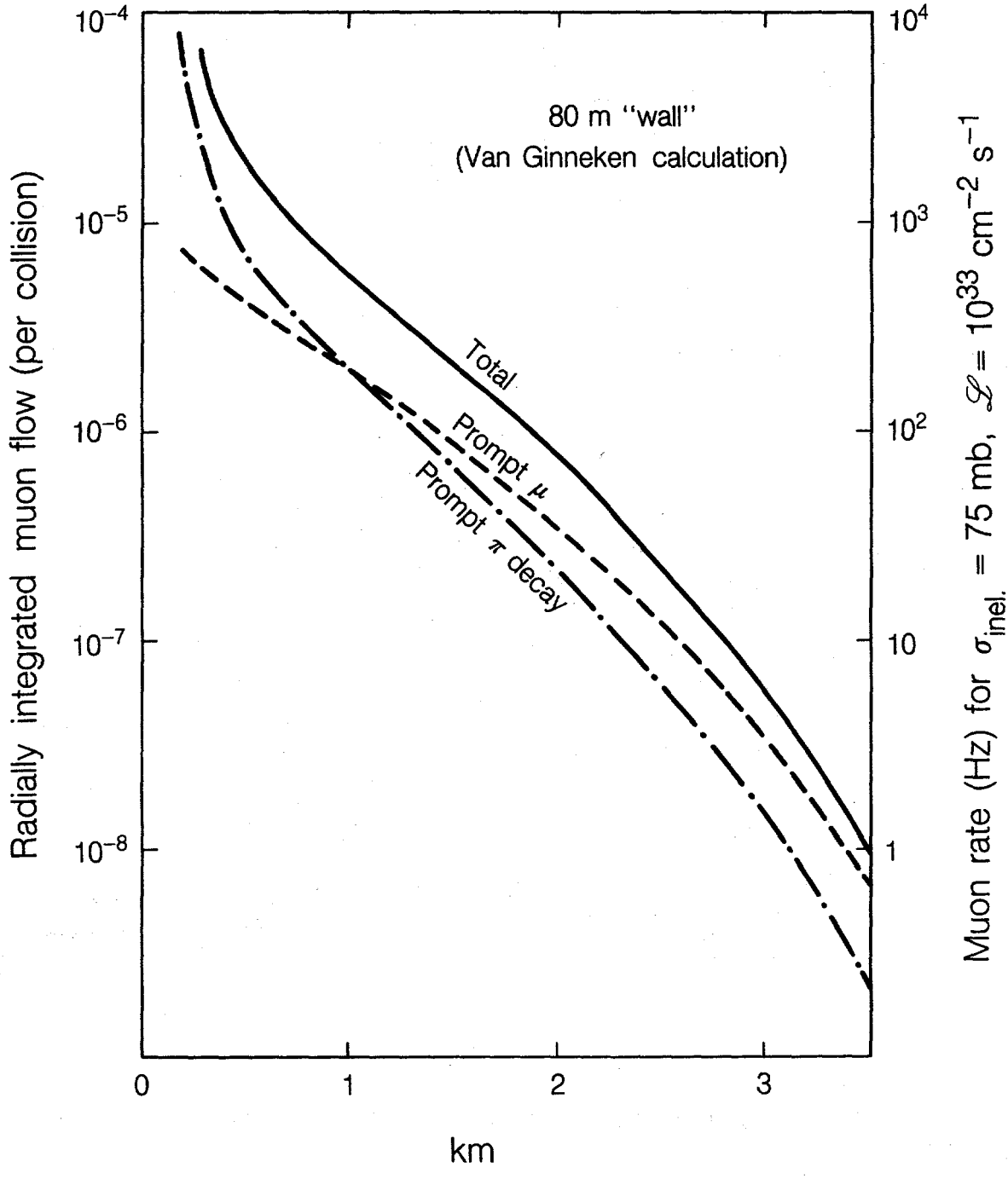

Fig. 1. Dependence of the radially integrated flux upon depth (z).

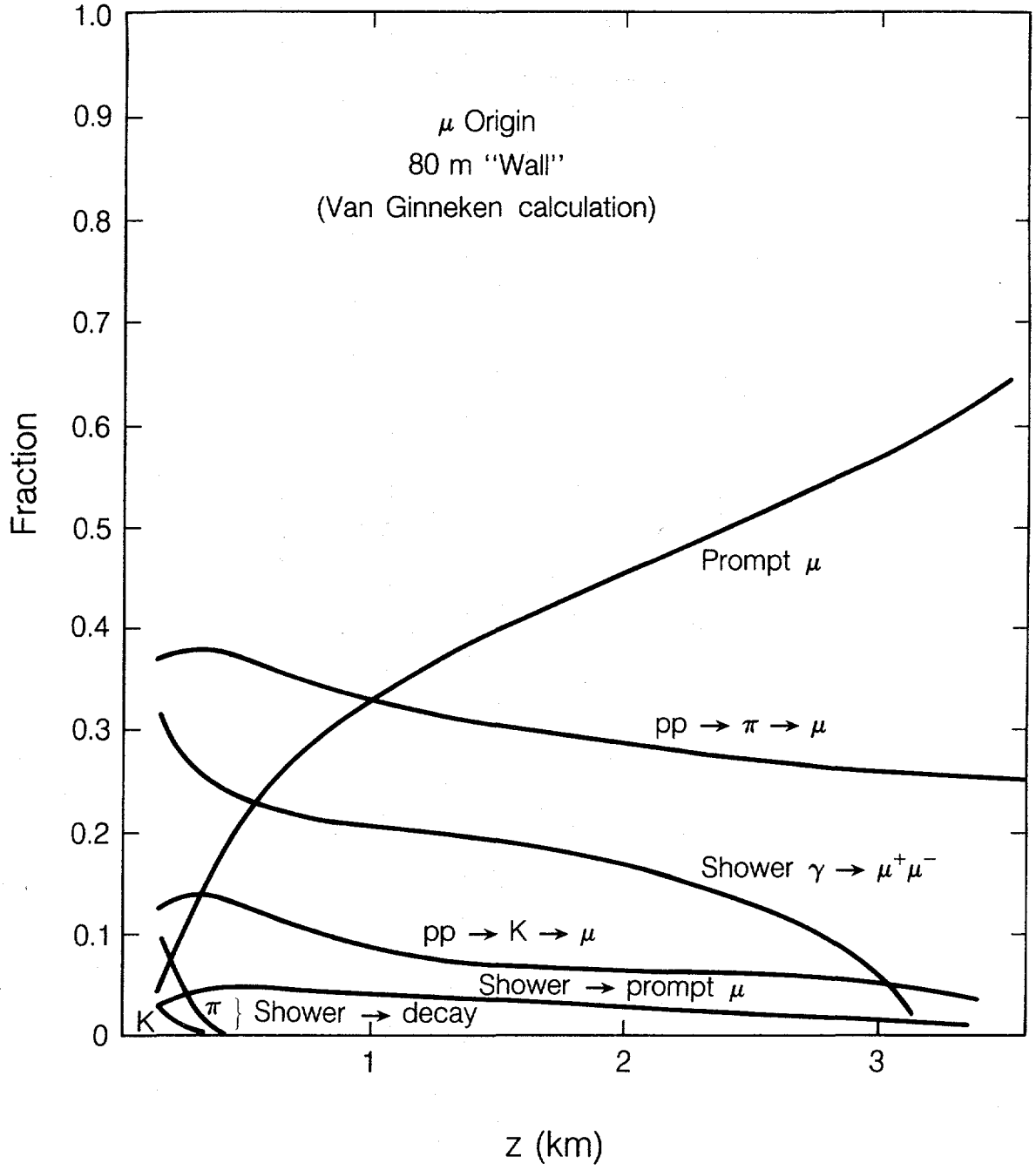

Fig. 2. Relative importance of different contributions as a function of z.

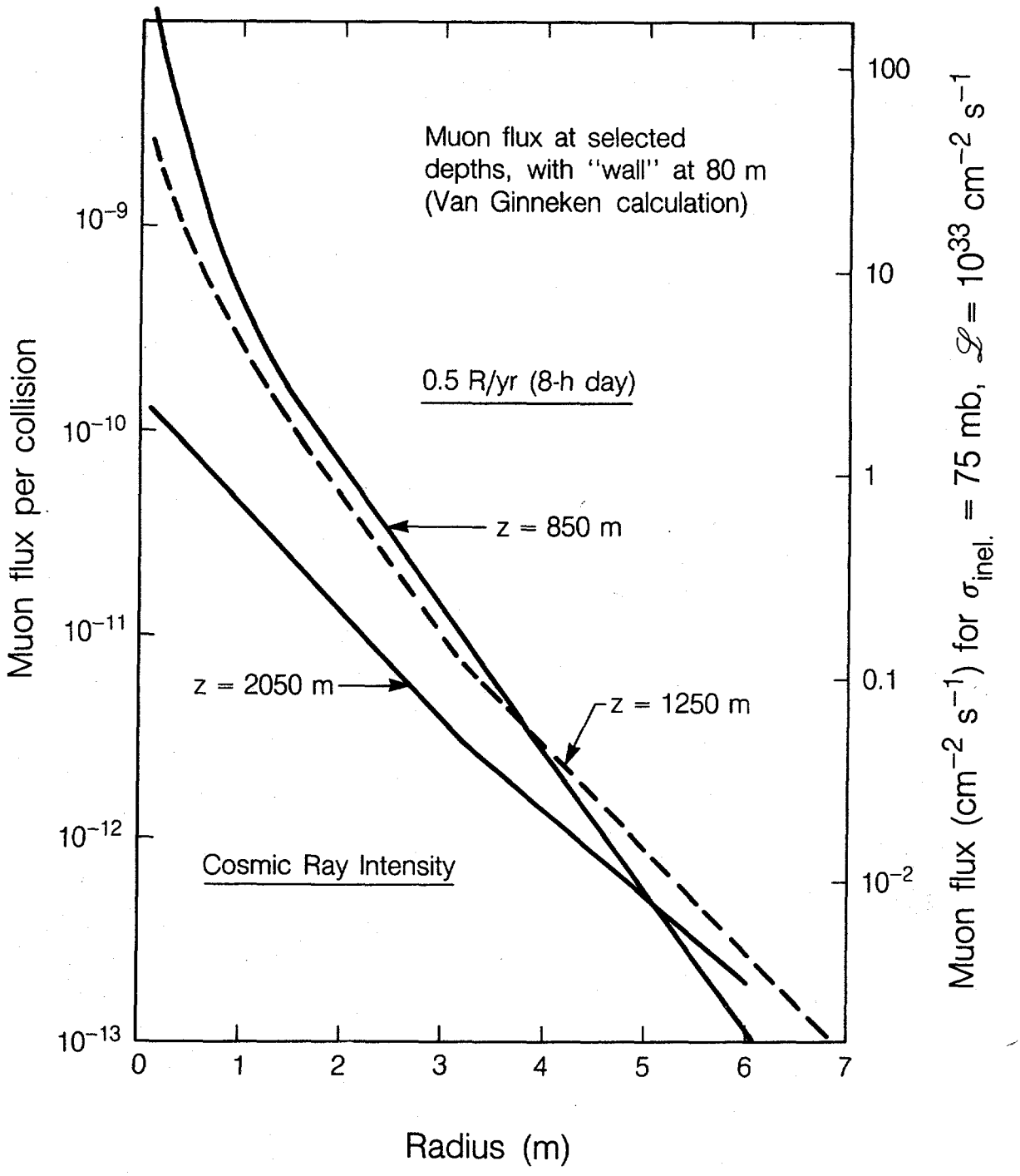

Fig. 3. Muon flux and radiation dose as a function of radial distance from the center of the beam spot at selected depths typical of proposed clustered IR separations.

GLOBAL SEARCHES IN QUADRUPOLE GEOMETRY FOR MINIMUM IR CHROMATICITY CONTRIBUTION

Steve Peggs
SSC Central Design Group

Introduction

This note forms a condensed summary of work performed by S. Peck at the Cornell Electron Storage Ring, which was reported in the proceedings of the 1984 Snowmass Workshop, page 384. It was originally presented by me as a series of viewgraphs, and has only been slightly modified and expanded here, for the ease of the reader. Interested readers are encouraged to refer back to the original article.

Method

Interaction region optics were studied from the 20 TeV collision point, out past a doublet or triplet of thick IR quads, to a boundary point 50 meters beyond the last quadrupole. The beta functions in both planes were propagated from equal initial values in both planes of

β^* = 0.4, 0.6, ... 2.0 meters out to the boundary, for intersection region free spaces of

L^* = 5, 10, 15 and 20 meters

and for assumed quadrupole strengths of

K = 0.003 to 0.009 m^{-2}

For a given combination of these initial conditions, a global computer search was made in the space of the quadrupole lengths and separations, to optimize the chromaticity contribution from the IR. Initially the step size for the global search was 0.1 meters in quadrupole length, and 1.0 meter in quadrupole separation. Typically, this led to the analysis of 200* 10* 200*

20* 200 configurations of a triplet optics. After the location of a global minimum on this scale, a local search was performed with 0.001 meter step size. The solution found in this way is unequivocally not merely at a local minimum of the "penalty function," but the best solution available. The confidence of these results came at the expense of about one day of VAX 780 CPU time.

Usually the maximum of the IR chromaticity contributions in the two transverse planes was minimized, often resulting in equal contributions in both planes. Sometimes the horizontal contribution was constrained to be three times the vertical contribution. This might be advantageous in SSC optics whose IR's are identical, and are symmetric about each collision point, where the horizontal sextupoles could more efficiently correct chromaticity than the vertical sextupoles, because of the larger dispersion at horizontal sextupoles. IR optics with peak values of

β_h or β_v > 20 kilometers anywhere, or with

β_h or β_h > 200 meters at the boundary point, were discarded as unsatisfactory.

Results

As a matter of convention in the figures which follow, doublet configurations are always marked with an open box, and triplet configurations with a triangle. XMAX or XI is always the minimum of the maximum (minimax) chromaticity contribution per half IR, so that a value of 8 would decrease the natural chromaticity of an SSC with 6 IR's by 96 units, in the worst plane. B represents the peak beta in either plane.

In all the cases shown here, the separation of the quadrupoles was 1 meter -- the lowest value it was allowed to reach, and always the optimum, for both

doublets and triplets. While closer quadrupoles mean stronger quadrupoles, the effect on the chromaticity was more than compensated by the decrease in peak betas. Typically, raising the separation form 1.0 meter to 10.0 meters raised the chromaticity contribution by only one or two per cent.

Figure 1 shows the dependency of the peak beta and the minimax chromaticity as a function of quadrupole strength, for various free space lengths, and for both doublet and triplet configurations. It is immediately clear that triplets are indeed far more efficient than doublets when the collison betas are equal, $\beta^* = 1.0$ meter in these cases. Noting the offset in the horizontal scale, it is also clear that large quadrupole field strengths K are useful in decreasing the chromaticity contribution, thus indirectly permitting lower β^* values to be reached. There is almost no advantage in having the free space L^* as low as 5.0 meters, although a reduction from the nominal value of 20 meters to 15 or even 10 meters might be advisable.

Figure 2 shows how the peak beta and the minimax chromaticity contribution vary as a function of β^*, for a family of qaudrupole field strengths K in a triplet configuration. Here again it is seen that high K values are advantageous, with peak beta or chromaticity being reduced by 50% or more when K is increased by a factor of two.

Figure 3 plots the integrated optimal strength, KL, of the first and second quadrupoles in a triplet versus the collision beta β^*, for a family of K values. It confirms the common wisdom that the focal length of the IR quadrupoles hardly varies at all as β^* is varied, in this case from 0.4 to 2.0 meters. Taken in conjunction with Fig. 2, it shows that the chromaticity increase associated with a collision beta decrease is almost entirely due to the increased betas at the IR triplet, and is not due to an increase in quadrupole strength.

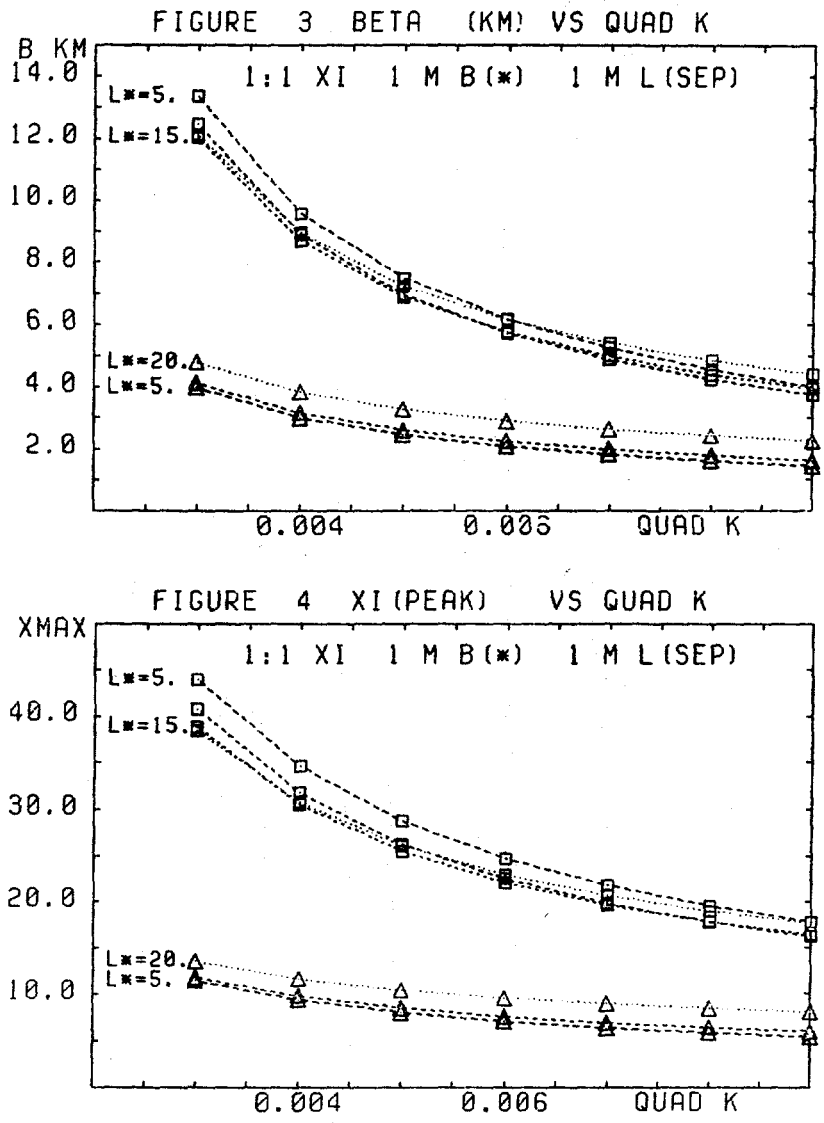

Fig. 1 Peak beta B, and minimax chromaticity contribution XMAX, versus quadrupole strength K, for various free spaces L*, with doublet and triplet configurations. Collision betas β* of 1.0 meter, quad separations of 1.0 meter.

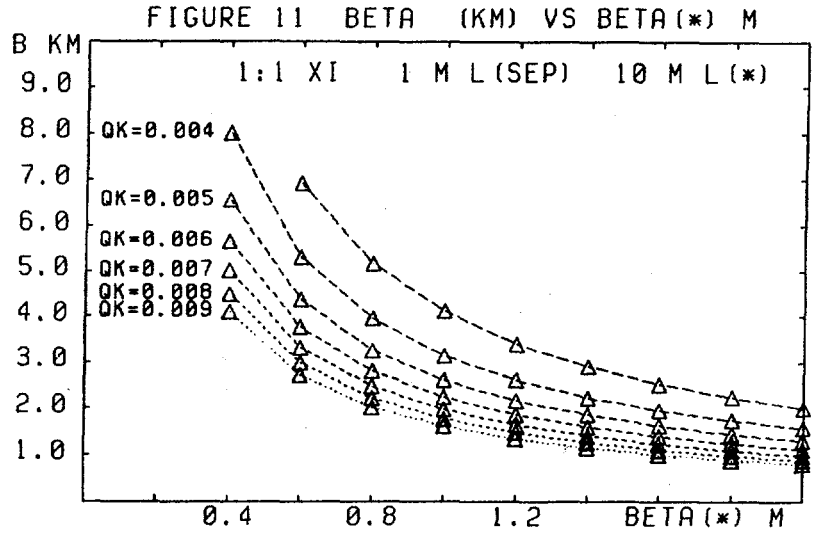

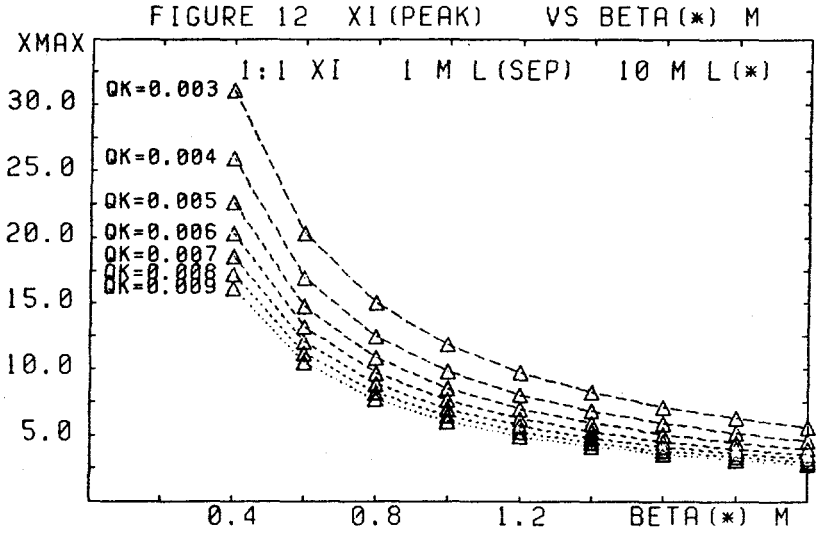

Fig. 2 Peak beta B, and minimax chromaticity contribution XMAX, versus collision beta β*, for various quadrupole field strengths K. Free space L* of 20 meters, quad separations of 1.0 meter.

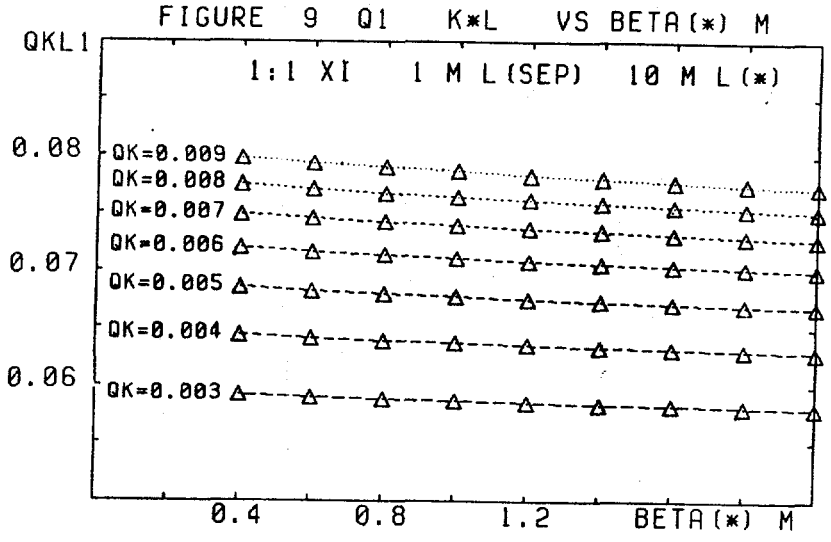

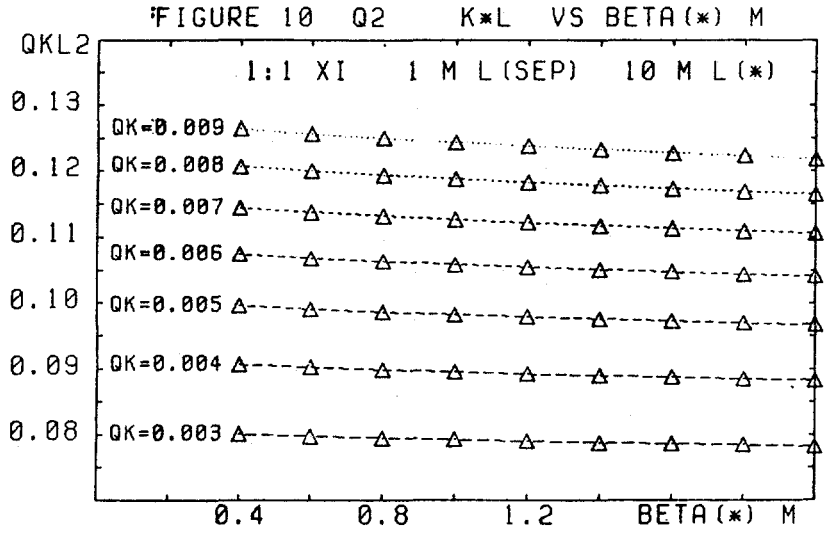

Fig. 3 Integrated strengths KL of the first two quadrupoles, versus collision beta β*, for various quadrupole field strengths K. Free space L* of 10 meters, quad separations of 1.0 meter.